BEST POSSIBLE SCAN

TID 4500 (57th Ed.)
UC-35
Nuclear Explosions-
Peaceful Applications

SC-RR-71 0056

AIRBLAST FROM PROJECT TRINIDAD DETONATIONS

L. J. Vortman
Underground Physics Division
Sandia Laboratories
Albuquerque, New Mexico
87115

June 1971

ABSTRACT

Airblast was measured from distances of a few hundred feet to about six miles from single one-ton surface, near surface, and buried explosions. Similar measurements were made perpendicular to and off the ends of buried single row-charges detonated simultaneously and with delays between charges in the rows, and buried double-row charges detonated simultaneously and with delays between rows. Explosives were either ammonium nitrate and fuel oil or aluminized ammonium nitrate slurry.

Single charges detonated at and near the surface gave peak overpressures and impulses close to those of TNT charges burst similarly. Buried single charges had positive impulses comparable to those from TNT, but had ground-shock-induced peak overpressures about twice those of TNT, and gas-venting peak overpressures from two to eight times those of TNT.

A one-ton charge placed at the bottom of a 14-inch-diameter unstemmed hole produced overpressures and airblast energy about midway between an equivalent surface burst and a completely stemmed explosion at the same depth.

Waveforms from all row-charge detonations were complex, and neither peak overpressures nor positive impulses could be related consistently to those from single charges or to smaller buried TNT charges in a more uniform medium.

No airblast damage occurred at either Jansen or Trinidad, Colorado at a maximum peak overpressure of 0.009 psi.

Key words: Plowshare, cratering, chemical explosives

ACKNOWLEDGMENTS

Airblast measurements described here were made by H. G. Laursen assisted by B. C. Holt, C. Csinnjinni, and M. E. Gilmer. J. L. Martinez and R. J. Beyatte were responsible for data reduction. J. W. Long made necessary adjustments to records, assisted in data correlation and analysis, and provided the data plots included in the Appendix. J. W. Reed served as scientific advisor in the field for two of the series and has made helpful suggestions in analysis and reporting of results. The work was sponsored by the U. S. Army Corps of Engineers Nuclear Cratering Group, Livermore, California.

CONTENTS

CONTENTS (cont)

CONTENTS (cont)

BLANK PAGE

AIRBLAST FROM PROJECT TRINIDAD DETONATIONS

Introduction and Objectives

Project TRINIDAD was a series of cratering experiments conducted with chemical explosives in interbedded sandstones and shales near Trinidad, Colorado. The series had multiple objectives, which included obtaining crater dimensions from single charges in interbedded sandstones and shales as a function of burial depth; determining the relative cratering effectiveness of aluminized ammonium nitrate slurry as against an ammonium nitrate/fuel oil combination; finding the effectiveness of row-charge cratering in non-level terrain; establishing the relative cratering effectiveness of simultaneous and delayed row-charge detonations, and investigating safety aspects such as ground motion and airblast resulting from single and row-charge detonations. Except for Shot D-1, all charges weighed one or two tons.

Table I summarizes the one-ton single-charge events. One-ton row-charge events are summarized in Table II, and side-hill shots in Table III.

TABLE I

Summary of Single-Charge Events - B Series

Shot No.	Explosive	Planned Charge-Burial Depth (ft)
B-1	ANFO[a]	16
B-2	ANFO	18
B-3	ANFO	20
B-4	AANS[b]	16
B-5	AANS	19
B-6	AANS	21.5
B-7	AANS	24
B-8	AANS	28
B-9	AANS	Cancelled
B-10[c]	AANS	-3.8
B-11[c]	AANS	-1.9
B-12[c]	AANS	0.0
B-13[c]	AANS	1.9
B-14	AANS	21.5
B-15[d]	AANS	21.5

(a) Ammonium nitrate and fuel oil.
(b) Aluminized ammonium nitrate slurry (TD-2).
(c) In spherical container.
(d) Unstemmed 14-inch-diameter hole.

TABLE II

Summary of Row-Charge Events - C Series

Shot No.	Number of Charges	Explosive	Planned Charge-Burial Depth (ft)	Charge Spacing (ft)	Delay (sec)
C-1	5	AANS[a]	18	32	0
C-2	5	AANS	20.4	25	0
C-3	7	AANS	23.5	18	0
C-4	5	AANS	20.4	25	0.050
C-5	5	AANS	20.4	25	0.025
C-6[b]	10	AANS	20.4	25	0

(a) Aluminized ammonium nitrate slurry (TD-2).
(b) Double row, 39 ft between rows.

TABLE III

Summary of Side-Hill Cuts - D Series

Shot No.	Explosive	Charge	Charge Weight (lbs)	Planned Charge-Burial Depth (ft)	Charge Spacing (ft)	Delay (sec)
D-1	ANFO[a]	A	300	13	10	None
		B	700	17.5	13	
		C	1200	20.5	14	
		D	1700	23.0	15	
		E	2000	23.5	16	
		F	2000	23.5	15	
		G	1200	20.5	12	
		H	500	16.0	9	
		I	200	11.0		
D-2	AANS (TD-1)	5 ea	2000	18	32	None
D-3	AANS (IR-10)					
	Uphill row(a)					
		6 ea	4000	25	35	None(b)
	Downhill row(a)					
		6 ea	2000	19	35	None(b)

(continued)

Table III continued

Shot No.	Explosive	Charge	Charge Weight (lbs)	Planned Charge-Burial Depth (ft)	Charge Spacing (ft)	Delay (sec)
D-4	AANS (TD-1) Uphill row(c)	A	2000	20	27	None(d)
		B	4000	25	28	"
		C	4000	28	25	"
		D	4000	28	25	"
		E	4000	28	26	"
		F	4000	26	29	"
		G	4000	25	33	"
		H	4000	24	35	"
		I	4000	24	35	"
		J	4000	24	33	"
		K	4000	25	33	"
		L	4000	24	36	"
		M	4000	22	35	"
		N	2000	18	--	"
	Downhill row(c)	A	2000	18	26	None(d)
		B	2000	18	28	"
		C	2000	21	24	"
		D	2000	21	22	"
		E	2000	22	22	"
		F	2000	21	25	"
		G	2000	19	27	"
		H	2000	19	29	"
		I	2000	18	29	"
		J	2000	19	27	"
		K	2000	19	24	"
		L	2000	22	20	"
		M	2000	23	19	"
		N	2000	23	19	"
		O	2000	23	19	"
		P	2000	23	20	"
		Q	2000	22	21	"
		R	2000	21	--	"

(a) Spacing between rows was 40 ft.
(b) Downhill row detonated 0.25 sec before uphill row.
(c) Spacing between rows was 46 ft.
(d) Downhill row detonated 0.141 sec before uphill row.

Background

Charges were detonated in an interbedded sandstone-and-shale medium. Air-blast measurements have been made on many single-charge chemical-explosive detonations, including shots in both dry soils[1-7] and dry rocks.[8-10] There have been no earlier airblast measurements on single charges detonated in sandstone or dry shale; and, while single-charge cratering explosions have been fired in wet shale,[11] no airblast measurements were made. TNT was used on all the cratering shots in soil for which airblast measurements were made, except for three shots in the CAPSA series,[7] where nitromethane was used. TNT was used for two of the three single-charge series in rock[8, 9] and nitromethane for the third.[10] Records from all measurements on single-charge shots except TUGBOAT[12] show waveforms consisting of a ground-shock-induced pulse followed by a gas-venting pulse, which is in turn followed by a negative phase. The interval between the two positive pulses characteristically lengthens with increased burial depth for a given medium, and, at greater burst depths where the interval is long, pressure may make a brief excursion below ambient between pulses. The interval is also medium-dependent and is relatively longer for media in which gas venting occurs relatively late. Peak overpressures of both pulses decrease with increased charge burial depth, the gas-venting peak decreasing more rapidly until, at depths at which gases are contained, there is no gas-venting pulse but only a ground-shock-induced pulse. In the Project TUGBOAT single-charge detonations[12] (and as noted later, some multiple-charge detonations in wet media), no gas-venting pulse was observed. It is presumed that the gas cavity, instead of venting early, continued to expand within a vertical column of ejecta until, when venting finally occurred, the cavity volume was so large that cavity pressures had dropped to nearly ambient. TUGBOAT was different in one other respect from previous cratering shots on which airblast measurements had been made in that aluminized ammonium nitrate slurry (AANS) was used. While the gas-venting pulse may also depend on the type of explosive, it is worth noting that in the case of nitromethane, strong venting pulses were observed on shots in both dry soil[7] and dry rock[10] but were absent from multiple-charge shots in saturated shale.[13-14] Figure 1 shows that for shots in dry alluvium,[7] nitromethane produces both ground-shock-induced and gas-venting peaks larger than for equal amounts of TNT.

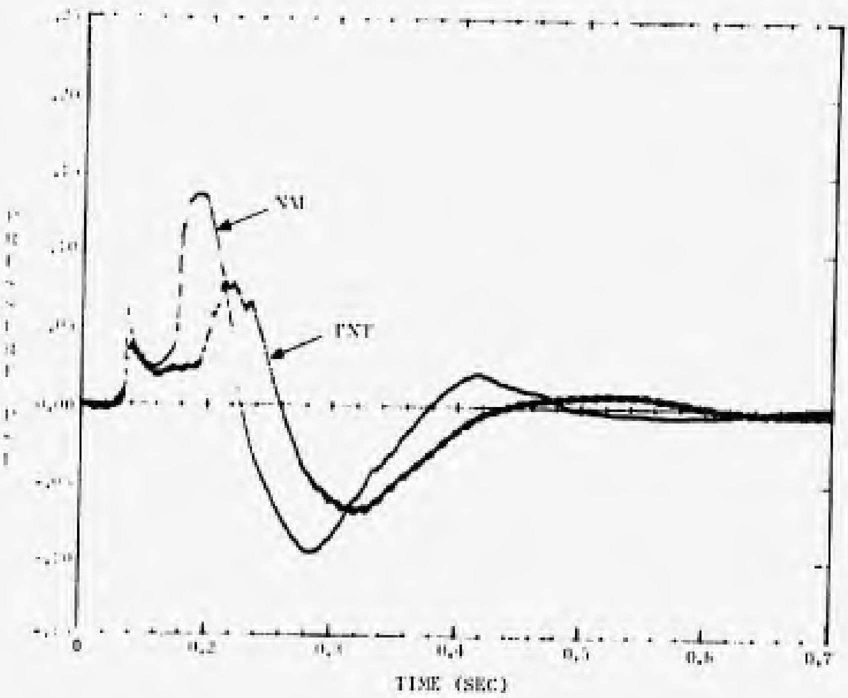

Figure 1. Airblast measured 140 feet from 1000-pound charges of nitromethane and TNT buried 12.5 feet deep

Airblast has been measured on TNT row charges in soil[15] and on nitromethane row charges in basalt[16] and wet shale.[13] The latter two, with the same explosive, one in a dry and one in a wet medium, respectively display the presence and absence of the gas-venting pulse noted earlier. Thus, a small or absent gas-venting pulse may be a characteristic of shots in water and saturated materials.

Attempts to relate airblast parameters to the number of charges[15] show that the ratio of airblast from a row charge to that from a single charge takes the form n^{α}, where n is the number of charges and α is dependent on azimuth, charge burial depth, spacing between charges, medium, and possibly on type of explosive. Measurements from the Project TRINIDAD row charges will permit evaluation of α for different explosives in a new medium together with different combinations of charge burial depth and spacing. Obviously, where a function is dependent on as many as five variables, it will take measurements on many series before the dependencies can be defined.

The TRINIDAD project included a series of surface and near-surface charges of AANS. Figure 2 shows a pressure-distance relationship cube-root-scaled to a 2000-pound charge, based on the references given below. Information from each source has been extrapolated to lower overpressures, as indicated by dashed extensions on the curve.

a. Kirkwood-Brinkley theoretical free-air curve for cast TNT[17] with linear extrapolation beyond 1.35 psi at the rate of the lowest overpressures calculated.

b. A similar but more recent calculation to lower overpressures.[18]

c. A surface-burst curve based on (a) and the 2W theory (perfect reflection assumed).

d. A measured surface-burst curve for hemispherical charges of cast TNT.[19]

e. Measurements made on surface bursts of various sizes of hemispherical ANFO charges.[20,21]

Figure 2 shows that the larger hemispherical ANFO charges produce peak overpressures equal to or slightly less than those produced by hemispherical charges of cast TNT.

There is no known reported airblast experience with aluminized ammonium nitrate slurries.

Instrumentation

Gages ·re either Statham unbonded strain gages, Dynisco bonded strain gages or Pace P-7 ·iable-reluctance gages. Signals were telemetered from the stations to the Corps ot .ngineers field office, where they were recorded on seven-track

Winston Research Corporation P-4000 tape recorders. Visicorder records were played back in the field to make possible field adjustment for expected pressures based on actual measurements.

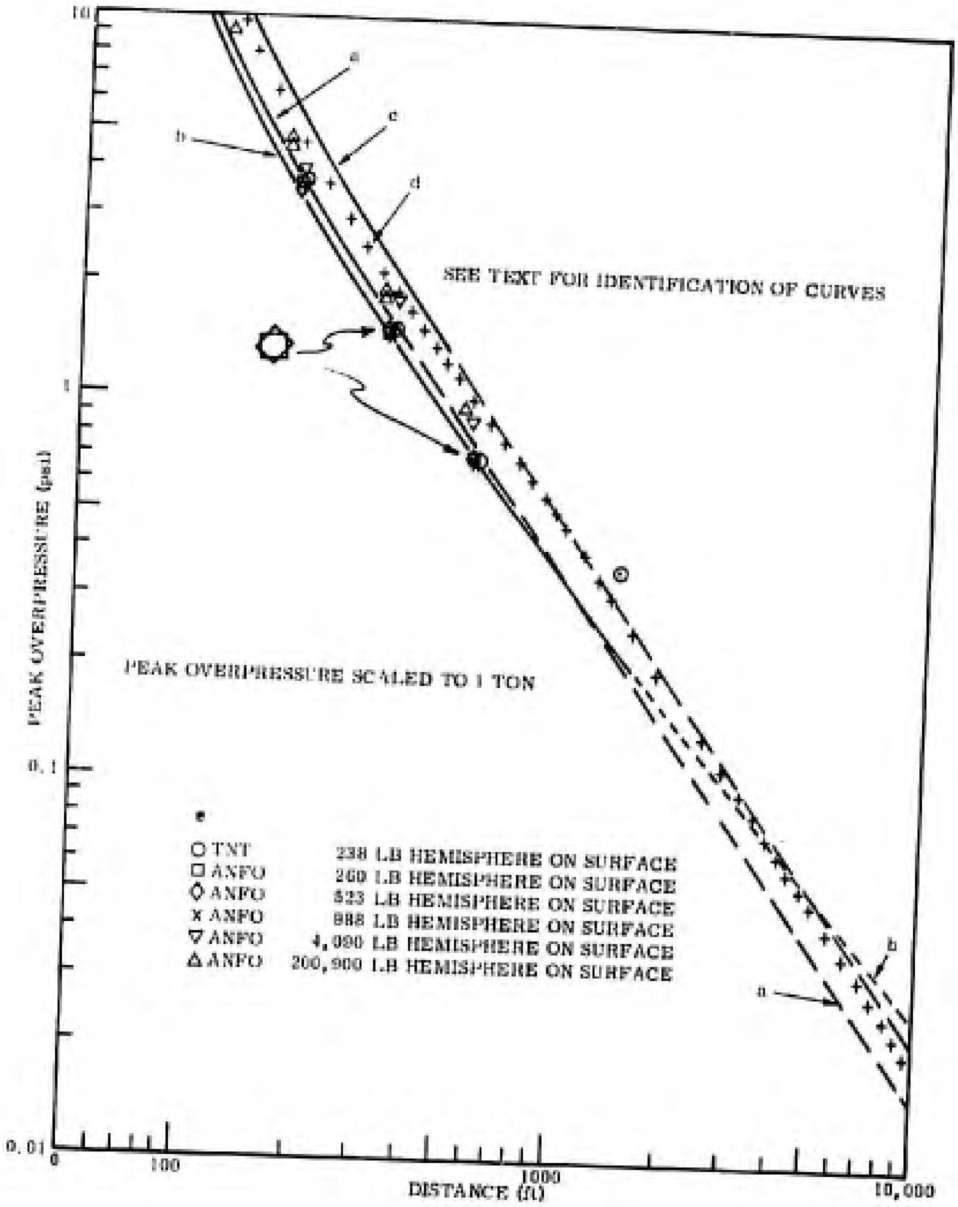

Figure 2. Peak overpressure vs distance for one-ton free air and surface bursts of TNT and ANFO

Plan of Measurements

The number and location of stations varied according to the complexity of a shot and the peak overpressures expected. For Shots B-1 to B-8, pressures were measured at three close-in stations ranging from 140 to 2000 feet. On all shots, the distances at which measurements were made were chosen to match the amplitude capability of gages in a particular canister, so as to minimize work in the field. On Shots B-10 to B-13, where higher overpressures were expected, the three close-in stations were augmented by stations at Sopris, Piedmont, Jansen, and Trinidad. Stations at Trinidad and Jansen had the primary objective of documenting overpressure for legal purposes in the event of claims for blast damage.

Stations at Trinidad and Jansen were retained on shots of the C series. On the simultaneous detonations, three stations were located off one end of the rows. For nonsimultaneous detonations, two stations were located perpendicular to the rows and two stations off each end of the rows.

On the D series, the stations at Trinidad and Jansen remained. On Shot D-1, two stations were placed perpendicular to and on each side of the row, to record terrain effects both uphill and downhill from the side-hill cut. Two stations were located off one end of the row in a direction approximately 90° from the azimuth to Jansen and Trinidad. On Shots D-2, D-3, and D-4, two stations were located perpendicular to the rows and three stations off the ends of the rows. The latter three were opposite the end of the row closest to Jansen and Trinidad; this was made necessary by terrain limitations on station locations.

Expected Peak Overpressures - B Series

Since there was no past experience on airblast measurements in a sandstone-shale medium, and little experience with this type of explosive at the planned charge burial depths, predictions were made on the basis of airblast from TNT charges buried in a variety of media. The following expressions had been derived[22] from data from past explosions for ground-shock-induced and gas-venting peak overpressures, and for positive-phase impulse as a function of range and charge burial depth based on buried charges detonated in a variety of media.

Ground-shock-induced peak overpressure:

$$\Delta p = \frac{5\left(\frac{r}{W^{1/3}}\right)^{-1.05}}{10 \exp\left[0.6\left(\frac{DOB}{W^{1/3}}\right)\right]} \tag{1}$$

Gas-venting peak overpressure:

$$\Delta p = \frac{70\left(\frac{r}{W^{1/3}}\right)^{-0.93}}{10 \exp\left[1.5\left(\frac{DOB}{W^{1/3}}\right)\right]} \tag{2}$$

Positive-phase impulse:

$$I = \frac{15\left(\frac{r}{W^{1/3}}\right)^{-0.5}}{10 \exp\left[0.56\left(\frac{r}{W^{1/3}}\right)^{0.17}\left(\frac{DOB}{W^{1/3}}\right)\right]} \tag{3}$$

DOB is the charge-burial depth in feet, r the horizontal distance from the epicenter in feet, Δp the peak overpressure in pounds per square inch, and I the scaled positive-phase impulse in psi-msec.

At a scaled distance of 5 ft/lb$^{1/3}$, or 63 feet from a 2000-pound charge, the above expressions give the peak overpressures shown in Fig. 3 as a function of scaled charge-burial depth. Figure 3 and an R^{-1} distance attenuation rate lead to the predictions of Table IV for the single-charge series. Predictions for Shots B-10 through B-13 are based on the surface-burst data of Fig. 2. Peak overpressures for the 14-inch-diameter unstemmed hole could only be predicted as being more than those of completely stemmed Shot B-6, and less than those of a surface burst. The large uncertainty was accommodated by using two double-gage canisters at two stations, with each canister covering two overlapping factors of 20 above peaks measured in Shot B-6.

Results - B Series

The results of the measurements of the B series are summarized in Appendix A, Tables A-1 through A-14. The data from these tables have been plotted vs distance in Figs. 4 through 11. Reproductions of pressure-time records and their integrals constitute Appendix B.

Subsurface Bursts, B-1 through B-8

Quality of Records -- No records were obtained for Station 1 on Shot B-2, or Station 2 on Shot B-7. Records for Station 2 on Shot B-2 and Station 1 on Shot B-7 were noisy. Peaks were limited on the low-range gage at one station on four shots and at two stations on one shot. Where peaks were on the high side of the uncertainty spanned by high- and low-range gages, it was anticipated that the low-range (high-sensitivity) gage would be overranged. The low-range gage used in Canister 6 on four of the shots apparently received mechanical damage between calibration and shot time, resulting in a very poor response characteristic, indicative of extraneous mechanical or acoustic damping. Records obtained by this gage show slow rise times, low, rounded peaks, and generally smaller impulses than by its companion high-range gage.

All other records obtained on the B series were quite good.

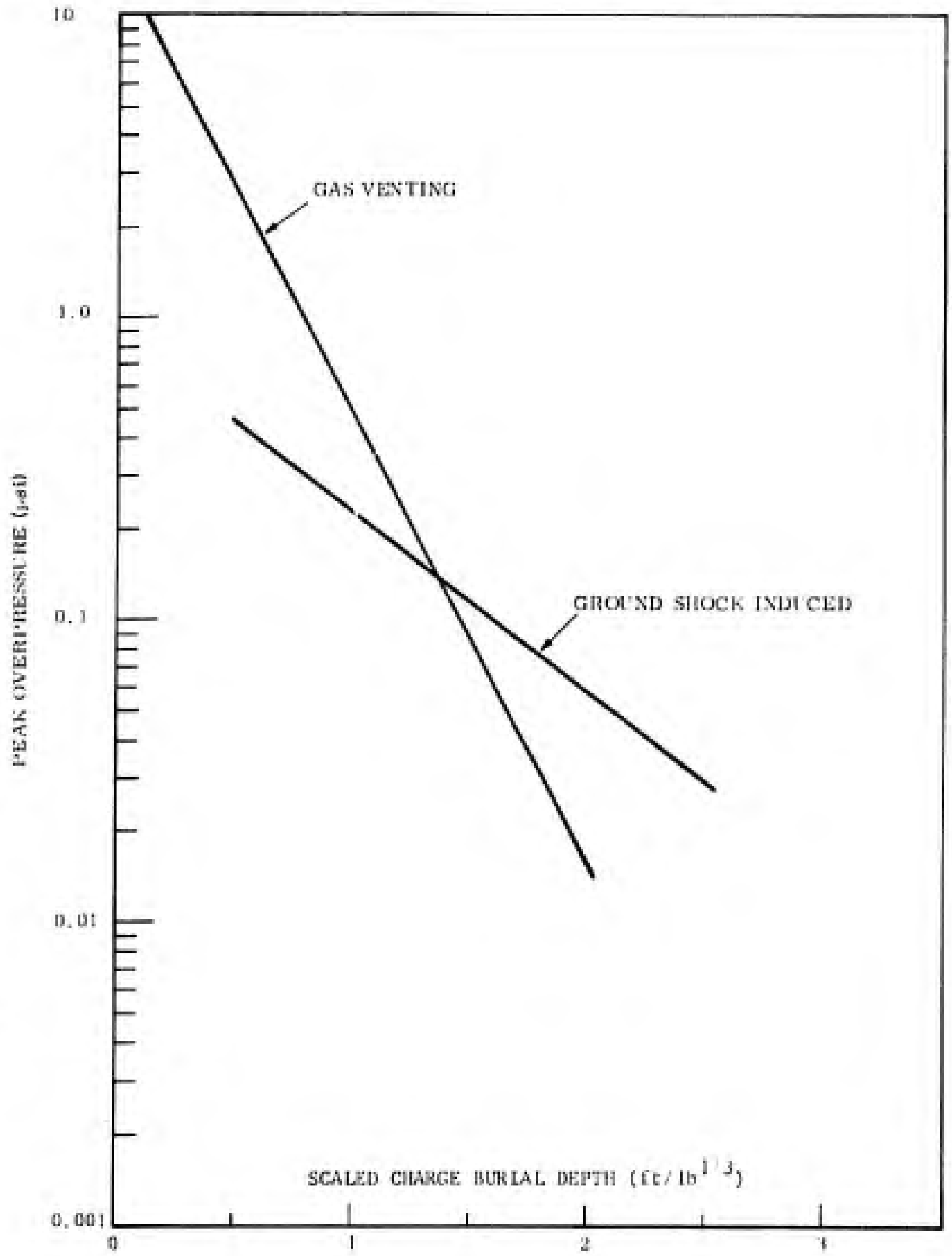

Figure 3. Peak overpressure as a function of scaled burial depth at a scaled distance of 5 $ft/lb^{1/3}$

TABLE IV

Expected Peak Overpressures

Shot No.	Scaled Burial Depth ($ft/lb^{1/3}$)	Expected Overpressure (psi) At 63 ft	At 630 ft*
B-1	1.27	0.20	0.02
B-2	1.43	0.13	0.013
B-3	1.39	0.10	0.01
B-4	1.27	0.20	0.02
B-5	1.51	0.11	0.011
B-6 (B-14)**	1.71	0.09	0.009
B-7	1.90	0.065	0.0065
B-8	2.22	0.045	0.0045
B-9	Cancelled		
B-10	-0.30	15	1.5
B-11	-0.15	15	1.5
B-12	0	10	1.0
B-13	0.15	9	0.9
B-14 (B-15)**	1.71	>0.09+	>0.009

* Assumes attenuation with distance of R^{-1}.

** Shot B-14 became B-15 and a shot like B-6 became B-14.

\+ Larger than B-6 because of 14-inch unstemmed hole.

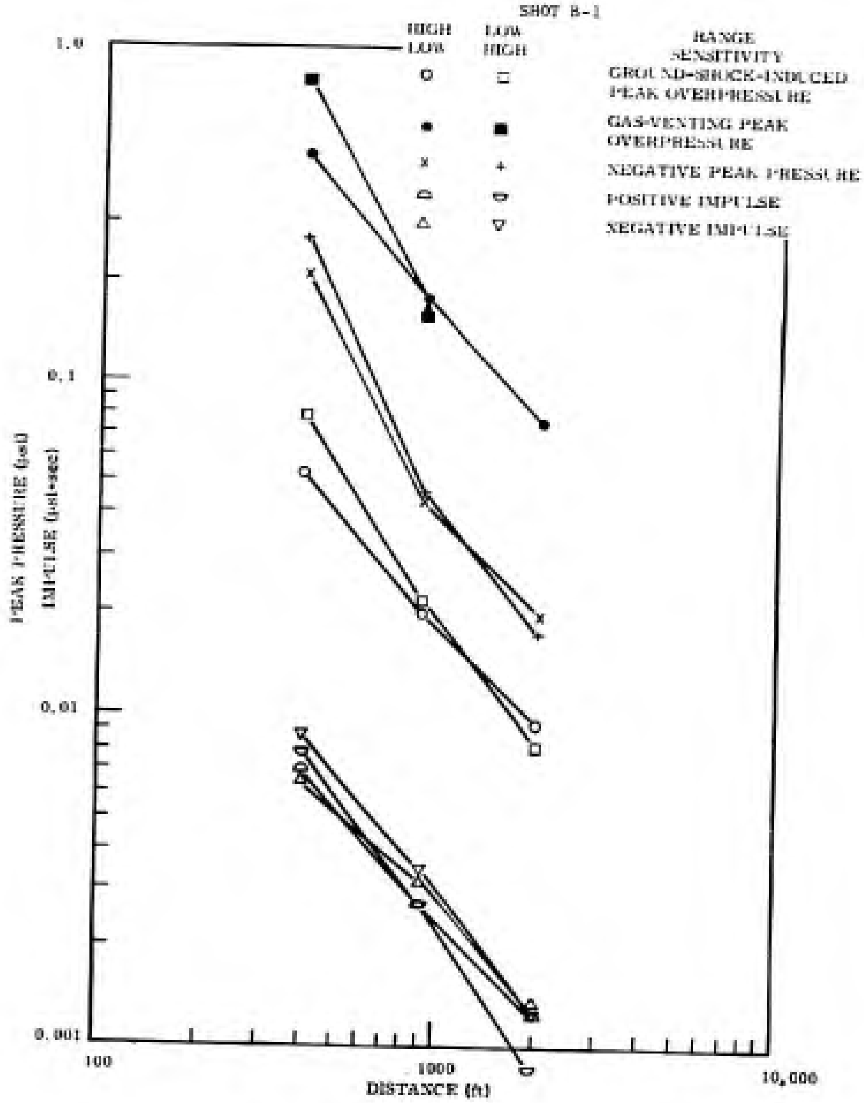

Figure 4. Airblast vs distance Shot B-1

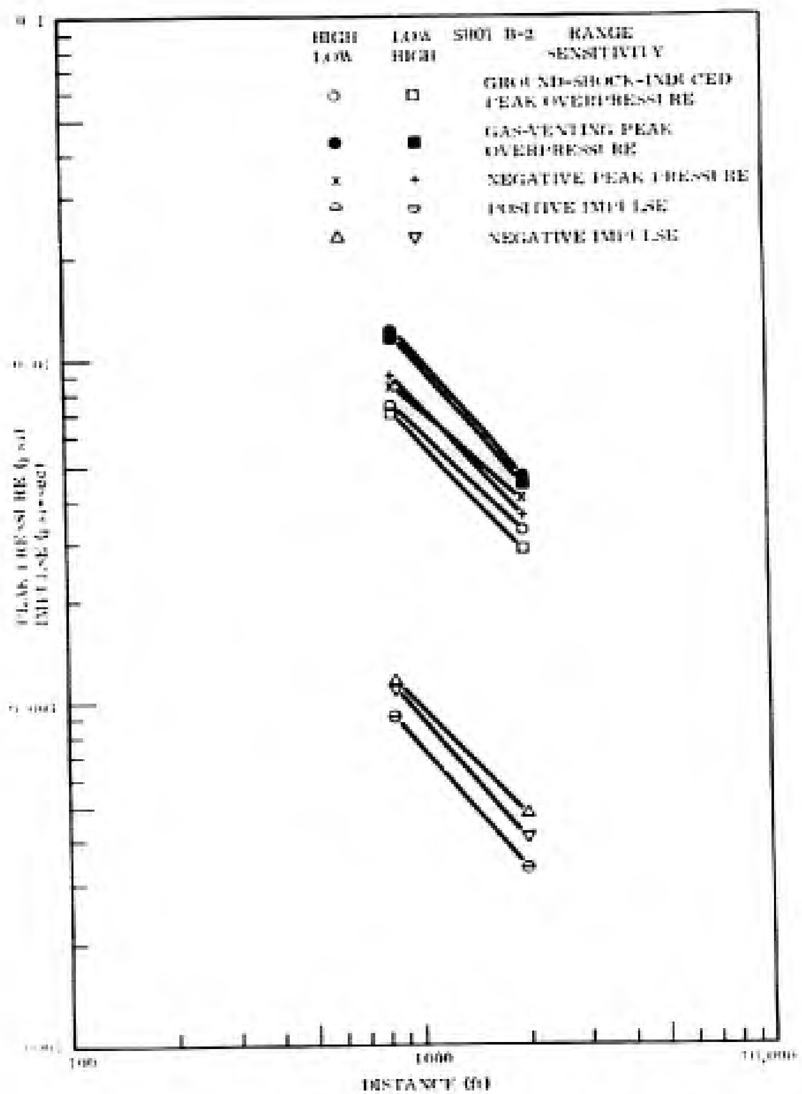

Figure 5. Airblast vs distance Shot B-2

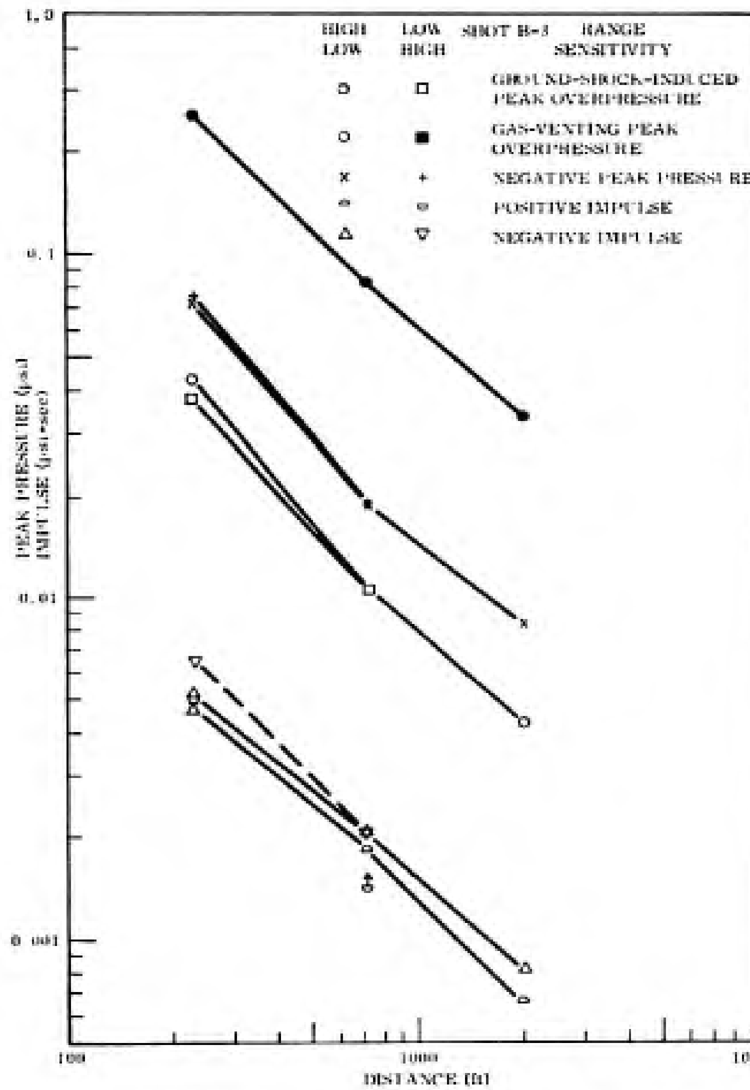

Figure 6. Airblast vs distance Shot B-3

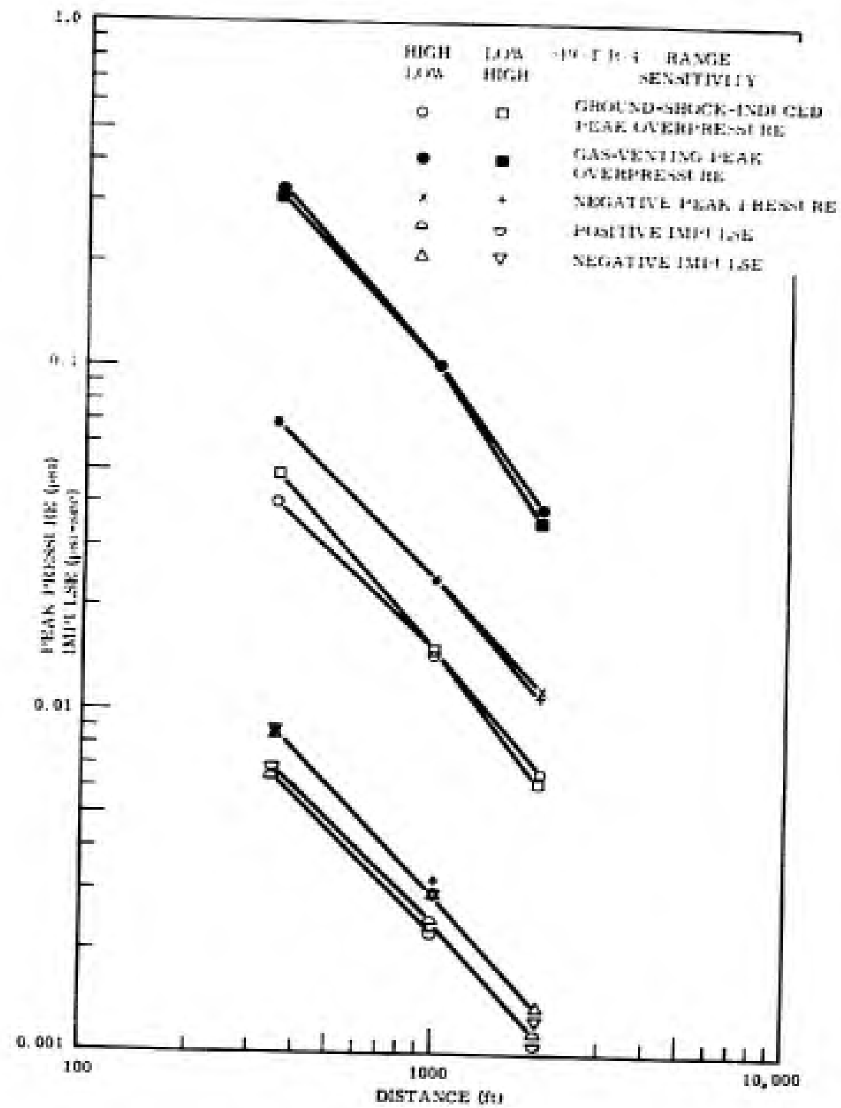

Figure 7. Airblast vs distance Shot B-4

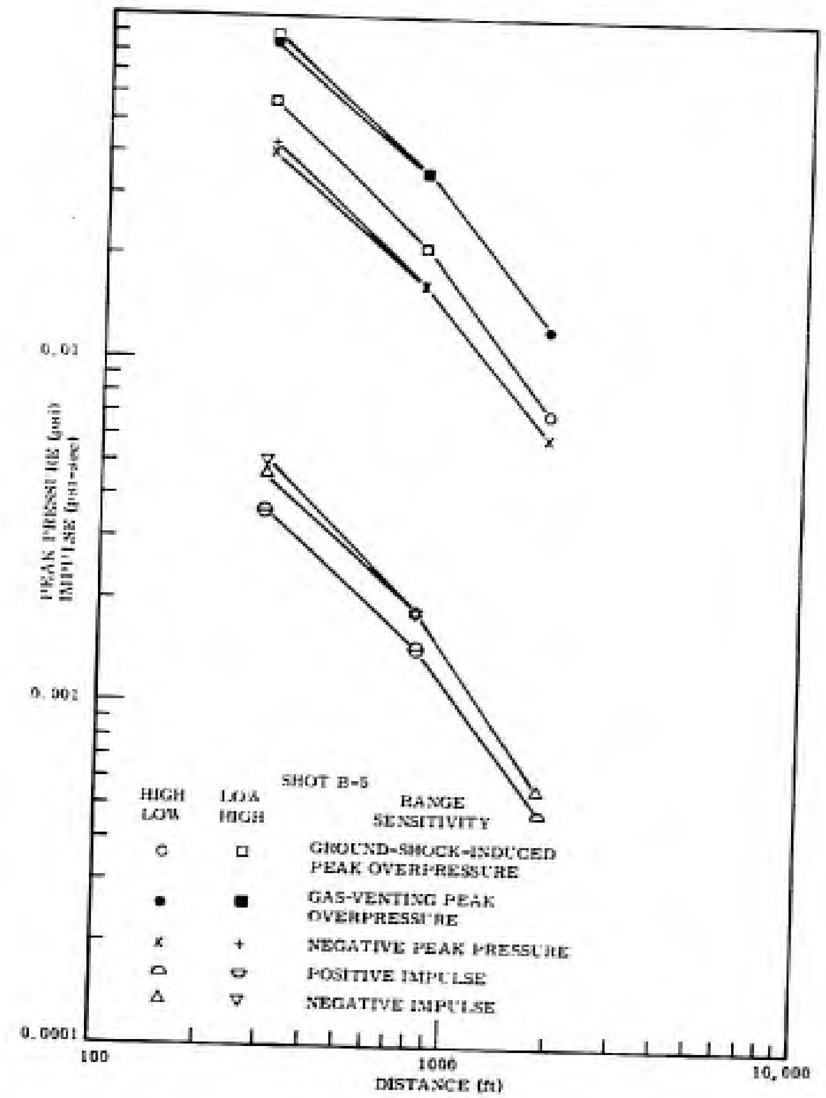

Figure 8. Airblast vs distance Shot B-5

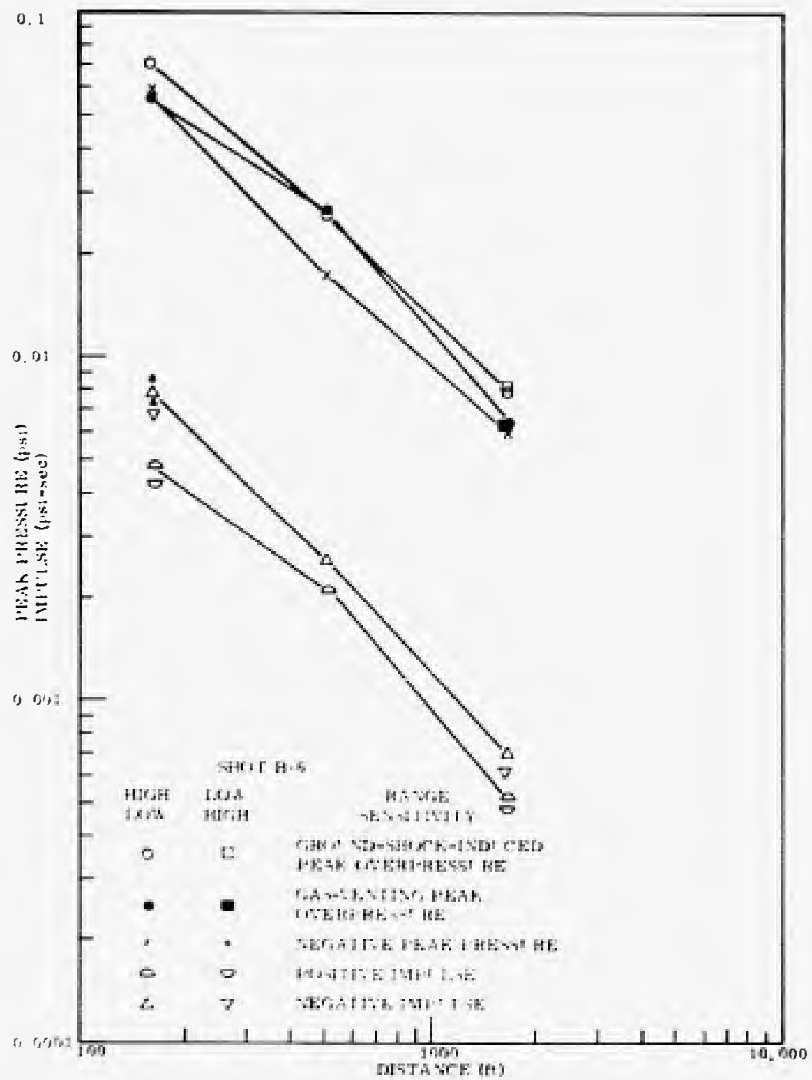

Figure 9. Airblast vs distance Shot B-6

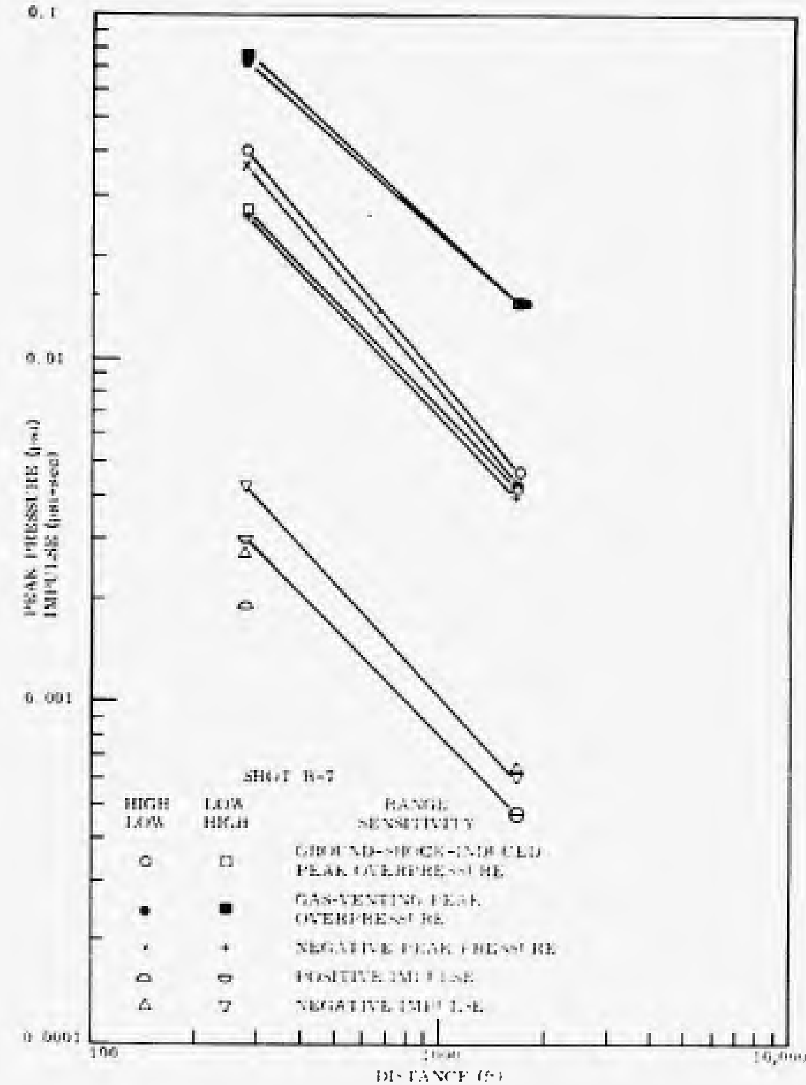

Figure 10. Airblast vs distance Shot B-7

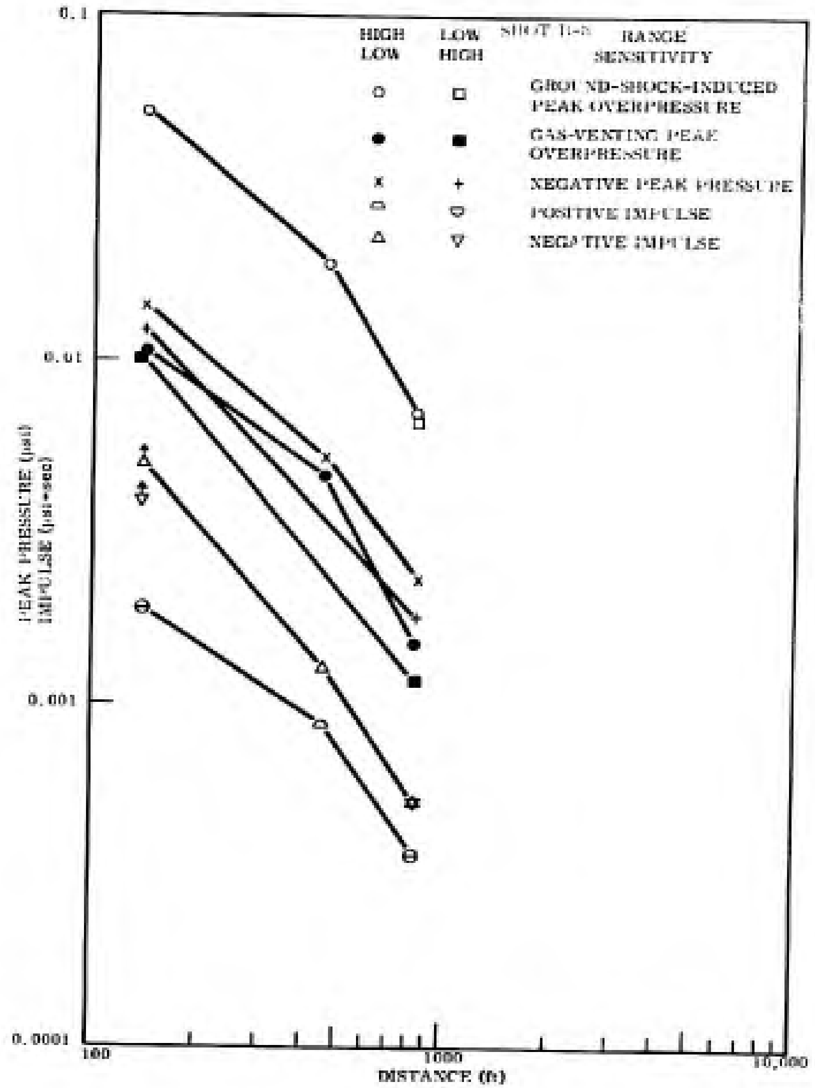

Figure 11. Airblast vs distance Shot B-8

Wave Shape -- Characteristic wave shapes included a ground-shock-induced pulse and a gas-venting pulse separated by an interval that increased with increased burial depth. For all but the deepest shot, the gas-venting pulse had a larger amplitude than the ground-shock-induced pulse. For the shallowest ANFO shot, the gas-venting pulse followed the ground-shock-induced pulse so closely that it is not possible to be certain that there are two separate pulses.

Ground-Shock-Induced Peak Overpressures -- For comparison, the ground-shock-induced and gas-venting peak overpressures have been plotted in Fig. 12 against burial depth for interpolation between measurements for 630 feet. This is approximately the logarithmic middle of the range of measurements. The comparison in Fig. 12 illustrates three points. The ground-shock-induced peak overpressures for four of the five AANS shots were about 2.1 times the prediction based on TNT charges. The ground-shock-induced peaks from the shallowest of the ANFO shots showed about the same increase. The two deeper ANFO shots had ground-shock-induced peaks only about 15 percent above those for TNT shots.

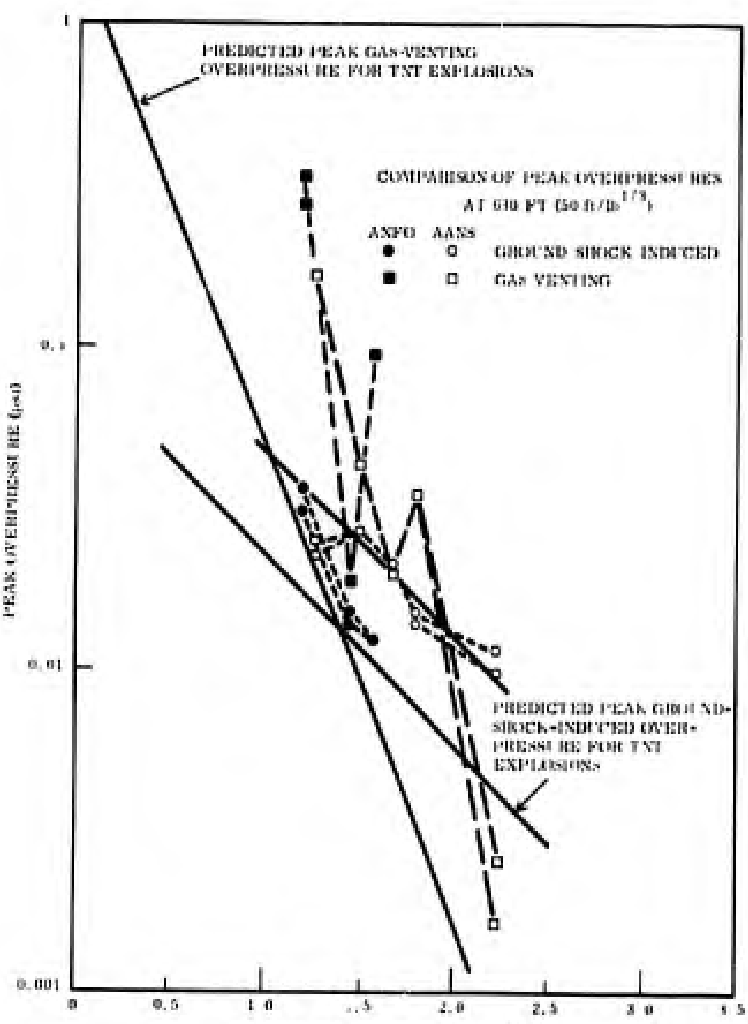

Figure 12. Comparison of measured and predicted peak overpressure

All shots were fired using detonators above ground and Primacord to the charge. On all shots, the Primacord between the detonator and the entry point into the ground was looped over a stake. The amount of Primacord above ground was equal to or greater than that below ground. On at least Shot B-6, an additional length of Primacord was coiled to one side of the epicenter. Unfortunately, on that shot, the airblast signal from the Primacord preceded the ground-shock-induced peak by about 17 msec. Because the Primacord spike originates at the epicenter and the ground-shock-induced pulse has an apparent origin at R = 2.2 DOB, the spike often is superimposed on the rise of the ground-shock-induced pulse. In most cases, it was possible to distinguish between this spike and the ground-shock-induced peak. On Shot B-1, however, the peak identified as ground-shock-induced may, in fact, be the Primacord spike; this could account for the peak being high with respect to the ground-shock-induced peaks of Shots B-2 and B-3. If such is the case, the ground-shock-induced pulse is inseparable from the gas-venting pulse, as would be the case in the event of an early stemming failure.

Gas-Venting Peak Overpressures -- Gas-venting peak overpressures for the AANS shots ranged from two to ten times the predictions based on TNT shots. The peaks for Shot B-7 appear to be high with respect to the other AANS data by about a factor of 3. The shallowest and deepest ANFO shots had gas-venting peak overpressures about ten times those for TNT shots. The other (Shot B-2) appears to be anomalous in that it had gas-venting peak overpressures only about 60 percent larger than TNT shots.

The irregularity of gas-venting peak overpressure with scaled burial depth has also been examined in terms of calculated time of venting. Venting time was calculated by assuming that: (a) sonic velocity in the medium was 6000 feet per second, (b) venting occurred immediately over ground zero, and (c) the source of the ground-shock-induced pulse was at R = 2.2 DOB. Scaled venting times have been plotted against scaled burial depth in Fig. 13. In the figure, Shot B-2 shows a low peak pressure because it vented quite late with respect to other charges. The scaled venting times for Shots B-5 and B-6 were also late compared to the others. This comparison, in contrast with that of Fig. 12, suggests that Shots B-5 and B-6 were anomalously low and that B-7 was in agreement with the other events. It is interesting to observe that the scaled venting time of Shot B-1 agrees with scaled venting times for TNT shots in basalt, whereas Shot B-2 agrees with venting times of TNT shots in alluvial soil. Most of the data indicate venting times about 60 percent of those for TNT shots in alluvial soil.

Positive-Phase Impulse -- Figure 14 shows impulse interpolated from Figs. 4 through 11 for 630 ft (50 ft/lb$^{1/3}$) compared with a prediction based on TNT shots in a variety of media. Here, too, Shot B-2 is low, suggesting a low-order detonation. Impulse for the deepest shot (B-8) is high because integration of the pressure-time record (see Appendix A) includes the contribution from a seismic wave train on which the air-transmitted pulses are superimposed. The pulses induced by the seismic wave train are less suppressed by charge burial than are either the ground-shock-induced or gas-venting pulses.

The prediction is based on a fit to airblast data from shots in several media. The variation from one medium to another in the fits to the data is greater than the scatter of six of the eight Trinidad shots about the prediction line based on the several media. The remarkable agreement between prediction and data of the six shots should increase one's confidence in coincidence.

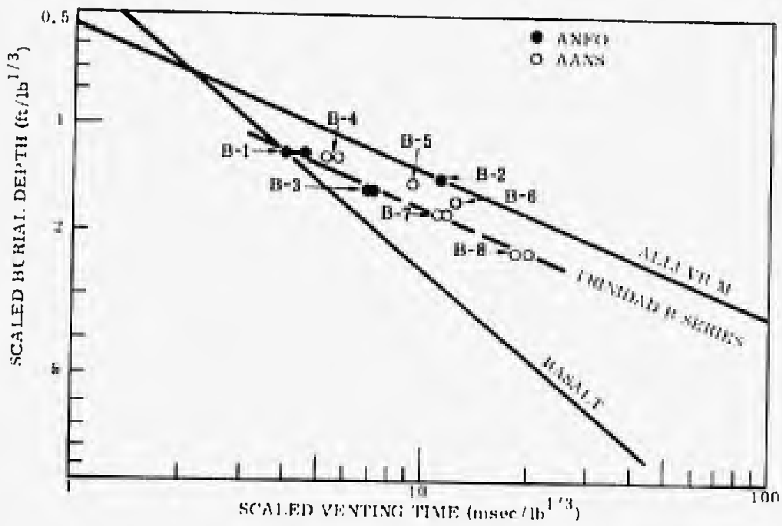

Figure 13. Scaled venting time as a function of scaled burial depth

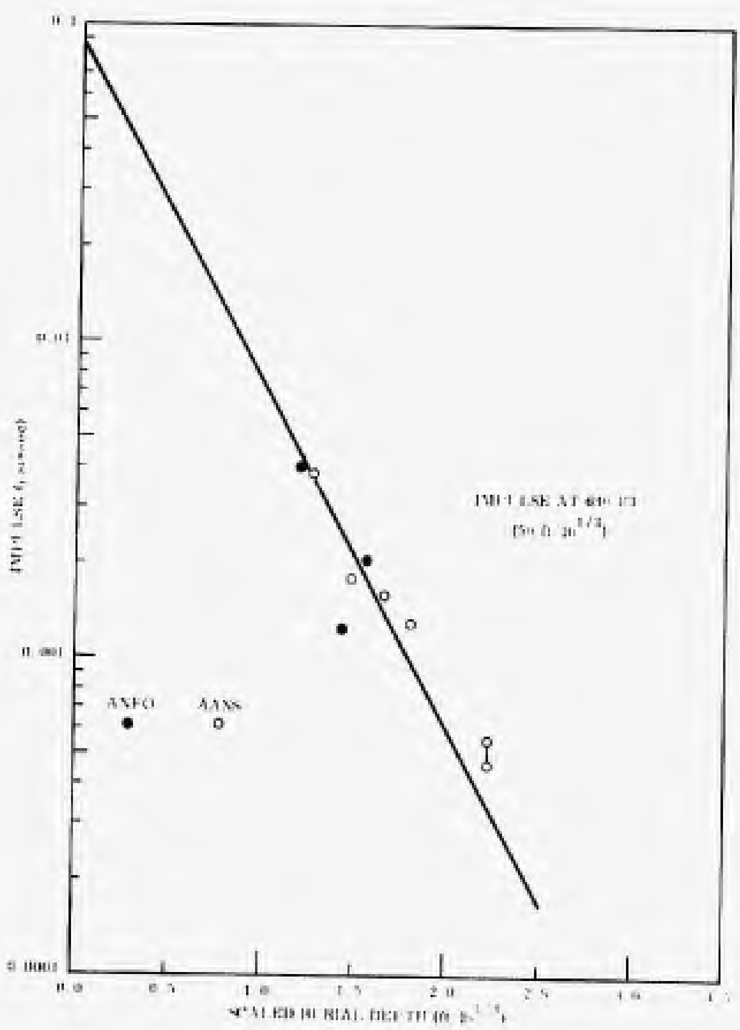

Figure 14. Comparison of measured impulse at 630 feet with prediction

Surface and Near-Surface Bursts - B-10 through B-13

Quality of Records -- Excellent records were obtained with the following exceptions. On Shot B-13, records at the Piedmont station were lost when the bleed plug on the gage canister was left open. At the Viola station, on the same shot, records on the low-range gage were lost and a poor record was obtained for the high-range gage. On the same shot, the negative peak on the high-range gage at the Jansen station was limited.

Wave Shape -- In general, the waveforms were characteristic of those of free air or surface bursts, with a sharp rise, decay into a negative phase, and recovery to ambient pressure. One notable characteristic was the increase in rise time with distance, the close stations having very short rise times and the more distant station at Trinidad having rise times approaching 100 milliseconds.

On Shot 11 a focus was recorded at Trinidad. Some suggestion of a refracted signal may appear at Piedmont, where a weak pulse follows the principal sinusoidal pulse by almost 1 second. At Jansen, the refracted pulse is almost identical with the pulse transmitted along the ground, and follows it by 0.8 second. At Trinidad, the pulse transmitted along the ground has become very weak and arrives at about 30 seconds. The focus from higher paths begins about 0.5 sec later and appears as a sinusoidal pulse with a strong spike superimposed on the later portion of the positive phase.

One other unusual characteristic appeared in the waveform measured at Station 2 on Shot B-12, where the negative phase ends abruptly with a sharp rise in pressure. A similar abrupt rise was observed on B-13 at Stations 1 and 2, and something of its character can still be seen in the rapid recovery from negative pressures at the Sopris station.

Peak Overpressures -- Peak overpressures are plotted versus distance in Fig. 15. At the three closest stations, differences between the four shots were relatively small. Because of atmospheric effects on attenuation with distance, differences increase significantly beyond 4000 feet.

Peak overpressures for a TNT hemisphere from Ref. 19 have been scaled to the Project TRINIDAD altitude and for the average temperature of the four events, and are shown in Fig. 15 as a line of plus signs. At the two closest stations, the results show good agreement with the TNT results. At the Sopris station and beyond, the order had changed somewhat, and the deepest shot, B-13, gave the highest peaks. Those for the surface burst, B-12, were below the peaks of B-13, and below those of the TNT hemisphere surface burst at the Sopris station and beyond. The pressures for the tangent surface shot (B-11) were below those of B-13 by a factor of 2 or more. A very high peak developed at Station 2 on B-12 due to an exceptionally sharp spike.

Positive-Phase Impulse -- Positive-phase impulses versus distance are compared for the four shots in Fig. 16. Positive-impulse data for TNT hemispherical charges have been added to Fig. 16 from Ref. 23. Differences between positive impulses of all shots and the TNT hemispheres are not great, although there is a tendency for the impulses to be smaller than for TNT hemispheres. Of the four shots, impulses for the deepest shot, B-13, were smallest at the closest stations and greatest beyond 9000 feet.

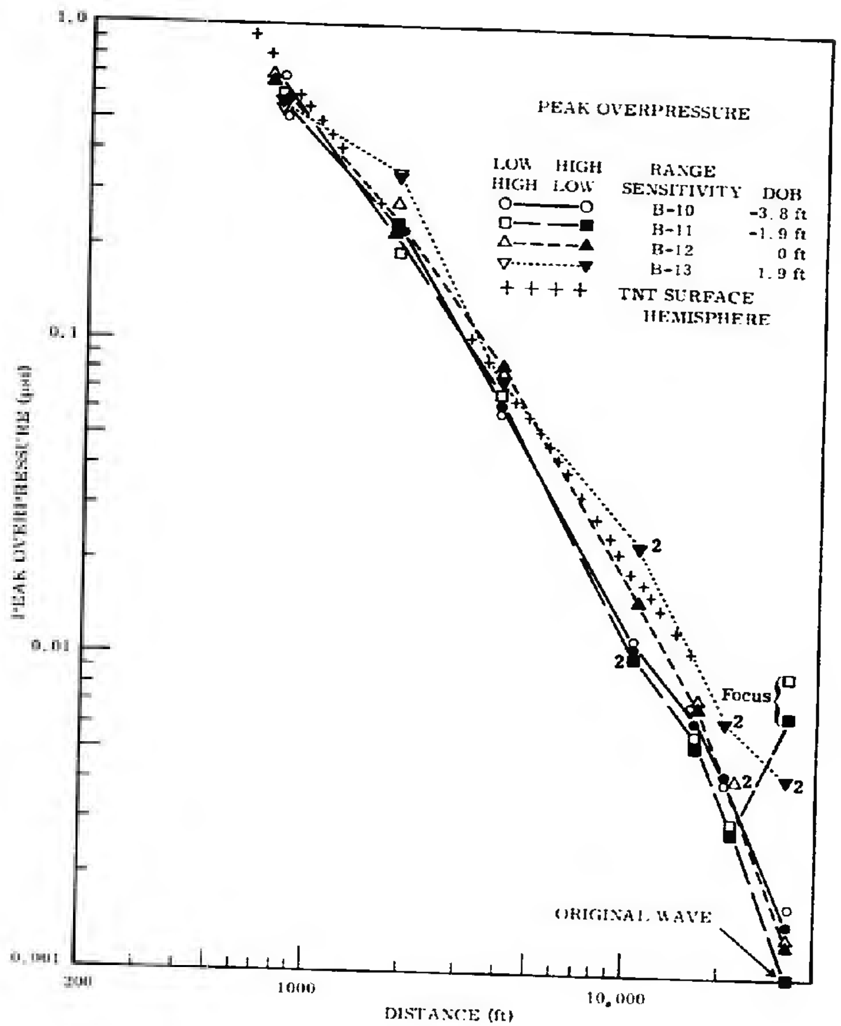

Figure 15. Peak overpressures vs distance, Shots B-10, B-11, B-12, and B-13

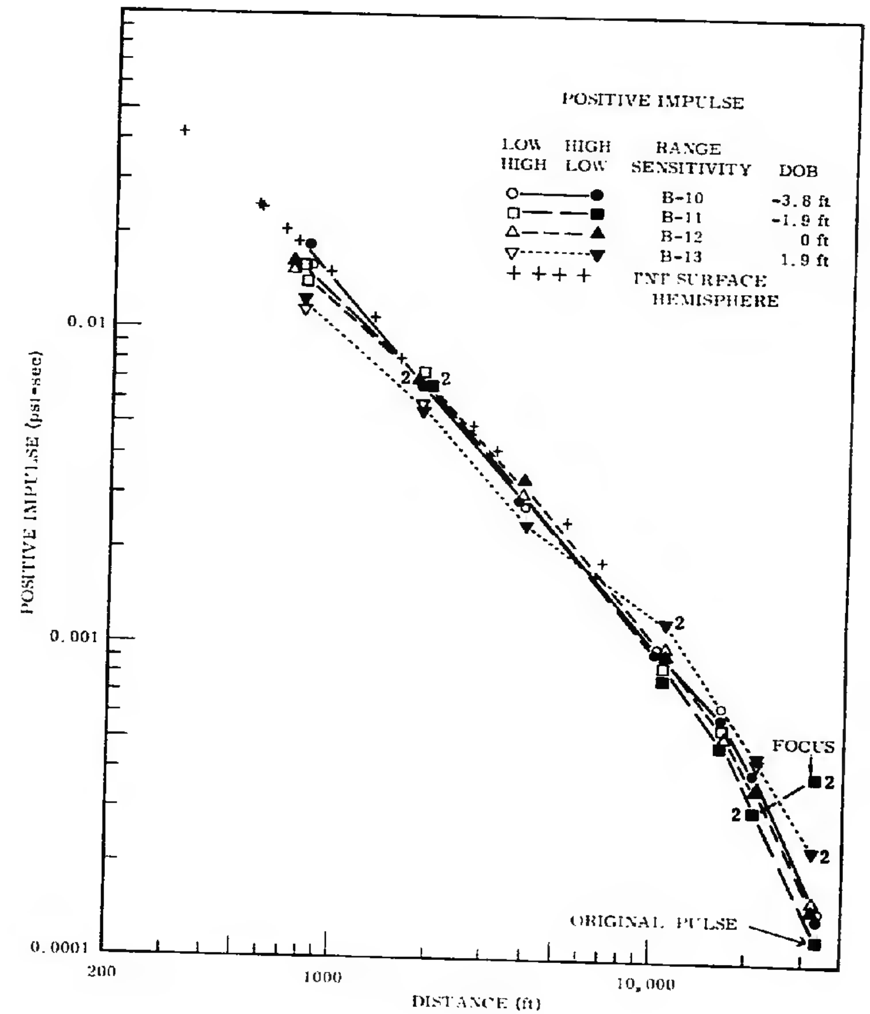

Figure 16. Positive impulse vs distance, Shots B-10, B-11, B-12, and B-13

The data show that atmospheric effects on attenuation exert a more significant influence on airblast than do small differences in depth or height of burst.

Focus -- No meteorological measurements other than surface temperature and wind direction and velocity were made; hence the effects on blast propagation of other meteorology must be presumed or deduced. Surface temperature was 37°F when Shot B-11 was fired, and surface-wind velocity was NE at 13 mph, or about 15 ft/sec in the direction of propagation toward Piedmont, Jansen, and Trinidad.

On all shots, rates of attenuation with distance increase for pressure (Fig. 15), impulse (Fig. 16), and energy (Fig. 17) beyond the Piedmont station. This is characteristic where a temperature gradient exists, with warmer temperatures at the ground, as is common for the season and time of day when these shots were fired.

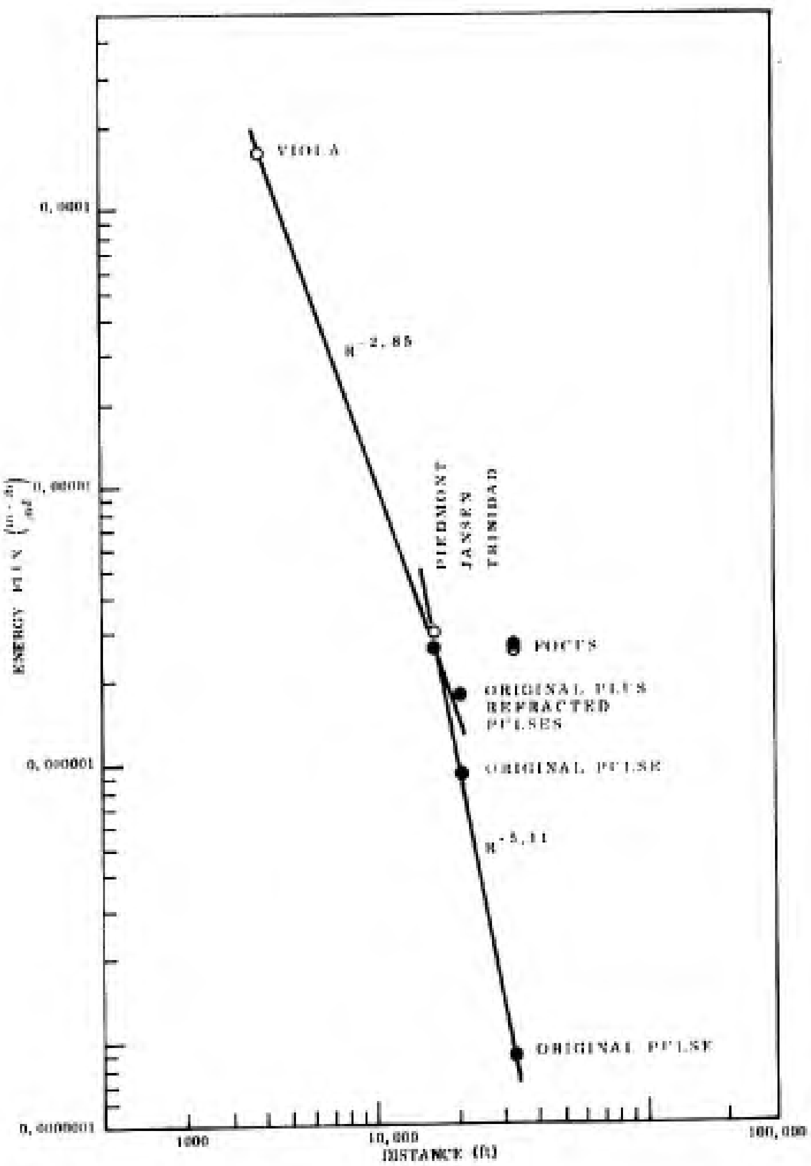

Figure 17. Energy flux vs distance for Shot B-11

Between Viola and Piedmont, the rate of attenuation for peak overpressures was $R^{-1.78}$, and for positive impulse was $R^{-1.23}$. From Piedmont to Trinidad, the rates were $R^{-2.53}$ and $R^{-2.15}$ respectively for the original pulse. The peak overpressure measured at Trinidad in the focus was 6.7 to 9 times that in the wave transmitted directly along the ground. The positive impulse in the focus pulse was about 3 to 3.5 times greater.

Attenuation of energy with distance presents an interesting change in rate, as illustrated in Fig. 17, which shows energy per unit area versus distance. Energy was attenuated at $R^{-2.85}$ to Piedmont but at $R^{-5.3}$ beyond. The refracted pulse at Jansen had energy nearly equal to that of the original pulse and, considering total energy, extends the $R^{-2.85}$ attenuation to Jansen. The energy per unit area in the focus at Trinidad was about 30 times that in the original wave propagated along the ground, and about 5 times that which would have been observed if attenuation to Trinidad had continued at $R^{-2.85}$.

Since neither temperature nor winds above the surface were determined, no precise source for the refracted wave can be isolated. An estimate using standard atmosphere conditions suggests refraction from an altitude of about 3000 feet above the ground.

<u>Bursts in Equivalent Stemmed and Unstemmed Holes - B-14 and B-15</u>

Shot B-14 was converted from an unstemmed shot to a stemmed shot and Shot B-15 was added to the series as the unstemmed experiment. It was detonated at the bottom of a 14-inch-diameter unstemmed hole. The burial depth was the same as for stemmed Shots B-6 and B-14. Since there was no prior experience on which to base pressure predictions for Shot B-15, a wider range of uncertainty had to be accommodated. Peak overpressures were expected to lie somewhere above those of an equivalent stemmed shot and below those of an equivalent surface burst. To accommodate the larger uncertainty for Shot B-15, canisters were removed from Sopris and Piedmont to provide dual canisters at Station 1 and Viola. The high-range and low-range canisters each contained two gages, and each pair covered a high and a low range. Because measured pressures were about midway between upper and lower limits, records were obtained by all four gages.

<u>Quality of Records</u> -- On Shot B-14, no information was obtained from the Jansen station. Records obtained from Station 1 were very noisy. At the Trinidad station, an approximately 30-Hz signal was recorded on the carrier. In addition, the record at Trinidad was poor because the low amplitude of the blast wave resulted in a very low signal-to-noise ratio.

On Shot B-15, no record was obtained by the high-range gage at Station 2. At Station 1, the high-range canister (No. 2) gave values consistently lower than the low-range canister (No. 9) by about 15 percent. Values for both gages in the high-range canister were consistent with each other, as were both gages in the low-range canister. No failures in calibration or equipment could be found to account for the difference, leading one to suspect that the low values for the high-range canister resulted from human error, most probably failure to remove the cloth tape used for weather protection over the canister intake port.

All other records on the two shots were good.

Wave Shape -- On the deeply buried shots, the waveform consisted of a ground-shock-induced pulse followed by a gas-venting pulse. On both shots, B-6 and B-14, the ground-shock-induced peak was slightly greater than that from venting gases. The two shots were different in the time sequence of venting, however, in that the separation between the two pulses was 0.1 second for Shot B-6 and only 0.065 second for Shot B-14. Since burial depth was the same for both shots, the difference in venting time must be attributed to geological variation, even though the charges were detonated only 360 feet apart.

The unstemmed hole of Shot B-15 made it, in essence, a vertical cannon. The ground-shock-induced pulse and the "muzzle blast" occurred at the same time and are inseparable. The combination provided the dominant first peak. This early pulse was followed by a negative phase that was interrupted by the gas-venting pulse, which has been identified as the second peak. The time separation for the two peaks is about 70 milliseconds, essentially the same as for Shot B-14.

Peak Overpressures -- Peak overpressures for the stemmed and unstemmed detonations are compared in Fig. 18, which also shows peak overpressures from the surface burst, B-12. Shot B-15 peak overpressures fall approximately midway between those of the surface-bursts and the completely contained shots out to about 5000 feet. The attenuation rate is almost exactly R^{-1} over the entire range. The much more rapid attenuation of peak overpressures from the surface-burst results in the overpressures being approximately equal at the Trinidad station.

Positive-Phase Impulse -- A similar comparison of por .tive-phase impulses is made in Fig. 19. At the closest station, positive impulses from the unstemmed shot are only 50 percent greater than those of the corresponding stemmed shots. Again, because of the more rapid attenuation of the surface burst and the approximate $R^{-0.8}$ rate of attenuation for B-15, the impulses for the unstemmed event nearly equal those of the surface burst at the Trinidad station.

Energy -- The meteorology for Shots B-14 and B-15 was not appreciably different from that for the surface-bursts, Shots B-10 through B-13. The latter were fired during the first four days of the week, and Shots B-14 and B-15 on the last day of the same week. The difference in rates of attenuation in the two cases is quite pronounced, leading to the speculation that the stronger shocks of the surface-burst start with an essentially hemispherical propagation, which results in loss of peak overpressure and impulse at the greater distances as meteorology prevents uniform distribution of energy through the hemisphere. By contrast, airblast from the unstemmed shot probably propagates initially as a vertically prolate dome, with a pressure and energy gradient decreasing from top to bottom. There is probably a tendency at the longer propagation ranges for more of the energy to feed down from the upper portion into levels closer to the ground than is true at the shorter ranges.

From Table V and Fig. 20, it is clear that energy in airblast from the unstemmed hole is about a factor of 20 below that of a surface-burst, and that complete stemming provides about another factor-of-10 reduction.

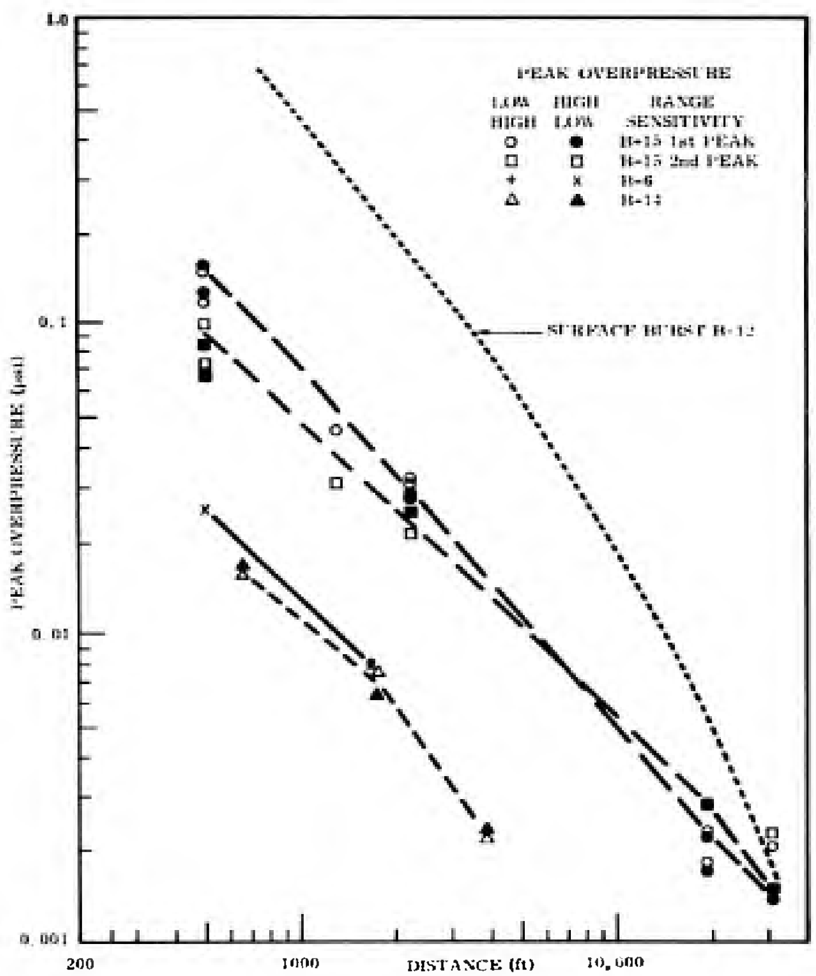

Figure 18. Peak overpressure vs distance for comparable stemmed and unstemmed detonations

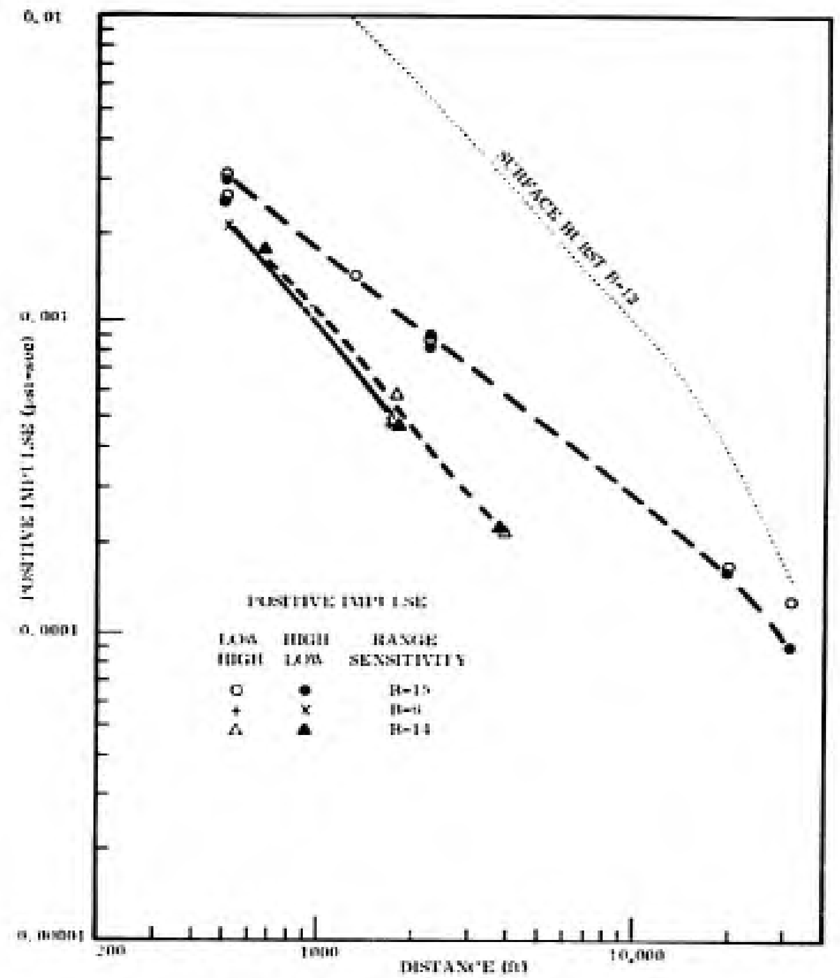

Figure 19. Positive impulse vs distance for comparable stemmed and unstemmed detonations

TABLE V

Comparison of Energy

Station →	1		Viola	
Distance ft →	500		2238	
	Percent	Equivalent Charge Weight (lbs)	Percent	Equivalent Charge Weight (lbs)
Surface Burst B-11	100	2000	100	2000
Unstemmed B-15	5	100	3.5	70
Completely Stemmed B-6, B-14	0.6	12	0.3	6

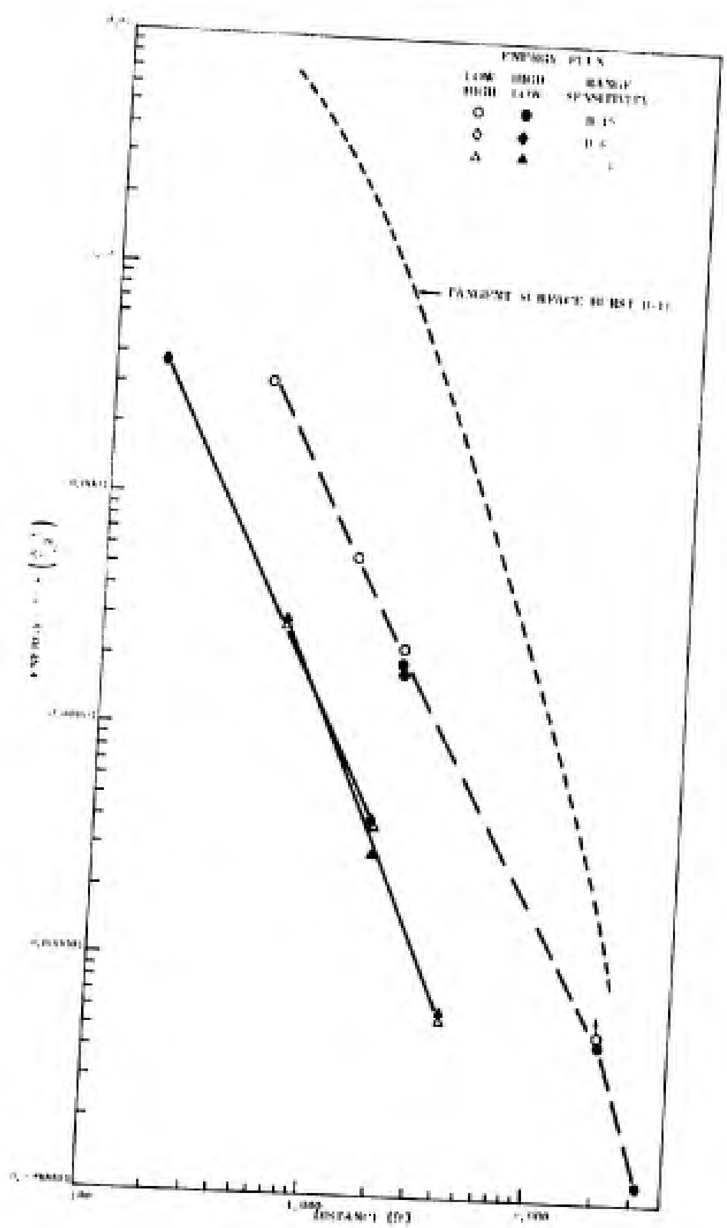

Figure 20. Energy flux vs distance for comparable stemmed and unstemmed detonations

At 500 feet, the unstemmed shot provided 8.3 times as much energy in airblast as did the equivalent stemmed shots at the same burial depth. It is impossible to apportion the energy in the airblast between the ground-shock-induced pulse, the cannon-muzzle pulse, and the gas-venting pulse.

Expected Peak Overpressures - C Series

Predictions for the C series were based on the measured results of the single-charge AANS shots of the B series.

The variation in peak overpressures for the single-charge AANS shots can be embraced by the predicted peak ground-shock-induced overpressure curve (for TNT) in Fig. 12 and another curve four times the amplitude of the first. The former was used for the low-range gage, the latter for the high-range gage, both modified by multipliers for row-charge detonations.

Multipliers of the single-charge results were based on Ref. 15. There, charges at DOB = 1.5 $ft/lb^{1/3}$ and spacing (S) = 2.0 $ft/lb^{1/3}$ showed that, for gas-venting peak overpressures, which were dominant at that scaled burial depth, the increase for row-charge over single-charge peak overpressure was as follows:

$$\frac{\Delta p_{row}}{\Delta p_{single}} = n^{\alpha}$$

Perpendicular to the row $\alpha = 0.42$, and off the end $\alpha = 0.06$. For a five-charge row, the ratios became 2 and 1.3 for the two azimuths respectively. Conservatism dictated rounding these values to 2.5 and 1.5 for Shot C-2, which had nearly the same scaled spacing and burial depth. The same ratios were used for C-1 and C-6. In the latter case peak overpressures off the end were increased by a factor of 2 for the double row. Perpendicular to the row an increase of only 1.5 was used. This was based on displacement of waveforms from one row by 34 msec relative to the other row, which, for a waveform like B-6, resulted in less than doubling. Thus, for C-6 the multipliers were 3.75 perpendicular to the row and 3 off the end. It should be noted that set ranges for this shot were established at a time when C-6 was to have been a non-simultaneous row, and would thus bear less relation to expected pressures than for other shots. C-6 was adapted to a simultaneous double row by changing station locations and, at stations that could not be relocated, by using gages different than those planned.

Scaled DOB (1.87 $ft/lb^{1/3}$) and scaled spacing (1.43 $ft/lb^{1/3}$) of Shot C-3 were close to those in another series (reported in Ref. 15) for which $\alpha = 0.68$ off the ends of the row and $\alpha = 0.87$ perpendicular to the row.

Ratios for a five-charge row are 3 and 4 respectively.

Results - C Series

The results of measurements on the C series are summarized in Appendix A, Tables A-15 through A-20. Reproductions of the pressure-time records and their integrals constitute Appendix C.

Quality of Records

The station at Trinidad was not operated for Shots C-3, C-4, or C-5. On C-1, C-2, and C-6, the calibration step was malfunctioning and, as a result, amplitude scales for those records are inaccurate. Pressure-time waveforms are valid, however. In addition, calibration steps were limited for the high-range gage on C-1 and C-2, and the record of the low-range gage on C-2 was degraded by noise averaging 16-17 cps. At the Jansen station, the transmitter drifted out of band on Shot C-2. Records obtained at Jansen on the other shots had values for the high gage that were low with respect to those of the low-range gage because of unstable calibration. A calibration was estimated to within ±15 percent and the data corrected accordingly. On Shot C-1, the transmitter for the E-3 station drifted out of band and no record was obtained. On Shot C-4, the 2E-2 station was nearly a mile back in Long Canyon, causing transmission to be intermittent. Transmission at shot time did not permit a signal to be obtained. A noisy and unusable record was obtained on Shot C-2 from the S-3 station.

On Shot C-6 no record was obtained at Station S-1 for the low-range gage. The high-range gage had an unstable calibration, but an accurate calibration was obtained by using identical calibrations from other shots. On Shot C-3 the values obtained for the low-range gage at Station E-3 also appear high with respect to those obtained by the high-range gage at the same station, and to pressures observed at other stations. No reason has been uncovered, although the canister for that gage was used on no other shot in the C series.

All other gages used in the C series provided excellent records.

Simultaneous Single Rows - Shots C-1, C-2, C-3

Shots C-1, C-2, and C-3 were fired in the order of increasing depth of burial and decreasing spacing between charges.

Wave Shape -- Perpendicular to the simultaneous single rows, the waveforms exhibit easily identifiable ground-shock-induced and gas-venting pulses. The former pulse is the smaller for the C-1 shot, is slightly larger than the gas-venting pulse for C-2, and is considerably larger for C-3. Thus, the increased depth of burial suppresses the gas-venting pulse more than the ground-shock-induced pulse; the suppression is not overcome by closer spacing of charges.

Off the end of the row, separate contributions of some but not all individual charges can be identified for the shot with the larger spacing, C-1. For Shots C-2 and C-3, with closer spacing, contribution of individual charges is quite indistinct.

At the Jansen and Trinidad stations, single positive and negative pulses were observed and, as in the case of C-2 at Trinidad and C-3 at Jansen, it is not clear that the two separate positive peaks are directly related to the two pulses.

Ground-Shock-Induced Peak Overpressures -- Perpendicular to the rows (Fig. 21), the ground-shock-induced peak overpressures were approximately the same for all three shots in spite of changes in charge spacing and burial depth, and the increase from 5 to 7 charges on Shot 3.

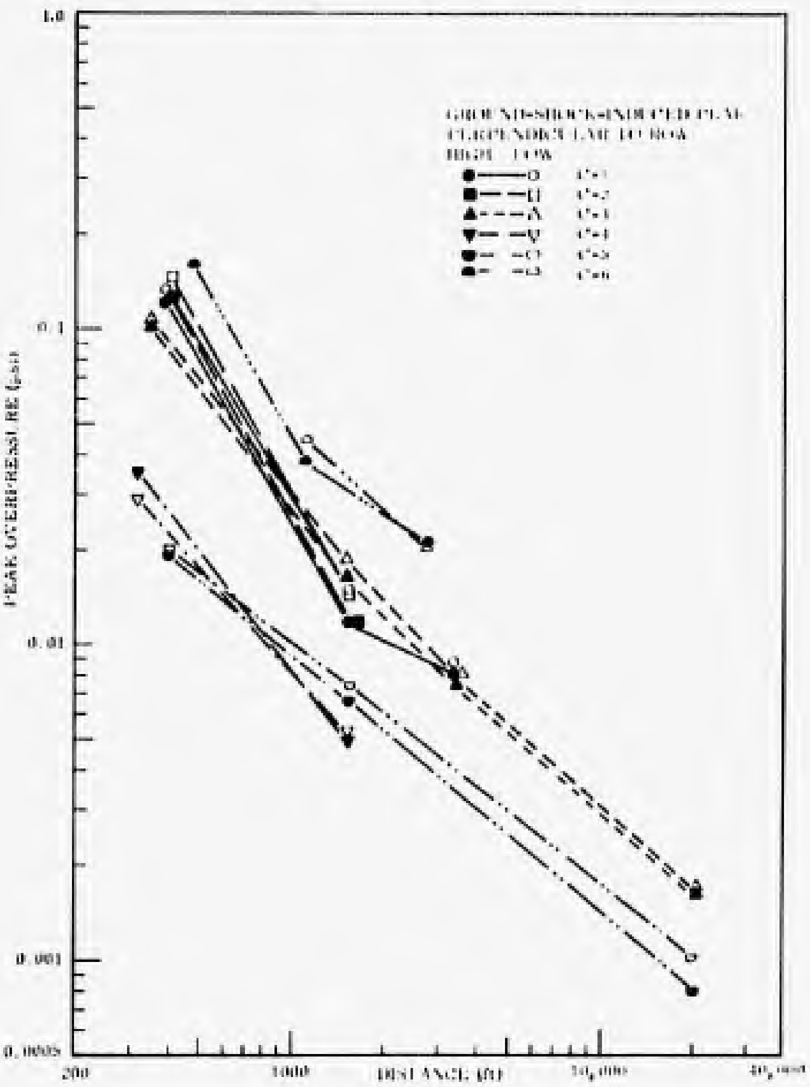

Figure 21. Ground-shock-induced peak overpressures vs distance perpendicular to row

Off the end of the rows (Fig. 22), the ground-shock-induced peaks were approximately the same for C-1 and C-3, but the C-2 peaks were roughly half those of the other two shots. Except for this latter case, azimuthal differences in the ground-shock-induced peak overpressures were small.

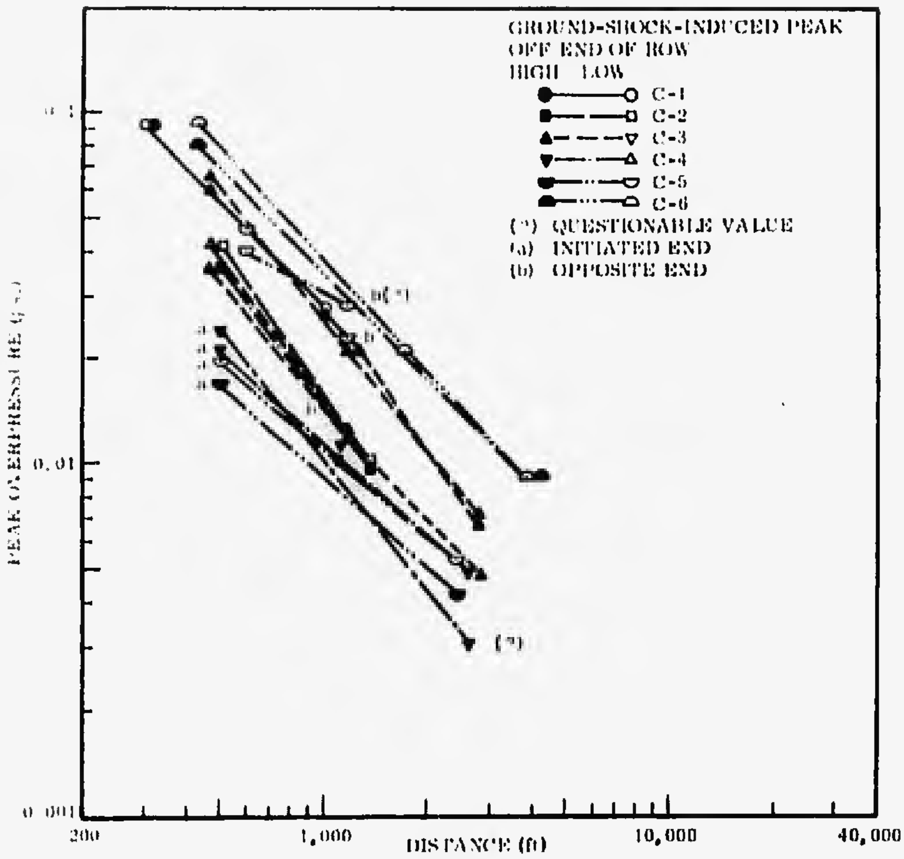

Figure 22. Ground-shock-induced peak overpressures vs distance off the ends of rows

Gas-Venting Peak Overpressures -- At the closest station, peaks perpendicular to the rows (Fig. 23) decreased in the order of the shots, but at the greater distances, different rates of attenuation for the different shots changed the order of and the spread between peak values. For example, at 750 feet the peaks for C-2 and C-3 were respectively 0.50 and 0.33 times those of C-1.

Off the ends of the rows (Fig. 24), the gas-venting peaks for C-2 and C-3 were 0.35 and 0.27 times those of C-1. Thus, we may conclude that deeper burial was more effective in reducing gas-venting peak overpressures than the closer spacing or the two additional charges of C-3 were in increasing it.

In comparing gas-venting peak overpressures perpendicular to the row and off the end, one can note that the azimuthal differences observed at the closest stations diminish at the greater distances. Azimuthal effects became relatively unimportant beyond 1,000, 1,500, and 3,000 feet for Shots C-1, C-2, and C-3. Thus, azimuthal effects were not preserved and the source appears to approach a point source as the distance to the place of observation is increased. This is not the conclusion one would have drawn from the small-charge work[15] and from the long-range measurements on PRE-GONDOLA III.[24]

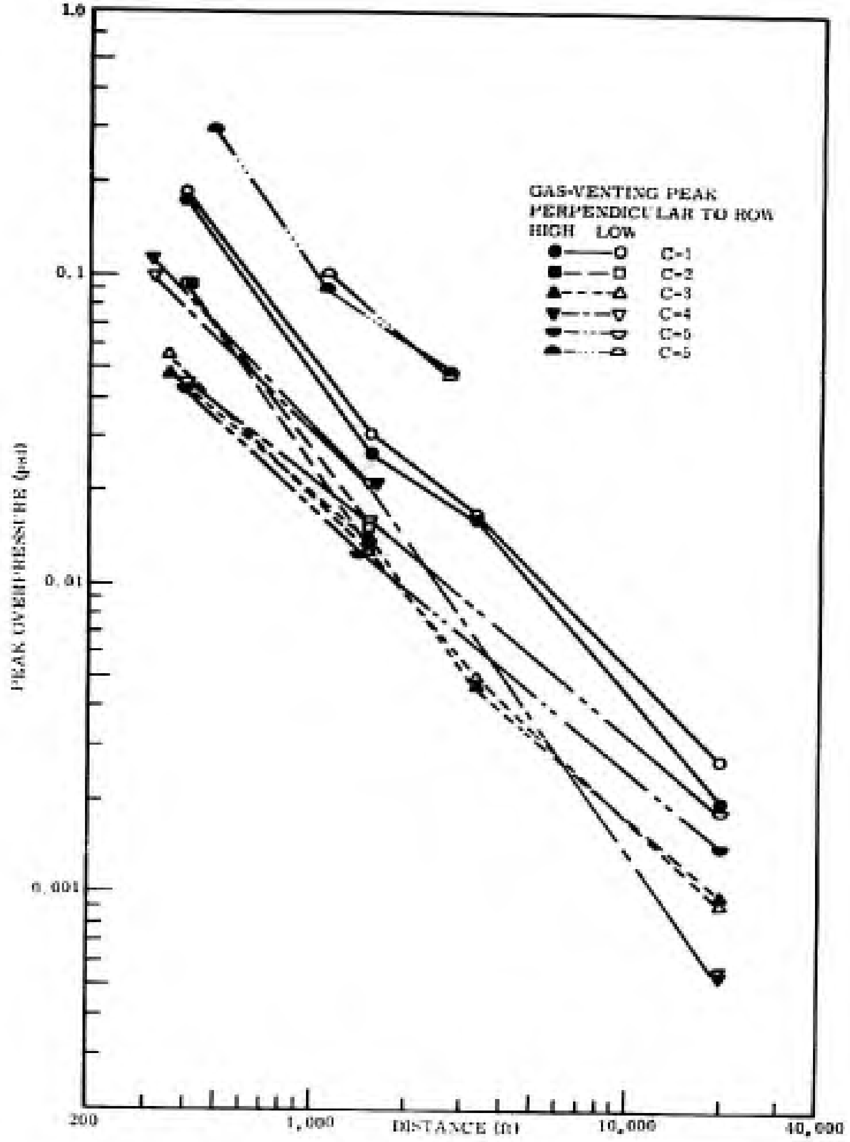

Figure 23. Gas-venting peak overpressures vs distance perpendicular to rows

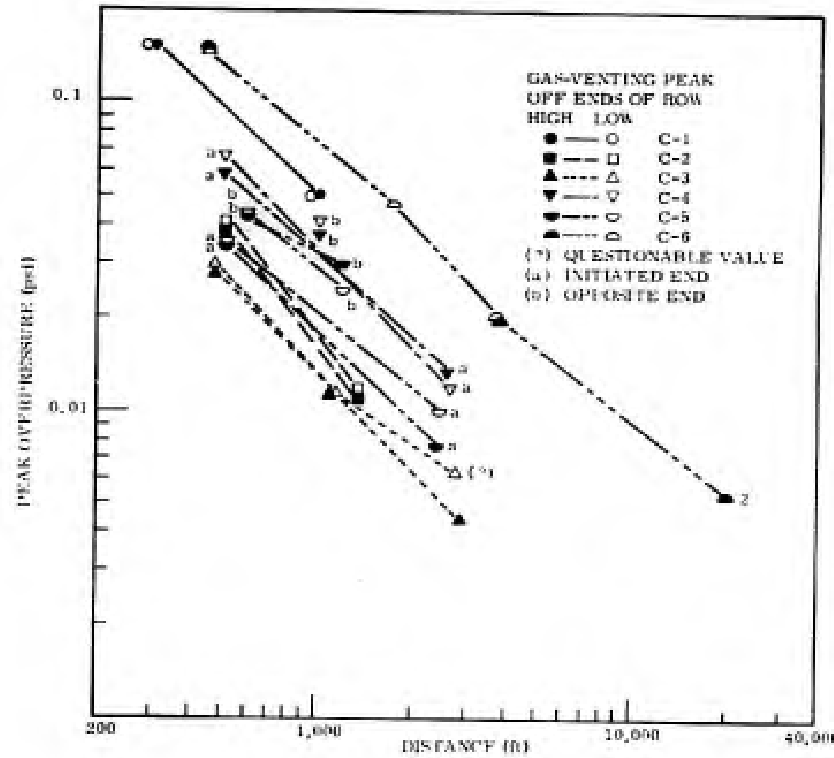

Figure 24. Gas-venting peak overpressures vs distance off ends of rows

Positive Phase Impulse -- Perpendicular to the rows (Fig. 25), the differences between the three shots caused by varying rates of impulse attenuation with distance tends to obscure the other trends. Differences are not large, however, at distances closer than 1,500 feet.

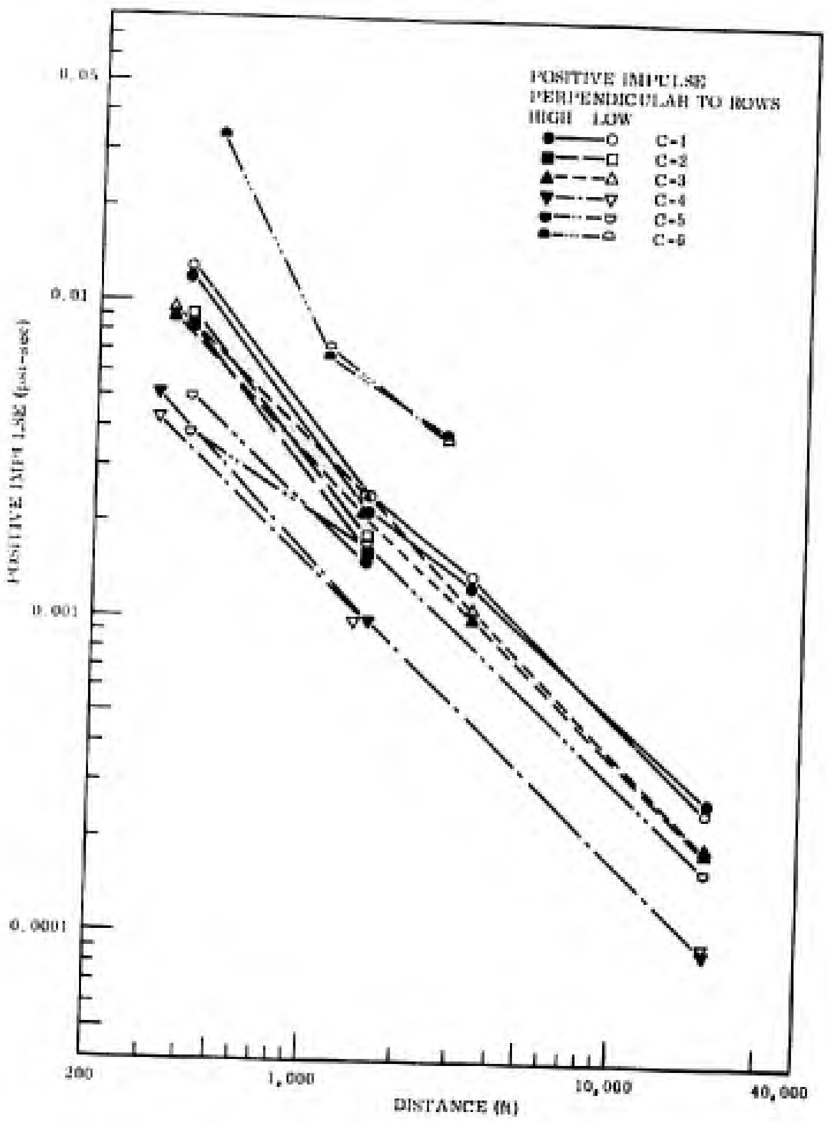

Figure 25. Positive-phase impulse vs distance perpendicular to rows

Off the ends of the rows (Fig. 26), positive-phase impulses for C-2 and C-3 were 0.6 and 0.75 times respectively those of C-1. Although the two additional charges of C-3 did not contribute to increased peak overpressures with respect to C-1, they did contribute additional impulse.

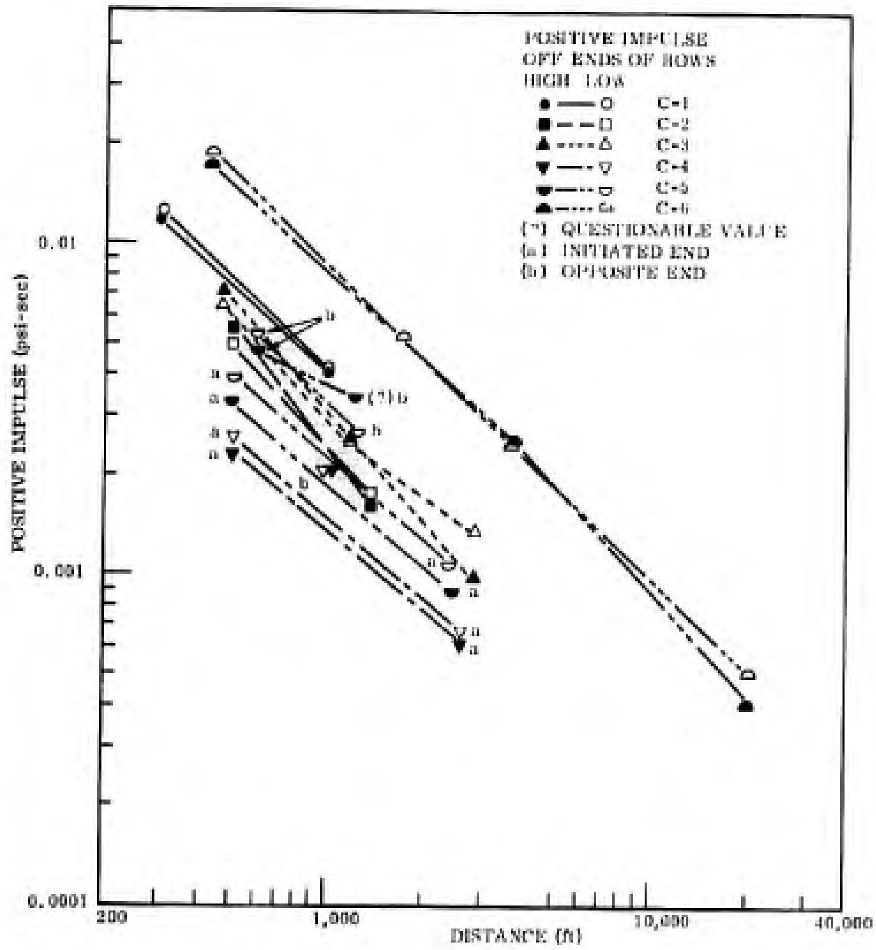

Figure 26. Positive-phase impulse vs distance off the ends of rows

Azimuthal effects of impulse were somewhat different for each of the three shots. On C-1, azimuthal differences had disappeared by about 1,000 feet. On C-2, impulse off the ends of the row was about 80 percent of that perpendicular to the row. The same ratio continued to approximately 2,000 feet. In the case of C-3, impulse at 750 feet was about the same in the two directions but, because of different rates of attenuation, that off the end of the row had become about 80 percent of the impulse perpendicular to the row by about 2,000 feet.

<u>Nonsimultaneous Single Rows - Shots C-4 and C-5</u>

Shot C-4 was detonated with 50-millisecond intervals between each two charges. For Shot C-5 the interval was 25 milliseconds. For both shots the charge detonated first was at the north end of the row--end 1E for purposes of station identification. The results for these two shots can be compared with those of C-2, for which the spacing and burial depth were the same, but where the charges were detonated simultaneously.

Wave Shape -- Perpendicular to the row, separate ground-shock-induced and gas-venting pulses could be observed. In the case of C-4, the gas-venting pulse was quite large with respect to the ground-shock-induced pulse, and the pulse shape was similar to that observed on some of the single charges (see waveforms of Shots B-3 and B-4 for examples.) Off both ends of the C-4 row, waveforms were similar to those perpendicular to the row.

Off the ends of C-5, there were two separate gas-venting pulses, and the reason for two sources is not understood. The records obtained at two stations off the end (opposite the initiation point of the first charge) are similar in having two separate peaks approximately equal in amplitude and separated by about 100 milliseconds. Although the first of these has been identified as ground-shock-induced, the identification may not be correct. Except for the two stations opposite the end on which the detonation was initiated on Shot C-5, waveforms at all stations on these two shots have a pronounced pulse early in what ordinarily would be the negative phase.

Ground-Shock-Induced Peak Overpressures -- Perpendicular to the two rows (Fig. 21), peak ground-shock-induced overpressures were approximately equal at 700 feet and had amplitudes approximately 0.3 times those of the corresponding simultaneous detonations. Because the attenuation rates were less than those of C-2, the overpressures tend to approach those of C-2 with increased distance. The peaks of C-5 attenuate with distance at a considerably lesser rate than those of C-4.

Off the ends of the rows (Fig. 22), pressures were measured at opposite ends. At 700 feet from C-4, the peaks at the end where the detonation was initiated, and at the opposite end, were 0.6 and 0.65 times respectively those of the simultaneous detonation. At 700 feet on C-5, the peaks were 0.5 and 1.5 times those of C-2 for the initiated and opposite ends respectively. For both C-4 and C-5, the initiated end had about the same peak overpressures as those measured perpendicular to the row.

Gas-Venting Peak Overpressures -- Perpendicular to the two rows (Fig. 23), between 400 and 1,500 feet, the gas-venting peaks for C-4 were approximately twice those of C-5. At greater distances, comparison is difficult because of the exceptionally rapid attenuation of gas-venting peaks on C-4. Comparison with C-2 is almost meaningless for the same reason.

Off the ends of the rows (Fig. 24), gas-venting peaks measured off the initiated end of C-4 are twice those of C-5. On the opposite end, the peaks measured on C-4 are 25 percent greater than those on the initiated end, which were approximately equal to the peaks measured perpendicular to the row. On C-5 the peaks measured on the end opposite from the initiated end were 40-50 percent greater than those measured off the initiated end, which, again, were about equal to perpendicular measurements.

Positive-Phase Impulse -- Perpendicular to the row (Fig. 25), positive-phase impulse for C-4 was approximately 2-1/2 times that of the simultaneous detonation. For C-5 it was also approximately 2-1/2 times as great at 400 feet but, because of attenuation less rapid than that of C-2, became only 1.5 times the values of C-2 at 1,500 feet. On both shots, positive-phase impulse measured off the initiated end was approximately equal (Fig. 26) to that measured perpendicular to the row. At

1,000 feet from the end opposite from the initiated end, impulses were 1.4 times those at the initiated end for C-4 (based on measurement at one station), and 1.6 times those at the initiated end for C-5. In this latter case the positive-phase impulse very closely approaches that observed off the end of C-2.

Simultaneous Double Row - Shot C-6

The charge spacing and burial depth for Shot C-6 was the same as for C-2. The spacing between the two rows was 39 feet.

Wave Shape -- The waveform perpendicular to the rows was not as expected. In the case of PRE-GONDOLA III (two rows of one-ton charges with a spacing of about 120 feet between rows), there were ground-shock-induced pulses only, and the separate peaks from each row were separated, as expected, by about 110 milliseconds. The waveform from Shot C-6, however, had both ground-shock-induced and gas-venting pulses. The separation of only about 35 milliseconds was small compared to the total duration of the positive phase, and the contributions of the individual rows could not be clearly identified.

Off the end of the double row, the pressure waveform was approximately sinusoidal, with no clearly identifiable contributions of separate charges or separate rows.

Ground-Shock-Induced Peak Overpressures -- At 1,100 feet, perpendicular to the rows (Fig. 21), the ground-shock-induced peak overpressures were about double those measured on Shot C-2.

Off the end of the rows (Fig. 22), the pressures were 2 to 2-1/2 times those of C-2, the variation resulting from different rates of attenuation with distance for the two shots. Comparison of pressures off the end of the row to those perpendicular to the row is difficult because of different rates of attenuation in the two directions. Pressures perpendicular were 25 percent higher than off the end at 1,000 feet, and 60 percent higher at 3,000 feet.

Gas-Venting Peak Overpressures -- Both perpendicular to the row and off the end of the rows (Figs. 23 and 24), gas-venting peak overpressures were four to five times those measured on C-2 at about 1,500 feet. Here again there were variations due to differences in rates of attenuation. Pressures measured perpendicular to the row were 30 to 50 percent greater than off the end of the row over the range of 1,000 to 3,000 feet.

Positive-Phase Impulse -- At 1,500 feet, both perpendicular to the row (Fig. 25) and off the end of the rows (Fig. 26), positive-phase impulse was about three times that of C-2. Off the end of the row, positive-phase impulse for this shot had a remarkably uniform attenuation from the close-in station all the way to Trinidad, at a rate of $R^{-0.93}$. Positive-phase impulses were essentially equal, perpendicular to and off the end of the row, over the range of 1,100 to 2,700 feet.

Predicting Row-Charge Airblast from Single-Charge Airblast

In an earlier effort,[15] air-blast parameters from row-charge detonations were compared with those from corresponding single-charge detonations. It was found that this ratio had the form n^{α}; that α was different for each air-blast parameter, and was also a function of charge burial depth and spacing. Since in that earlier series the same explosive and medium were used for single and row charges, it was presumed that the use of a ratio would eliminate the effect of both. The C series provides an opportunity to examine these relationships for larger charges with a new medium and new explosives.

Since charge-burial depth and spacing are different for each of the C series shots, there is advantage in reducing these two variables to a single one. The one chosen is the line-charge-equivalent scaled burial depth, Δ, i.e., $ft/(lb/ft)^{1/2}$, where DOB is scaled according to the square root of the equivalent explosive energy per unit length. Table VI summarizes pertinent data for the shots. The last column of the table illustrates the point that, when spacing is varied, burial depth is also changed to optimize effectiveness of explosive excavation, and that this effectiveness is achieved over a relatively small range of line-charge equivalent scaled depths of burst. Shot C-6 has been included in the table and in the following comparisons, even though it consisted of two five-charge rows rather than a single ten-charge row.

TABLE VI

Line-Charge Equivalent Scaled Burial Depths

Series or Shots	Charge Weight (lb)	Explosive	Medium	Cube-root Scaled Spacing $(ft/lb^{1/3})$	Cube-root Scaled DOB $(ft/lb^{1/3})$	Square-root Scaled DOB $[ft/(lb/ft)^{1/2}]$
A (Ref. 15)	64	TNT	Playa	1.31	1.73	1.98
B (Ref. 15)	64	TNT	Playa	2.00	1.50	2.18
C-1	2000	AANS	Sandstone shale	2.54	1.43	2.28
C-2	2000	AANS	Sandstone shale	1.98	1.58	2.22
C-3	2000	AANS	Sandstone shale	1.43	1.83	2.19
C-6	2000	AANS	Sandstone shale	1.98	1.58	2.22

Comparisons are made in Figs. 27, 28, and 29 between ground-shock-induced peak overpressure, gas-venting peak overpressure, and positive-phase impulses, both perpendicular to the rows and off the ends. The lines are fits from Ref. 15 to data from rows of 2, 5, 11, and, in one case, 25 charges. The pressure-distance relationships from which the ratios were obtained differed little in attenuation rates, so ratios were based on intercepts, where attenuation rates of row charges were forced to agree with those of the corresponding single charges. Thus, ratios of a given row-charge parameter to a corresponding single-charge parameter were constant over the range where measurements were made. Single charges were at exactly the same burial depth as the corresponding row charges.

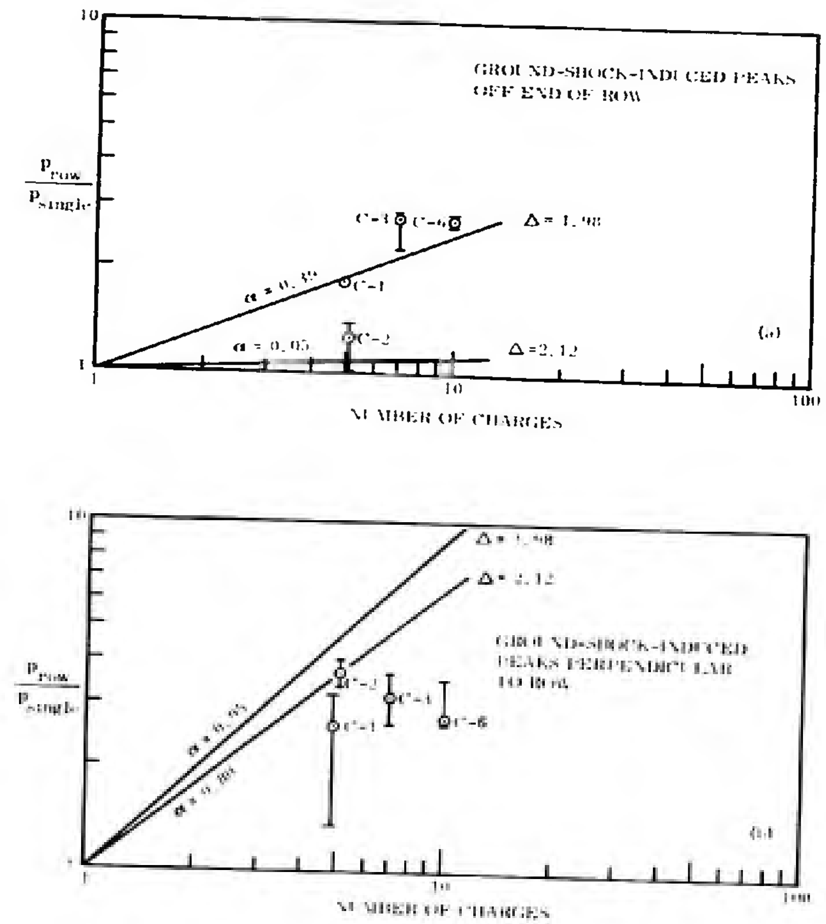

Figure 27. Ratio of row-charge to single-charge ground-shock-induced peak overpressures as a function of number of charges

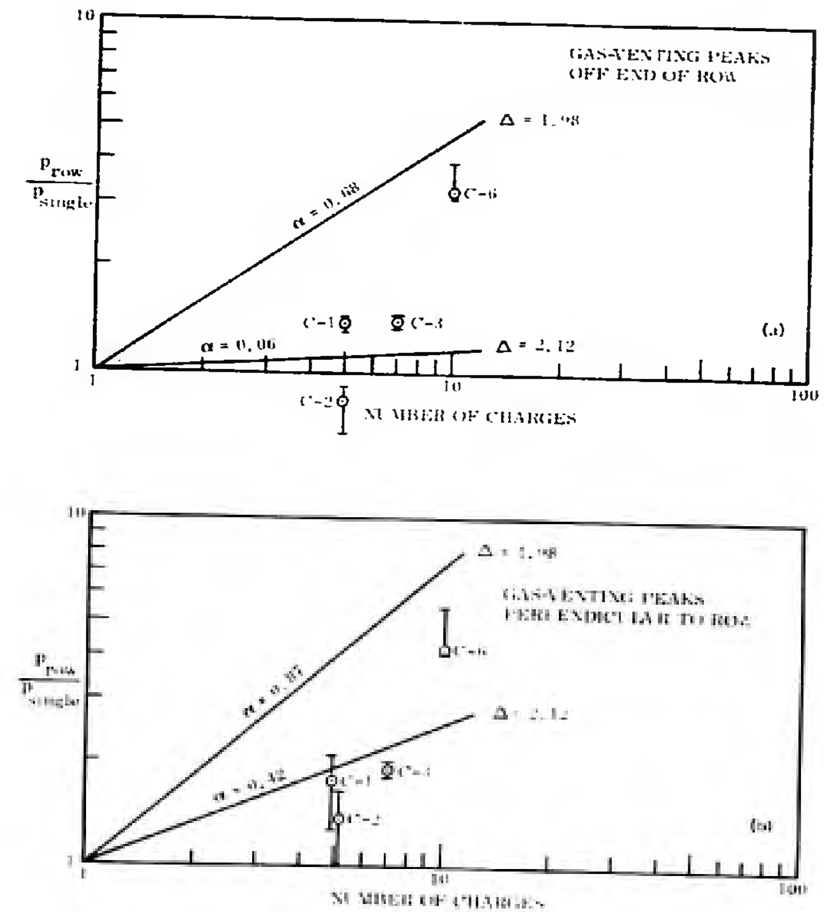

Figure 28. Ratio of row-charge to single-charge gas-venting peak overpressures as a function of number of charges

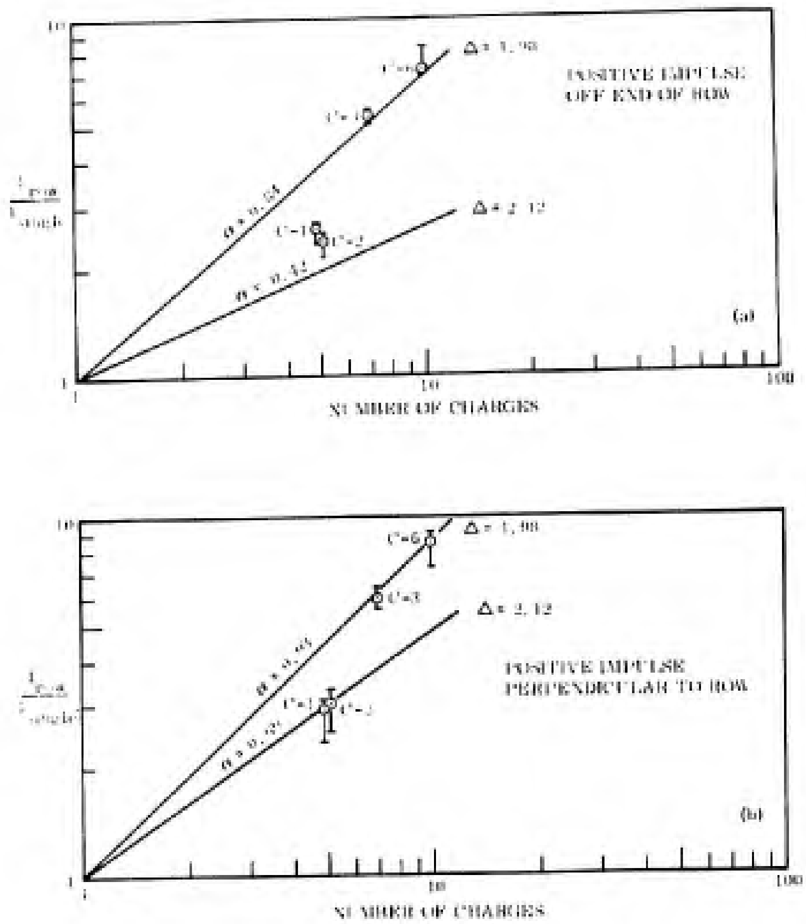

Figure 29. Ratio of row-charge to single-charge positive impulse as a function of number of charges

For the C series shots, these factors contribute to uncertainty:

1. Single-charge shots were not at exactly the same burial depth as the row charges, so some interpolation was necessary.

2. Interpolation was difficult because of irregular depth-of-burst dependence of the single charges--see Fig. 12. Interpolation was based on 2.1 times the TNT ground-shock-induced peak overpressure prediction line of Fig. 12, and 5 times the TNT gas-venting peak overpressure prediction line. For positive impulse the line of Fig. 14 was used. For single charges, an attenuation rate of R^{-1} about the 630-foot intercept from Figs.12 and 14 was assumed.

For the C series shots, the value was based on a 630-foot intercept of an R^{-1} approximation to the data over the range of the first to second stations (or to the third station if Station 2 was missing). "Error bars" about the circles indicate the spread due to a variable attenuation rate of the row-charge blastwave over a range from about 300 to 1,500 feet.

3. Attenuation rates for the single charges were close to R^{-1}, while those of the row charges were often quite different.

The results of Figs. 27-29 are quite unsatisfying inasmuch as there are neither consistent agreements between the ratios for the C series and those of the earlier work, nor consistent trends established for the C series itself. If ratios are truly dependent on Δ, agreement between C-3 and the $\Delta = 2.12$ line would be expected; yet C-3 is as often in agreement with the $\Delta = 1.98$ line as with the $\Delta = 2.12$ line.

The lack of agreement is larger than could be accounted for by differences in attenuation rate. Because of the great variation in gas-venting peak overpressures with burial depth, a significant cause would involve the choice of interpolation. Variation with depth of burst was much less for the other two parameters, so the cause of lack of agreement probably lies elsewhere than in the interpolation.

A more probable explanation is that the wave shapes of airblasts from both single and multiple charges are so complex in their dependence on spacing, burial depth, and azimuth that they cannot be represented properly by so simple a ratio. It is also possible that medium and explosive dependence is not removed by using single- and row-charge data from shots with similar media and types of explosive.

Predictions and Results - D Series

Results of the measurements made on the D series are summarized in Appendix A, Tables A-21 through A-24. Reproductions of the pressure-time records and their integrals constitute Appendix D.

In the D series, the only station for which records were not obtained was the Trinidad station on Shot D-4. Also at Trinidad, the record for the low-range gage on Shot D-1 was noisy and unusable. At Station E-2 on the same shot, the low-range gage was noisy but usable. Other records were among the best of the program. Calibration stability problems developed on Shots D-1 and D-2 for both gages at Trinidad and for the E-3 high gage. It was possible to correct the data by using the calibration for Shot D-3, which was stable and had the same value as for D-1 and D-2.

Prediction of overpressures for the D series was complicated and made less accurate by the fact that D-1 made use of ammonium nitrate and fuel oil explosive, whereas the explosive for the other three was aluminized ammonium nitrate slurry. An IR-10 slurry was used for Shot D-3, and then the TD-1 slurry was used for Shots D-2 and D-4.

Since each shot in the D series was quite different from the other three, each will be discussed separately.

Shot D-1

Shot D-1 was a single-row detonation; the charge weights, spacings, and burial depths are listed in Table VII. Charge weights were unequal, as were spacings and burial depths. Table VII also lists the scaled spacings and scaled burial depths for the shot. Average scaled burial depth was 1.92 ft/lb$^{1/3}$ and average scaled spacing averaged 1.29 ft/lb$^{1/3}$. Average charge weight was 1089 pounds. Prediction was made as if the row were nine equal charges, with uniform scaled spacing and scaled burial depth, and with each equal to the average value for Shot D-1. The pressure-distance function for a single 1089-pound charge at a scaled burial depth of 1.92 ft/lb$^{1/3}$ was determined and increased for a row charge by using data of Ref. 15 to estimate overpressure off the end of and perpendicular to the row. Although the uncertainty was greater because of the variation in parameters, experience on the C series had shown that a fairly large range of uncertainty could be accommodated by using two gages at each station.

TABLE VII

Charge Placement Shot D-1

Charge	A		B		C		D		E		F		G		H		I
[illegible] (lb)	500		[illegible]		1200		1700		2000		2000		1200		500		200
[illegible] Depth (ft)	[illegible]		[illegible]		[illegible]		22.3		23.0		[illegible]		20.2		15.7		11.5
[illegible]	[illegible]		[illegible]		[illegible]		[illegible]		[illegible]		1.88		1.90		1.98		1.97
[illegible] (ft)						[illegible]		[illegible]		16		15		12		9	
[illegible]																	
[illegible]		[illegible]		[illegible]		[illegible]		1.26		[illegible]		[illegible]		[illegible]		[illegible]	
[illegible]		[illegible]		[illegible]		[illegible]		1.19		[illegible]		1.41		1.51		[illegible]	
[illegible]																	
[illegible]			[illegible]		2.10		2.07		1.99		2.12		[illegible]		[illegible]		2.14
[illegible]	[illegible]		[illegible]		[illegible]		[illegible]		2.06		2.05		[illegible]		2.11		

Measurements were made perpendicular to the row in both directions. Since the shot was to excavate a side-hill cut, it was desirable to make measurements in both up- and downhill directions to examine the results for terrain effects. Measurements were also made off the Charge I end.

Wave Shape -- At the closest stations perpendicular to the row in both directions, the waveform was a very sharp short-duration spike of an amplitude that was quite large with respect to the rest of the signal. By the time it reached the second station in both directions, the spike was becoming broader and of lower amplitude.

At the two closest stations in each direction, the spike was followed by a lower and longer-duration spike. Although both of these coincide in time with the ground-shock-induced pulse, the spike with the very short duration may well have resulted from the Primacord detonation on the ground surface. Perpendicular to the row, the gas-venting pulse was a minor one. Off the end of the row at all stations, a dominant ground-shock-induced pulse was followed approximately 0.2 second later by a gas-venting pulse. Waveforms at the more distant Jansen station were similar. The one record obtained at Trinidad shows a simple sinusoidal pulse.

Peak Overpressures - Figure 30 shows peak overpressures for both the ground-shock-induced and gas-venting pulses. Peaks measured at Jansen are shown as an extension of those measured off the ends of the row at the closer stations. Perpendicular to the row there was very little difference between the two directions, indicating that terrain effects were small. If the largest-amplitude spike is used at the closest stations, the attenuation rates to the second stations are very large with respect to the rates off the end of the row. If the second peak is used, however, attenuation rates more nearly match those in the other direction. This argues strongly that the first very sharp spike must indeed be attributed to detonation of the surface Primacord. Ground-shock-induced peaks were about eight times the gas-venting peaks.

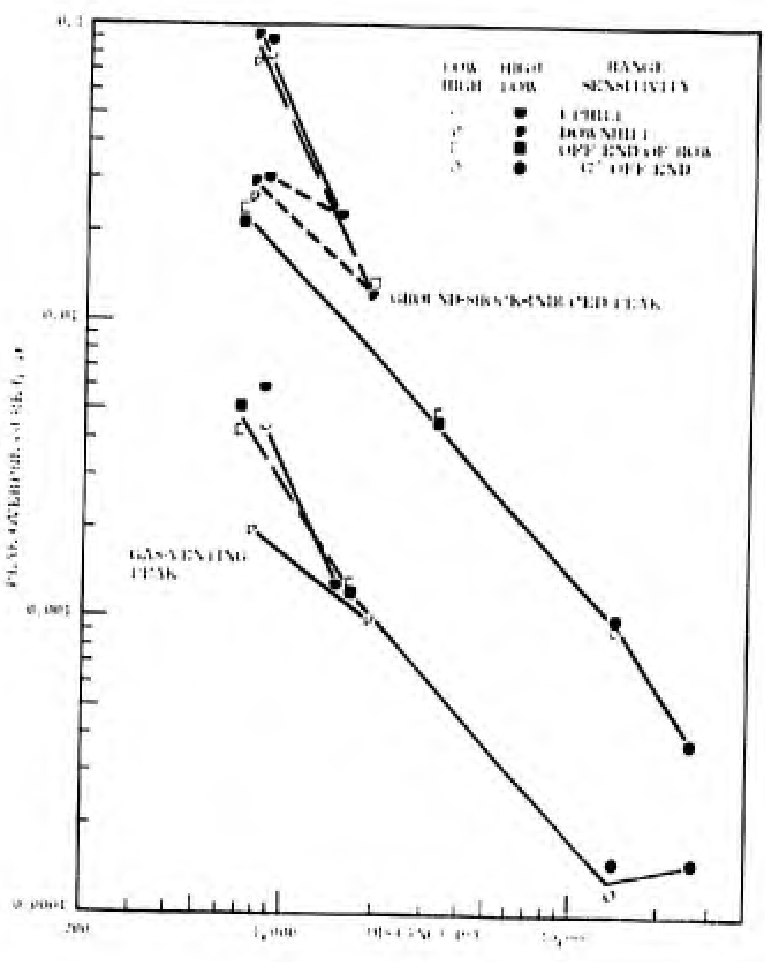

Figure 30. Peak overpressure vs distance for Shot D-1

Positive Phase Impulse -- Positive-phase impulse has been plotted versus distance in Fig. 31. The differences in impulse in the three directions are small, although that from the uphill direction is slightly lower than off the end, and that in the downhill direction slightly larger, again indicating that terrain effects were small.

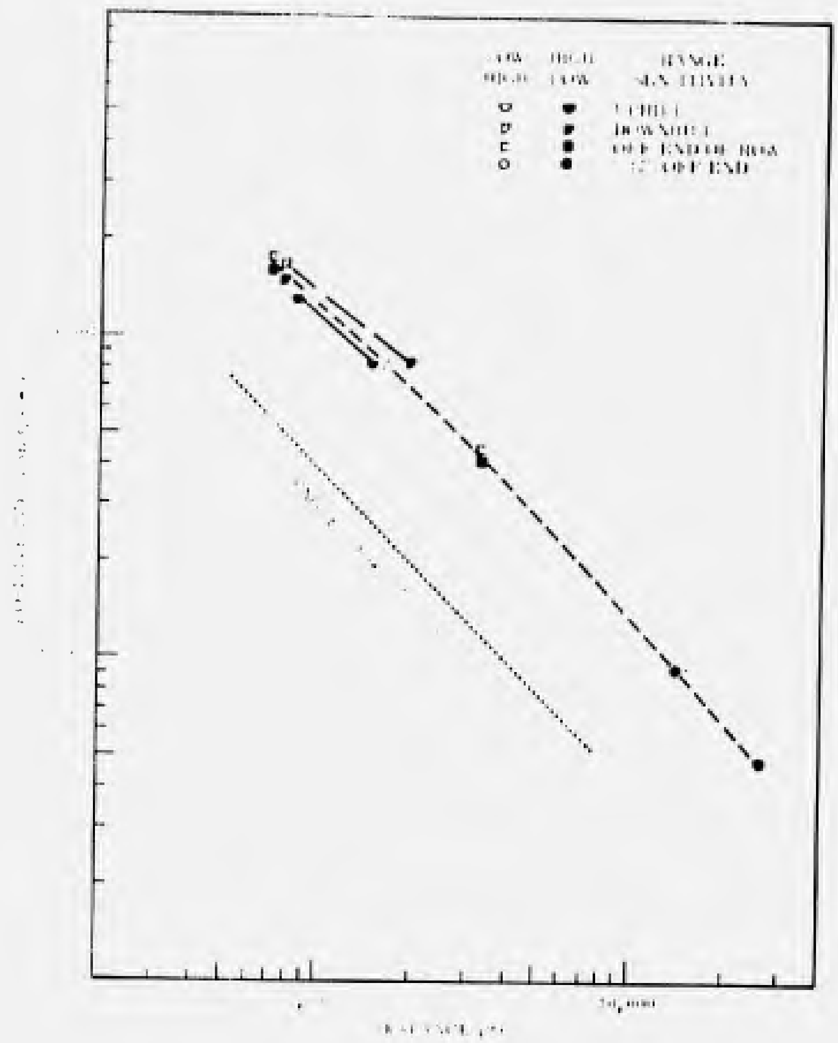

Figure 31. Positive impulse vs distance for Shot D-1

Positive-phase impulse versus distance for a single 1089-pound charge at the average scaled burial depth of the row has been added to the figure. Over most of the range of measurement, the impulse from the row charge was 3 to 3-1/2 times that of the equivalent single charge. If one compares this ratio of impulse for a 9-charge row to the impulse for a single charge with other data in Fig. 29, the results are no more satisfying than for the C series. Note, too, that the average line-charge equivalent scaled burial depth (Δ) is 2.15 compared with 2.12 for shots in the series in Fig. 29.

Shot D-2

Shot D-2 was a single-row detonation consisting of five one-ton charges spaced 32 feet apart. Actual burial depths for Shots A through E are given in Table A-22. The average scaled depth was 1.4 ft/lb$^{1/3}$. Prediction was made by assuming that overpressures would be comparable to those of Shots C-1 and C-2. Stations E-1, E-2, and E-3 were off the Charge E end, while that at Jansen was about 27° from the axis of the Charge A end.

Wave Shape -- Perpendicular to the row, the gas-venting pulse gave greater amplitudes than the ground-shock-induced pulse, while off the end of the row, the ground-shock-induced pulse gave the larger amplitudes. Between Station E-3 at 3,740 feet, and Jansen at about 14,000 feet, the two positive pulses merged into one pulse with a single peak.

Peak Overpressures -- Figure 32 shows ground-shock-induced and gas-venting peak overpressures versus distance, both perpendicular to the row and off the end of the row. As in the case of Shot D-1, a large-amplitude, short-duration spike has been attributed to Primacord detonation, and the ground-shock-induced peak has been identified as a lower-amplitude peak at a slightly later time. Ground-shock-induced peaks perpendicular to the row were about 1.5 times those off the end of the row, but the gas-venting peaks perpendicular to the row were between 4 and 5 times those off the end.

Positive-Phase Impulse -- Perpendicular to the row, positive-phase impulses (Fig. 33) were about twice those measured at comparable distances off the end of the row. Shot D-2 had an equivalent line-charge scaled burial depth of 2.23 ft/(lb/ft)$^{1/2}$. Row-charge and single-charge ratios from Fig. 33 at about 1,500 feet agree with the Δ = 2.12 line of Fig. 29 off the end of the row, but are high when compared with results perpendicular to the row.

Comparison of Shots D-2 and C-1 -- Both Shots C-1 and D-2 were rows of five one-ton charges. The spacing and burial depths were identical, 32 and 18 feet respectively. C-1 was fired beneath a slope of approximately 5° and D-2 beneath a slope of about 18°. The geology was similar, though not identical, in the two locations, which were 6,425 feet apart.

Perpendicular to the rows, the ground-shock-induced peak overpressures for D-2 averaged about 2-1/2 times those of C-1, whereas off the end they were 1.6 times those of C-1. Gas-venting peak overpressures perpendicular to D-2 averaged three times those of C-1, and off the end they were only 70 percent of those of C-1. Positive-phase impulse measured perpendicular to D-2 was 1.6 times that perpendicular to C-1, and impulse measured off the end of D-2 was about 75 percent of that of C-1. In the vicinity of Jansen and Trinidad, differences between the two shots were small.

Shot D-3

Shot D-3 was the detonation of a double row in the geometry shown in Fig. 34. The pre-shearing holes were loaded with Primacord in order to fix the uphill crater

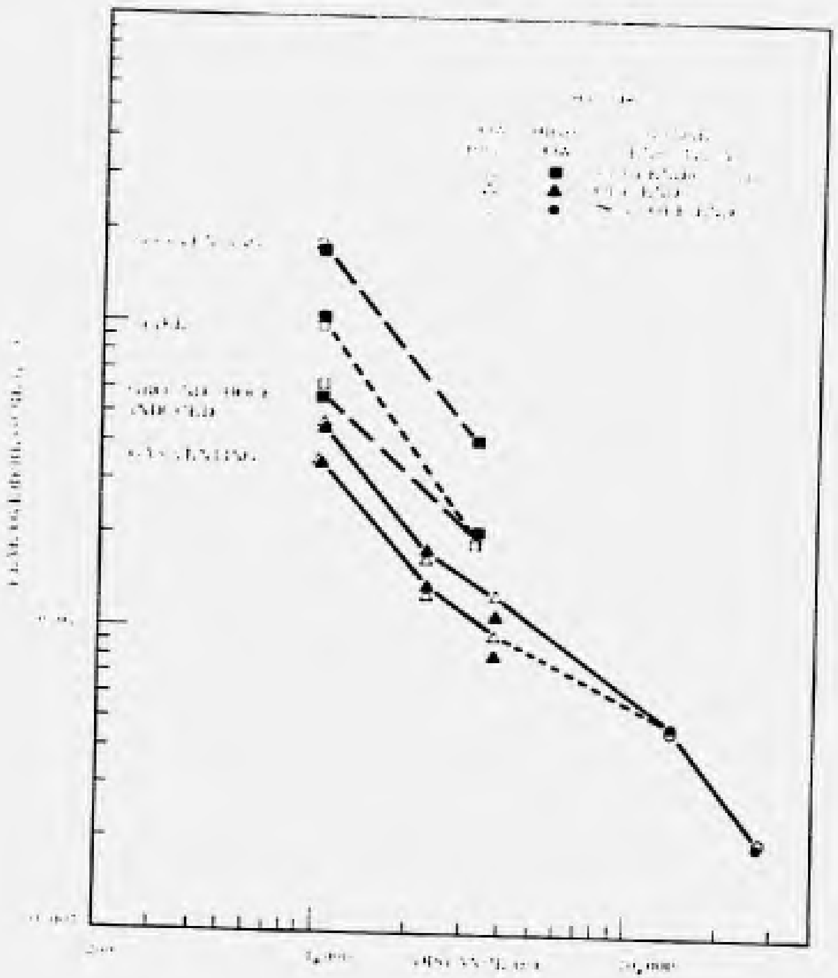

Figure 32. Peak overpressure vs distance for Shot D-2

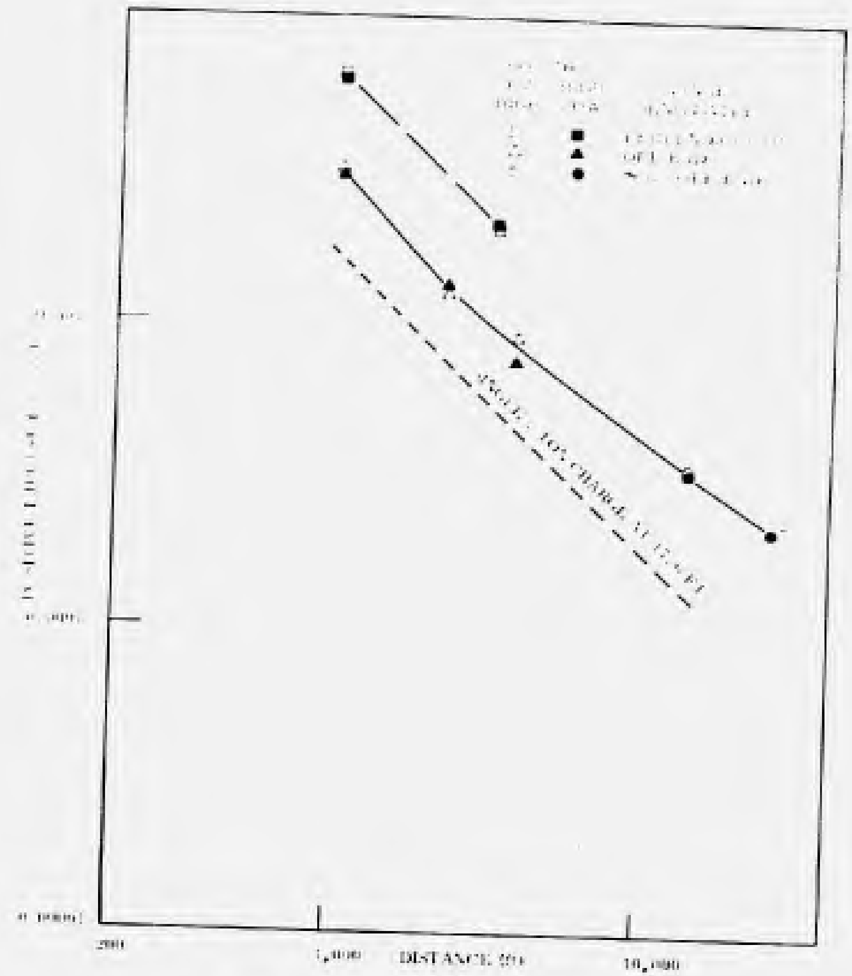

Figure 33. Positive impulse vs distance for Shot D-2

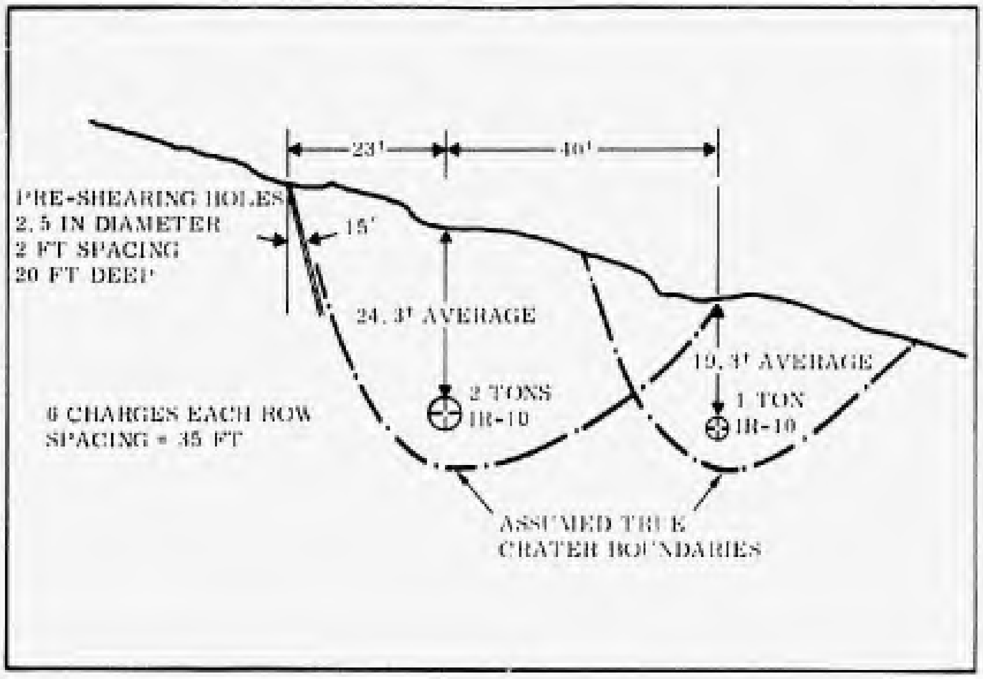

Figure 34. Layout for Shot D-3

boundary. The Primacord was detonated at zero time, the one-ton row was detonated 50 milliseconds after zero time, and the two-ton row 300 milliseconds after zero. Charges in the row were 35 feet apart. Burial depth for the one-ton row charges A through F are given in Table A-23. Scaled burial depth was 1.5? ft/lb$^{1/3}$ for both rows. There is some evidence that the two-ton charge, D (fourth from the east), produced a low-order detonation.

Wave Shape -- Perpendicular to the row, the waveform consisted of two major positive pulses, each followed by a negative pulse. The first positive pulse contains both the ground-shock-induced and the gas-venting peaks from the one-ton row. These are preceded by spikes from the Primacord detonation and the pre-shearing holes. The second positive pulse coincides with that expected from the gas-venting pulse of the two-ton row. The ground-shock-induced pulse of the two-ton row appears to coincide with the first negative pulse, and may be related to the minor perturbation occurring near the bottom of that negative pulse.

Off the end of the rows the waveform consists of three positive pulses. The first two are separated by a decrease to about ambient pressure, and the second and third are separated by a brief but pronounced negative phase. The third is followed by a broad negative phase, which in turn is followed by a final positive phase with small amplitude. Observed from the end of the row, the source appears to have a length of 175 feet. Assuming simultaneity of each separate row source, the source would span an interval of approximately 155 milliseconds between a signal from the closest charge and a comparable signal from the farthest charge. If the time interval between ground-shock-induced and gas-venting pulses is assumed to be equal to that interpolated from shots in the B series, the time span of each pulse can be estimated, as illustrated in Fig. 35. It thus appears that the first positive pulse can be associated with the pre-shearing shots plus the ground-shock-induced and gas-venting pulses of the one-ton row. The second peak must be associated with the gas-venting pulse from the more distant one-ton charges, and the ground-shock-induced peak from the closest charges in the two-ton row. The final pulse requires contributions from the ground-shock-induced pulses of distant two-ton charges and the gas-venting pulses of all two-ton charges. A single one-ton-charge detonation has a positive-phase duration of about 0.25 second. Where times of arrival from nearest to farthest charges are separated by 0.15 second, the negative phase of the closest charge coincides with part of the positive phase from the farthest charge. With a six-charge row the interaction of waveforms is very complex and is not explored further in this report.

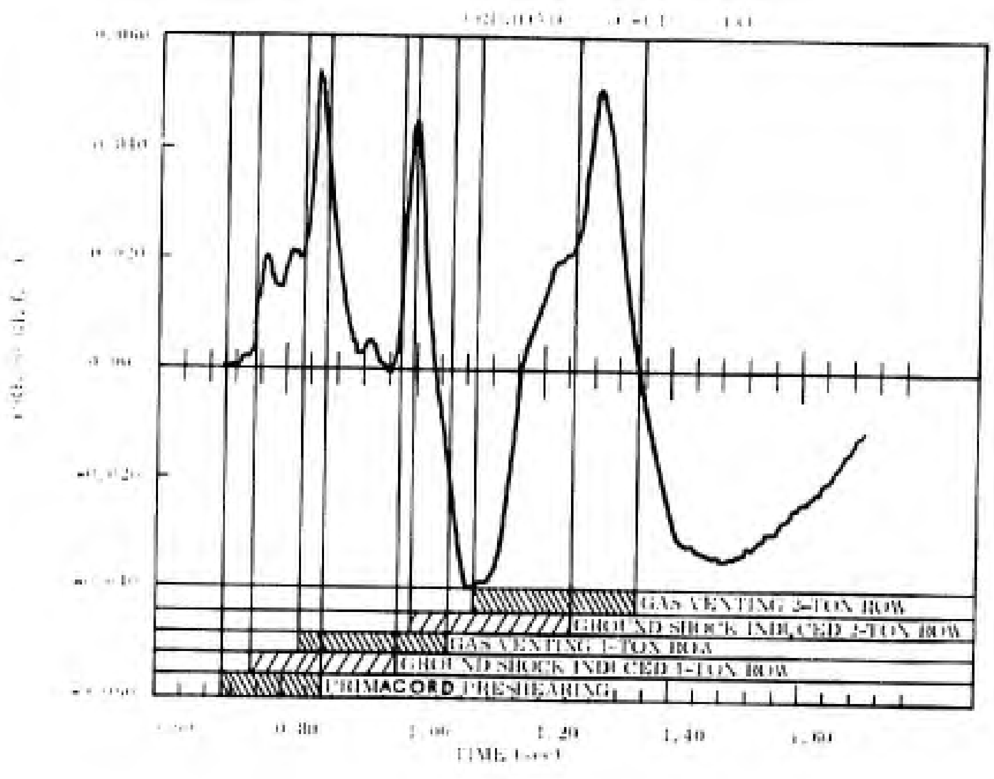

Figure 35. Sequence of airblast pulses off end of Shot D-3

Peak Overpressures -- Peak overpressures have been plotted as functions of distance in Fig. 36. Perpendicular to the rows, the ground-shock-induced peak from the one-ton row is consistently lower than the other two peaks. Due to changes in wave shape, the gas-venting peak from the one-ton row is larger than that from the two-ton row at the closest station, but is smaller at the more distant station.

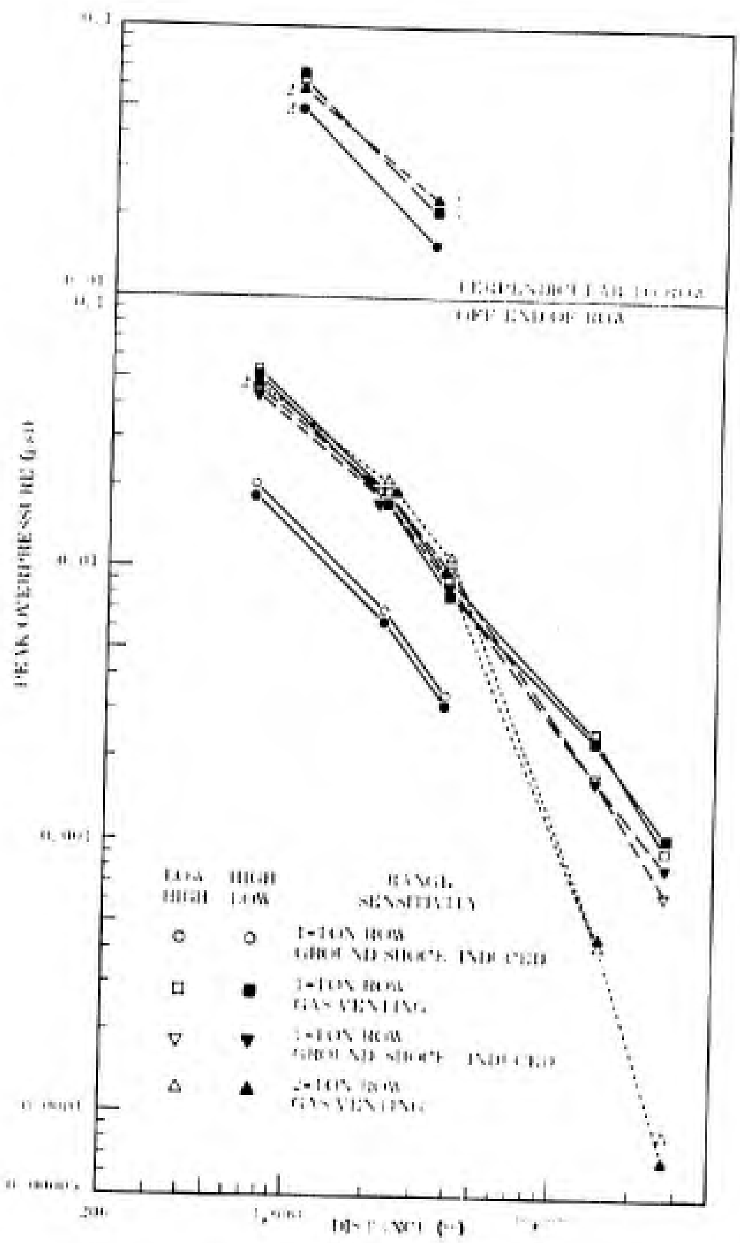

Figure 36. Peak overpressure vs distance for Shot D-3

At all stations off the ends of the rows, the ground-shock-induced peak from the one-ton row is noticeably lower than other peaks. In the region from about 2,000 to 4,000 feet the other three peaks are about equal. At the greater distances, the gas-venting peak from the one-ton row remains about 35 percent greater than the ground-shock-induced peak from the two-ton row. At these two distant stations, what appears to be the gas-venting pulse from the two-ton row has a very much decreased amplitude. The peaks perpendicular to the row are about 50 percent greater than those off the ends of the rows in the region from about 2,000 to 3,000 feet.

Positive-Phase Impulse -- In Fig. 37 the positive-phase impulse, both perpendicular to and off the ends of the rows, has been plotted versus distance. Two values of impulse are shown. The upper values are the total positive impulse derived from the contributions of both rows. The lower values are for the one-ton row above. At the closest stations, both the total impulse and the one-ton row impulse perpendicular to the rows are about 50 percent greater than their equivalents off the end of the rows. The total impulse in each direction is 1.8 to 1.9 times the one-ton row impulse in the same direction. At the distant stations, maximum and total impulses converge, and the reason for the convergence can be seen in the impulse-time curves in Appendix D.

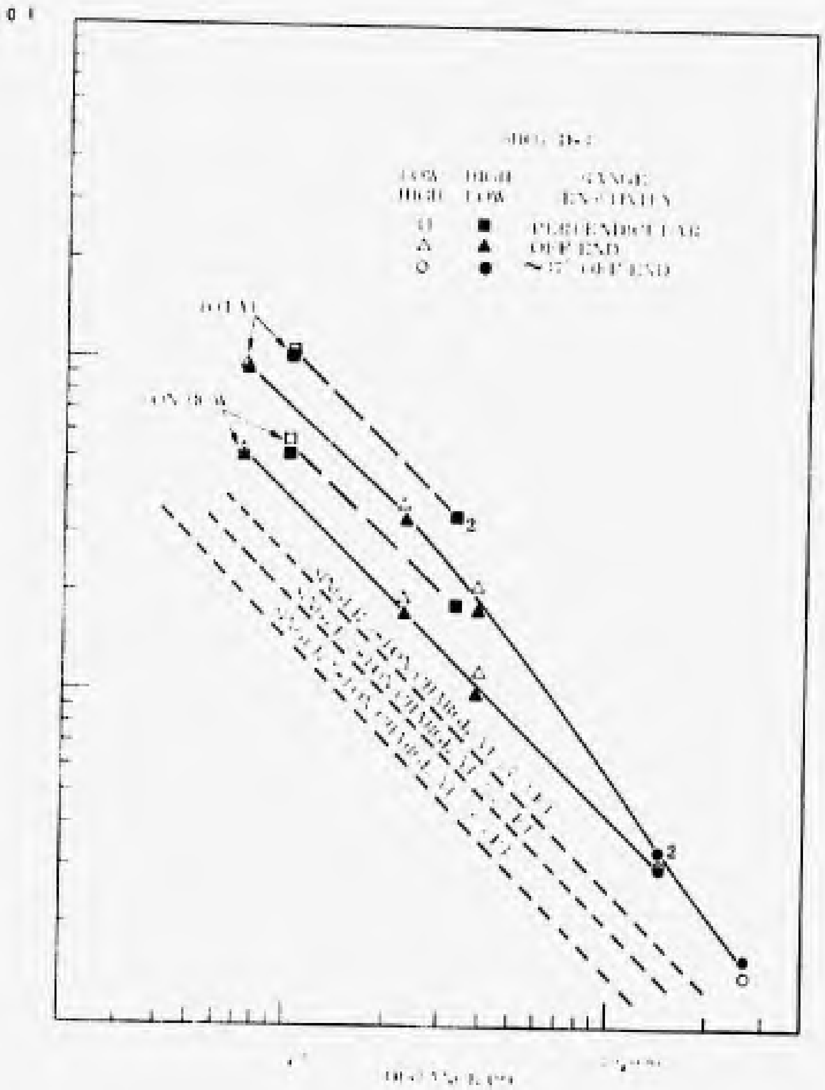

Figure 37. Positive impulse vs distance for Shot D-3

Impulse-distance values for single 1, 2, and 3-ton charges at comparable scaled burial depths have been added to the figure. From these one may obtain row-charge to single-charge impulse ratios for comparison with Fig. 29. If the one-ton row impulse is used and compared with the one-ton single-charge impulse, ratios of 4.0 and 2.8 are obtained respectively for the perpendicular and off the ends of the rows. Since Δ equals 2.55 for the one-ton row, agreement with other data in Fig. 29 is not especially good. The agreement is not improved if one chooses instead to consider the double row as being equivalent to a single row of 3-ton charges, and this impulse is compared with the total impulse. In this case Δ equals 2.12. It does not appear that a meaningful comparison could be made on the basis of a two-ton row.

Shot D-4

Shot D-4 consisted of the detonation of a row of 18 one-ton charges and, after a short delay, a row of 12 two-ton charges flanked on each end by a single one-ton charge. Pre-shearing holes loaded with Primacord were detonated at zero time, the one-ton row charge at 9 msec, and the two-ton row at 150 msec. The cross section was similar to that of Fig. 34 except that the spacing between rows was 46 feet and the slope of the ground profile was considerably less at the east end. Both the one-ton charges were emplaced in 30-inch-diameter holes. Holes for the one-ton charges were underreamed, producing charges with a height-to-diameter ratio close to one. Holes for the two-ton charges were not underreamed, and the 30-inch-diameter cylinder of explosive was approximately 10 feet high. The depths of burial given in Table A-24 are to the mid-height of the explosive cylinder. This large L/D ratio would probably cause gas venting to occur relatively earlier than for an equivalent spherical charge buried in the same depth.

Wave Shape -- Wave shapes for this event were quite complex and varied significantly with azimuth about the rows. On the north perpendicular line (closest to the one-ton row), the ground-shock-induced pulse from the one-ton row arrived first, followed by a pulse which included the combined contributions of the gas-venting pulse of the one-ton row and the ground-shock-induced pulse of the two-ton row. This in turn was followed by a brief negative phase and the gas-venting pulse from the two-ton row, which were followed by a final negative phase. Along the south perpendicular (nearest the subsequent detonation of the two-ton row), the first signal resulted from the nearby Primacord used for the pre-shearing holes. This was followed by the ground-shock-induced pulse of the one-ton row. The gas-venting pulse of the one-ton row is superimposed on the ground-shock-induced pulse of the two-ton row; the ground-shock-induced pulse of the two-ton row can be identified with an intermediate peak on the rising slope of the same pulse. This single positive phase was followed by a conventional negative phase.

Off the end of the rows the complex waveform and the sequence of pulses is as illustrated in Fig. 38. The ground-shock-induced pulse from the nearest one-ton charge is the first pulse observed. This is followed at an appropriate time by the gas-venting pulse from the nearest one-ton charge, superimposed on the ground-shock-induced pulse from a somewhat more distant charge in the one-ton row. Because of the 400-foot length of the rows, the interval spanned by the contribution of any one signal is approximately 0.36 second. Thus, off the end of the D-3 shot, positive-phase contributions of a given pulse are in part offset by negative-phase

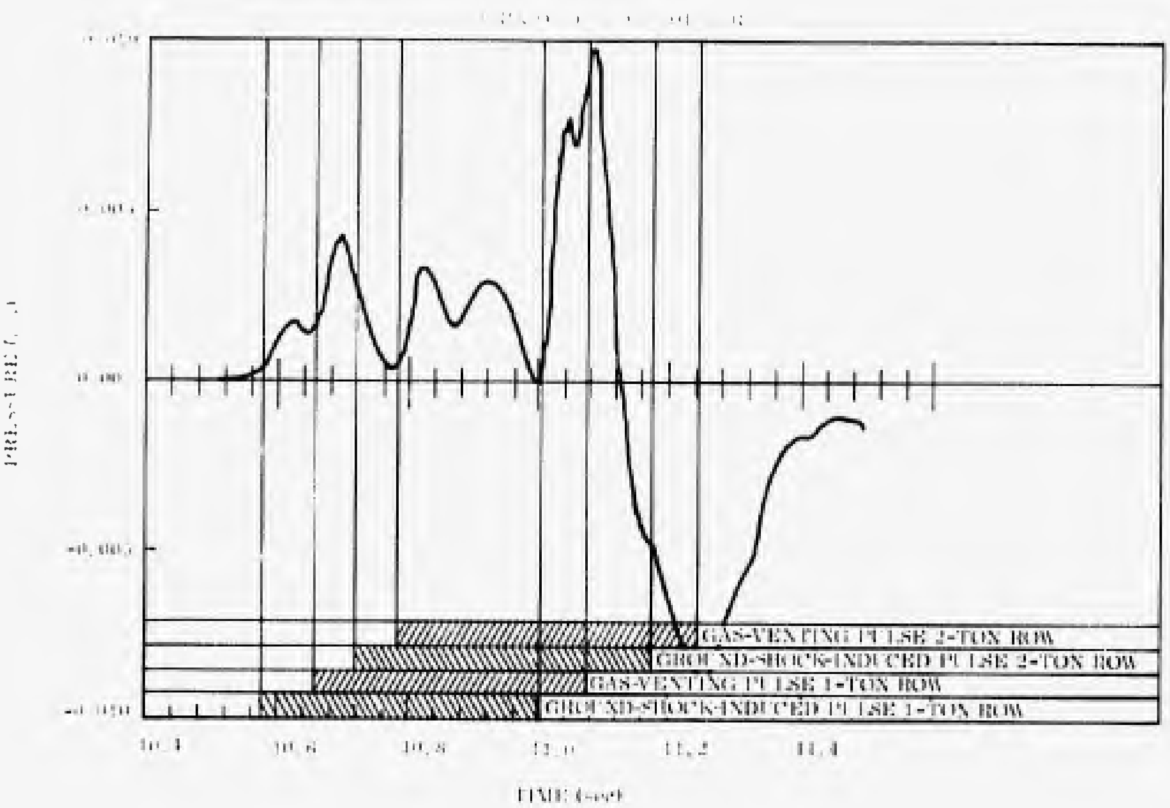

Figure 38. Sequence of airblast pulses off end of Shot D-4

contributions of earlier pulses with differences in time related to the positions of the contributing charges. In Table A-24, peaks after the first two whose source could be defined have been identified by numbers 4 through 6 because of the impossibility of assigning them a specific source.

Figure 38 shows that the final and dominant peak had contributions from the gas-venting pulse of the one-ton row, together with gas-venting and ground-shock-induced peaks from the two-ton row. The train of positive pulses was followed by a substantial negative phase.

Peak Overpressures -- Figure 39 shows ground-shock-induced peak overpressures both perpendicular to and off the ends of the rows. Those along the north perpendicular are from 2.3 to almost 10 times those measured off the end, the difference being due to the very low attenuation rate of ground-shock-induced peaks along the north perpendicular. The single measurement along the south perpendicular had values approximately 75 percent of those measured along the north perpendicular. Rates of attenuation off the end of the row are greater than those for gas-venting peaks from the one-ton row (Fig. 40), but are in agreement with those of the third peak measured off the end of the row (Fig. 41).

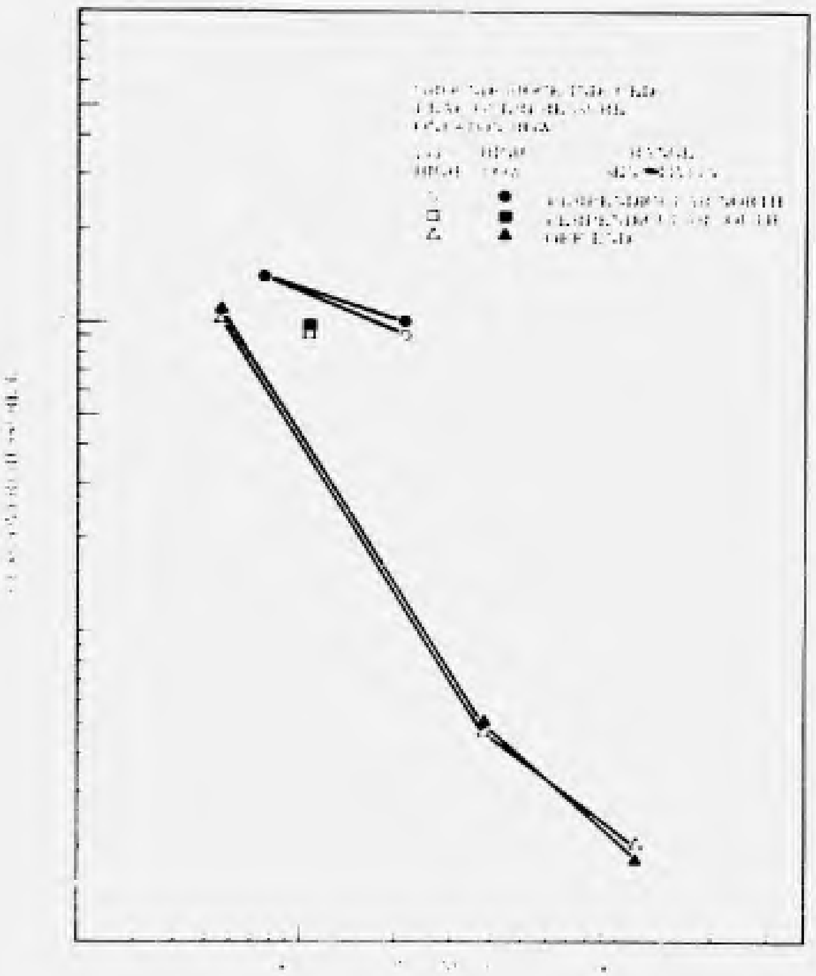

Figure 39. Peak ground-shock-induced overpressures vs distance for Shot D-4

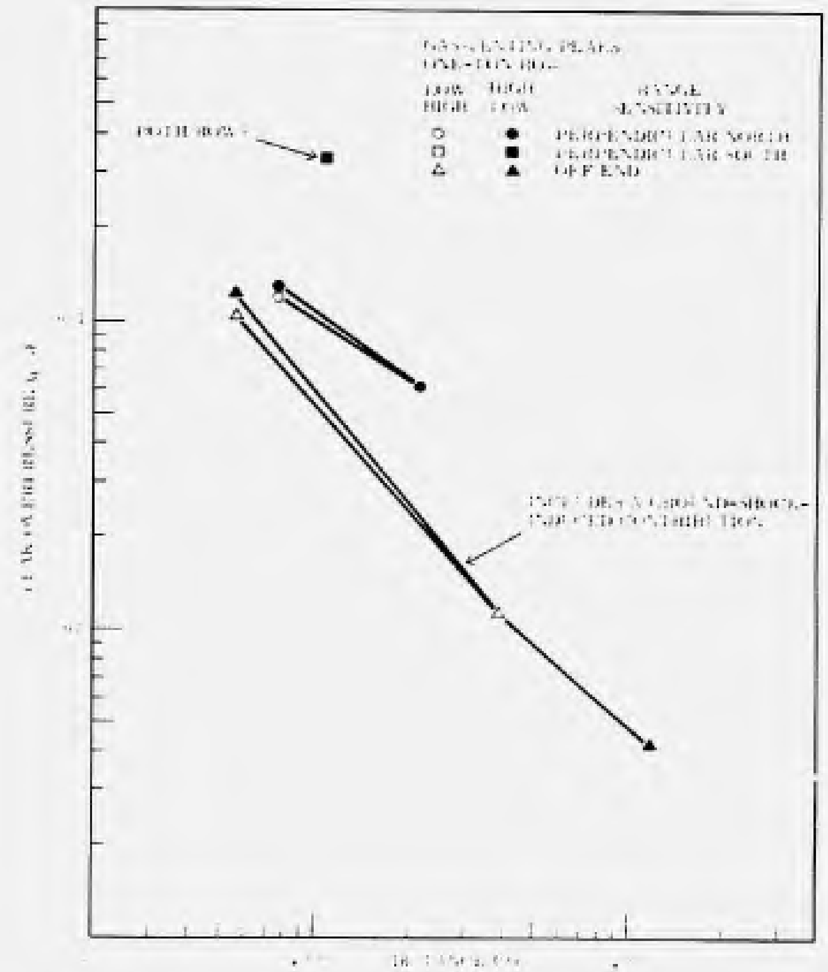

Figure 40. Peak gas-venting overpressures vs distance for Shot D-4

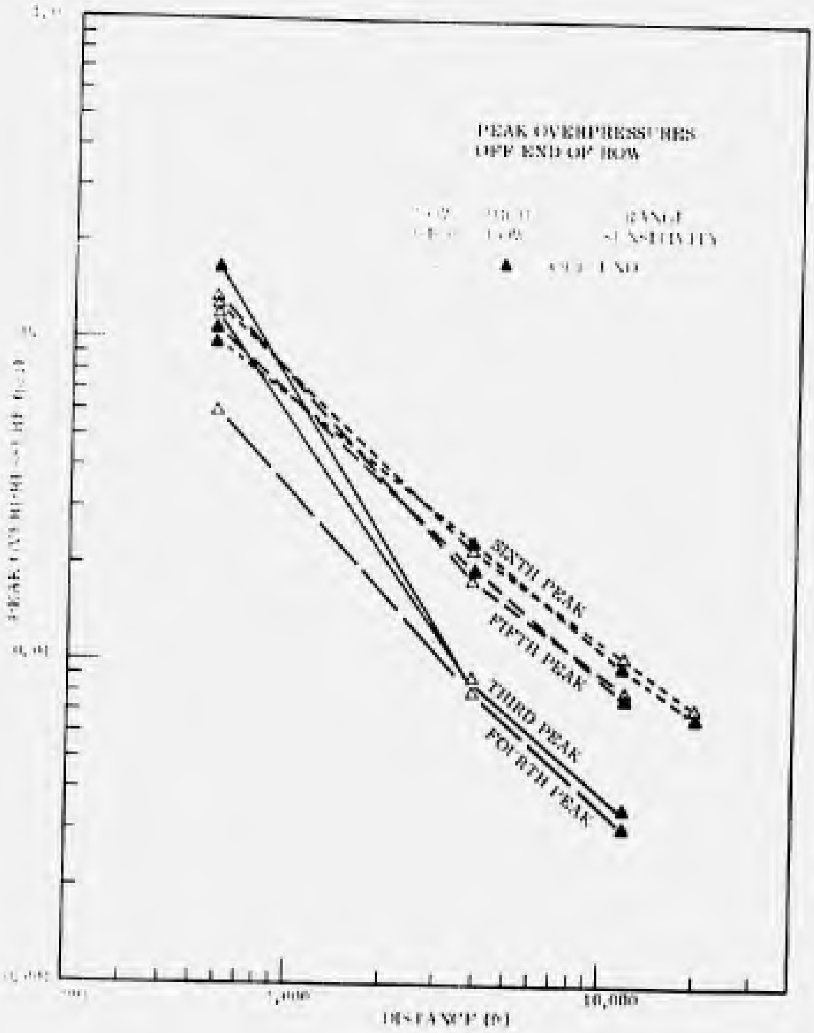

Figure 41. Unassigned peak overpressures vs distance from Shot D-4

Gas-venting peaks measured along the north perpendicular attenuated more rapidly than did the ground-shock-induced peaks, but, again, less rapidly than gas-venting peaks measured off the ends (Fig. 40). Those measured along the north perpendicular were from 1.7 to 2.5 times those measured off the end. Values measured along the south perpendicular were considerably larger because the gas-venting peaks of the two rows coincided.

Figure 42 shows the peak overpressures measured perpendicular to the two-ton rows. Only here was it possible to clearly define a contribution of the two-ton rows. As stated above, measurements along the south perpendicular were large because of the contributions of the other row. Ground-shock-induced peaks measured along the south perpendicular were larger than those along the north perpendicular by about 30 percent, but the latter includes an inseparable contribution from the gas-venting pulse of the one-ton row.

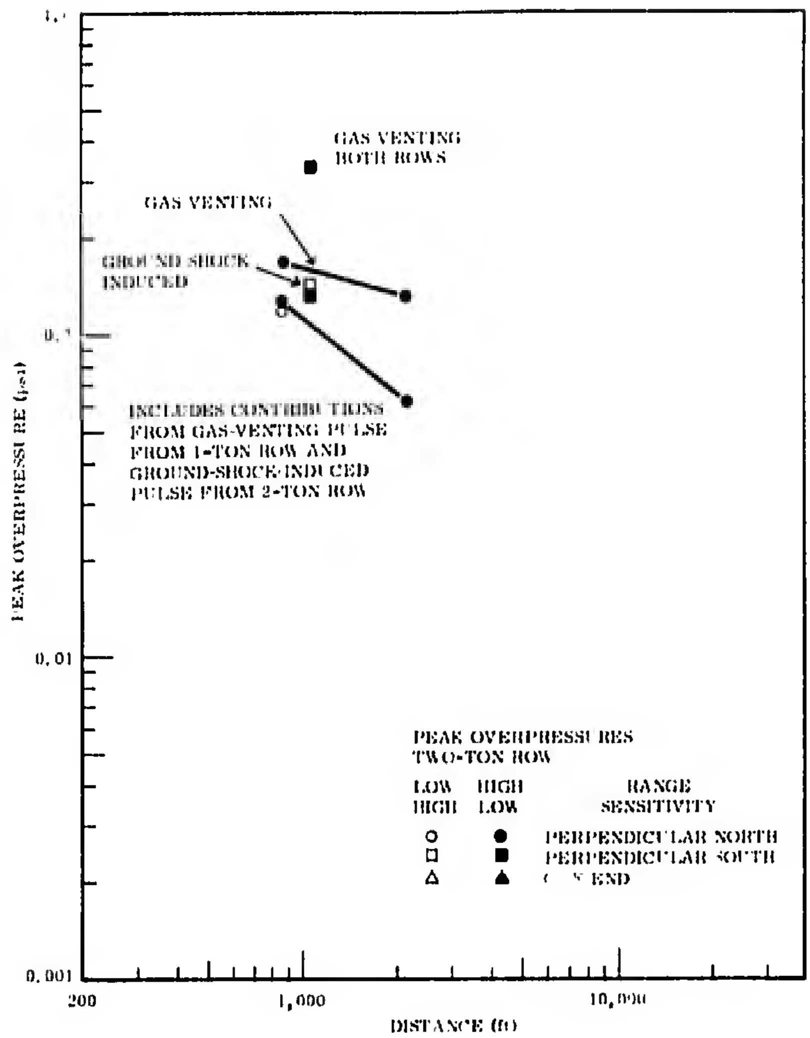

Figure 42. Peak overpressure vs distance from 2-ton row of Shot D-4

The four peaks that follow the ground-shock-induced and gas-venting peaks measured off the ends of the rows are shown in Fig. 41. The third and fourth peaks become nearly equal by the second and third stations. It should be kept in mind that the divergence at the closest station may be a result of those records having been purged of electrically induced amplitude shifts. The fifth and sixth peaks, which constitute the dominant pulse measured off the ends, were nearly equal and attenuated at about the same rate. The dominant peak observed at the Trinidad station has been attributed to attenuation of the sixth peak solely on the basis of the extrapolation illustrated in Fig. 41.

Positive-Phase Impulse -- Positive-phase impulse measured along the south perpendicular was approximately 40 percent greater than that measured along either the north perpendicular or off the ends of the rows (Fig. 43). Values measured at the close station along the north perpendicular were 80 percent of those measured off the end, whereas those measured at the far station were 50 percent greater.

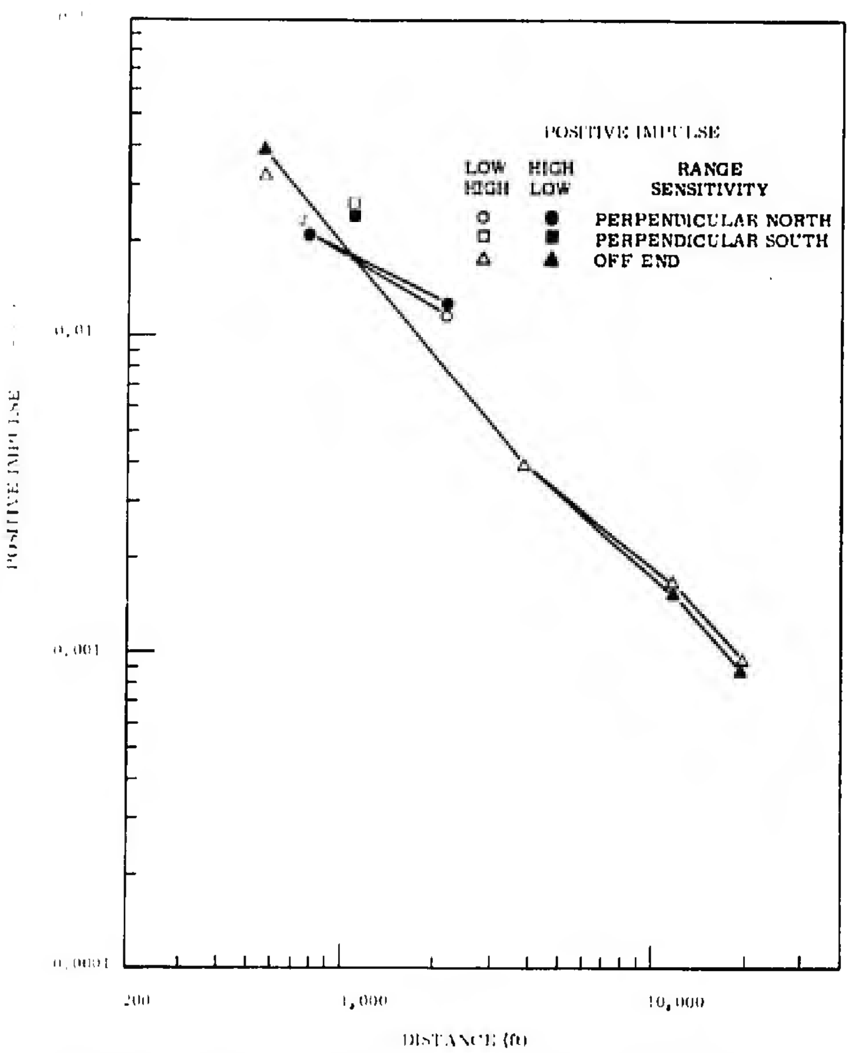

Figure 43. Positive impulse vs distance from Shot D-4

Damage Potential of TRINIDAD Airblast

Maximum overpressures recorded at Trinidad were 0.0067 to 0.009 psi on Shot B-11, where a focus was recorded. Probabilities of damage, based on San Antonio experience for the Medina explosion, were shown[25] to be

$$D = 3.71 \times 10^{-3} A^{1.22} \Delta p^{2.78}$$

where D is damage intensity in broken panes per thousand, A is pane area in square feet, and Δp is incident overpressure in millibars. Numbers of typical pane sizes for San Antonio in 1963 are shown in Table VIII, together with the total glass in Trinidad based on the 1970 census, and an assumption that the two cities are alike in glass distribution as related to population. (The difference in the ages of the cities may detract from the accuracy of the assumption, but there is no way to verify this.) Assuming modal values of 1, 6, 25, and 50 ft^2 respectively for size categories A through D gives breakage probabilities (per thousand) of 0.00043, 0.0038, 0.022, and 0.051 for 0.0067 psi, and 0.00099, 0.0088, 0.050, and 0.117 for 0.009 psi. Relating these probabilities to the estimated window census for Trinidad leads to the probabilities of breakage shown on the last two lines of Table VIII for the two overpressures. It was noted earlier that the differences in overpressure were related to the overpressure spike rather than to the overall wave; i.e., impulses were equal. Since the large value came from the more sensitive gage, it may be the more accurate of the two.

TABLE VIII

Probability of Glass Breakage

	Pane Size Category				
	A	B	C	D	
	2 ft^2	2-9 ft^2	9-40 ft^2	40 ft^2	Total
Panes/Person in San Antonio	10.6	8.20	0.14	0.04	19.0
Thousands of Panes in Trinidad	103.0	79.7	1.36	0.39	184.45
Broken Panes Expected at 0.0067 psi	0.044	0.303	0.030	0.020	0.40
Broken Panes Expected at 0.009 psi	0.103	0.701	0.068	0.046	0.92

Table VIII suggests that the probability of breaking even one pane in Trinidad was less than one. More than three months after Shot B-11, no claims for glass breakage had been filed. Since probability increases as $\Delta p^{2.78}$, it would appear that from a purely economic standpoint, overpressures 2 or 3 times larger would have been acceptable for a project of the magnitude of TRINIDAD. It also should be noted that the next highest overpressure recorded at Trinidad was about half that observed on Shot B-11.

Summary and Conclusions

Airblast measurements were made on Project TRINIDAD as functions of distance on 24 detonations. There were nine buried single charges; four were detonated on or near the surface, and one was detonated at the bottom of a 14-inch unstemmed hole. There were three simultaneously detonated single rows with different combinations of spacing and burial depth, two nonsimultaneously detonated rows, and one shot involving simultaneous detonation of two equal parallel rows. The last series consisted of four detonations, the first three being side-hill cuts, and the last a cross-hill cut. The first detonation involved nine unequal charges with unequal spacings and burial depths. The second was a simultaneous five-charge detonation with uniform charge weight, spacing, and burial depth. The third side-hill cut consisted of six one-ton charges detonated 0.25 second before detonation of a row of six two-ton charges 40 feet from the one-ton row.

The three buried single charges of ANFO gave ground-shock-induced peak overpressures approximately equal to those of TNT, but the gas-venting peak overpressures were approximately 10 times those to be expected from a TNT shot. Ground-shock-induced peak overpressures from the AANS detonations were about twice those to be expected from TNT detonations, whereas the gas-venting peaks were 2-10 times greater. By contrast, positive-phase impulses were almost exactly what would have been expected from TNT detonations.

The four surface and near-surface bursts gave no consistent differences that could be attributed to charge location with respect to the surface. Peak overpressures and impulses were close to those previously measured on surface detonations of TNT or ANFO. Meteorological effects on blast attenuation with distance were more pronounced than the effects of height or depth of burst.

A one-ton AANS charge detonated at a depth of 20.9 feet at the bottom of a 14-inch-diameter unstemmed hole gave peak overpressures approximately midway between those of an equivalent surface burst and those of a completely stemmed detonation at the same burial depth. The energy in the airblast from the unstemmed hole was approximately 10 times that of a stemmed shot and 1/20th that of an equivalent surface burst.

For the simultaneous rows, the ground-shock-induced peak overpressures were approximately equal. Closer spacing and an increase in the number of charges from five to seven for the closest spacing was insufficient to offset the decrease in gas-venting peak overpressures caused by the greater burial depths. (However, the two additional charges for the shot with the closest spacing and greatest burial depth did increase the positive-phase impulse for that shot.)

The two nonsimultaneous row-charge detonations had delays of 25 and 50 milliseconds between detonations of each two charges. Perpendicular to the rows, the ground-shock-induced peaks were approximately equal to but below those from an equivalent simultaneous detonation. Off the end at which the first charge was detonated, the ground-shock-induced peaks again were approximately equal to and less than for a simultaneous detonation. On the opposite end, the ground-shock-induced peaks for the 50-millisecond delay were less than for the 25-millisecond delay; the peaks for the latter were greater than for a simultaneous detonation. Perpendicular to the rows, gas-venting peak overpressures for the 50-millisecond delay were twice those for the 25-millisecond delay. On the end opposite the initiated end, gas-venting peak overpressures were 1.25 times and 1.4 times those off the initiated end for the 50- and 25-millisecond delays respectively. Perpendicular to the row, positive-phase impulses for both delayed shots were approximately 2-1/2 times those for a simultaneous detonation. Off the initiated end, impulses were about equal to those perpendicular to the row, and off the opposite end, they were 1.4 and 1.6 times the impulses of a simultaneous detonation for the 50- and 25-millisecond delays respectively.

Ground-shock-induced peak overpressures perpendicular to the simultaneous double-row detonation were approximately twice those of a single-row detonation, whereas off the end they were from 2 to 2-1/2 times as great. Gas-venting peak overpressures both perpendicular and off the end were 4 to 5 times those of a single-row detonation. Gas-venting peak overpressures measured perpendicular to the double row were 1.3 to 1.5 times those measured off the ends of the rows. Positive-phase impulses showed little azimuthal variation, and those measured perpendicular to the double row were approximately three times those measured perpendicular to a single row.

An effort to relate the number of charges to the ratios of row-charge airblast to single-charge airblast parameters showed no consistent agreement with earlier work for which relationships had been derived.

The unequal-charge side-hill cut, where measurements were made both uphill and downhill perpendicular to the row, showed that terrain effects were relatively small. Ground-shock-induced peak overpressures measured on that detonation were 8 times the gas-venting peak overpressures. The five-charge side-hill cut had gas-venting peaks larger than ground-shock-induced peaks perpendicular to the row; they were smaller off the end of the row. Ground-shock-induced peaks perpendicular to the row were 1.5 times those off the end, whereas gas-venting peaks were 4 to 5 times those observed off the end.

The delayed detonation of a one-ton and two-ton row provided complex waveforms, especially off the ends of the rows; there the waveform consisted of three approximately equal peaks. The first two were identified as the ground-shock-induced and gas-venting peaks of the one-ton row and the third as a gas-venting peak from the two-ton row detonated 0.25 second later. The ground-shock-induced peak for the two-ton row was counteracted by the negative phase following the gas-venting pulse from the one-ton row. Perpendicular to the rows, the largest of the three peaks was less than 50 percent greater than the small one. Off the end of the rows, the three peaks were approximately equal in the 2,000-4,000 feet range, but at greater distances the gas-venting peaks from the two-ton row attenuated more rapidly than the rest.

The delayed one-ton and two-ton cross-hill cut gave peak ground-shock-induced overpressures perpendicular to the one-ton row (detonated first) that were greater than those perpendicular to the two-ton row. Gas-venting peak overpressures perpendicular to the two-ton row were more than three times those in the opposite direction, due to the addition of pulses from both rows. The complex waveforms off the ends of the rows had six distant peaks. The first was clearly associated with the ground-shock-induced pulse from the nearest one-ton charge. The second was attributed to the gas-venting pulse of that same charge, together with a contribution from the ground-shock-induced pulses of a more distant one-ton charge. The four subsequent peaks, including the largest and last, were a result of complex interaction of positive and negative pulses from several charges. Azimuthal variation of positive impulse was not pronounced.

Maximum overpressure recorded at Trinidad on any shot was 0.009 psi. Estimates of a window census for Trinidad suggest that the probability of breaking even one window was close to one.

REFERENCES

1. Vaile, R. B., Jr., Surface Structure Program, Underground Explosion Tests At Dugway, AFSWP-298, Stanford Research Institute, Menlo Park, California, March 1952.

2. Doll, E. B., High Explosive Tests, Operation Jangle, WT-365, Armed Forces Special Weapons Project, October-November 1951.

3. Sachs, D. C., and Swift, L. M., Small Explosion Tests Project MOLE, Vols. I and II, AFSWP-291, Stanford Research Institute, Menlo Park, California, December 1955.

4. Murphey, B. F., and Ames, E. S., Air Pressure Versus Depth of Burst, SC-TM-42-59(51), Sandia Laboratories, Albuquerque, New Mexico, February 1959.

5. Vortman, L. J., et al, 20-Ton HE Cratering Experiment in Desert Alluvium, Project STAGECOACH, SC-4596(RR), Sandia Laboratories, Albuquerque, New Mexico, May 1962.

6. Perret, W. R., et al, Project SCOOTER Final Report, SC-4602(RR), Sandia Laboratories, Albuquerque, New Mexico, October 1963.

7. Unpublished data, The CAPSA Series, Sandia Laboratories, Albuquerque, New Mexico.

8. Murphey, B. F., High Explosive Crater Studies: Tuff, SC-4574(RR), Sandia Laboratories, Albuquerque, New Mexico, April 1961.

9. Vortman, L. J., et al, 20-Ton and 1/2-Ton High Explosive Cratering Experiments in Basalt Rock, Project BUCKBOARD, SC-4675(RR), Sandia Laboratories, Albuquerque, New Mexico, November 1960.

10. Reed, J. W., and Vortman, L. J., Airblast Measurements, Project PRE-SCHOONER II, PNE-512F, Sandia Laboratories, Albuquerque, New Mexico, February 1968.

11. Kurtz, M. K., Jr., Project PRE-GONDOLA I, PNE-1102, U. S. Army Corps of Engineers, Nuclear Cratering Group, Livermore, California, May 1968.

12. Vortman, L. J., Airblast from Project TUGBOAT Detonations, SC-1212-70-541, Sandia Laboratories, Albuquerque, New Mexico, November 1970.

13. Keefer, J. M., Jackson, W. F., and Lefevre, D. P., "Close-in Airblast from a Row of Buried Charges," Ballistic Research Laboratories, Aberdeen Proving Ground, Maryland, Chapter in Project PRE-GONDOLA II, Summary Report, U. S. Corps of Engineers, Nuclear Cratering Group, Livermore, California, to be published.

14. Vortman, L. J., "Close-in Airblast Measurements," Sandia Laboratories, Albuquerque, New Mexico, Chapter in Project PRE-GONDOLA III, Phase I, Summary Report, PNE-1114, U. S. Corps of Engineers, Nuclear Cratering Group, Livermore, California.

15. Vortman, L. J., Airblast and Craters from Rows of Two to Twenty-five Charges, SC-RR-68-655, Sandia Laboratories, Albuquerque, New Mexico, January 1969.

16. Vortman, L. J., Close-in Airblast from a Row Charge in Basalt, PNE-608F Sandia Laboratories, Albuquerque, New Mexico, August 4, 1965.

17. Kirkwood, J. G., and Brinkley, S. R., Jr., Theoretical Blast-Wave Curves for Cast TNT, OSRD-5481, Office of Scientific Research and Development, August 23, 1945.

18. Lehto, D. L., and Larson, R. A., Long Range Propagation of Spherical Shock Waves from Explosions in Air, NOLTR-69-88, U. S. Naval Ordnance Laboratory, White Oak, Silver Spring, Maryland, July 22, 1969.

19. Kingery, C. N., and Pannill, B. F., Peak Overpressure vs. Scaled Distance for TNT Surface Bursts (Hemispherical Charges), BRL-MR-1518, Ballistic Research Laboratories, Aberdeen Proving Ground, Maryland, April 1964.

20. Sadwin, L. D., and Pittman, J. F., Airblast Characteristics of AN/FO, Phase I, NOLTR-69-82, U. S. Naval Ordnance Laboratory, White Oak, Maryland, April 30, 1969.

21. Sadwin, L. D., and Swisdak, M. M., Jr., Blast Characteristics of 20 and 100 Ton Hemispherical AN/FO Charges, NOL Data Report, NOLTR-70-32, U. S. Naval Ordnance Laboratory, White Oak, Maryland, March 17, 1970.

22. Vortman, L. J., "Close-in Airblast From Underground Detonations" in Procedings of Symposium on Engineering with Nuclear Explosives, January 14-16, 1970. The American Nuclear Society and the U. S. Atomic Energy Commission, May 1970, pp. 1508-1543.

23. Kingery, C. N., Air Blast Parameters Versus Distance for Hemispherical TNT Surface Bursts, BRL R 1344, Aberdeen Proving Ground, Maryland, September 1966.

24. Reed, J. W., PRE-GONDOLA III-Microbarograph Measurements, PNE-1118, Sandia Laboratories, Albuquerque, New Mexico, to be published.

25. Reed, J. W., Pape, B. J., Minor, J. E., and DeHart, R. C., Evaluation of Window Pane Damage Intensity in San Antonio Resulting from Medina Facility Explosion on November 13, 1963, Annals of the New York Academy of Sciences, Vol. 152, Art. 1, October 28, 1968.

BLANK PAGE

APPENDIX A

Summary of Airblast Measurements

TABLE A-1

Summary of Airblast Measurements

Shot No. B-1

Date 08-13-70
Time 0900
Temp. 67°F

Depth 15.2 ft.
Expl. ANFO
Wind SSW 5-6

Station	1L	1H	2L	2H	3L	3H
Distance	400	400	900	900	2000	2000
Canister	3	3	4	4	5	5
Gage	D39998	D44001	S1741	D44067	S1745	S1632
Expected Overpressure (psi)	0.4	1.0	0.15	0.325	0.032	0.10
Cal Step (psi)	0.307	1.36	0.093	0.25	0.031	0.051
Arrival Time (sec)	0.265	0.269	0.710	0.710	1.682	1.683
Ground-shock-induced-peak (psi)	0.08	0.054	0.022	0.020	0.0081	0.0094
Time of Peak (sec)	0.272	0.272	0.715	0.716	1.686	1.688
Gas Venting Peak (psi)	0.805	0.48	>0.162(limited)	0.18	Limited	0.076
Time of Peak (sec)	0.287	0.288	0.726	0.727	-	1.696
Negative Peak (psi)	0.27	0.215	0.049	0.045	0.0175	0.02
Time of Peak (sec)	0.329	0.328	0.776	0.778	1.749	1.751
Positive Impulse (psi-sec)	0.0079	0.0061	0.00278	0.00273	>0.00088	0.00124
Negative Impulse (psi-sec)	0.0090	0.0067	0.00341	0.00325	>0.00125	0.00138

TABLE A-2

Summary of Airblast Measurements

Shot No. B-2

Date 08-14-70
Time 1100
Temp. 90°F

Depth 18.0 ft.
Expl. ANFO
Wind Calm

Station	1L	1H	2L	2H	3L	3H
Distance	350	350	850	850	2000	2000
Canister	3	3	4	4	5	5
Gage	D39998	D44001	S1741	D44067	S1745	S1632
Expected Overpressure (psi)	0.4	1.0	0.15	0.325	0.032	0.1
Cal Step (psi)	0.307	1.36	0.093	0.25	0.031	0.051
Arrival Time (sec)	No Record	No Record	~0.760	~0.760	1.759	1.758
Ground-shock-induced Peak (psi)	No Record	No Record	0.0070 ± 0.0015	0.0073 ± 0.0015	0.00290	0.00324
Time of Peak (sec)	No Record	No Record	0.779	0.781	1.782	1.784
Gas Venting Peak (psi)	No Record	No Record	0.0120 ± 0.0015	0.0118 ± 0.0015	0.0044	0.0046
Time of Peak (sec)	No Record	No Record	0.880	0.871	1.873	1.878
Negative Peak (psi)	No Record	No Record	~0.009	0.0087 ± 0.0015	0.0036	0.0041
Time of Peak (sec)	No Record	No Record	~0.980	0.986	1.984	1.995
Positive Impulse (psi-sec)	No Record	No Record	0.00091	0.00092	0.00033	0.00034
Negative Impulse (psi-sec)	No Record	No Record	0.00114	0.00110	0.00041	0.00048

TABLE A-3

Summary of Airblast Measurements

Shot No. 5-3

Date 06-12-73 Time 0810 Temp. 63°F Depth 19.7 ft. Expl. ANFO Wind SW 0-2

Station	1L	1H	2L	2H	3L	3H
Distance	230	230	720	720	2020	2020
Canister	4	4	5	5	6	6
Gage	S1471	I44067	S1745	S1632	P17844	S1626
Expected Overpressure (psi)	0.065	0.325	0.02	0.10	0.0065	0.0365
Cal Step (psi)	0.093	0.025	0.031	0.051	0.0144	0.046
Arrival Time (sec)	0.231	0.233	0.667	0.669	?	1.735
Ground-shock-induced Peak (psi)	0.038	0.043	0.0107	0.0104	?	0.00416
Time of Peak (sec)	0.239	0.240	0.675	0.676	?	1.742
Gas Venting Peak (psi)	Limited	0.255	Limited	0.082	Limited	0.0332
Time of Peak (sec)	-	0.277	-	0.711	?	1.774
Negative Peak (psi)	0.075	0.0723	0.019	0.0195	0.0047(a)	0.0084
Time of Peak (sec)	0.322	0.329	0.755	0.759	?	1.824
Positive Impulse (psi-sec)	>0.00495	0.00472	>0.00143	0.00184	>0.000485(a)	0.000656
Negative Impulse (psi-sec)	>0.00655	0.00551	>0.00210	0.00208	>0.000680(a)	0.000818

(a) Values are not correct, see text.

TABLE A-4

Summary of Airblast Measurements

Shot No. B-4

Date 08-13-70 Depth. 15.9 ft.
Time 1400 Expl. AANS
Temp. 89°F Wind NNE 7

Station	1L	1H	2L	2H	3L	3H
Distance	350	350	1000	1000	2000	2000
Canister	4	4	5	5	7	7
Gage	S1471	D44067	S1745	S1632	P12688	S1670
Expected Overpressure (psi)	0.065	0.325	0.02	0.1	0.002	0.01
Cal Step (psi)	0.093	0.25	0.031	0.051	0.0113	0.039
Arrival Time (sec)	0.324	0.325	0.896	0.897	1.774	1.772
Ground-shock-induced Peak (psi)	0.048	0.34	0.015	0.0145	0.0061	0.0066
Time of Peak (sec)	0.340	0.341	0.911	0.914	1.794	1.795
Gas Venting Peak (psi)	0.317	0.328	Limited	0.101	0.0360	0.0386
Time of Peak (sec)	0.366	0.367	-	0.936	1.819	1.818
Negative Peak (psi)	0.07	0.070	0.024	0.0245	0.011	0.0115
Time of Peak (sec)	0.471	0.477	1.059	1.061	1.899	1.900
Positive Impulse (psi-sec)	0.00681	0.00650	>0.00227	0.00246	0.00107	0.00112
Negative Impulse (psi-sec)	0.00889	0.00858	>0.00287	0.00296	0.00126	0.00135

TABLE A-5

Summary of Airblast Measurements

Shot No. B-5

Date 08-11-70
Time 1400
Temp. 81°F

Depth 18.6 ft.
Expl. AANS
Wind ENE 0-3

Station	1L	1H	2L	2H	3L	3H
Distance	295	295	810	810	1845	1845
Canister	4	4	5	5	6	6
Gage	S1471	D44067	S1745	S1632	P1784	S1626
Expected Overpressure (psi)	0.065	0.325	0.02	0.1	0.0065	0.0365
Cal Step (psi)	0.093	0.25	0.031	0.051	0.0144	0.046
Arrival Time (sec)	0.415	0.420	0.863	0.864	?	1.771
Ground-shock-induced Peak (psi)	0.057	0.057	0.021	0.0205	0.0028(a)	0.007
Time of Peak (sec)	0.427	0.429	0.875	0.877	1.801	1.777
Gas Venting Peak (psi)	0.090	0.0856	0.0315	0.0354	0.00615(a)	0.0123
Time of Peak (sec)	0.494	0.496	0.941	0.943	1.852	1.842
Negative Peak (psi)	0.043	0.0415	0.0161	0.0167	0.0047(a)	0.006
Time of Peak (sec)	0.626	0.620	1.073	1.075	1.995	1.982
Positive Impulse (psi-sec)	0.00367	0.00363	0.00141	0.00149	0.000231(a)	0.000487
Negative Impulse (psi-sec)	0.00507	0.00468	0.00182	0.00186	0.000263(a)	0.000570

(a) Values are not correct, see text.

TABLE A-6

Summary of Airblast Measurements

Shot No. B-6

Date 08-10-70 | Depth 20.9 ft.
Time 1115 | Expl. AANS
Temp. 79°F | Wind W 0-5

Station	1L	1H	2L	2H	3L	3H
Distance	163	163	510	510	1670	1670
Canister	5	5	6	6	7	7
Gage	S1745	S1632	P17844	S1626	P12688	S1670
Expected Overpressure (psi)	0.02	0.1	0.0065	0.0365	0.002	0.01
Cal Step (psi)	0.031	0.051	0.0144	0.046	0.0113	0.039
Arrival Time (sec)	0.338	0.339	?	0.659	1.643	1.646
Ground-shock-induced Peak (psi)	Limited	0.0705	0.0127(a)	0.0260	0.00803	0.0078
Time of Peak (sec)	-	0.370	0.685	0.686	1.677	1.678
Gas Venting Peak (psi)	Limited	0.0556	0.0133(a)	0.0262	0.0064	0.0064
Time of Peak (sec)	-	0.472	0.796	0.784	1.779	1.779
Negative Peak (psi)	Limited	0.0585	Limited	0.0173	Limited	0.006
Time of Peak (sec)	-	0.604	-	0.920	-	1.902
Positive Impulse (psi-sec)	>0.00427	0.0048	0.0015(a)	0.00210	0.00048	0.00052
Negative Impulse (psi-sec)	>0.00703	0.0077	0.0018(a)	0.00259	0.00062	0.00070

(a) Values are not correct, see text.

TABLE A-7

Summary of Airblast Measurements

Shot No. B-7

Date 08-12-70   Depth 22.6 ft.
Time 1440   Expl. AANS
Temp. 82°F   Wind S 9

Station	1L	1H	2L	2H	3L	3H
Distance	275	275	830	830	1630	1630
Canister	4	4	5	5	7	7
Gage	S1471	D44067	S1745	S1632	P12688	S1670
Expected Overpressure (psi)	0.065	0.325	0.02	0.10	0.002	0.01
Cal Step (psi)	0.093	0.25	0.031	0.051	0.0113	0.039
Arrival Time (sec)	0.259	0.250			1.430	1.430
Ground-shock-induced Peak (psi)	0.0264	0.0404 ± 0.005	No Record	No Record	0.00426	0.00466
Time of Peak (sec)	0.275	0.278	No Record	No Record	1.450	1.451
Gas Venting Peak (psi)	0.076	0.073 ± 0.005	No Record	No Record	0.0148	0.0149
Time of Peak (sec)	0.357	0.363	No Record	No Record	1.526	1.527
Negative Peak (psi)	0.026	0.037 ± 0.005	No Record	No Record	0.0040	0.0044
Time of Peak (sec)	0.507	0.437	No Record	No Record	1.675	1.665
Positive Impulse (psi-sec)	0.00300	0.00194	No Record	No Record	0.000464	0.000472
Negative Impulse (psi-sec)	0.00436	0.00274	No Record	No Record	0.000627	0.000633

TABLE A-8

Summary of Airblast Measurements

Shot No. B-8

Date 08-11-70 Depth 28.1 ft.
Time 0835 Expl. AANS
Temp. 67°F Wind WSW 8

Station	1L	1H	2L	2H	3L	3H
Distance	140	140	460	460	835	835
Canister	5	5	6	6	7	7
Gage	S1745	S1632	P17844	S1626	P12688	S1670
Expected Overpressure (psi)	0.02	0.1	0.0065	0.0365	0.002	0.01
Cal Step (psi)	0.031	0.051	0.0144	0.046	0.0113	0.039
Arrival Time (sec)	0.305	0.307	0.580	0.580	0.918	0.917
Ground-shock-induced Peak (psi)	Limited	0.0528	0.0101(a)	0.0190	>0.0067(lim)	0.0070
Time of Peak (sec)	-	0.329	0.620	0.616	0.951	0.951
Gas Venting Peak (psi)	0.0104	0.0107	0.0015(a)	0.0046	0.00117	0.0015
Time of Peak (sec)	0.491	0.495	0.779	0.772	1.115	1.124
Negative Peak (psi)	0.0123	0.0145	0.00375(a)	0.0052	0.0018	0.0023
Time of Peak (sec)	0.684	0.684	0.968	0.950	1.304	1.281
Positive Impulse (psi-sec)	>0.00193	0.00189	0.00075(a)	0.000869	0.000360	0.00037
Negative Impulse (psi-sec)	>0.00393	0.00499	0.00118(a)	0.00139	0.000518	0.00052

(a) Values are not correct, see text.

TABLE A-9

Summary of Airblast Measurements

Shot No. B-10

Date 10-8-7[illegible] Time [illegible] Temp. [illegible] F

Depth 3.6 ft. above surface Expl. [illegible] Wind [illegible]

Station	1 L	1 H	2 L	2 H	Tilda L	Tilda H	Sopris L	Sopris H	Piedmont L	Piedmont H	Jansen L	Jansen H	Trinidad L	Trinidad H
Distance	724	724	1840	1840	3941	3941	10,620	10,620	16,350	16,350	20,750	20,750	32,400	32,400
Canister	1	1	2	2	3	3	4	4	9	9	5	5	10	10
Gage	44487	[illegible]	44061	44060	39968	[illegible]	1784	44001	1782	44068	1745	[illegible]	[illegible]	[illegible]
Set Range (psi)	7.5	[illegible]	7.5	2.5	[illegible]	2.5	0.15	0.5	0.15	0.5	0.15	[illegible]	0.15	0.15
Cal Step (psi)	2.54	4.7	[illegible]	0.485	0.33	[illegible]	0.098	0.25	0.031	0.117	0.031	0.51	0.0689	0.033
Arrival Time (sec)	0.570	0.570	1.603	1.604	3.587	3.575	9.699	9.699	14.965	14.985	19.144	19.143	30.146	30.139
Positive Peak (psi)	0.51	0.59	0.225	0.230(a)	0.060	0.063	0.0114	0.0110	0.0079	0.0065	0.00405	0.00425	0.00168(b)	0.00146
Time of Peak (sec)	0.576	0.577	1.610	1.609	3.594	3.583	9.753	9.755	15.050	15.058	19.226	19.227	30.235	30.241
Negative Peak (psi)	0.205	0.30	0.096	0.309(a)	0.038	0.035	0.0105	0.0110	0.0063	0.0058	0.00240	[illegible]	0.00104(b)	0.00090,0.00152
Time of Peak (sec)	0.703	0.686	1.759	1.757	3.741	3.737	9.942	9.911	15.203	15.199	19.339	19.372	30.404	30.409
Positive Impulse (psi-sec)	0.0162	0.0177	0.0068	0.0067(a)	0.0028	0.0029	0.00100	0.00098	0.00066	0.00060	0.000551	0.000400	0.000149(b)	0.000136
Negative Impulse (psi-sec)	0.0170	0.0196	0.0076	0.0073(a)	0.0031	0.0033	0.00109	0.00109	0.00071	0.00062	0.000343	0.000340	0.000197(b)	0.000185

(a) Recorded values multiplied by 1.37 to correct for unstable calibration.

(b) Recorded values multiplied by 0.87 to correct for unstable calibration.

TABLE A-10

Summary of Airblast Measurements

Shot No. [illegible]

Date [illegible] Time [illegible] Temp. [illegible]

Depth 1.0 ft. above surface Expl. [illegible] Wind [illegible]

Station	[illegible] L	[illegible] H	[illegible] L	[illegible] H	[illegible] L	[illegible] H	[illegible] L	[illegible] H	[illegible] L	[illegible] H	[illegible] L	[illegible] H	Trinidad L	Trinidad H
Distance	[illegible]	[illegible]	[illegible]	[illegible]	[illegible]	[illegible]	10,645	10,645	[illegible]	[illegible]	[illegible]	[illegible]	32,300	[illegible]
[illegible]	[illegible]	[illegible]	[illegible]	[illegible]	3	3	4	4	[illegible]	9	[illegible]	5	[illegible]	[illegible]
Gage	[illegible]	[illegible]	[illegible]	[illegible]	[illegible]	[illegible]	1791	[illegible]	[illegible]	[illegible]	[illegible]	[illegible]	[illegible]	[illegible]
Set Range (psi)	[illegible]	[illegible]	[illegible]	[illegible]	[illegible]	[illegible]	[illegible]	0.5	[illegible]	[illegible]	[illegible]	[illegible]	0.15	0.15
Arrival Time (ms)	[illegible]	[illegible]	[illegible]	[illegible]	[illegible]	[illegible]	[illegible]	[illegible]	[illegible]	[illegible]	[illegible]	[illegible]	29,900	29,900
Positive Peak (psi)	[illegible]	[illegible]	[illegible]	[illegible]	[illegible]	[illegible]	[illegible]	[illegible]	[illegible]	[illegible]	[illegible]	[illegible]	[illegible]	[illegible]
Time of Peak (ms)	[illegible]	[illegible]	[illegible]	[illegible]	[illegible]	[illegible]	[illegible]	[illegible]	[illegible]	[illegible]	[illegible]	[illegible]	[illegible]	[illegible]
Negative Peak (psi)	[illegible]	[illegible]	[illegible]	[illegible]	[illegible]	[illegible]	[illegible]	[illegible]	[illegible]	[illegible]	[illegible]	[illegible]	[illegible]	[illegible]
Time of Peak (ms)	[illegible]	[illegible]	[illegible]	[illegible]	[illegible]	[illegible]	[illegible]	[illegible]	[illegible]	[illegible]	[illegible]	[illegible]	[illegible]	[illegible]
Positive Impulse (psi-sec)	[illegible]	[illegible]	[illegible]	[illegible]	[illegible]	[illegible]	[illegible]	[illegible]	[illegible]	[illegible]	[illegible]	[illegible]	[illegible]	[illegible]
Negative Impulse (psi-sec)	[illegible]	[illegible]	[illegible]	[illegible]	[illegible]	[illegible]	[illegible]	[illegible]	[illegible]	[illegible]	[illegible]	[illegible]	[illegible]	[illegible]

(a) Measured value multiplied by [illegible]

(b) Measured value multiplied by [illegible]

TABLE A-11

Summary of Airblast Measurements

[illegible]	[illegible]	[illegible]	[illegible]	[illegible]	[illegible]	[illegible]	[illegible]	[illegible]	[illegible]	[illegible]	[illegible]	[illegible]
[illegible]	[illegible]	[illegible]	[illegible]	[illegible]	[illegible]	[illegible]	[illegible]	[illegible]	[illegible]	[illegible]	[illegible]	[illegible]
[illegible]	[illegible]	[illegible]	[illegible]	[illegible]	[illegible]	[illegible]	[illegible]	[illegible]	[illegible]	[illegible]	[illegible]	[illegible]
[illegible]	[illegible]	[illegible]	[illegible]	[illegible]	[illegible]	[illegible]	[illegible]	[illegible]	[illegible]	[illegible]	[illegible]	[illegible]
[illegible] (psi)	[illegible]	[illegible]	[illegible]	[illegible]	[illegible]	[illegible]	[illegible]	[illegible]	[illegible]	[illegible]	[illegible]	[illegible]
[illegible] (psi)	[illegible]	[illegible]	[illegible]	[illegible]	[illegible]	[illegible]	[illegible]	[illegible]	[illegible]	[illegible]	[illegible]	[illegible]
Arrival Time (sec)	[illegible]	[illegible]	[illegible]	[illegible]	[illegible]	[illegible]	[illegible]	[illegible]	[illegible]	[illegible]	[illegible]	[illegible]
Positive Peak (psi)	[illegible]	[illegible]	[illegible]	[illegible]	[illegible]	[illegible]	[illegible]	[illegible]	[illegible]	[illegible]	[illegible]	[illegible]
Time of Peak (sec)	[illegible]	[illegible]	[illegible]	[illegible]	[illegible]	[illegible]	[illegible]	[illegible]	[illegible]	[illegible]	[illegible]	[illegible]
Negative Peak (psi)	[illegible]	[illegible]	[illegible]	[illegible]	[illegible]	[illegible]	[illegible]	[illegible]	[illegible]	[illegible]	[illegible]	[illegible]
Time of Peak (sec)	[illegible]	[illegible]	[illegible]	[illegible]	[illegible]	[illegible]	[illegible]	[illegible]	[illegible]	[illegible]	[illegible]	[illegible]
Positive Impulse (psi-sec)	[illegible]	[illegible]	[illegible]	[illegible]	[illegible]	[illegible]	[illegible]	[illegible]	[illegible]	[illegible]	[illegible]	[illegible]
Negative Impulse (psi-sec)	[illegible]	[illegible]	[illegible]	[illegible]	[illegible]	[illegible]	[illegible]	[illegible]	[illegible]	[illegible]	[illegible]	[illegible]

(a) True peak not recorded.

(b) Measured values multiplied by [illegible]

TABLE A-12

Summary of Airblast Measurements

[illegible]	[illegible]	[illegible]	[illegible]	[illegible]	[illegible]	[illegible]	[illegible]	[illegible]	[illegible]	[illegible]	[illegible]	[illegible]	[illegible]	[illegible]
[illegible]	[illegible]	[illegible]	[illegible]	[illegible]	[illegible]	[illegible]	[illegible]	[illegible]	[illegible]	[illegible]	[illegible]	[illegible]	[illegible]	[illegible]
[illegible]	[illegible]	[illegible]	[illegible]	[illegible]	[illegible]	[illegible]	[illegible]	[illegible]	[illegible]	[illegible]	[illegible]	[illegible]	[illegible]	[illegible]
[illegible]	[illegible]	[illegible]	[illegible]	[illegible]	[illegible]	[illegible]	[illegible]	[illegible]	[illegible]	[illegible]	[illegible]	[illegible]	[illegible]	[illegible]
[illegible]	[illegible]	[illegible]	[illegible]	[illegible]	[illegible]	[illegible]	[illegible]	[illegible]	[illegible]	[illegible]	[illegible]	[illegible]	[illegible]	[illegible]
[illegible]	[illegible]	[illegible]	[illegible]	[illegible]	[illegible]	[illegible]	[illegible]	[illegible]	[illegible]	[illegible]	[illegible]	[illegible]	[illegible]	[illegible]
[illegible]	[illegible]	[illegible]	[illegible]	[illegible]	[illegible]	[illegible]	[illegible]	[illegible]	[illegible]	[illegible]	[illegible]	[illegible]	[illegible]	[illegible]
[illegible]	[illegible]	[illegible]	[illegible]	[illegible]	[illegible]	[illegible]	[illegible]	[illegible]	[illegible]	[illegible]	[illegible]	[illegible]	[illegible]	[illegible]
[illegible]	[illegible]	[illegible]	[illegible]	[illegible]	[illegible]	[illegible]	[illegible]	[illegible]	[illegible]	[illegible]	[illegible]	[illegible]	[illegible]	[illegible]
[illegible]	[illegible]	[illegible]	[illegible]	[illegible]	[illegible]	[illegible]	[illegible]	[illegible]	[illegible]	[illegible]	[illegible]	[illegible]	[illegible]	[illegible]
[illegible]	[illegible]	[illegible]	[illegible]	[illegible]	[illegible]	[illegible]	[illegible]	[illegible]	[illegible]	[illegible]	[illegible]	[illegible]	[illegible]	[illegible]
[illegible]	[illegible]	[illegible]	[illegible]	[illegible]	[illegible]	[illegible]	[illegible]	[illegible]	[illegible]	[illegible]	[illegible]	[illegible]	[illegible]	[illegible]
[illegible]	[illegible]	[illegible]	[illegible]	[illegible]	[illegible]	[illegible]	[illegible]	[illegible]	[illegible]	[illegible]	[illegible]	[illegible]	[illegible]	[illegible]

TABLE A-13

Summary of Airblast Measurements

[illegible]

Date [illegible] Depth [illegible]
Time [illegible] Rep. [illegible]
Temp. [illegible] Wind [illegible]

Station	1 L	1 R	2 L	2 R	Vicia L	Vicia R	Carpet L	Carpet R	[illegible] L	[illegible] R
Distance	[illegible]	[illegible]	[illegible]	[illegible]	3830	[illegible]	[illegible]	[illegible]	[illegible]	[illegible]
Canister	[illegible]	[illegible]	[illegible]	[illegible]	5	5	[illegible]	[illegible]	[illegible]	[illegible]
Gage	[illegible]	[illegible]	[illegible]	[illegible]	[illegible]	[illegible]	[illegible]	[illegible]	[illegible]	[illegible]
Set Range (psi)	1.0	2.5	0.15	0.5	0.25	0.15	0.15	0.15	[illegible]	[illegible]
Cal Step (psi)	0.11	0.41	0.031	0.117	[illegible]	[illegible]	0.0016	[illegible]	[illegible]	[illegible]
Arrival Time (sec)	0.574	0.583	1.565	1.551	3.459	3.440	(a)	(a)	−25.75	−25.75
[illegible]-and-shock-induced Peak (psi)	1	1	0.0075	0.0065	0.00290	0.00231	(a)	(a)	0.0067	0.0054
Time of Peak (sec)	T	T	1.597	1.598	3.496	3.494	(a)	(a)	−25.78	−25.78
Gas Venting Peak (psi)	.016	.017	0.0066	0.0055	0.00185	0.00086	(a)	(a)	0.0044	0.0042
Time of Peak (sec)	0.634	0.666	1.657	1.697	3.560	3.359	(a)	(a)	−25.835	−25.635
Negative Peak (psi)	0.013	0.024	0.0057	0.0053	0.00095	0.00211	(a)	(a)	0.0047	0.0065
Time of Peak (sec)	0.839	0.851	1.814	1.834	3.730	3.781	(a)	(a)	−30.02	−30.02
Positive Impulse (psi-sec)	0.00175	0.00177	0.000487	0.000471	0.000213	0.000271	(a)	(a)	0.0000376	0.0000386
Negative Impulse (psi-sec)	0.00180	0.00182	0.000777	0.000606	0.000251	0.000289	(a)	(a)	0.0000574	0.0000612

(a) Lost.

TABLE A-14

Summary of Airblast Measurements

Shot No. [illegible]

Date [illegible]   Depth 20.0 ft.
Time [illegible]   Expl. [illegible]
Temp. [illegible]   Wind [illegible]

Station	BP L	BP H	11 L	11 H	2 L	2 H	Viola-High L	Viola-High H	Viola-Low L	Viola-Low H	Jansen L	Jansen H	Trinidad L	Trinidad H
Distance	500	500	500	500	1900	1900	2938	2938	2238	2238	14,45[illegible]	14,4[illegible]	21,190	21,190
Transducer	2	2	9	9	4	4	3	3	5	5	[illegible]	[illegible]	11	11
Gage	44971	46060	1742	[illegible]	1741	[illegible]	39908	44002	[illegible]	1630	1641	[illegible]	1763	1677
Set Range (psi)	2.5	2.5	0.15	0.5	0.15	0.5	1.0	2.5	0.15	0.15	0.15	0.5	0.15	0.15
Cal Step (psi)	[illegible]	0.485	0.041	0.117	0.043	0.75	0.11	0.41	0.032	0.051	[illegible]	[illegible]	0.0042	0.0054
Arrival Time (sec)	0.519	0.52[illegible]	0.521	0.519	1.018	(b)	1.996	1.996	2.004	2.006	17.[illegible]	17.[illegible]	28.296	28.292
First Positive Peak (psi)	0.1183(c)	0.1970(c)	0.1519	0.1570	0.0456	(b)	0.0317	0.0391	0.0229	0.0300	[illegible]	[illegible]	0.0029	0.00135
Time of Peak (sec)	0.527	0.525	0.524	0.523	1.029	(b)	2.004	2.002	2.013	2.012	[illegible]	[illegible]	28.322	28.327
Second Positive Peak (psi)	0.0297(c)	0.0463(c)	0.0996	0.0976	0.032	(b)	0.0293	0.0251	0.0219	0.0214	[illegible]	[illegible]	0.00227	0.00146
Time of Peak (sec)	0.536	0.534	0.534	0.536	~1.095	(b)	2.034	2.075	2.049	2.049	17.7[illegible]	17.7[illegible]	28.424	28.421
First Negative Peak (psi)	[illegible]	[illegible]	[illegible]	[illegible]	0.0043	(b)	0.0056	0.0180	0.0116	0.0112	[illegible]	[illegible]	0.00196	0.00156
Time of Peak (sec)	0.597	0.559	0.557	0.555	1.056	(b)	2.037	2.037	2.044	2.046	17.775	17.775	28.[illegible]	28.[illegible]
Second Negative Peak (psi)	[illegible]	[illegible]	[illegible]	[illegible]	0.012	(b)	~0.008	~0.008	0.008	~0.008	-	-	-	-
Time of Peak (sec)	[illegible]	[illegible]	[illegible]	[illegible]	~1.2[illegible]	(b)	~2.017	~2.017	2.0176	~2.017	-		-	-
Total Positive Impulse (psi-sec)	[illegible]	[illegible]	[illegible]	[illegible]	[illegible]	(b)	0.00087	0.0084	[illegible]	[illegible]	[illegible]	[illegible]	[illegible]	0.00086
Total Negative Impulse (psi-sec)	[illegible]	[illegible]	[illegible]	[illegible]	[illegible]	(b)	0.00109	0.0048	0.00099	[illegible]	[illegible]	[illegible]	[illegible]	[illegible]

(a) Limited.

(b) Lost.

(c) Values are suspect.

TABLE A-15

Summary of Airblast Measurements

[illegible]	[illegible]	[illegible]	[illegible]	[illegible]	[illegible]	[illegible]	[illegible]	[illegible]	[illegible]	[illegible]	[illegible]	[illegible]	[illegible]	[illegible]	[illegible]	[illegible]	[illegible]	[illegible]
[illegible]	[illegible]	[illegible]	[illegible]	[illegible]	[illegible]	[illegible]	[illegible]	[illegible]	[illegible]	[illegible]	[illegible]	[illegible]	[illegible]	[illegible]	[illegible]	[illegible]	[illegible]	[illegible]
[illegible]	[illegible]	[illegible]	[illegible]	[illegible]	[illegible]	[illegible]	[illegible]	[illegible]	[illegible]	[illegible]	[illegible]	[illegible]	[illegible]	[illegible]	[illegible]	[illegible]	[illegible]	[illegible]
[illegible] (psi)	[illegible]	[illegible]	[illegible]	[illegible]	[illegible]	[illegible]	[illegible]	[illegible]	[illegible]	[illegible]	[illegible]	[illegible]	[illegible]	[illegible]	[illegible]	[illegible]	[illegible]	[illegible]
[illegible] (psi)	[illegible]	[illegible]	[illegible]	[illegible]	[illegible]	[illegible]	[illegible]	[illegible]	[illegible]	[illegible]	[illegible]	[illegible]	[illegible]	[illegible]	[illegible]	[illegible]	[illegible]	[illegible]
Arrival Time (sec)	[illegible]	[illegible]	[illegible]	[illegible]	[illegible]	[illegible]	[illegible]	[illegible]	[illegible]	[illegible]	[illegible]	[illegible]	[illegible]	[illegible]	[illegible]	[illegible]	[illegible]	[illegible]
[illegible] peak (psi)	[illegible]	[illegible]	[illegible]	[illegible]	[illegible]	[illegible]	[illegible]	[illegible]	[illegible]	[illegible]	[illegible]	[illegible]	[illegible]	[illegible]	[illegible]	[illegible]	[illegible]	[illegible]
Time of Peak (sec)	[illegible]	[illegible]	[illegible]	[illegible]	[illegible]	[illegible]	[illegible]	[illegible]	[illegible]	[illegible]	[illegible]	[illegible]	[illegible]	[illegible]	[illegible]	[illegible]	[illegible]	[illegible]
2nd Positive Peak (psi)	[illegible]	[illegible]	[illegible]	[illegible]	[illegible]	[illegible]	[illegible]	[illegible]	[illegible]	[illegible]	[illegible]	[illegible]	[illegible]	[illegible]	[illegible]	[illegible]	[illegible]	[illegible]
Time of Peak (sec)	[illegible]	[illegible]	[illegible]	[illegible]	[illegible]	[illegible]	[illegible]	[illegible]	[illegible]	[illegible]	[illegible]	[illegible]	[illegible]	[illegible]	[illegible]	[illegible]	[illegible]	[illegible]
Negative Peak (psi)	[illegible]	[illegible]	[illegible]	[illegible]	[illegible]	[illegible]	[illegible]	[illegible]	[illegible]	[illegible]	[illegible]	[illegible]	[illegible]	[illegible]	[illegible]	[illegible]	[illegible]	[illegible]
Time of Peak (sec)	[illegible]	[illegible]	[illegible]	[illegible]	[illegible]	[illegible]	[illegible]	[illegible]	[illegible]	[illegible]	[illegible]	[illegible]	[illegible]	[illegible]	[illegible]	[illegible]	[illegible]	[illegible]
Positive Impulse (psi-sec)	[illegible]	[illegible]	[illegible]	[illegible]	[illegible]	[illegible]	[illegible]	[illegible]	[illegible]	[illegible]	[illegible]	[illegible]	[illegible]	[illegible]	[illegible]	[illegible]	[illegible]	[illegible]
Negative Impulse (psi-sec)	[illegible]	[illegible]	[illegible]	[illegible]	[illegible]	[illegible]	[illegible]	[illegible]	[illegible]	[illegible]	[illegible]	[illegible]	[illegible]	[illegible]	[illegible]	[illegible]	[illegible]	[illegible]

NOTES: Tamp- A = [illegible]
B = [illegible]
C = [illegible]
D = [illegible]
E = [illegible]

AVERAGE: [illegible] ft/lb[1/3]

(a) Transmitter drifted off band.
(b) Includes undefinable contributions from [illegible] of the ground surface.
(c) Calibration limited, wave shape is valid.
(d) Values are questionable because of unstable calibration steps; wave shape is valid.
(e) Measured values have been multiplied by [illegible] to correct for unstable calibration; probable accuracy ± 25 per cent.

TABLE A-16

Summary of Airblast Measurements

Shot No. [illegible]

Date [illegible] — Depth [illegible] — Time [illegible] — Expl. [illegible] — Temp. [illegible] — Wind [illegible]

Station	[illegible] L	[illegible] R	[illegible] L	[illegible] R	[illegible] L	[illegible] R	[illegible] L	[illegible] R	[illegible] L	[illegible] R	[illegible] L	[illegible] R	Jansen L	Jansen R	Trinidad L	Trinidad R
Distance	[illegible]	[illegible]	[illegible]	[illegible]	[illegible]	[illegible]	[illegible]	[illegible]	[illegible]	[illegible]	[illegible]	[illegible]	[illegible]	[illegible]	[illegible]	[illegible]
Transducer	[illegible]	[illegible]	[illegible]	[illegible]	[illegible]	[illegible]	[illegible]	[illegible]	[illegible]	[illegible]	[illegible]	[illegible]	[illegible]	[illegible]	7	7
Gage	[illegible]	[illegible]	[illegible]	[illegible]	[illegible]	[illegible]	[illegible]	[illegible]	[illegible]	[illegible]	[illegible]	[illegible]	[illegible]	[illegible]	[illegible]	[illegible]
Cal. Range (psi)	[illegible]	[illegible]	[illegible]	[illegible]	[illegible]	[illegible]	[illegible]	[illegible]	[illegible]	[illegible]	[illegible]	[illegible]	[illegible]	[illegible]	[illegible]	[illegible]
Cal. Step (psi)	[illegible]	[illegible]	[illegible]	[illegible]	[illegible]	[illegible]	[illegible]	[illegible]	[illegible]	[illegible]	[illegible]	[illegible]	[illegible]	[illegible]	[illegible]	[illegible]
Arrival Time (sec)	[illegible]	[illegible]	[illegible]	[illegible]	[illegible]	[illegible]	[illegible]	[illegible]	[illegible]	[illegible]	[illegible]	[illegible]	[illegible]	[illegible]	[illegible]	[illegible]
Ground-shock-induced peak (psi)	[illegible]	[illegible]	[illegible]	[illegible]	(a)	(a)	[illegible]	[illegible]	[illegible]	[illegible]	[illegible]	[illegible]	[illegible]	[illegible]	(a)	[illegible]
Time of Peak (sec)	[illegible]	[illegible]	[illegible]	[illegible]	(a)	(a)	[illegible]	[illegible]	[illegible]	[illegible]	[illegible]	[illegible]	[illegible]	[illegible]	(a)	[illegible]
Gas Venting Peak (psi)	[illegible]	[illegible]	[illegible]	[illegible]	(a)	(a)	[illegible]	[illegible]	[illegible]	[illegible]	[illegible]	[illegible]	[illegible]	[illegible]	(a)	[illegible]
Time of Peak (sec)	[illegible]	[illegible]	[illegible]	[illegible]	(a)	(a)	[illegible]	[illegible]	[illegible]	[illegible]	[illegible]	[illegible]	[illegible]	[illegible]	(a)	[illegible]
Negative Peak (psi)	[illegible]	[illegible]	[illegible]	[illegible]	(a)	(a)	[illegible]	[illegible]	[illegible]	[illegible]	[illegible]	[illegible]	[illegible]	[illegible]	(a)	[illegible]
Time of Peak (sec)	[illegible]	[illegible]	[illegible]	[illegible]	(a)	(a)	[illegible]	[illegible]	[illegible]	[illegible]	[illegible]	[illegible]	[illegible]	[illegible]	(a)	[illegible]
Positive Impulse (psi-sec)	[illegible]	[illegible]	[illegible]	[illegible]	(a)	(a)	[illegible]	[illegible]	[illegible]	[illegible]	[illegible]	[illegible]	[illegible]	[illegible]	[illegible]	[illegible]
Negative Impulse (psi-sec)	[illegible]	[illegible]	[illegible]	[illegible]	(a)		[illegible]	[illegible]	[illegible]	[illegible]	[illegible]	[illegible]	[illegible]	[illegible]	[illegible]	[illegible]

DEPTHS: [illegible]

AVERAGE: [illegible]

(a) Record noisy and unreadable.
(b) Record lost.
(c) Transmitter drifted out of band.
(d) [illegible]
(e) [illegible]

TABLE A-17

Summary of Airblast Measurements

Shot No. [illegible]

Date [illegible] Depth See below
Time [illegible] Yield [illegible]
Temp. ___ Wind [illegible]

Station	[illegible] L	[illegible] H	[illegible] L	[illegible] H	[illegible] L	[illegible] H	E-1 L	E-1 H	E-2 L	E-2 H	E-3 L	E-3 H	[illegible] L	[illegible] H	Trinidad L	Trinidad H
Distance	949	949	1530	1530	2390	2390	447	447	[illegible]	[illegible]	9791	9791	[illegible]	[illegible]	[illegible]	[illegible]
Canister	3	3	9	9	10	10	4	4	5	5	11	11	[illegible]	[illegible]	[illegible]	[illegible]
Gage	39998	44001	1742	44068	1667	1744	1741	44067	1745	3432			[illegible]	[illegible]	[illegible]	[illegible]
Set Range (psi)	0.1	0.4	0.03	0.12	0.04	0.04	0.04	0.15	0.0125	0.05	0.004	0.015	[illegible]	[illegible]	0.004	0.005
Cal Step (psi)	0.11	0.41	0.031	0.117	[illegible]	[illegible]	0.0093	0.85	0.031	[illegible]	[illegible]	[illegible]	[illegible]	[illegible]	[illegible]	0.0137
Arrival Time (sec)	0.304	0.305	1.368	~1.334	~2.900	~2.900	0.408	0.408	1.029	1.030	[illegible]	[illegible]	[illegible]	[illegible]	(a)	(a)
Ground-shock-induced peak (psi)	0.109	0.101	0.0188	0.0042	[illegible]	[illegible]	0.042,0.066	0.036,0.060	[illegible]	[illegible]	[illegible]	[illegible]	[illegible]	[illegible] (c)	(a)	(a)
Time of Peak (sec)	0.331	0.330	1.397	1.394	[illegible]	2.946	0.416,0.438	0.417,0.439	[illegible]	[illegible]	[illegible]	[illegible]	[illegible]	[illegible]	(a)	(a)
Max Venting Peak (psi)	0.0947	0.048	0.0127	0.0140	0.0050	0.0048	0.0298	0.0281	0.0113	0.0115	[illegible]	[illegible]	[illegible]	[illegible] (c)	(a)	(a)
Time of Peak (sec)	0.467	0.467	1.544	1.555	3.093	3.094	0.379	0.381	1.206	1.206	[illegible]	[illegible]	[illegible]	[illegible]	(a)	(a)
Negative Peak (psi)	0.046	0.042	0.0110	0.0106	0.0043	0.0046	0.032	0.0304	0.0107	0.0113	[illegible] (c)	0.0048	[illegible]	[illegible] (c)	(a)	(a)
Time of Peak (sec)	0.684	0.644	1.865	1.858	3.370	3.370	0.793	0.790	1.450	1.433	2.904	2.906	17.972	17.974	(a)	(a)
Positive Impulse (psi-sec)	0.0094	0.00896	0.0025	0.0022	0.00108	0.00103	0.0065	0.0072	0.00252	0.00263	0.00137(c)	0.00099	0.000195	0.000188 (c)	(a)	(a)
Negative Impulse (psi-sec)	0.0138	0.0130	0.0034	0.0031	0.00149	0.00145	0.0097	0.0092	0.00346	0.00305	0.00209(b)	0.00149	0.000225	0.000206 (c)	(a)	(a)

DEPTHS: Charge A - 23.15
B - 22.[illegible]
C - 23.[illegible]
D - 22.[illegible]
E - 22.7
F - 22.7
G - 23.55

AVERAGE: 23.04 (1.83 ft/lb$^{1/3}$)

(a) Station not on.
(b) Values are [illegible] high; reason unknown.
(c) Measured values have been multiplied by 1.55 to correct for unstable calibration; probable accuracy ± 15 per cent

TABLE A-18

Summary of Airblast Measurements

Shot No. [illegible]

Station	[illegible]	[illegible]	[illegible]	[illegible]	[illegible]	[illegible]	[illegible]	[illegible]	[illegible]	[illegible]	[illegible]	[illegible]	Jasper L	Jasper H	Trinidad L	Trinidad H
Distance	[illegible]	[illegible]	[illegible]	[illegible]	[illegible]	[illegible]	[illegible]	[illegible]	[illegible]	[illegible]	[illegible]	[illegible]	[illegible]	[illegible]	51,400	51,400
Canister	[illegible]	[illegible]	[illegible]	[illegible]	[illegible]	[illegible]	[illegible]	[illegible]	[illegible]	[illegible]	[illegible]	[illegible]	[illegible]	[illegible]	7	7
Gage	[illegible]	[illegible]	[illegible]	[illegible]	[illegible]	[illegible]	[illegible]	[illegible]	[illegible]	[illegible]	[illegible]	[illegible]	[illegible]	[illegible]	[illegible]	[illegible]
Set Range (psi)	[illegible]	[illegible]	[illegible]	[illegible]	[illegible]	[illegible]	[illegible]	[illegible]	[illegible]	[illegible]	[illegible]	[illegible]	[illegible]	[illegible]	[illegible]	0.009
Cal Step (psi)	[illegible]	[illegible]	[illegible]	[illegible]	[illegible]	[illegible]	[illegible]	[illegible]	[illegible]	[illegible]	[illegible]	[illegible]	[illegible]	[illegible]	[illegible]	[illegible]
Arrival Time (sec)	[illegible]	[illegible]	[illegible]	[illegible]	[illegible]		[illegible]	[illegible]	[illegible]	[illegible]	(b)	(b)	[illegible]	[illegible]	(a)	(a)
Ground-shock-induced peak (psi)	[illegible]	[illegible]	[illegible]	[illegible]	[illegible]	[illegible]	[illegible]	[illegible]	[illegible]	[illegible]	(b)	(b)			(a)	(a)
Time of Peak (sec)	[illegible]	[illegible]	[illegible]	[illegible]	[illegible]	[illegible]	[illegible]	[illegible]	[illegible]	[illegible]	(b)	(b)			(a)	(a)
Max Positive Peak (psi)	[illegible]	[illegible]	[illegible]	[illegible]	[illegible]	[illegible]	[illegible]	[illegible]	[illegible]	[illegible]	(b)	(b)	[illegible]	[illegible](c)	(a)	(a)
Time of Peak (sec)	[illegible]	[illegible]	[illegible]	[illegible]	[illegible]	[illegible]	[illegible]	[illegible]	[illegible]	[illegible]	(b)	(b)	[illegible]	[illegible]	(a)	(a)
Negative Peak (psi)	[illegible]	[illegible]	[illegible]	[illegible]	[illegible]	[illegible]	[illegible]	[illegible]	[illegible]	[illegible]	(b)	(b)	[illegible]	[illegible](c)	(a)	(a)
Time of Peak (sec)	[illegible]	[illegible]	[illegible]	[illegible]	[illegible]	[illegible]	[illegible]	[illegible]	[illegible]	[illegible]	(b)	(b)	[illegible]	[illegible]	(a)	(a)
Positive Impulse (psi-sec)	[illegible]	[illegible]	[illegible]	[illegible]	[illegible]	[illegible]	[illegible]	[illegible]	[illegible]	[illegible]	(b)	(b)	[illegible]	[illegible](c)	(a)	(a)
Negative Impulse (psi-sec)	[illegible]	[illegible]	[illegible]	[illegible]	[illegible]	[illegible]	[illegible]	[illegible]	[illegible]	[illegible]	(b)	(b)	[illegible]	[illegible](c)	(a)	(a)

(a) Station not [illegible].

(b) Signal could not be transmitted from station location.

(c) Measured values have been multiplied by [illegible] to correct for [illegible] calibration; probable accuracy ± [illegible] per cent.

TABLE A-19

Summary of Airblast Measurements

Shot No. [illegible]

Date [illegible] Time [illegible] Temp. ______ Depth See below Rel. [illegible] Wind [illegible]

Station	[illegible] L	[illegible] H	[illegible] L	[illegible] H	1EI L	1EI H	LED L	LED H	2E1 L	2E1 H	2RE L	2RE H	[illegible] 1	[illegible] 2	[illegible] 1	[illegible] 2
Distance	[illegible]	[illegible]	[illegible]	[illegible]	[illegible]	[illegible]	2452	2452	[illegible]	[illegible]	[illegible]	[illegible]	[illegible]	[illegible]	[illegible]	[illegible]
Canister	3	3	4	5	4	4	19	10	2	2	5	5	*	*	*	*
Gage	[illegible]	[illegible]	[illegible]	[illegible]	[illegible]	[illegible]	1667	1744	4400.1	4400.0	[illegible]	[illegible]	[illegible]	[illegible]	[illegible]	[illegible]
Set Range (psi)	[illegible]	[illegible]	0.075	[illegible]	[illegible]	[illegible]	0.098	0.087	0.175	[illegible]	0.13	[illegible]	[illegible]	[illegible]	[illegible]	[illegible]
Cal Step (psi)	[illegible]	[illegible]	0.051	0.107	0.098	[illegible]	0.0099	0.0156	[illegible]	0.488	0.032	[illegible]	0.0604	0.0108	0.0013	0.0107
Arrival Time (sec)	~0.3	~0.35	1.348	~1.380	~0.42	0.41	2.122	2.14	0.590	~0.4	1.176	1.100	17.378		(a)	(a)
Ground-shock-induced peak (psi)	~0.021	0.024	0.0073	.0067	.0090	0.0164	0.00326	0.0047	0.0449	0.041	0.0233	0.026	[illegible]	0.00075(b)	(a)	(a)
Time of Peak (sec)	~0.38	~0.35	1.401	1.400	0.460	0.462	2.181	2.150	0.664	0.660	1.157	1.157	~17.4	~17.4	(a)	(a)
Gas Venting Peak (psi)	0.047	0.04	0.06	.0524	0.0350,0.0137	0.0946,0.0855	0.0100,0.0800	0.00773,0.0046	0.0438	0.040	0.0245	0.0304	0.0018,0.0012	0.0004,0.00092(b)	(a)	(a)
Time of Peak (sec)	0.710	~0.710	1.543	~1.540	0.595,0.005	0.578,0.605	2.309,2.389	2.310,2.384	0.750	0.755	1.275	1.274	~17.5,~17.575	~17.5,~17.575	(a)	(a)
Negative Peak (psi)	~0.021	~0.024	0.006	~0.008	0.0025	0.017	0.0046,0.00763	0.00296,0.0056	0.0387	0.032	0.0034	0.0029	0.0016	0.0006(b)	(a)	(a)
Time of Peak (sec)	~0.70	~0.70	1.73	~1.73	0.717	0.714	2.436,2.690	2.436,2.681	0.861	0.865	1.379	1.384	17.65	17.65	(a)	(a)
Positive Impulse (psi-sec)	0.0027(d)	0.0050	0.001	0.0025	0.00390	0.0033	0.00100	0.00088	0.0058	0.0047	0.0025	0.0034	0.00011	(c)	(a)	(a)
Negative Impulse (psi-sec)	0.0064(d)	0.0065	0.0037	0.0029	0.00496	0.005	0.0155	0.00138	0.0062	0.0063	0.0034	0.0042	0.000350	(c)	(a)	(a)

DEPTHS: Charge A = 19.9
B = 20.4
C = 20.0
D = 20.15
E = 20.5

AVERAGE: 20.19 (1.60 ft/lb$^{1/3}$)

(a) Station not on.

(b) Measured values have been multiplied by 1.8 to correct for [illegible] calibration; probably accuracy ± 15 per cent.

(c) Integration not valid

(d) Doubtful value.

TABLE A-20

Summary of Airblast Measurements

Shot No. [illegible]

Date [illegible] Depth See below
Time [illegible] Expl. [illegible]
Temp. [illegible] Wind [illegible]

Station	[illegible] I	[illegible] H	[illegible] I	[illegible] H	[illegible] I	[illegible] H	K-1 I	K-1 H	[illegible] I	[illegible] H	K-3 I	K-3 H	[illegible] I	[illegible] H	Trinidad I	Trinidad H
Distance	[illegible]	[illegible]	[illegible]	[illegible]	[illegible]	[illegible]	[illegible]	[illegible]	[illegible]	[illegible]	[illegible]	[illegible]	[illegible]	[illegible]	31,300	31,300
Canister	[illegible]	[illegible]	[illegible]	[illegible]	[illegible]	[illegible]	[illegible]	[illegible]	[illegible]	[illegible]	18	[illegible]	[illegible]	[illegible]	7	7
Gage	[illegible]	[illegible]	[illegible]	[illegible]	[illegible]	[illegible]	[illegible]	[illegible]	[illegible]	[illegible]	[illegible]	[illegible]	[illegible]	[illegible]	[illegible]	[illegible]
Set Range (psi)	[illegible]	[illegible]	[illegible]	[illegible]	[illegible]	[illegible]	[illegible]	[illegible]	[illegible]	[illegible]	0.01	0.04	[illegible]	[illegible]	[illegible]	0.009
Cal Step (psi)	[illegible]	[illegible]	[illegible]	[illegible]	[illegible]	[illegible]	[illegible]	[illegible]	[illegible]	[illegible]	[illegible]	[illegible]	[illegible]	[illegible]	[illegible]	0.0027
Arrival Time (sec)	(b)	[illegible]	[illegible]	[illegible]	[illegible]	[illegible]	[illegible]	[illegible]	[illegible]	(b)	[illegible]	[illegible]	[illegible]	[illegible]	[illegible]	~28.0
Groundshock-induced peak (psi)	(b)	[illegible]	[illegible]	[illegible]	[illegible]	[illegible]	[illegible](a)	[illegible]	[illegible]	(b)	[illegible]	[illegible]	-	-	-	-
Time of Peak (sec)	(b)	[illegible]	[illegible]	[illegible]	[illegible]	[illegible]	[illegible]	[illegible]	[illegible]	(b)	[illegible]	[illegible]	-	-	-	-
Gas Venting Peak (psi)	(b)	[illegible]	[illegible]	[illegible]	[illegible]	[illegible]	[illegible]	[illegible]	[illegible]	(b)	[illegible]	[illegible]	[illegible]	[illegible](e)	[illegible](d)	0.00087(d)
Time of Peak (sec)	(b)	[illegible]	[illegible]	[illegible]	[illegible]	[illegible]	[illegible]	[illegible]	[illegible]	(b)	[illegible]	[illegible]	[illegible]	17.7	[illegible]	28.102
Negative Peak (psi)	(b)	[illegible]	[illegible]	[illegible]	[illegible]	[illegible]	[illegible]	[illegible]	[illegible]	(b)	[illegible]	[illegible]	[illegible]	[illegible](e)	[illegible](d)	0.00035(d)
Time of Peak (sec)	(b)	[illegible]	[illegible]	[illegible]	[illegible]	[illegible]	[illegible]	[illegible]	[illegible]	(b)	[illegible]	[illegible]	[illegible]	[illegible]	28.2	28.200
Positive Impulse (psi-sec)	(b)	[illegible]	[illegible]	[illegible]	[illegible]	[illegible]	[illegible]	[illegible]	[illegible]	(b)	[illegible]	[illegible]	[illegible]	[illegible](e)	0.000059(d)	0.00005(d)
Negative Impulse (psi-sec)	(b)	[illegible]	[illegible]	[illegible]	[illegible]	[illegible]	[illegible]	[illegible]	[illegible]	(b)	[illegible]	[illegible]	[illegible]	[illegible](e)	0.000070(d)	0.00008(d)

DEPTHS: [illegible]

AVERAGE: [illegible]

(a) May be premature spike.
(b) Lost.
(c) Measured values have been multiplied by 1.7 to correct for unstable [illegible] probable accuracy ± 15 per cent.
(d) Values are questionable because of unstable calibration steps [illegible].
(e) Measured values have been multiplied by [illegible] based on calibration step of [illegible] to correct for unstable calibration step.

TABLE A-21

Summary of Airblast Measurements

Shot No. [illegible]

Date 1-17-70 | Time 1115 | Temp. 51 F | Depth See below | Expl. AANFO | Wind NE 5

Station	[illegible] L	[illegible] H	[illegible] L	[illegible] H	DS-1 L	DS-1 H	DS-2 L	DS-2 H	E-1 L	E-1 H	E-2 L	E-2 H	[illegible] L	[illegible] H	[illegible] L	[illegible] H
Distance	[illegible]	[illegible]	[illegible]	[illegible]	775	775	[illegible]	1900	700	704	3260	3260	[illegible]	[illegible]	[illegible]	[illegible]
Transducer	[illegible]	[illegible]	5	5	[illegible]	8	[illegible]	10	4	4	7	7	11	[illegible]	4	[illegible]
Gage	[illegible]	[illegible]	1749	[illegible]	[illegible]	[illegible]	897	1944	1961	4487	[illegible]	[illegible]	1743	1827	[illegible]	[illegible]
Set Range (psi)	[illegible]	[illegible]	[illegible]	[illegible]	[illegible]	[illegible]	[illegible]	0.09	[illegible]	[illegible]	[illegible]	[illegible]	[illegible]	[illegible]	[illegible]	[illegible]
Cal Step (psi)	[illegible]	[illegible]	[illegible]	[illegible]	[illegible]	[illegible]	[illegible]	[illegible]	0.093	[illegible]	[illegible]	[illegible]	[illegible]	[illegible]	[illegible]	[illegible]
Arrival Time (sec)	[illegible]	[illegible]	[illegible]	[illegible]	[illegible]	[illegible]	1.619	1.621	0.636	0.636	2.096	2.098	[illegible]	[illegible]	(c)	[illegible]
Ground-shock-induced peak (psi)	[illegible]	[illegible]	[illegible]	[illegible]	[illegible]	[illegible](a)	[illegible]	0.0024	[illegible]	[illegible]	[illegible]	[illegible]	[illegible]	[illegible]	(b)	–
Time of Peak (sec)	[illegible]	[illegible]	[illegible]	[illegible]	[illegible]	[illegible](a)	[illegible]	1.676	0.706	0.706	3.067	3.066	12.450	12.509	(b)	–
Gas Venting Peak (psi)	[illegible]	[illegible]	[illegible]	0.0013	[illegible]	(a)	[illegible]	0.001	[illegible]	[illegible]	0.0013	0.0012	[illegible]	[illegible]	(b)	[illegible](c)
Time of Peak (sec)	[illegible]	[illegible]	[illegible]	[illegible]	[illegible]	(a)	[illegible]	1.899	[illegible]	[illegible]	3.279	3.278	12.747	12.745	(b)	-83.99
Negative Peak (psi)	[illegible]	[illegible]	[illegible]	[illegible]	[illegible]	0.0015(a)	[illegible]	0.0035	[illegible]	[illegible]	[illegible]	[illegible]	[illegible]	[illegible]	(b)	[illegible](c)
Time of Peak (sec)	[illegible]	[illegible]	[illegible]	[illegible]	[illegible]	[illegible](a)	[illegible]	2.052	[illegible]	[illegible]	[illegible]	[illegible]	[illegible]	[illegible]	(b)	-84.29
Positive Impulse (psi-sec)	[illegible]	[illegible]	[illegible]	[illegible]	[illegible]	[illegible](a)	[illegible]	0.00064	[illegible]	0.00162	0.00045	[illegible]	[illegible]	[illegible]	(b)	[illegible](c)
Negative Impulse (psi-sec)	[illegible]	[illegible]	[illegible]	0.00129	[illegible]	[illegible](a)	[illegible]	0.00105	[illegible]	0.00225	0.00058	0.00057	[illegible]	0.000111	(b)	[illegible](c)

Charge	Burial Depth (ft)
A	[illegible]
B	17.1
C	20.2
D	[illegible]
E	[illegible]
F	24.7
G	20.2
H	25.7
I	11.4

(a) Noisy record.
(b) Noisy and unusable record.
(c) Values measured have been multiplied by 2.1 based on D-3 calibration to correct for unstable calibration.

TABLE A-22

Summary of Airblast Measurements

Shot No. E-2

Date [illegible] | Depth See below
Time [illegible] | Expl. AANS [illegible]
Temp. [illegible] °F | Wind Calm

Station	[illegible] L	[illegible] H	[illegible]	[illegible]	E-1 L	E-1 H	E-2 L	E-2 H	E-3 L	E-3 H	Jansen L	Jansen H	Trinidad L	Trinidad H
Distance	[illegible]	[illegible]	[illegible]	[illegible]	[illegible]	[illegible]	[illegible]	2240	[illegible]	[illegible]	[illegible]	[illegible]	24,500	24,500
Canister	[illegible]	[illegible]	[illegible]	[illegible]	[illegible]	6	[illegible]	[illegible]	7	7	[illegible]	[illegible]	4	4
Gage	[illegible]	[illegible]	[illegible]	[illegible]	[illegible]	[illegible]	[illegible]	[illegible]	[illegible]	[illegible]	[illegible]	1627	1631	[illegible]
Set Range (psi)	[illegible]	[illegible]	[illegible]	[illegible]	[illegible]	[illegible]	[illegible]	[illegible]	[illegible]	[illegible]	[illegible]	[illegible]	0.0025	0.0025
Cal Step (psi)	[illegible]	[illegible]	[illegible]	[illegible]	[illegible]	[illegible]	[illegible]	[illegible]	[illegible]	[illegible]	[illegible]	[illegible]	0.0043	0.0107
Arrival Time (sec)	[illegible]	[illegible]	[illegible]	[illegible]	[illegible]	[illegible]	1.07[illegible]	[illegible]	3.303	3.303	[illegible]	[illegible]	23.745	23.784
Groundshock-induced peak (psi)	[illegible]	[illegible]	[illegible]	[illegible]	[illegible]	.454	[illegible]	[illegible]	.125	[illegible](b)	-	-	-	-
Time of Peak (sec)	[illegible]	[illegible]	[illegible]	[illegible]	[illegible]	[illegible]	[illegible]	[illegible]	[illegible]	[illegible]	-	-	-	-
Max Positive Peak (psi)	[illegible]	[illegible]	[illegible]	[illegible]	[illegible]	[illegible]	[illegible]	[illegible]	[illegible]	[illegible](b)	[illegible]	[illegible]	0.00211(c)	0.00205(d)
Time of Peak (sec)	[illegible]	[illegible]	[illegible]	[illegible]	[illegible]	[illegible]	[illegible]	[illegible]	[illegible]	[illegible]	[illegible]	[illegible]	23.959	23.962
Negative Peak (psi)	[illegible]	[illegible]	[illegible]	[illegible]	[illegible]	[illegible]	[illegible]	[illegible]	[illegible]	[illegible](b)	(a)	[illegible]	0.00252(c)	0.00252(d)
Time of Peak (sec)	[illegible]	[illegible]	[illegible]	[illegible]	[illegible]	[illegible]	[illegible]	[illegible]	[illegible]	[illegible]	(a)	[illegible]	24.114	24.12
Positive Impulse (psi-sec)	[illegible]	[illegible]	[illegible]	[illegible]	[illegible]	[illegible]	[illegible]	[illegible]	[illegible]	[illegible](b)	[illegible]	[illegible]	0.000222(c)	0.000220(d)
Negative Impulse (psi-sec)	[illegible]	[illegible]	[illegible]	[illegible]	[illegible]	[illegible]	[illegible]	[illegible]	[illegible]	[illegible](b)	(a)	[illegible]	0.000099(c)	0.000097(d)

Charge	Burst Depth (ft)
[illegible]	[illegible]

(a) Failed.
(b) Values measured have been multiplied by 1.53 based on E-[illegible] calibration to correct for unstable calibration.
(c) Values measured have been multiplied by [illegible] based on E-[illegible] calibration to correct for unstable calibration.
(d) Values measured have been multiplied by [illegible] based on E-3 calibration to correct for unstable calibration.

TABLE A-23

Summary of Airblast Measurements

Shot No. D-3

Date 11-14-72   Time 1015   Temp. 45°F

Depth See below   Expl. AANS IF-10   Wind Calm

Station	S-1 L	S-1 H	S-2 L	S-2 H	E-1 L	E-1 H	E-2 L	E-2 H	E-3 L	E-3 H	Jansen L	Jansen H	Trinidad L	Trinidad H
Distance	1000	1000	3216	3216	720	720	2220	2220	3815	3815	14,3[illegible]	14,3[illegible]	26,[illegible]	26,[illegible]
Canister	4	-	5	5	9	9	10	10	7	7	11	11	[illegible]	[illegible]
Gage	1741	4467	1745	1636	1742	4468	1667	1744	1634	1676	1743	1627	1631	1626
Set Range (psi)	0.14	0.14	0.045	0.045	0.065	0.065	0.03	0.03	0.015	0.015	0.005	0.005	0.0027	0.0027
Cal Step (psi)	0.093	0.24	0.031	0.031	0.0295	0.1175	0.0049	0.0195	0.011	0.011	0.0042	0.0042	0.0043	[illegible]
Arrival Time	0.904	0.90[illegible]	2.933	2.934	-0.74	0.728	2.073	2.074	3.530	3.533	12.981	12.985	24.667	24.663
1-Ton Row														
Ground-shock-induced peak (psi)	0.05	0.05	0.0155	0.0158	0.0204	[illegible]	0.0079	0.0064	0.00349	0.00312	-	-	-	-
Time of Peak (sec)	0.944	0.944	3.023	3.011	0.770	0.771	2.091	2.092	3.551	3.554	-	-	-	-
Gas Venting Peak (psi)	0.0647	0.0660	0.0206	0.0212	0.0539	0.0512	0.0193	0.0177	0.0094	0.00815	0.00247	0.00238	0.000957	0.001062
Time of Peak (sec)	0.997	0.998	3.060	3.061	0.851	0.851	2.167	2.167	3.631	3.627	13.152	13.153	24.669	24.642
2-Ton Row														
Ground-shock-induced peak (psi)	-	-	-	-	0.0449	0.0432	0.0194	0.0177	0.00995	0.00885	0.00173	0.00169	0.000659	0.000813
Time of Peak (sec)	-	-	-	-	1.000	0.998	2.316	2.316	3.777	3.776	13.432	13.432	24.956	24.556
Gas Venting Peak (psi)	0.0578	0.0580	0.0232	0.0239	0.0508	0.0487	0.0212	0.0194	0.01103	0.00967	0.00042	0.00045	0.000065	0.000067
Time of Peak (sec)	1.327	1.324	3.380	3.380	1.283	1.243	2.597	2.599	4.060	4.060	13.696	13.690	25.253	25.256
First Negative Peak (psi)	0.0463	0.0460	0.0133	0.0135	0.0402	0.0340	0.0165	0.0159	0.0086	0.0086	0.00126	0.00125	0.000701	0.000787
Time of Peak (sec)	1.160	1.181	3.240	3.242	1.086	1.112	2.405	2.407	3.880	3.876	13.496	13.495	25.050	25.051
Second Negative Peak (psi)	0.0160	0.0160	0.0057	0.0057	0.0350	0.0330	0.0138	0.0137	0.00795	0.00690	0.00084	0.00084	0.00065	0.00061
Time of Peak (sec)	1.503	1.513	3.617	3.615	1.479	1.483	2.742	2.748	4.271	4.278	13.847	13.845	25.578	25.583
Maximum Positive Impulse (psi-sec)	0.00566	0.00528	0.00185	0.00185	0.00604	0.00614	0.00228	0.00209	0.00126	0.00110	0.000306	0.000300	0.000142	0.000160
Total Maximum Positive Impulse (psi-sec)	0.01036	0.01019	0.00339	0.00341	0.00964	0.00945	0.00369	0.00340	0.00204	0.00178	0.000338	0.000334	0.000144	0.000161
Maximum Negative Impulse (psi-sec)	0.00648	0.00601	0.00235	0.00242	0.00936	0.00892	0.00329	0.00303	0.00176	0.00152	0.000261	0.000253	0.000234	0.000249
Total Maximum Negative Impulse (psi-sec)	0.01238	0.01153	0.00403	0.00416	0.01296	0.01232	0.00470	0.00434	0.00254	0.01220	0.000377	0.000369	0.000317	0.000344

Charge	Burial Depth (ft) One-Ton Row	Burial Depth (ft) Two-Ton Row
A	19.0	23.0
B	19.0	24.2
C	18.9	25.0
D	19.5	25.0
E	19.5	24.0
F	19.7	24.4

TABLE A-24

Summary of Airblast Measurements

Shot No. [illegible]

Date [illegible] Depth See below
Time [illegible] Expl. [illegible]
Temp [illegible] Wind Calm

Item	[illegible] L	[illegible] H	[illegible] L	[illegible] H	[illegible] L	[illegible] H	E-1 L	E-1 H	E-2 L	E-2 H	E-3 L	E-3 H	Jensen L	Jensen H	Trinidad L	Trinidad H
Distance	[illegible]	[illegible]	[illegible]	[illegible]	[illegible]	[illegible]	[illegible]	560	[illegible]	[illegible]	[illegible]	[illegible]	[illegible]	[illegible]	[illegible]	[illegible]
Canister	[illegible]	[illegible]	[illegible]	[illegible]	[illegible]	[illegible]	3	3	4	4	5	5	7	7	[illegible]	[illegible]
Gage	[illegible]	[illegible]	[illegible]	[illegible]	[illegible]	[illegible]	[illegible]	[illegible]	[illegible]	[illegible]	[illegible]	[illegible]	[illegible]	[illegible]	[illegible]	[illegible]
[illegible] Range (psi)	[illegible]	[illegible]	[illegible]	[illegible]	[illegible]	[illegible]	[illegible]	[illegible]	[illegible]	[illegible]	[illegible]	[illegible]	[illegible]	[illegible]	[illegible]	[illegible]
[illegible] Step (psi)	[illegible]	[illegible]	[illegible]	[illegible]	[illegible]	[illegible]	[illegible]	[illegible]	[illegible]	[illegible]	[illegible]	[illegible]	[illegible]	[illegible]	[illegible]	[illegible]
Arrival Time (ms)	[illegible]	[illegible]	[illegible]	[illegible]	[illegible]	[illegible]	[illegible]	[illegible]	[illegible]	[illegible]	[illegible]	[illegible]	[illegible]	[illegible]	(g)	(g)
[illegible]																
[illegible] peak (psi)	[illegible]	[illegible]	[illegible]	[illegible]	[illegible]	[illegible]	[illegible]	[illegible]	[illegible]	[illegible]	[illegible]	[illegible]	-	-	(g)	(g)
Time of Peak (ms)	[illegible]	[illegible]	[illegible]	[illegible]	[illegible]	[illegible]	[illegible]	[illegible]	[illegible]	[illegible]	[illegible]	[illegible]	-	-	(g)	(g)
Gas venting Peak (psi)	[illegible]	[illegible]	[illegible]	[illegible]	[illegible]	[illegible]	[illegible]	[illegible]	[illegible]	[illegible]	[illegible]	[illegible]	[illegible]	[illegible]	(g)	(g)
Time of Peak (ms)	[illegible]	[illegible]	[illegible]	[illegible]			[illegible]	[illegible]	4.537	3.541	[illegible]	[illegible]	[illegible]	[illegible]	(g)	(g)
[illegible]																
[illegible] peak (psi)	[illegible]	[illegible]	[illegible]	[illegible]	[illegible]	[illegible]	-	-	-	-	-	-	-	-	(g)	(g)
Time of Peak (ms)	[illegible]	[illegible]	[illegible]	[illegible]	[illegible]	[illegible]	-	-	-	-	-	-	-	-	(g)	(g)
Gas venting Peak (psi)	[illegible]	[illegible]	[illegible]	[illegible]	[illegible]	[illegible]	-	-	-	-	-	-	-	-	(g)	(g)
Time of Peak (ms)	[illegible]	[illegible]	[illegible]	[illegible]	[illegible]	[illegible]	-	-	-	-	-	-	-	-	(g)	(g)
[illegible]																
Third Peak (psi)	-	-	-	-	-	-	[illegible]	[illegible]	[illegible]	[illegible]	[illegible]	[illegible]	-	-	(g)	(g)
Time of Peak (ms)	-	-	-	-	-	-	[illegible]	[illegible]	[illegible]	[illegible]	[illegible]	[illegible]	-	-	(g)	(g)
Fourth Peak (psi)	-	-	-	-	-	-	[illegible]		[illegible]	[illegible]	[illegible]	[illegible]	-	-	(g)	(g)
Time of Peak (ms)	-	-	-	-	-	-	[illegible]		[illegible]	[illegible]	[illegible]	[illegible]	-	-	(g)	(g)
Fifth Peak (psi)	-	-	-	-	-	-	[illegible]	[illegible]	[illegible]	[illegible]	[illegible]	[illegible]	-	-	(g)	(g)
Time of Peak (ms)	-	-	-	-	-	-	[illegible]	[illegible]	[illegible]	[illegible]	[illegible]	[illegible]	-	-	-	(g)
[illegible] Peak (psi)	-	-	-	-	-	-	[illegible]	[illegible]	[illegible]	[illegible]	[illegible]	[illegible]	[illegible]	[illegible]	(g)	(g)
Time of Peak (ms)	-	-	-	-	-	-	[illegible]	[illegible]	[illegible]	[illegible]	[illegible]	[illegible]	[illegible]	[illegible]	(g)	(g)
First Negative Peak (psi)	[illegible]	[illegible]	[illegible]	[illegible]			-	-	-	-	-	-	-	-	(g)	(g)
Time of Peak (ms)	[illegible]	[illegible]	[illegible]	[illegible]	[illegible]	[illegible]	-	-	-	-	-	-	-	-	(g)	(g)
Second Negative Peak (psi)	[illegible]	[illegible]	[illegible]	[illegible]	[illegible]	[illegible]	[illegible]	[illegible]	[illegible]	[illegible]	Limited	[illegible]	[illegible]	[illegible]	(g)	(g)
Time of Peak (ms)	[illegible]	[illegible]	[illegible]	[illegible]	[illegible]	[illegible]		1.17	[illegible]	[illegible]	-	[illegible]	[illegible]	[illegible]	(g)	(g)
First Positive Impulse (psi-ms)	[illegible]	[illegible]	[illegible]	[illegible]	-	-	-	-	-	-	-	-	-	-	(g)	(g)
Second Positive Impulse (psi-ms)	[illegible]	[illegible]	[illegible]	[illegible]	-	-	-	-	-	-	-	-	-	-	(g)	(g)
Total Positive Impulse (psi-ms)	[illegible]	[illegible]	[illegible]	[illegible]	[illegible]	[illegible]	[illegible]	[illegible]	[illegible]	[illegible]	[illegible]	[illegible]	[illegible]	[illegible]	(g)	(g)
First Negative Impulse (psi-ms)	[illegible]	[illegible]	[illegible]	[illegible]	-	-	-	-	-	-	-	-	-	-	(g)	(g)
Second Negative Impulse (psi-ms)	[illegible]	[illegible]	[illegible]	[illegible]	-	-	-	-	-	-	-	-	-	-	(g)	(g)
Total Negative Impulse (psi-ms)	[illegible]	[illegible]	[illegible]	[illegible]	[illegible]	[illegible]	[illegible]	[illegible]	[illegible]	[illegible]	Limited	[illegible]	[illegible]	[illegible]	(g)	(g)

CHARGE	BURIAL DEPTH (ft)	
	[illegible]	[illegible]
[illegible]	[illegible]	[illegible]
[illegible]	[illegible]	18.9 (crater)

(a) Gas venting pulse of [illegible] coincides with ground-shock-induced pulse of [illegible].
(b) Gas venting pulses of both [illegible] coincide.
(c) In first negative phase.
(d) Record parent of electrically-induced shifts in amplitude, hence, values and pulse identification may not be accurate.
(e) [illegible] of gas venting pulse from near charge and ground-shock-induced pulse of a more distant charge.
(f) Calibration was lost for this gage and overpressure values were estimated by setting positive phase impulse of high range gage equal to that of low range gage.
(g) [illegible]

BLANK PAGE

APPENDIX B

Pressure-Time Records for the B Series

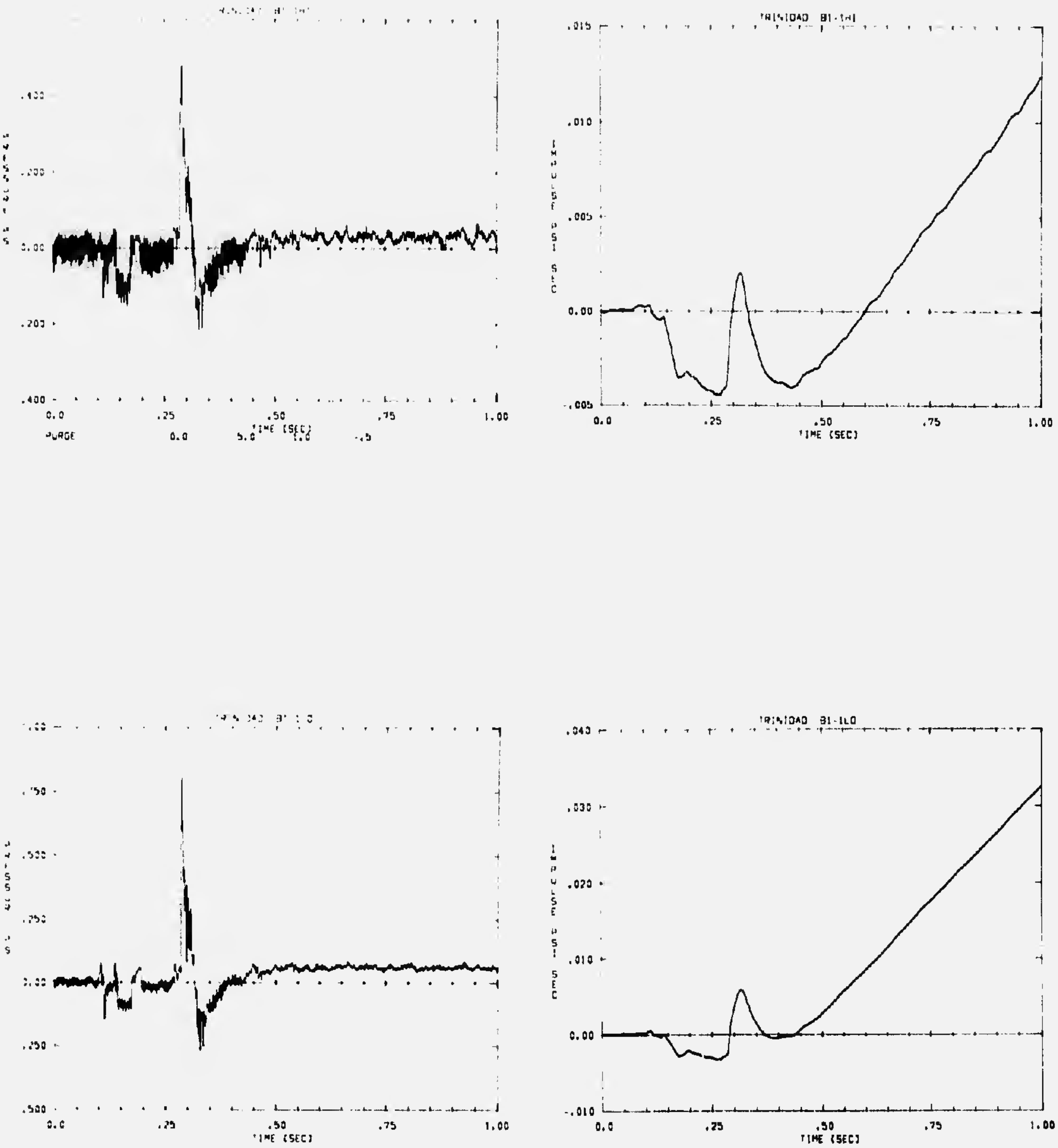

Figure B-1. Pressure-time and impulse-time for high-range gage (upper) and low-range gage (lower) for TRINIDAD Shot B-1, Station 1

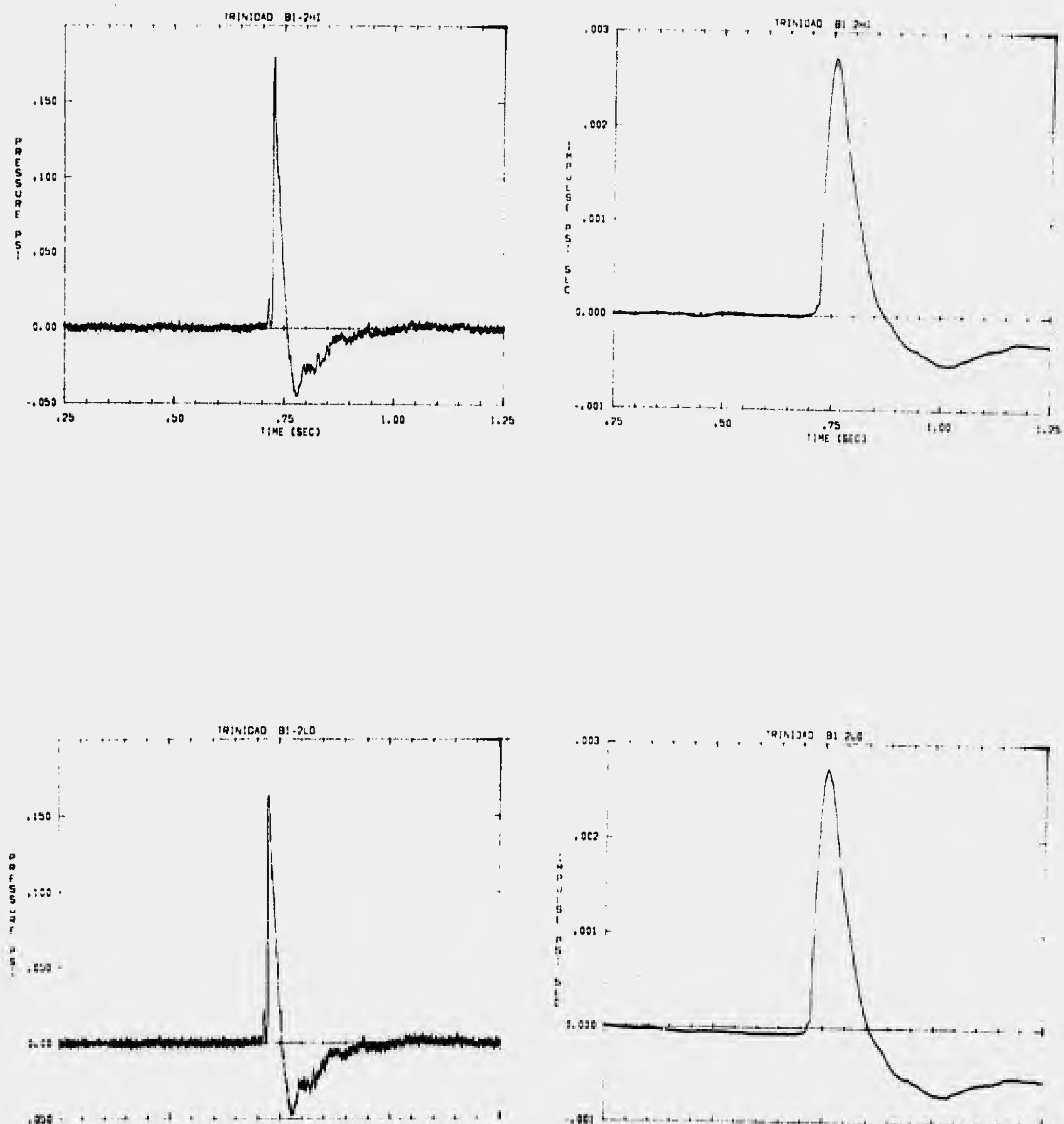

Figure B-2. Pressure-time and impulse-time for high-range gage (upper) and low-range gage (lowe1) for TRINIDAD Shot B-1, Station 2

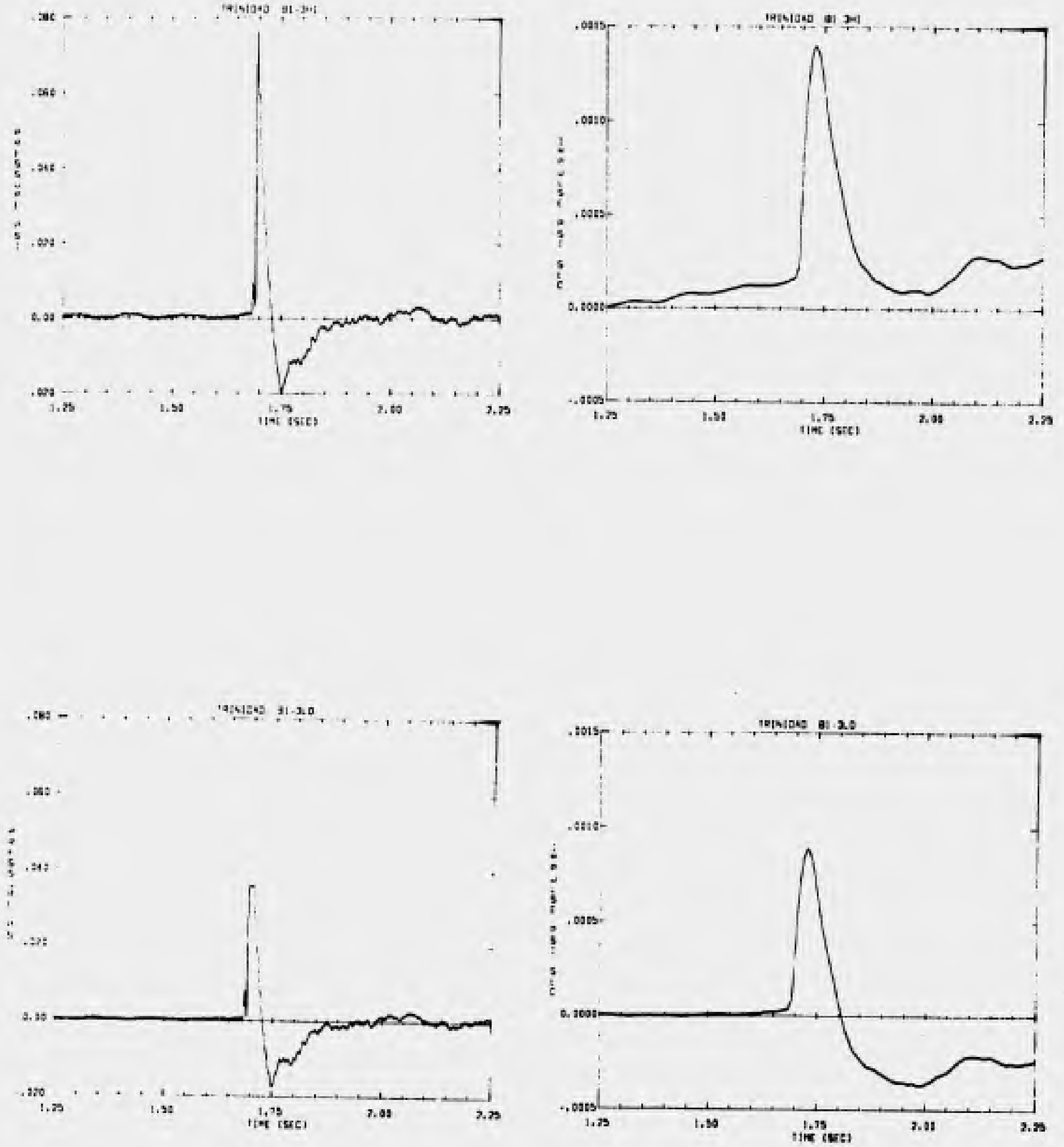

Figure B-3. Pressure-time and impulse-time for high-range gage (upper) and low-range gage (lower) for TRINIDAD Shot B-1, Station 3

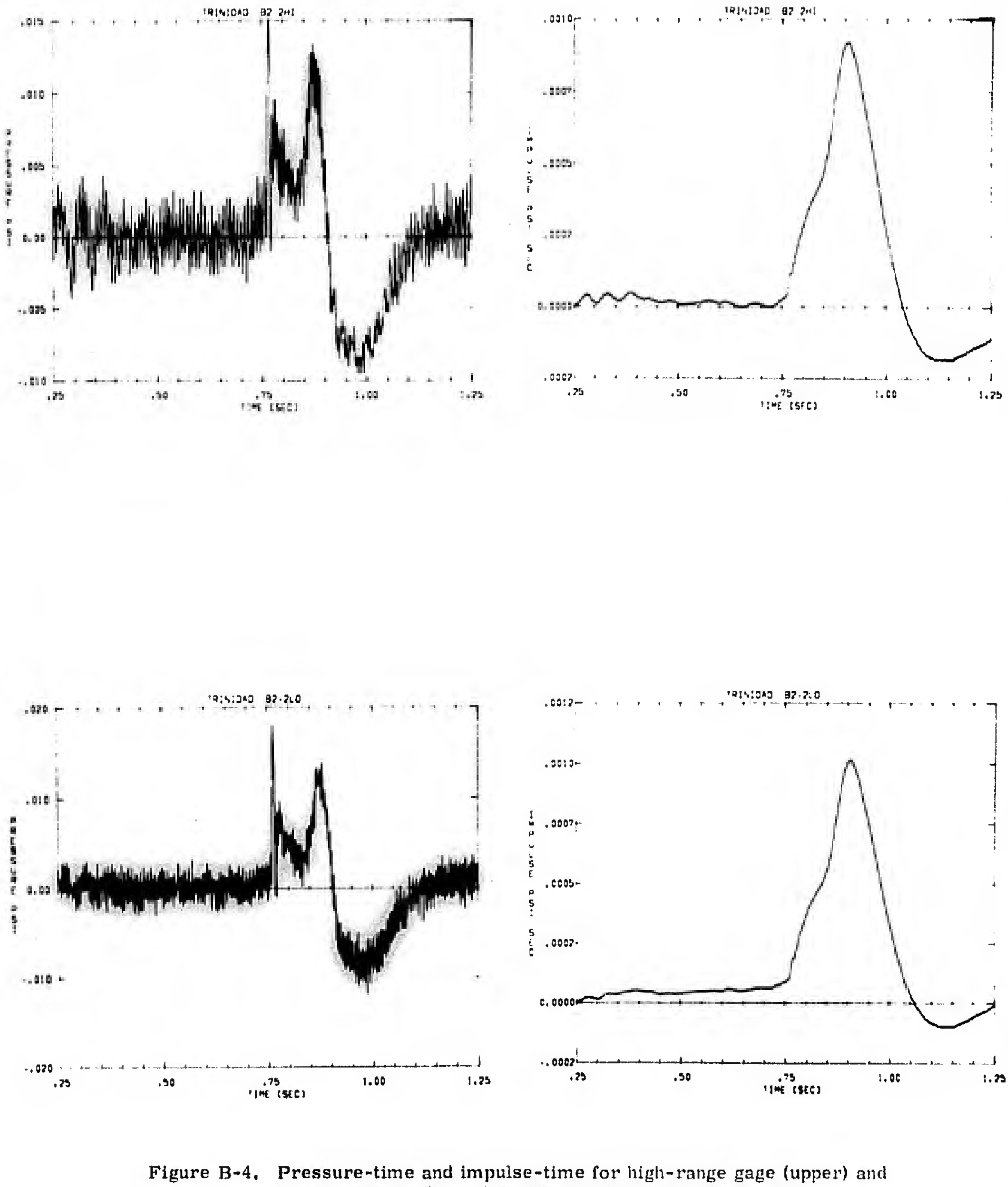

Figure B-4. Pressure-time and impulse-time for high-range gage (upper) and low-range gage (lower) for TRINIDAD Shot B-2, Station 2

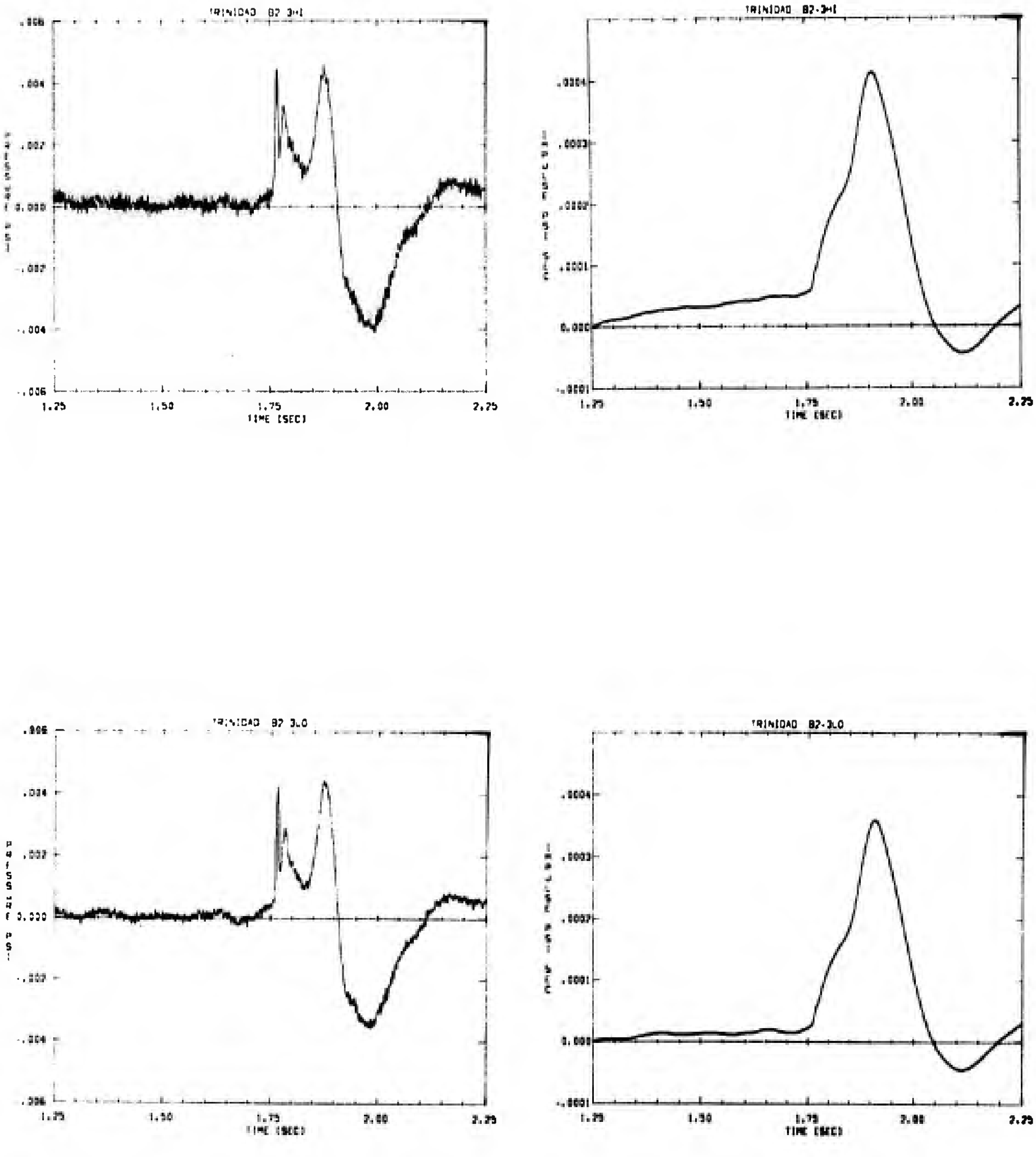

Figure B-5. Pressure-time and impulse-time for high-range gage (upper) and low-range gage (lower) for TRINIDAD Shot B-2, Station 3

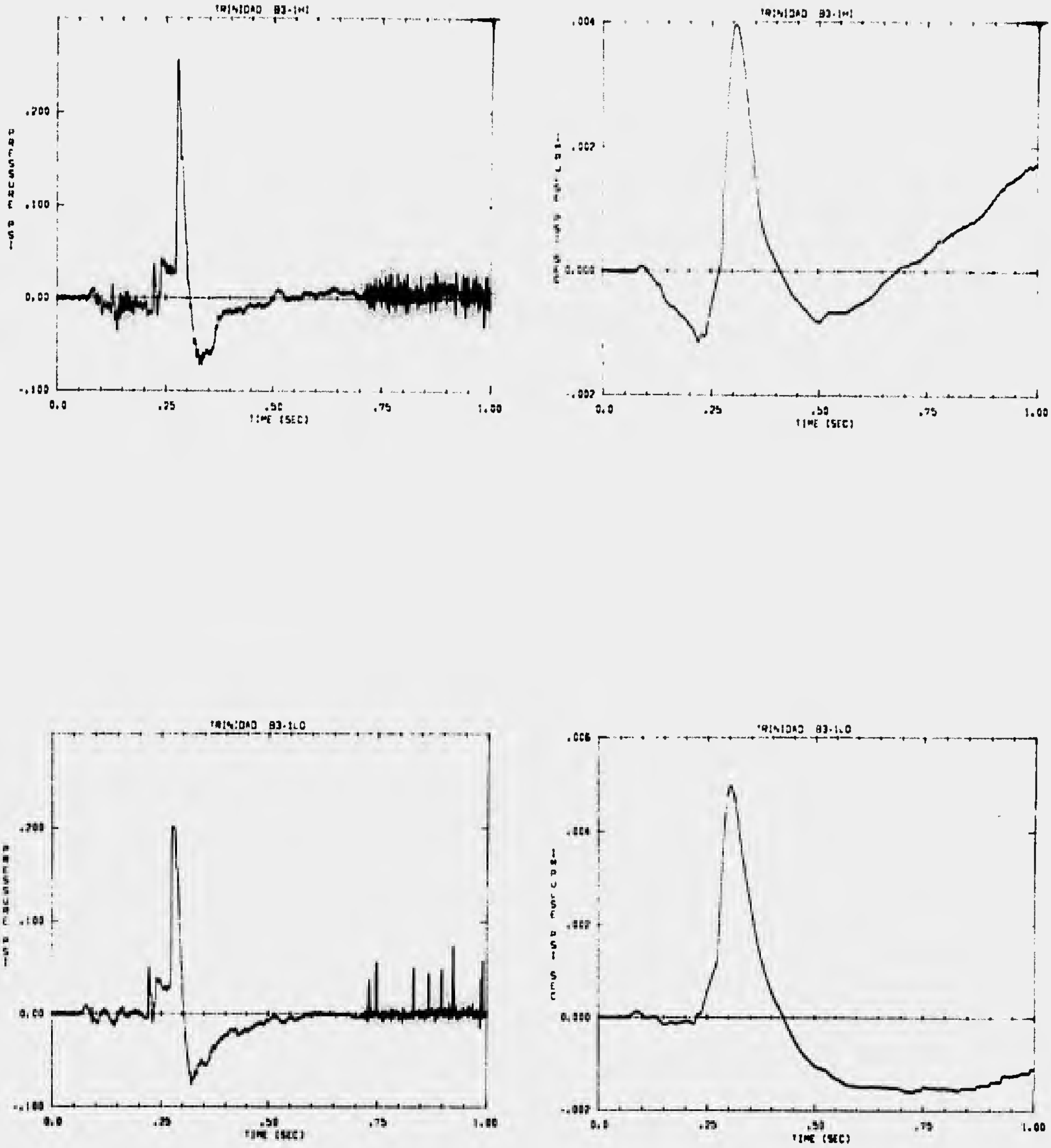

Figure B-6. Pressure-time and impulse-time for high-range gage (upper) and low-range gage (lower) for TRINIDAD Shot B-3, Station 1

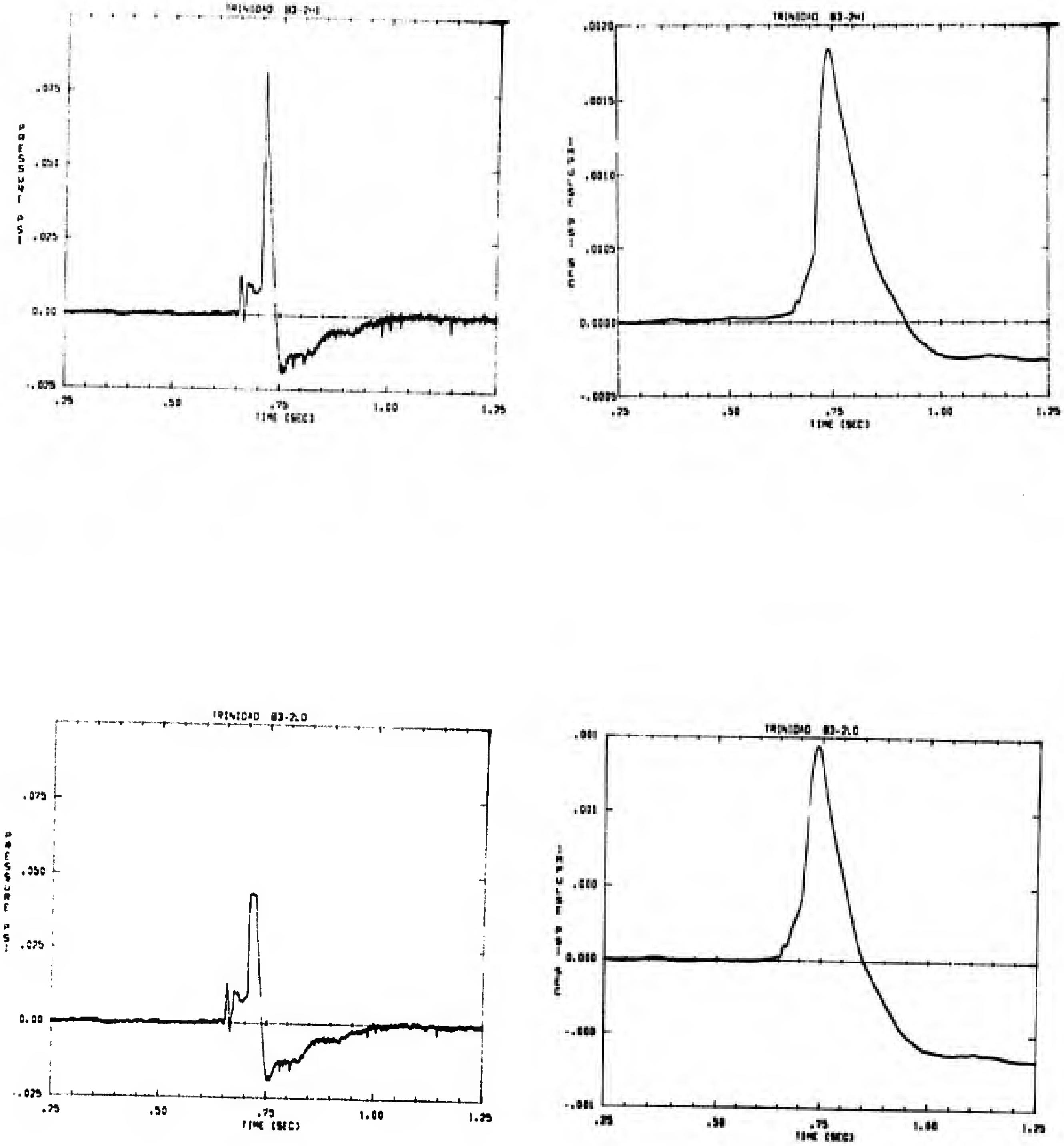

Figure B-7. Pressure-time and impulse-time for high-range gage (upper) and low-range gage (lower) for TRINIDAD Shot B-3, Station 2

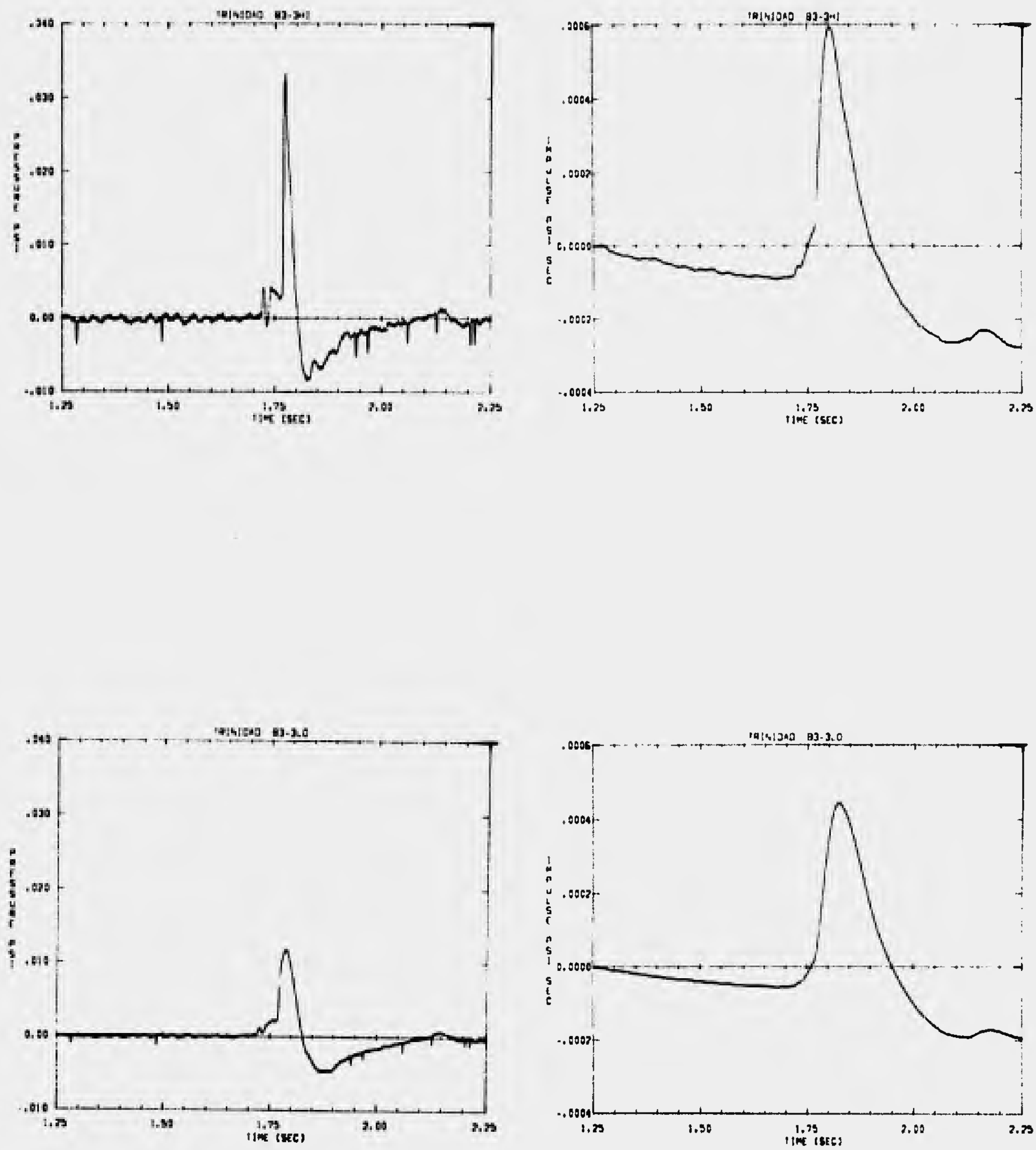

Figure B-8. Pressure-time and impulse-time for high-range gage (upper) and low-range gage (lower) for TRINIDAD Shot B-3, Station 3

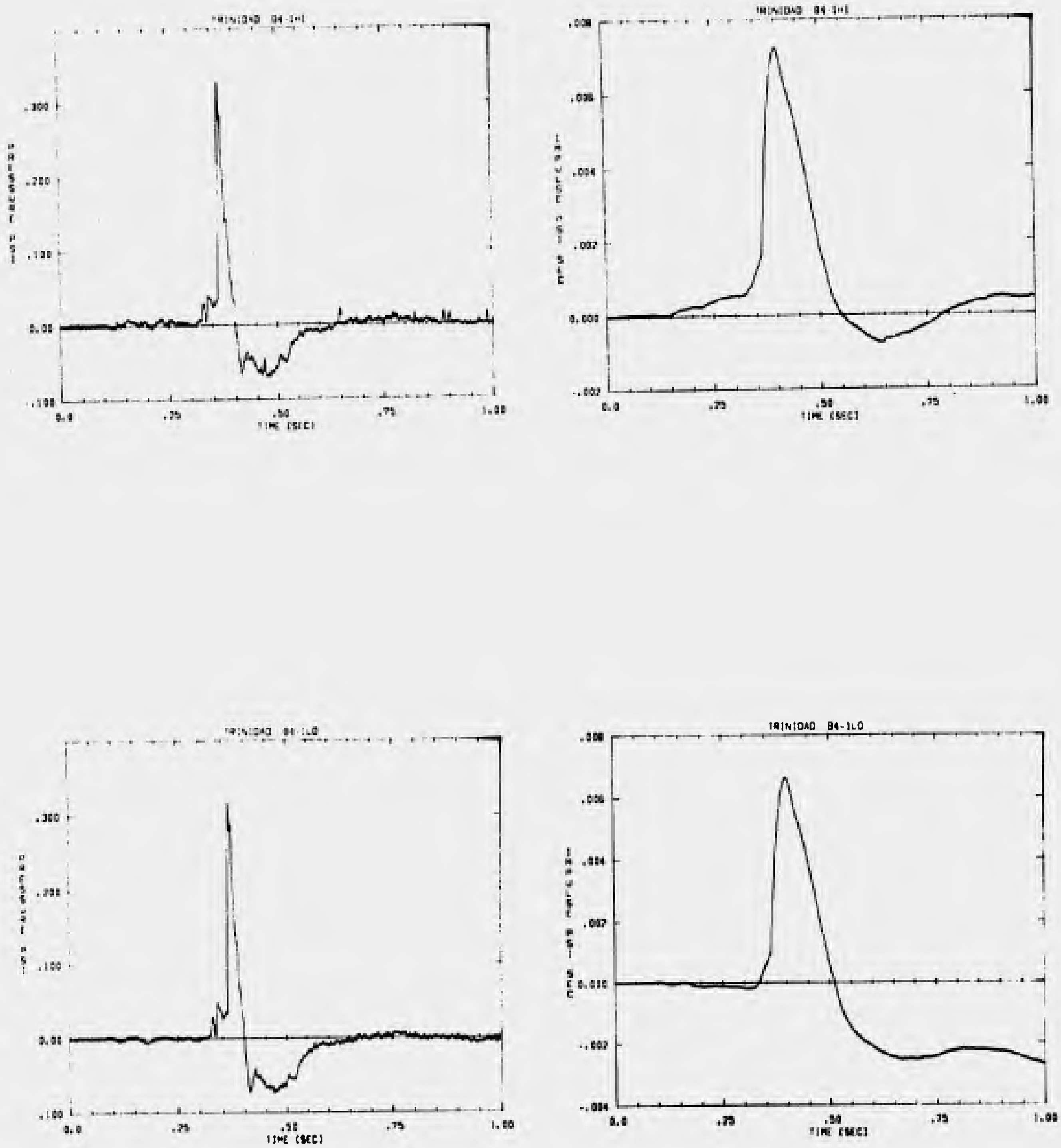

Figure B-9. Pressure-time and impulse-time for high-range gage (upper) and low-range gage (lower) for TRINIDAD Shot B-4, Station 1

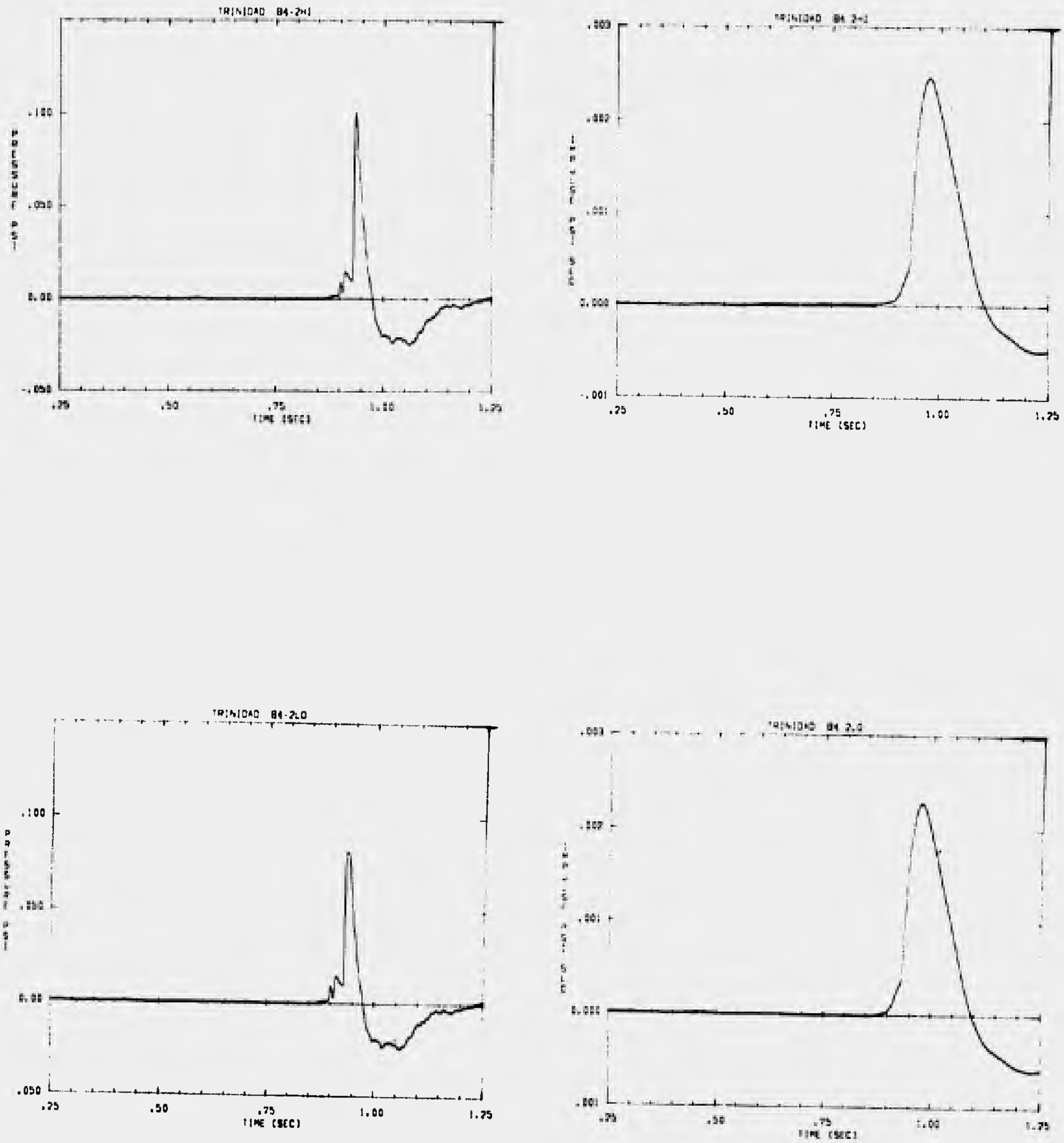

Figure B-10. Pressure-time and impulse-time for high-range gage (upper) and low-range gage (lower) for TRINIDAD Shot B-4, Station 2

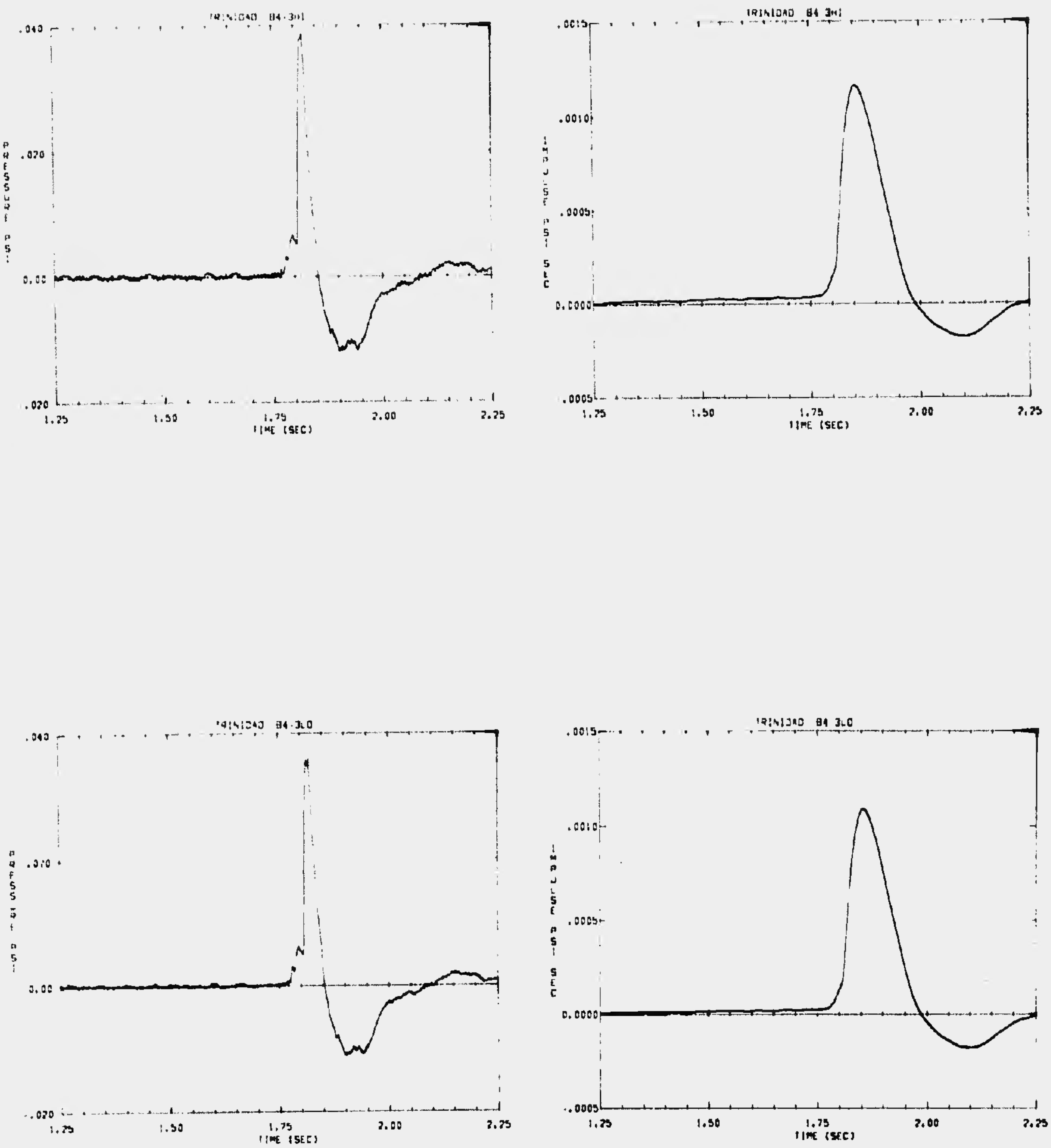

Figure B-11. Pressure-time and impulse-time for high-range gage (upper) and low-range gage (lower) for TRINIDAD Shot B-4, Station 3

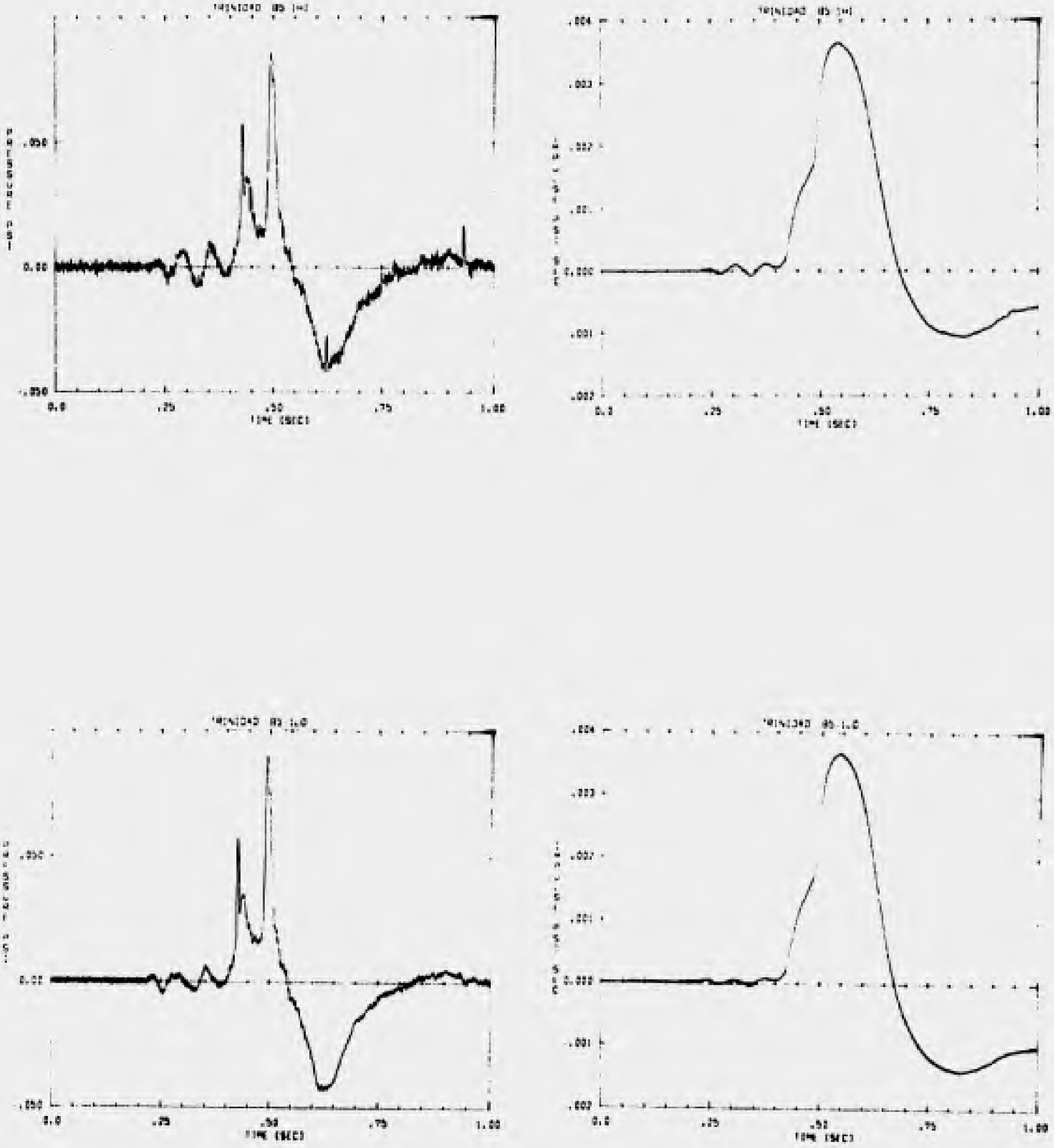

Figure B-12. Pressure-time and impulse-time for high-range gage (upper) and low-range gage (lower) for TRINIDAD Shot B-5, Station 1

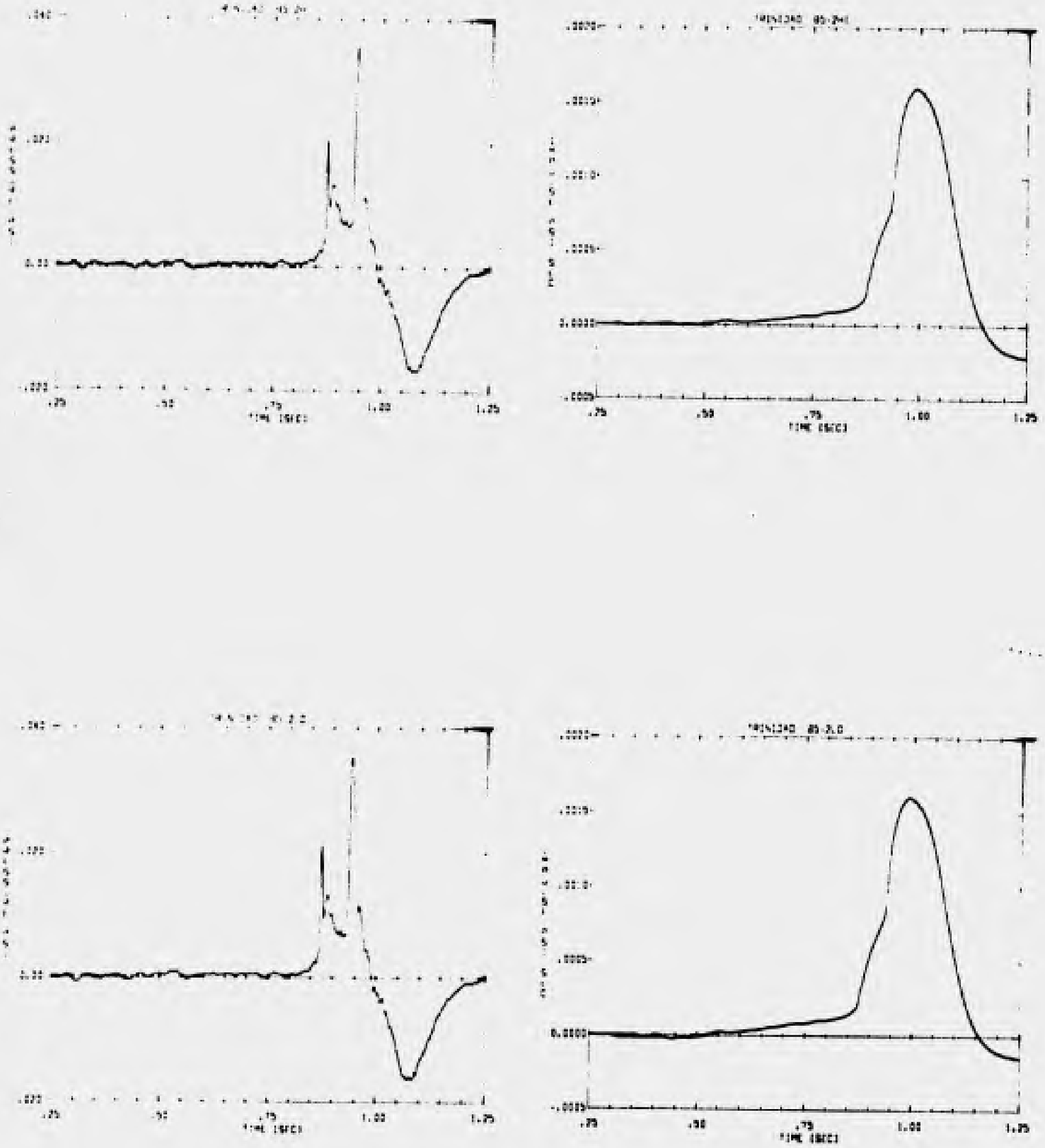

Figure B-13. Pressure-time and impulse-time for high-range gage (upper) and low-range gage (lower) for TRINIDAD Shot B-5, Station 2

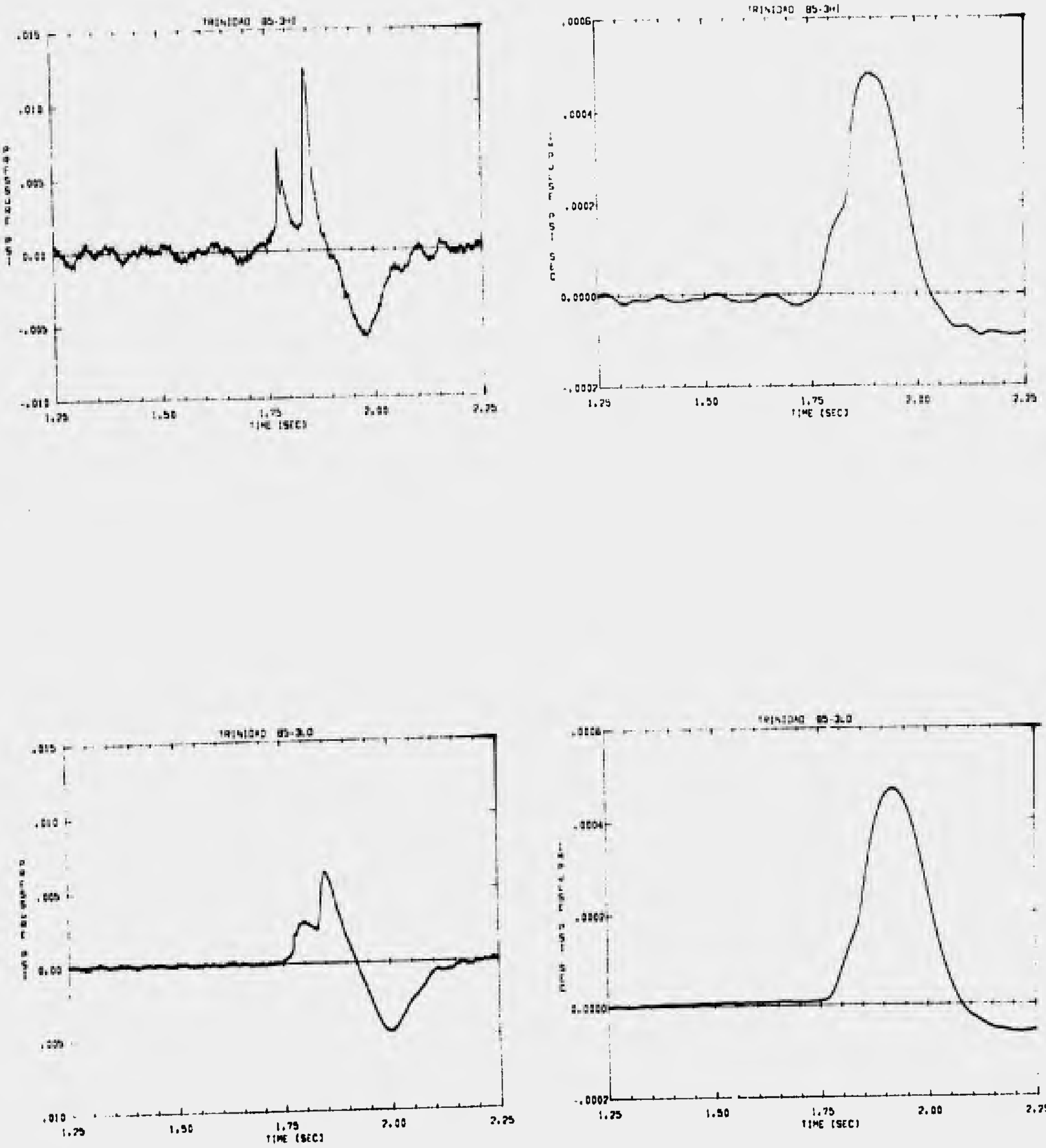

Figure B-14. Pressure-time and impulse-time for high-range gage (upper) and low-range gage (lower) for TRINIDAD Shot B-5, Station 3

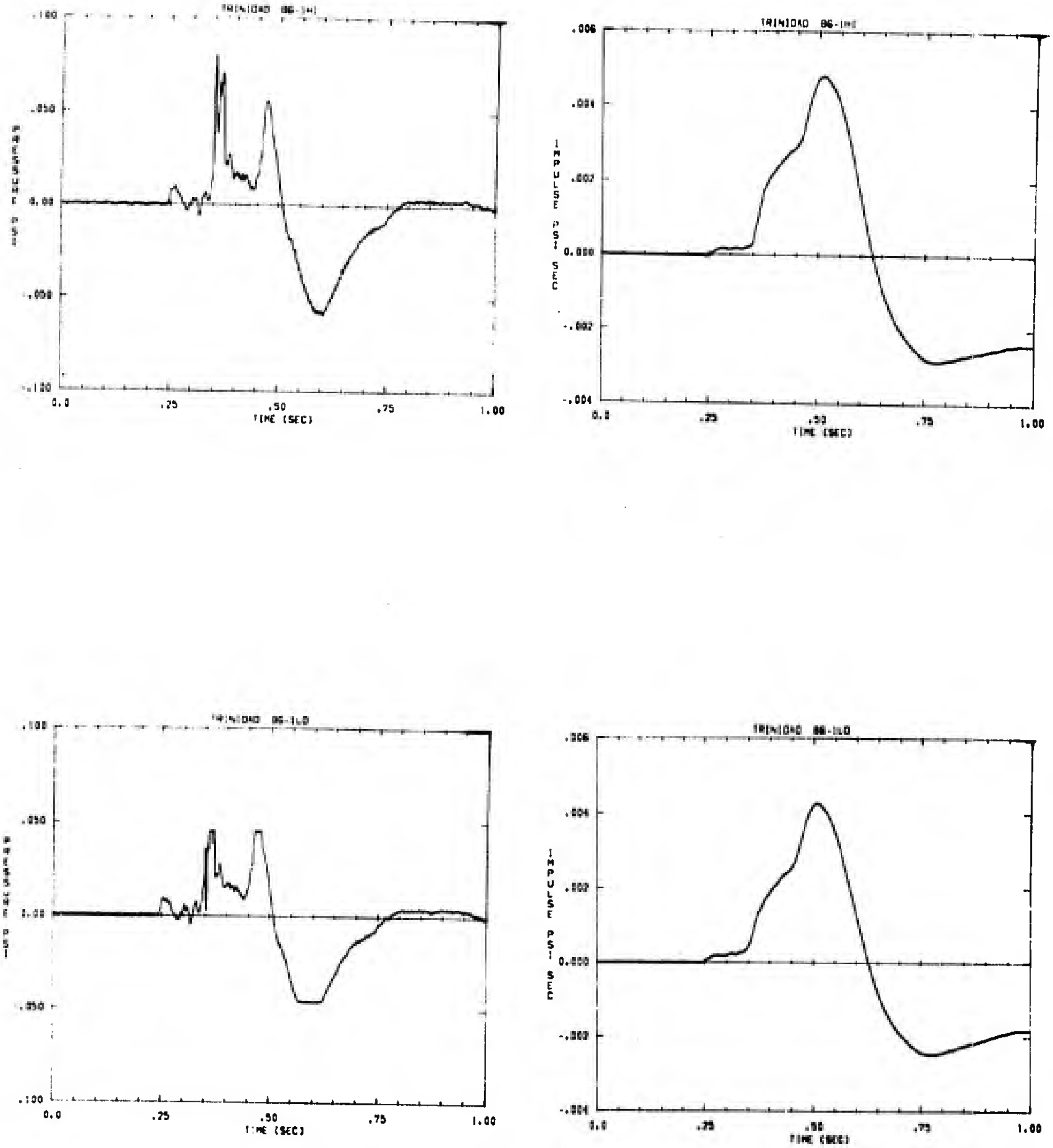

Figure B-15. Pressure-time and impulse-time for high-range gage (upper) and low-range gage (lower) for TRINIDAD Shot B-6, Station 1

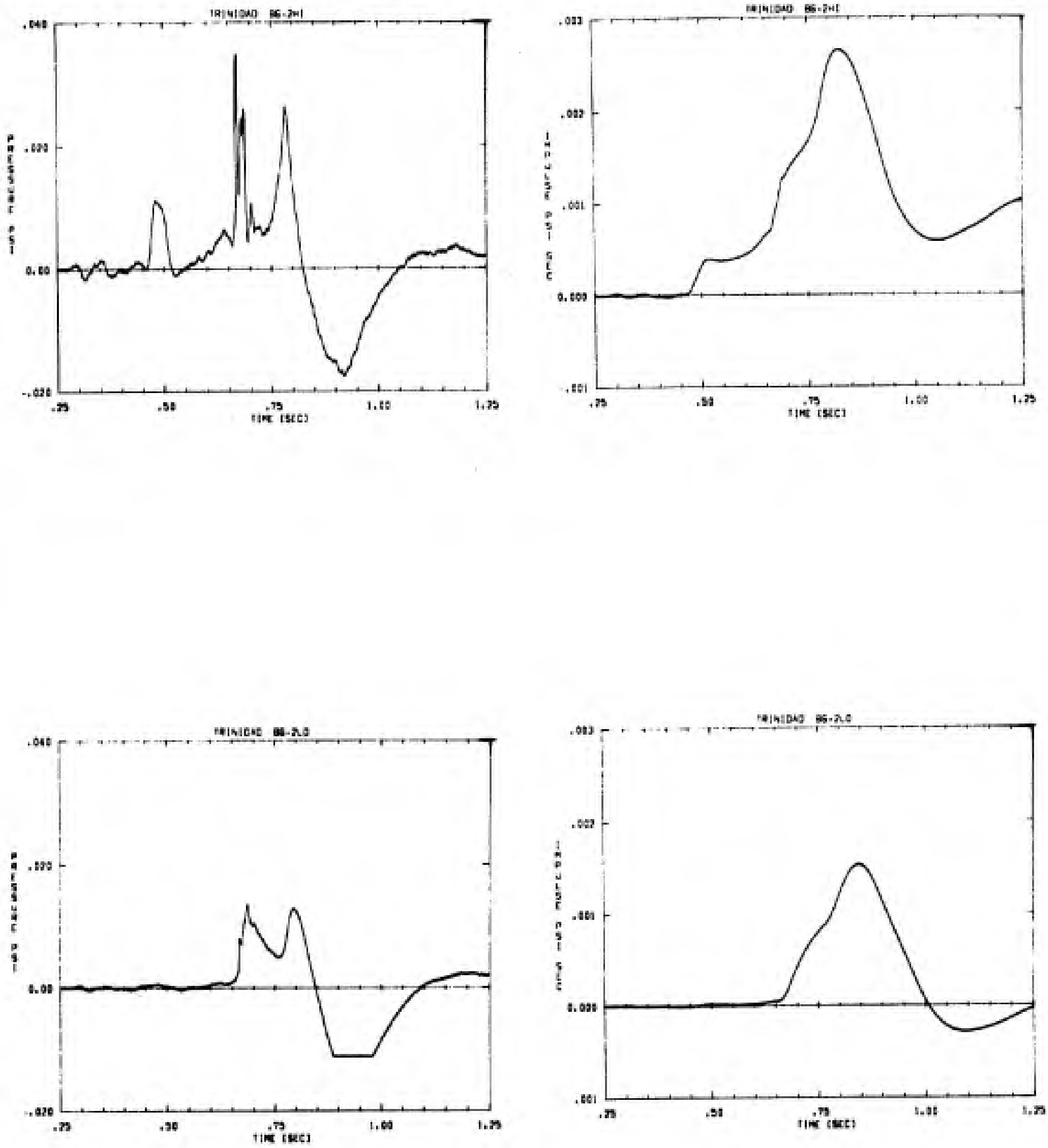

Figure B-16. Pressure-time and impulse-time for high-range gage (upper) and low-range gage (lower) for TRINIDAD Shot B-6, Station 2

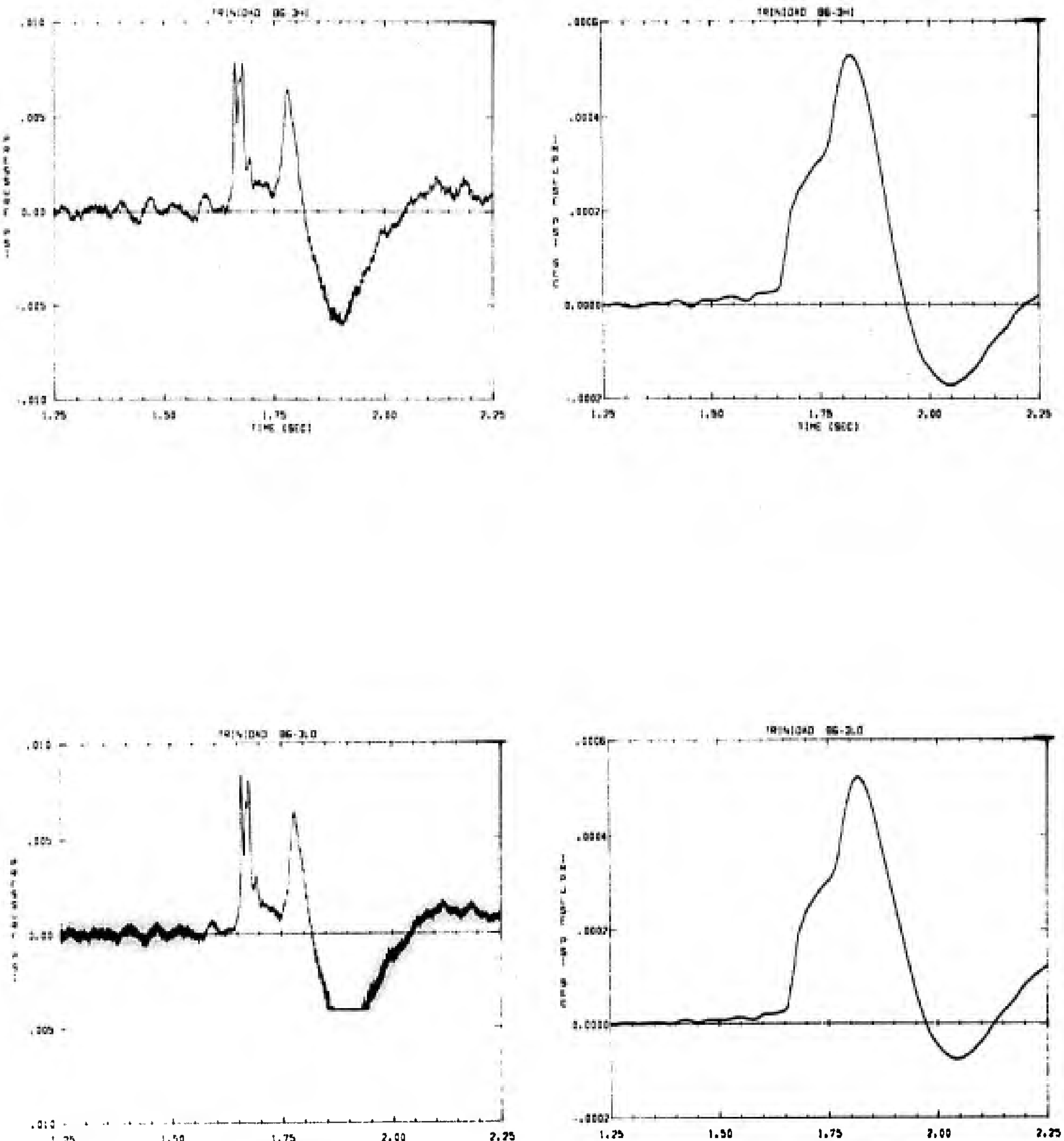

Figure 17. Pressure-time and impulse-time for high-range gage (upper) and low-range gage (lower) for TRINIDAD Shot B-6, Station 3

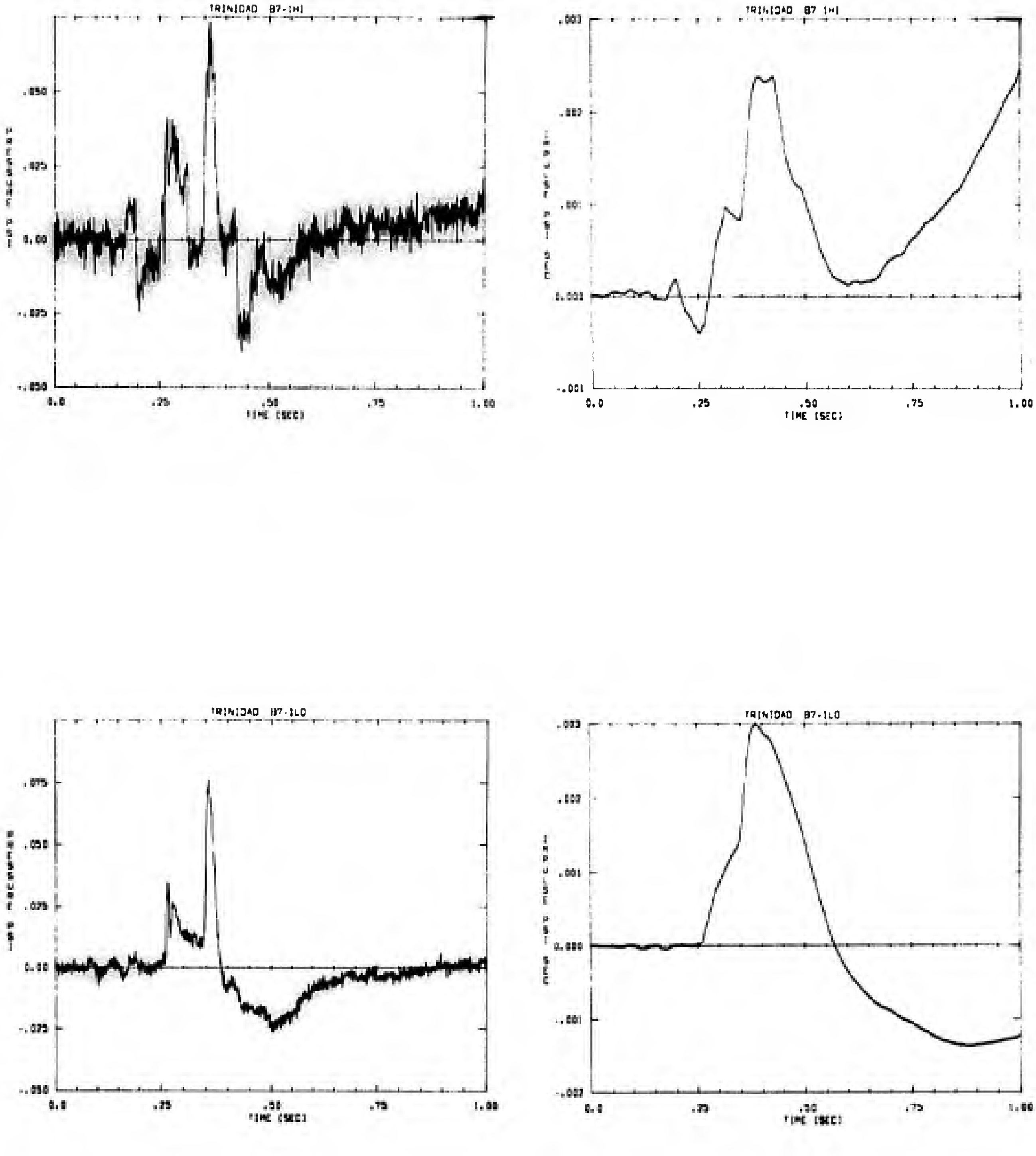

Figure B-18. Pressure-time and impulse-time for high-range gage (upper) and low-range gage (lower) for TRINIDAD Shot B-7, Station 1

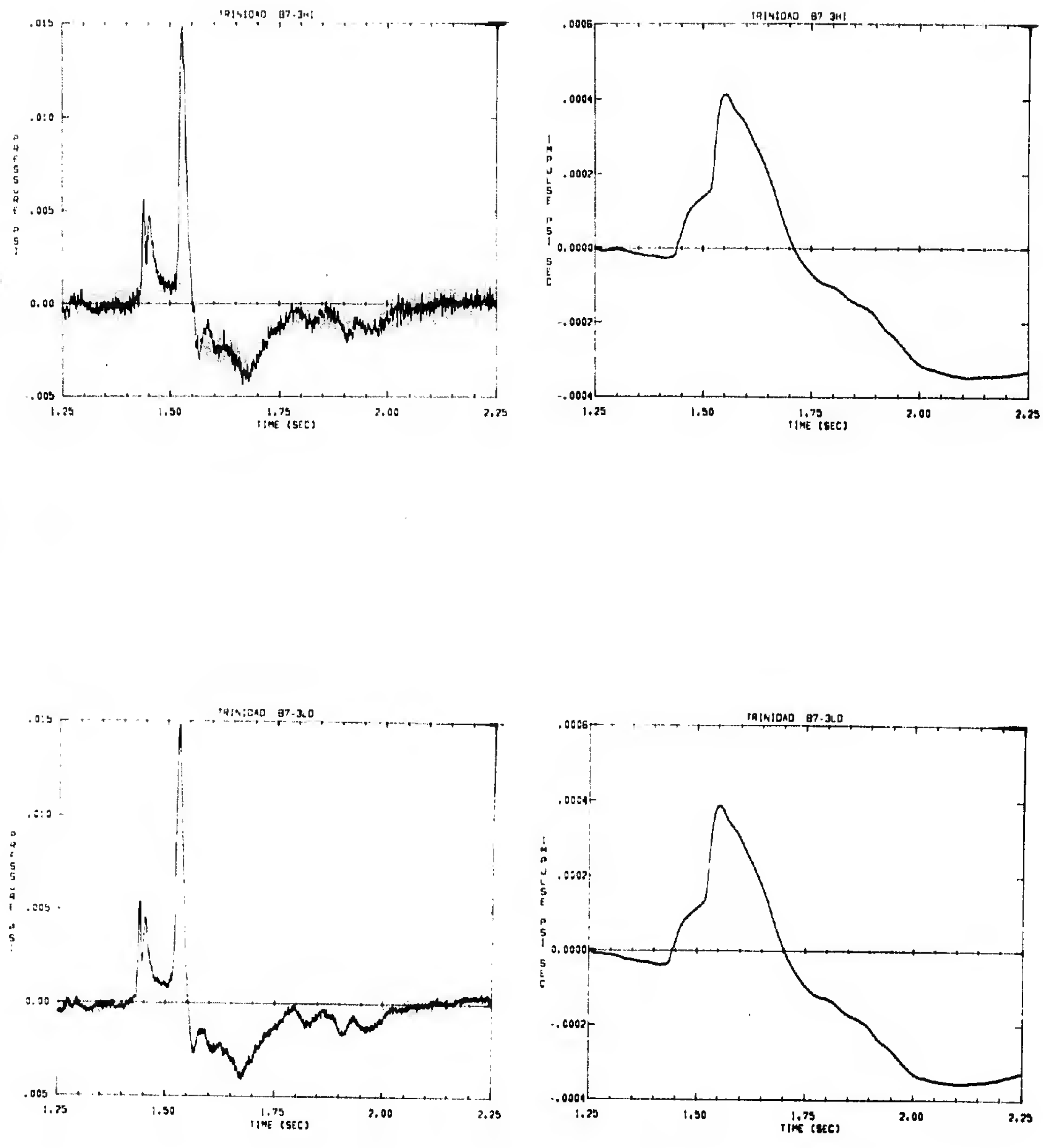

Figure B-19. Pressure-time and impulse-time for high-range gage (upper) and low-range gage (lower) for TRINIDAD Shot B-7, Station 3

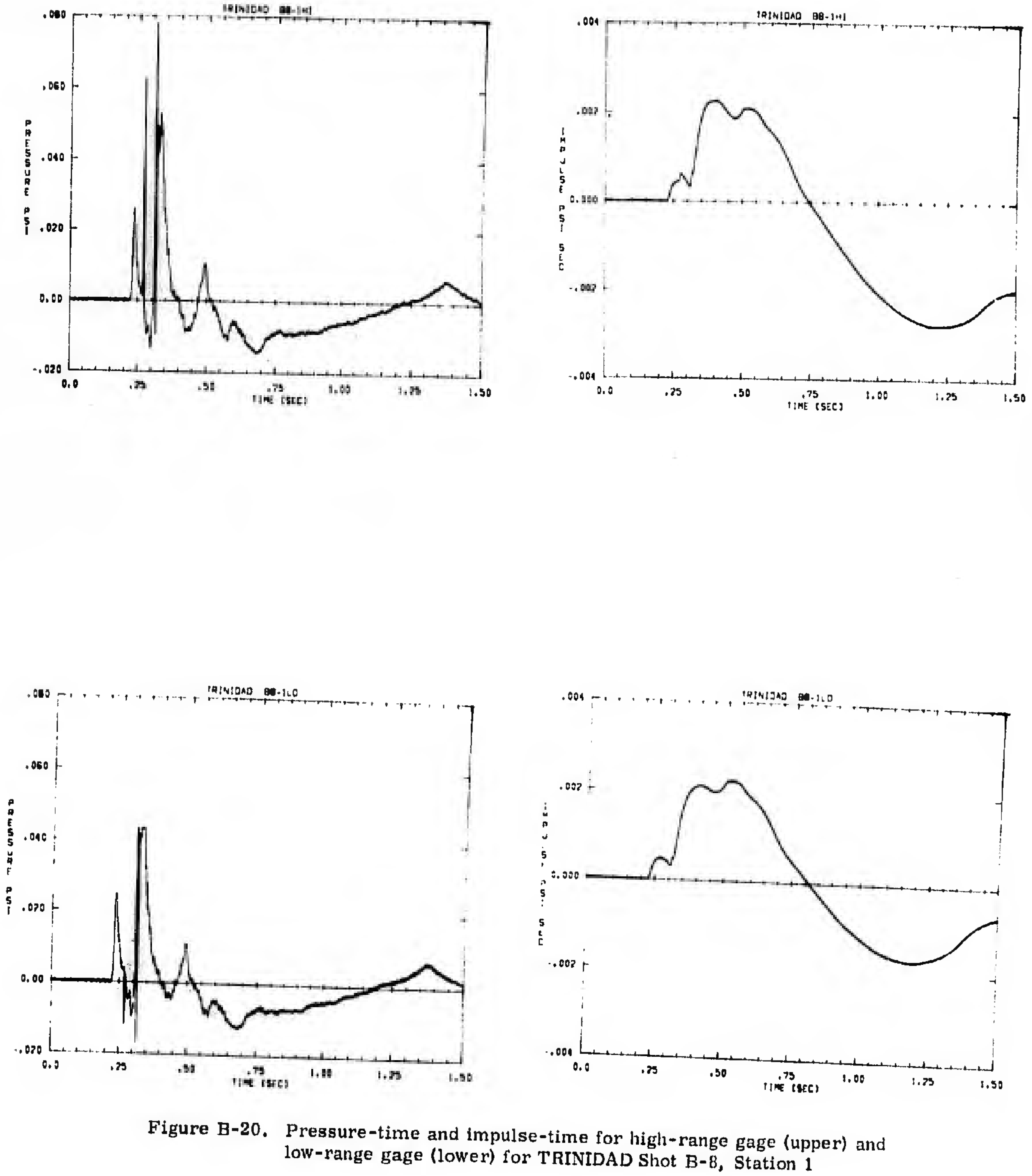

Figure B-20. Pressure-time and impulse-time for high-range gage (upper) and low-range gage (lower) for TRINIDAD Shot B-8, Station 1

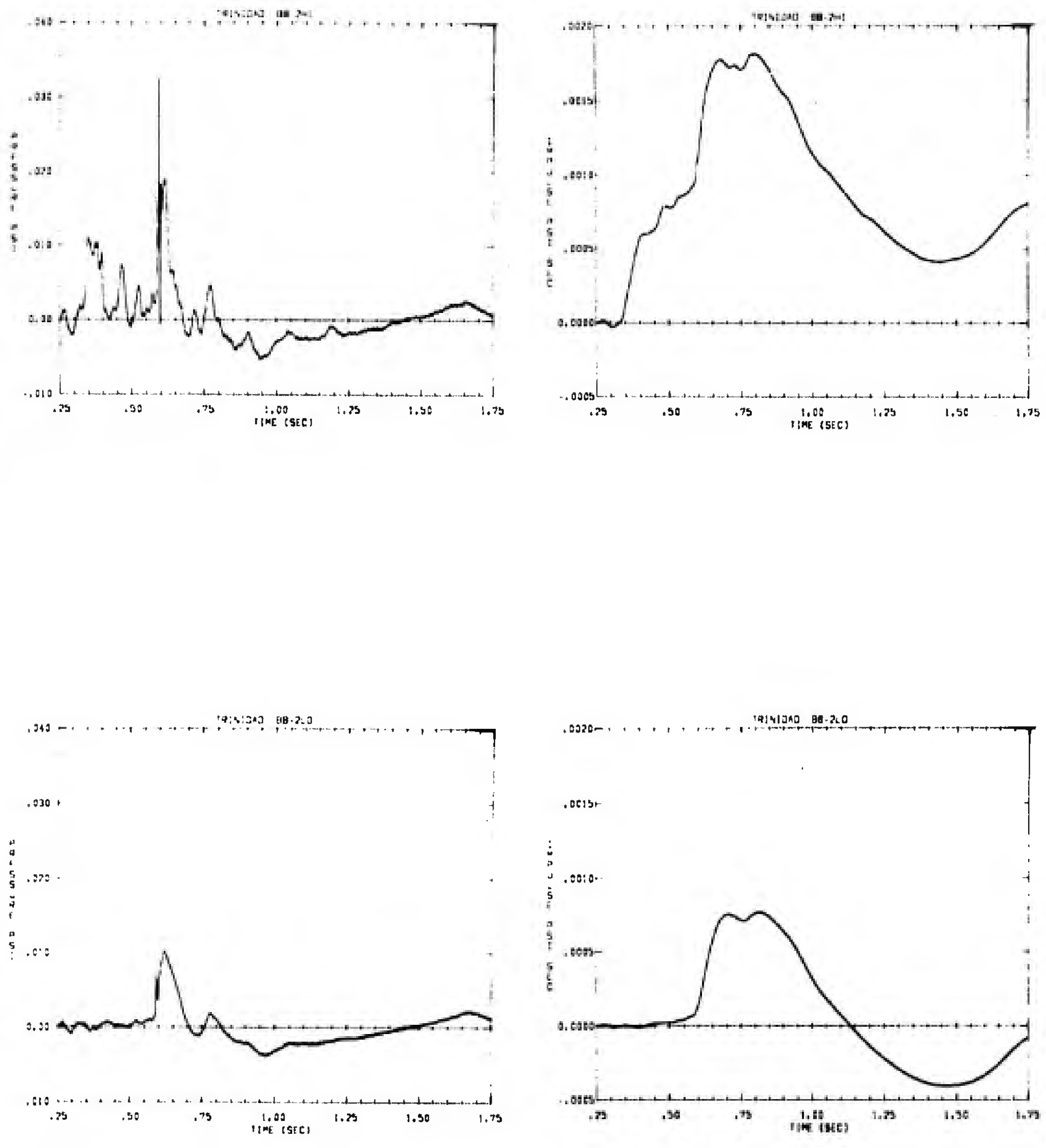

Figure B-21. Pressure-time and impulse-time for high-range gage (upper) and low-range gage (lower) for TRINIDAD Shot B-8, Station 2

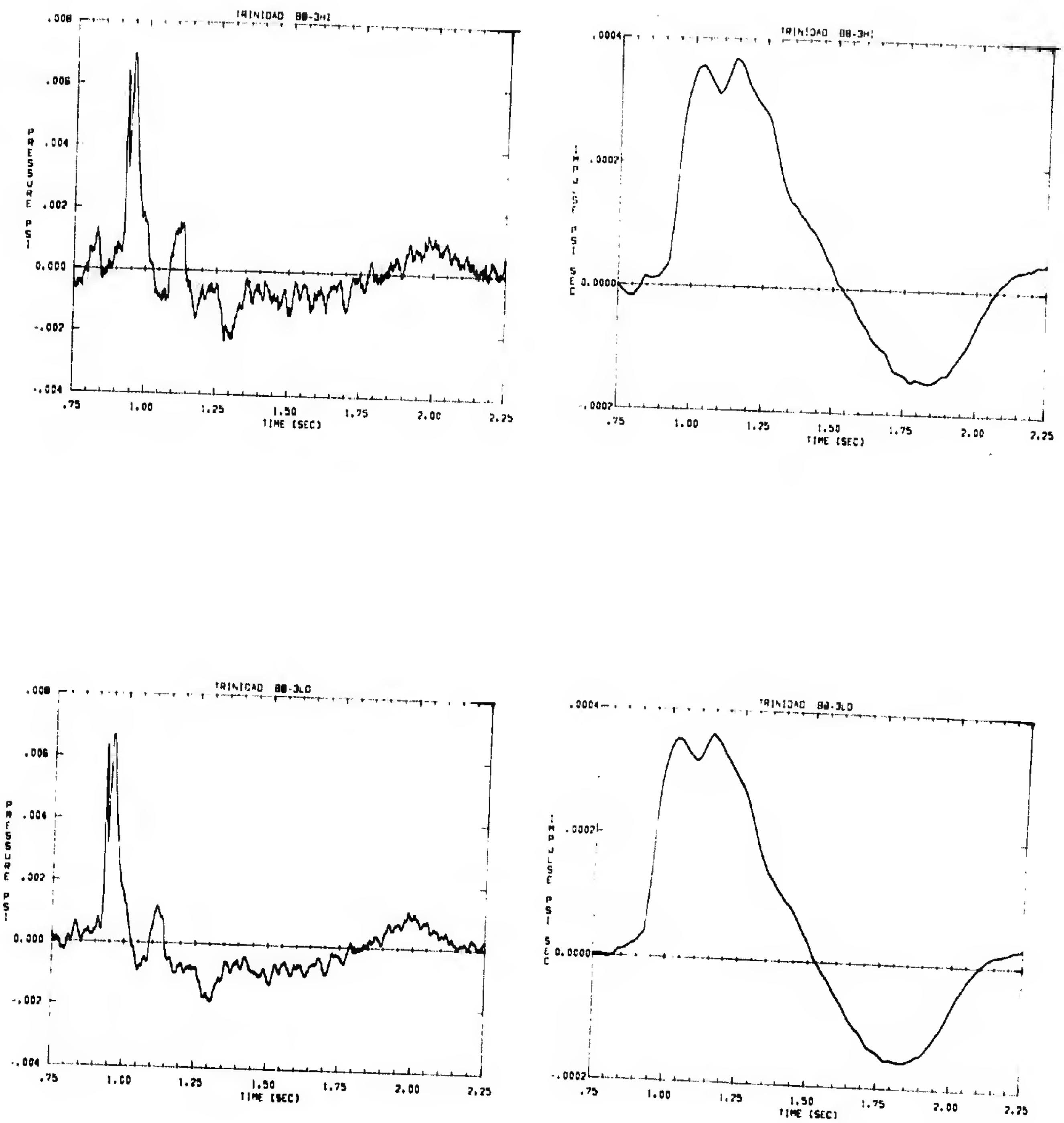

Figure B-22. Pressure-time and impulse-time for high-range gage (upper) and low-range gage (lower) for TRINIDAD Shot B-8, Station 3

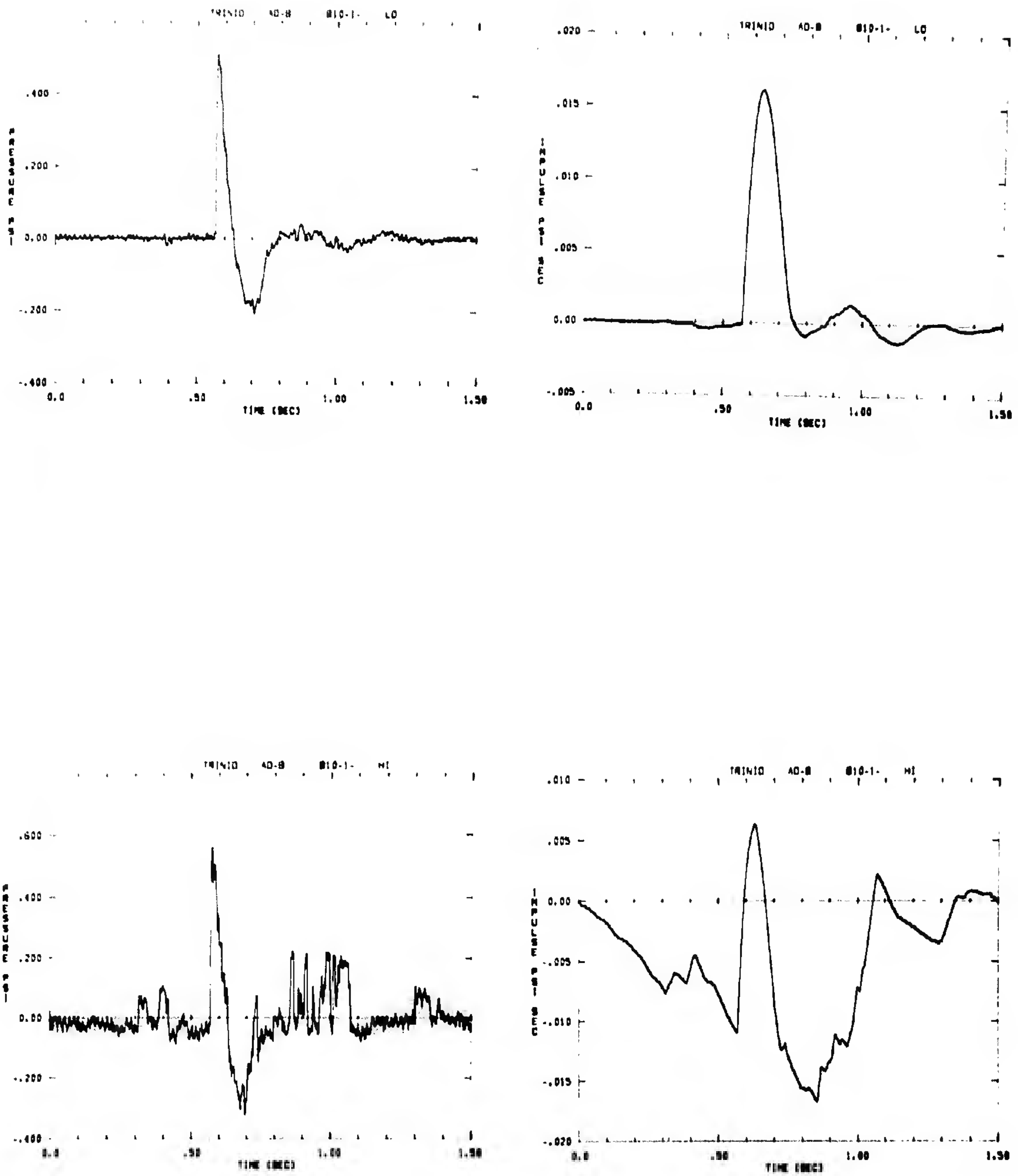

Figure B-23. Pressure-time and impulse-time for low-range gage (upper) and high-range gage (lower) for TRINIDAD Shot B-10, Station 1

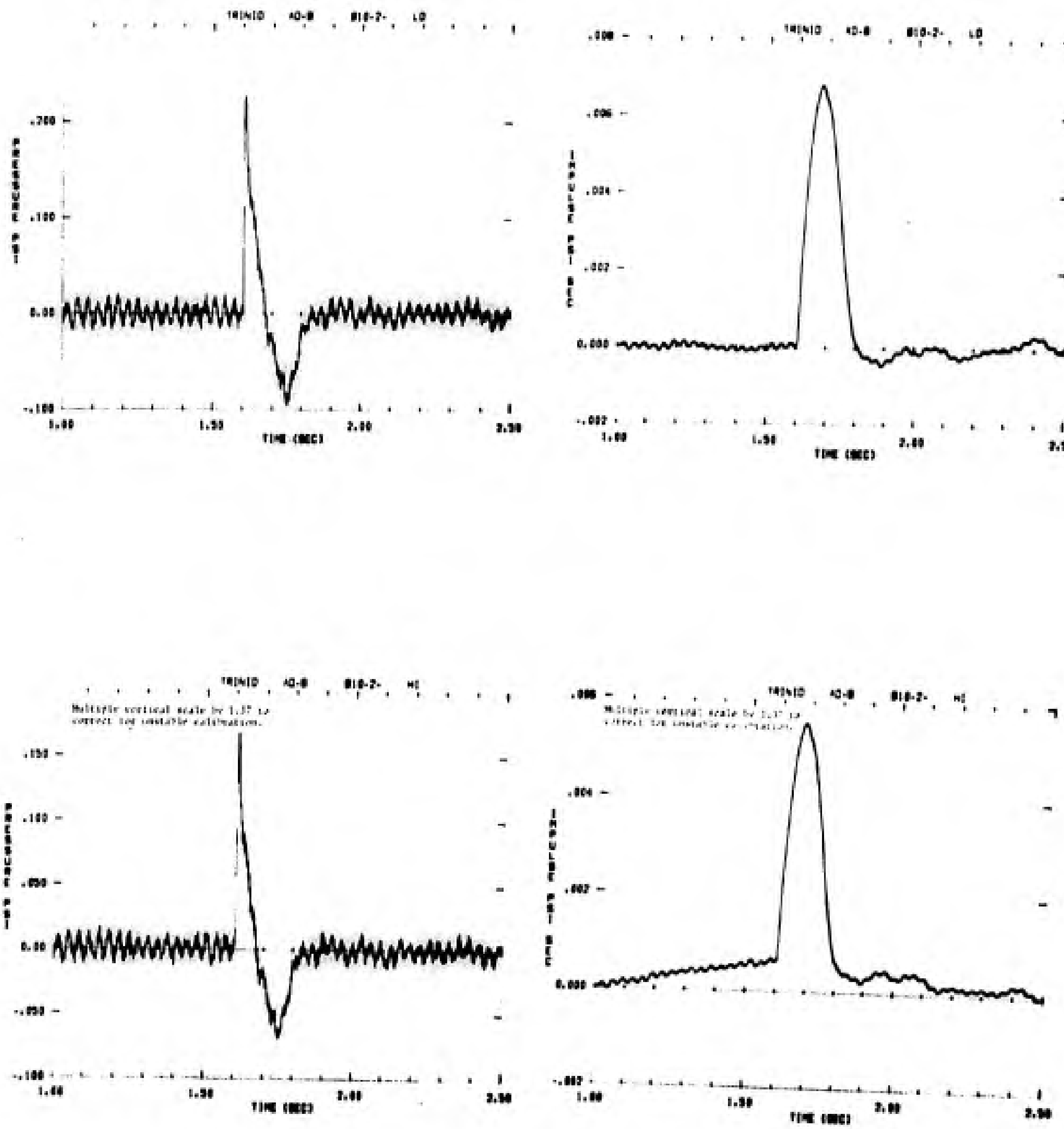

Figure B-24. Pressure-time and impulse-time for low-range gage (upper) and high-range gage (lower) for TRINIDAD Shot B-10, Station 2

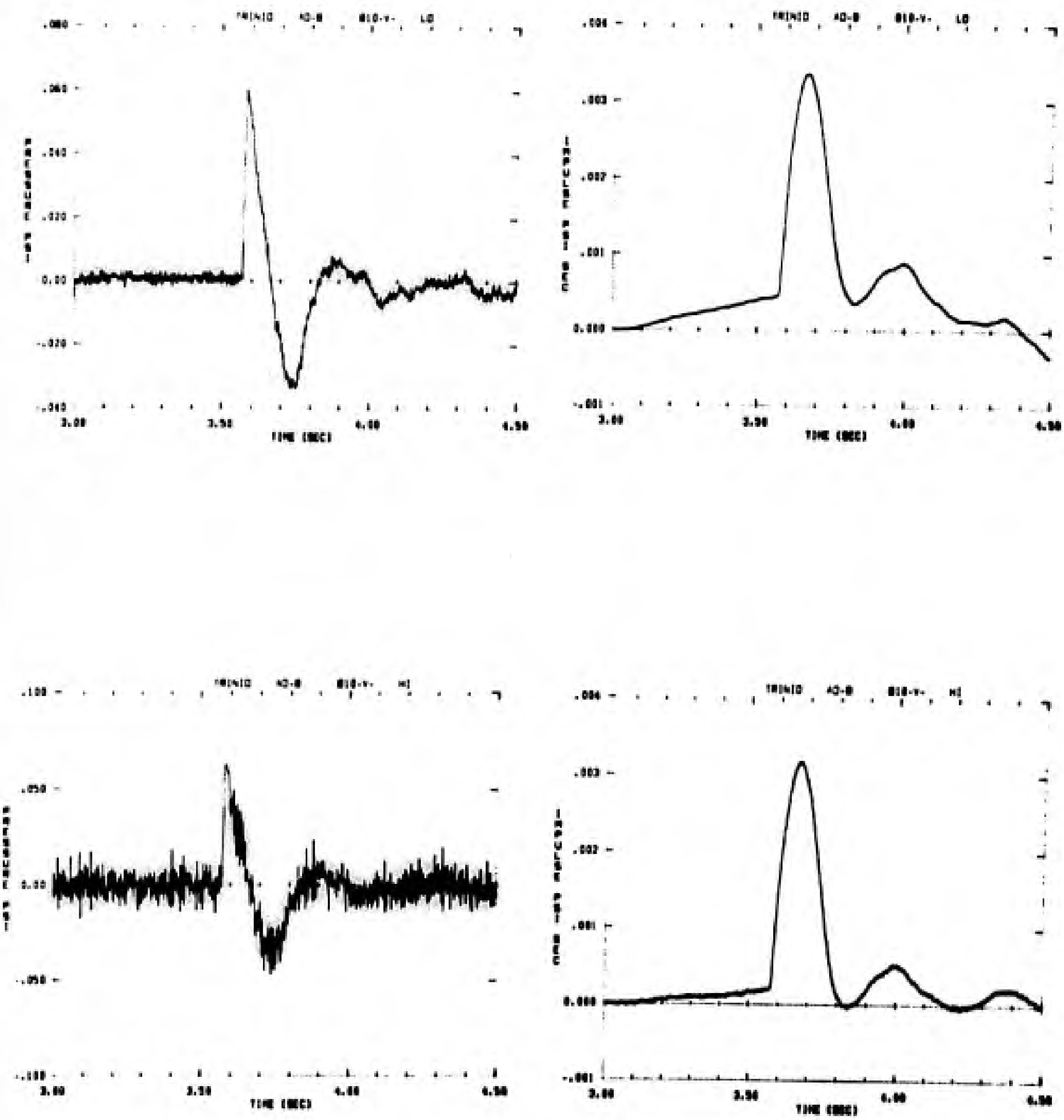

Figure B-25. Pressure-time and impulse-time for low-range gage (upper) and high-range gage (lower) for TRINIDAD Shot B-10, Station Viola

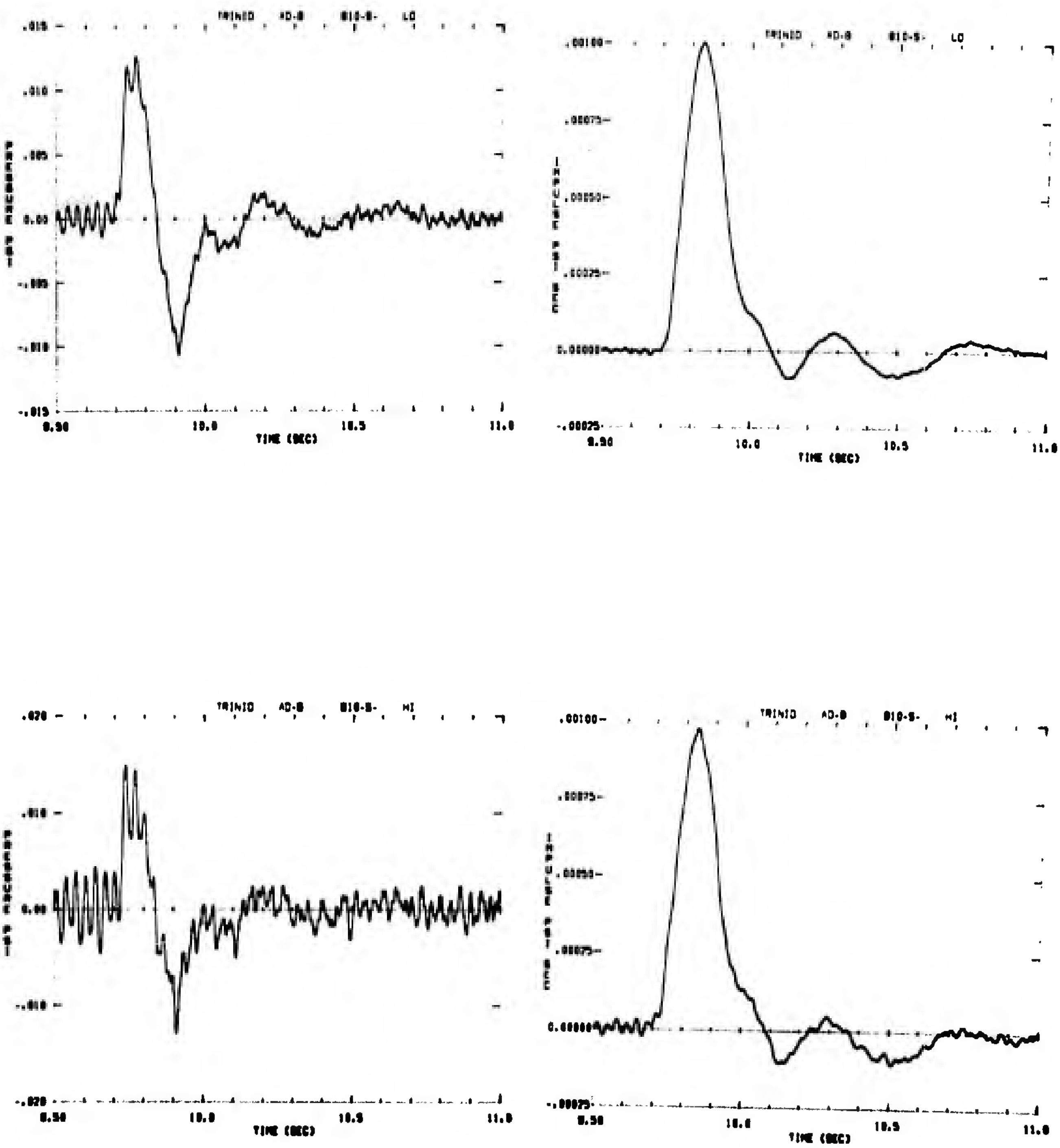

Figure B-26. Pressure-time and impulse-time for low-range gage (upper) and high-range gage (lower) for TRINIDAD Shot B-10, Station Sopris

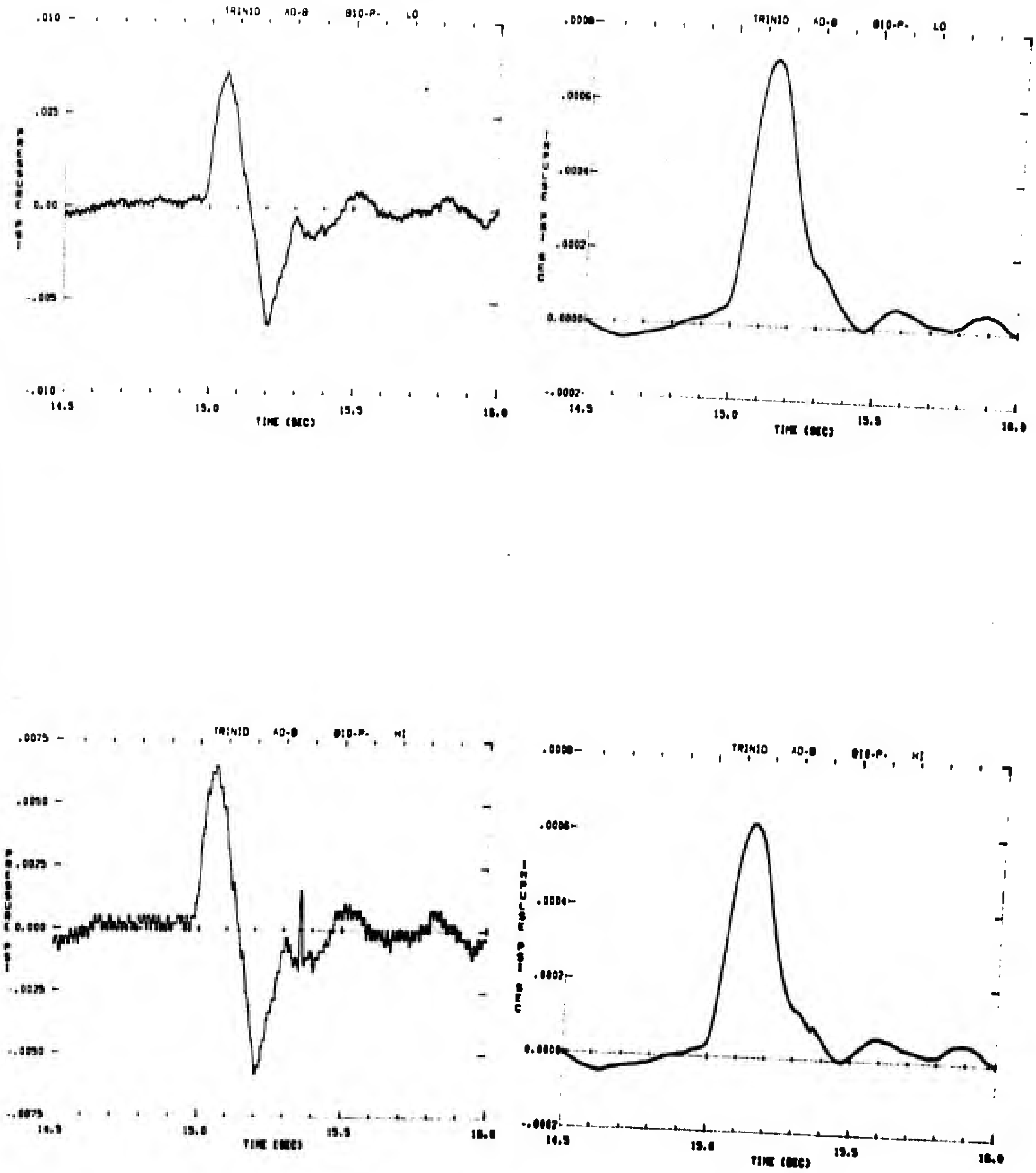

Figure B-27. Pressure-time and impulse-time for low-range gage (upper) and high-range gage (lower) for TRINIDAD Shot B-10, Station Piedmont

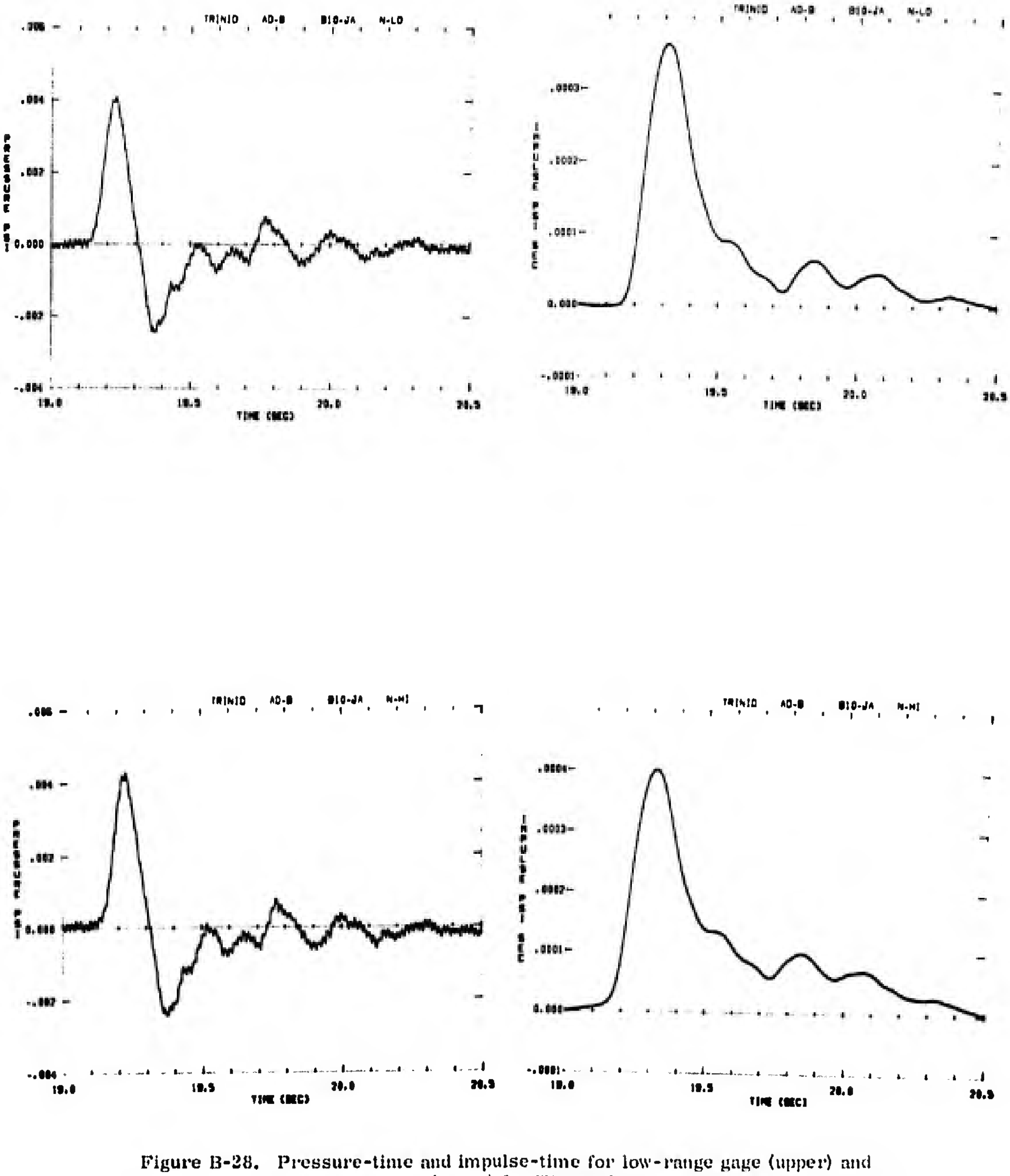

Figure B-28. Pressure-time and impulse-time for low-range gage (upper) and high-range gage (lower) for TRINIDAD Shot B-10, Station Jansen

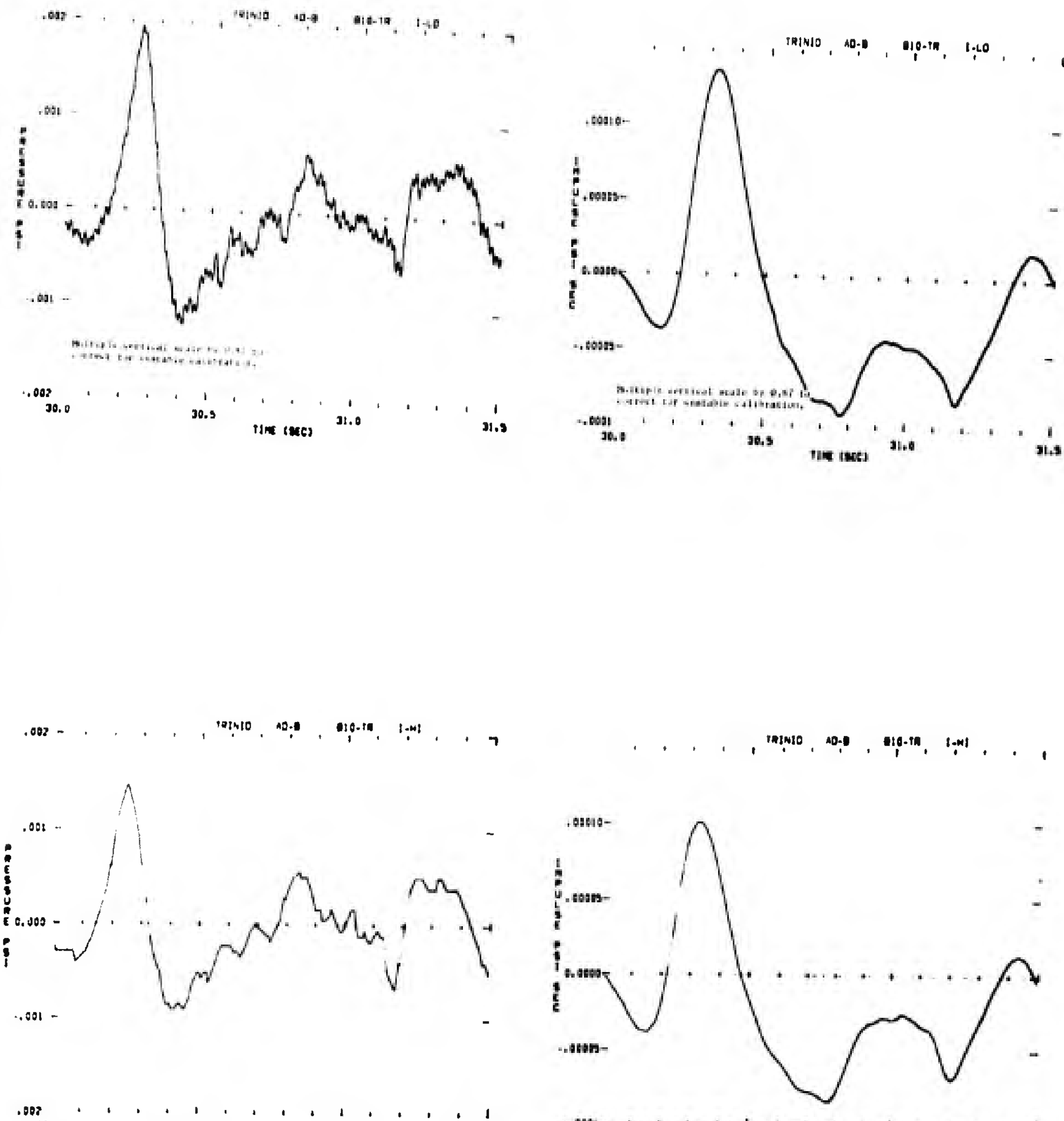

Figure B-29. Pressure-time and impulse-time for low-range gage (upper) and high-range gage (lower) for TRINIDAD Shot B-10, Station Trinidad

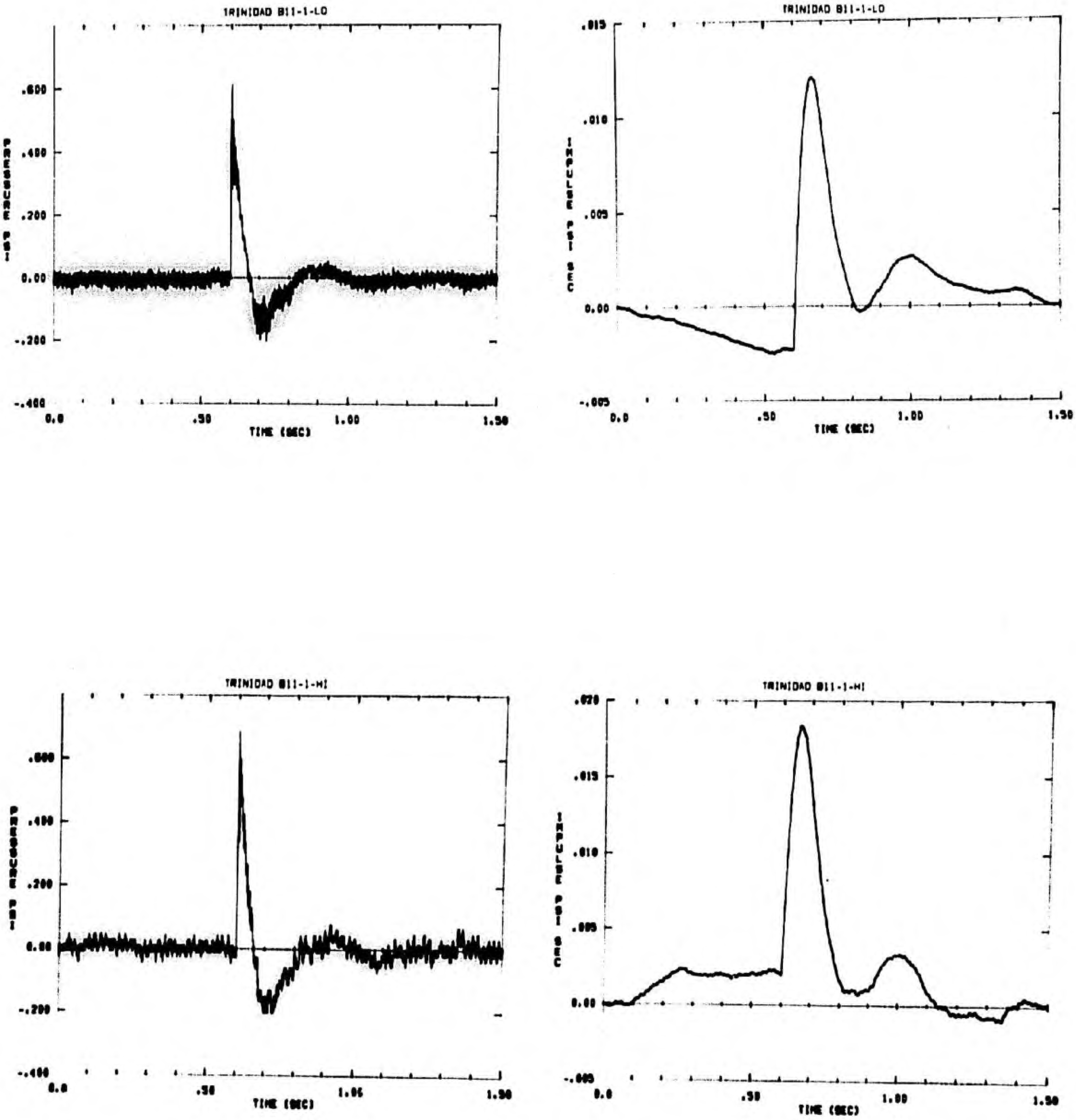

Figure B-30. Pressure-time and impulse-time for low-range gage (upper) and high-range gage (lower) for TRINIDAD Shot B-11, Station 1

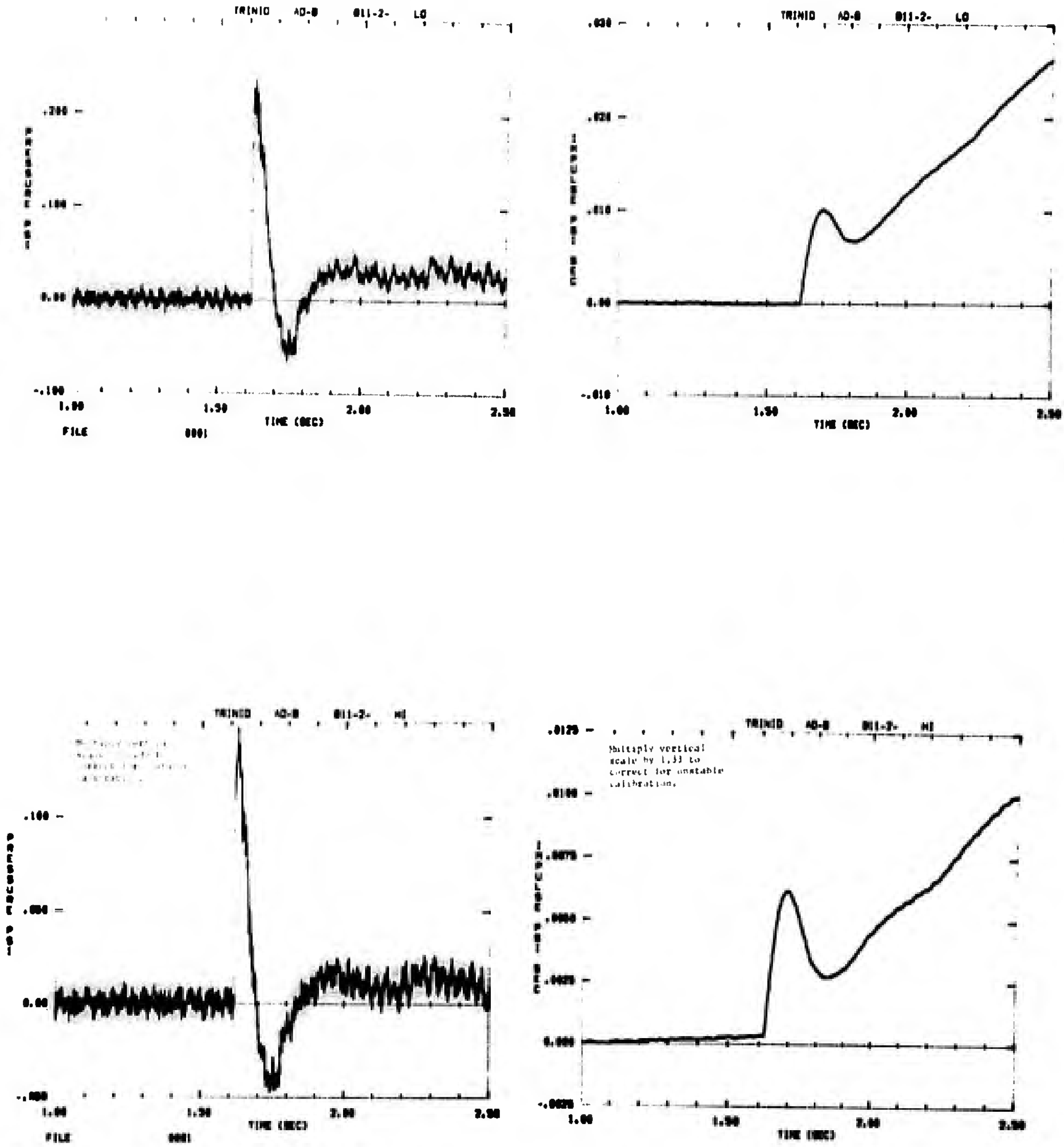

Figure B-31. Pressure-time and impulse-time for low-range gage (upper) and high-range gage (lower) for TRINIDAD Shot B-11, Station 2

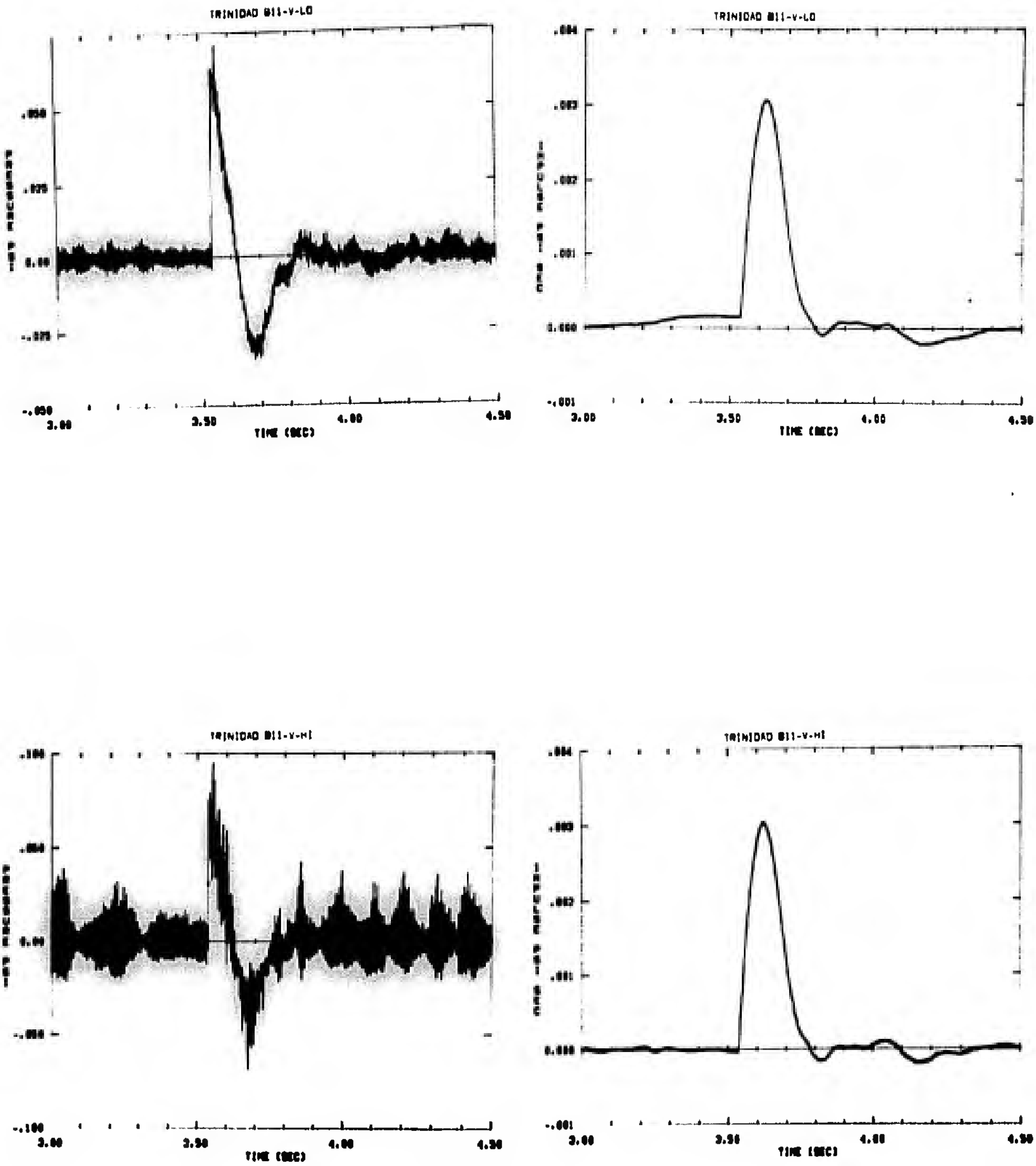

Figure B-32. Pressure-time and impulse-time for low-range gage (upper) and high-range gage (lower) for TRINIDAD Shot B-11, Station Viola

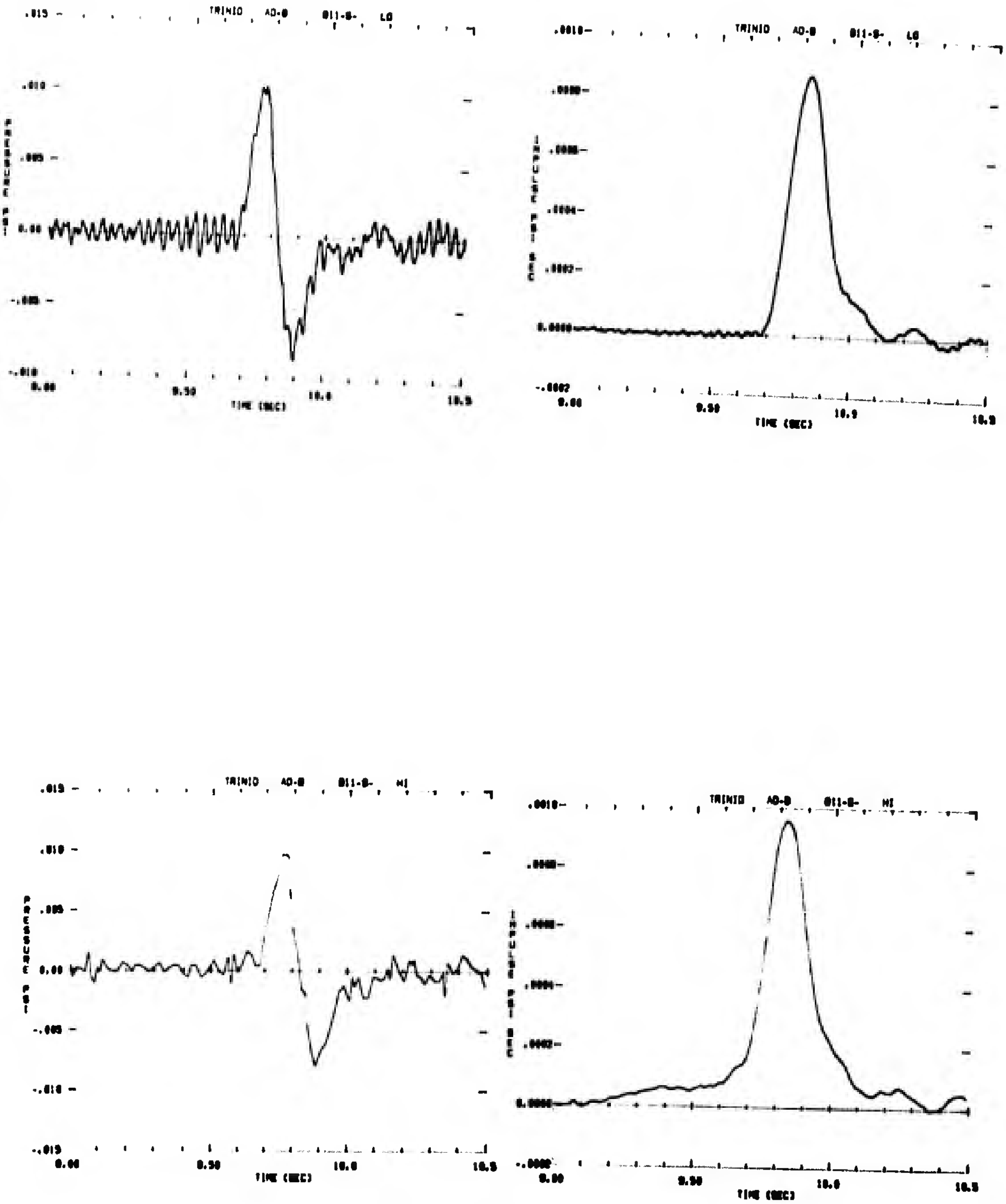

Figure B-33. Pressure-time and impulse-time for low-range gage (upper) and high-range gage (lower) for TRINIDAD Shot B-11, Station Sopris

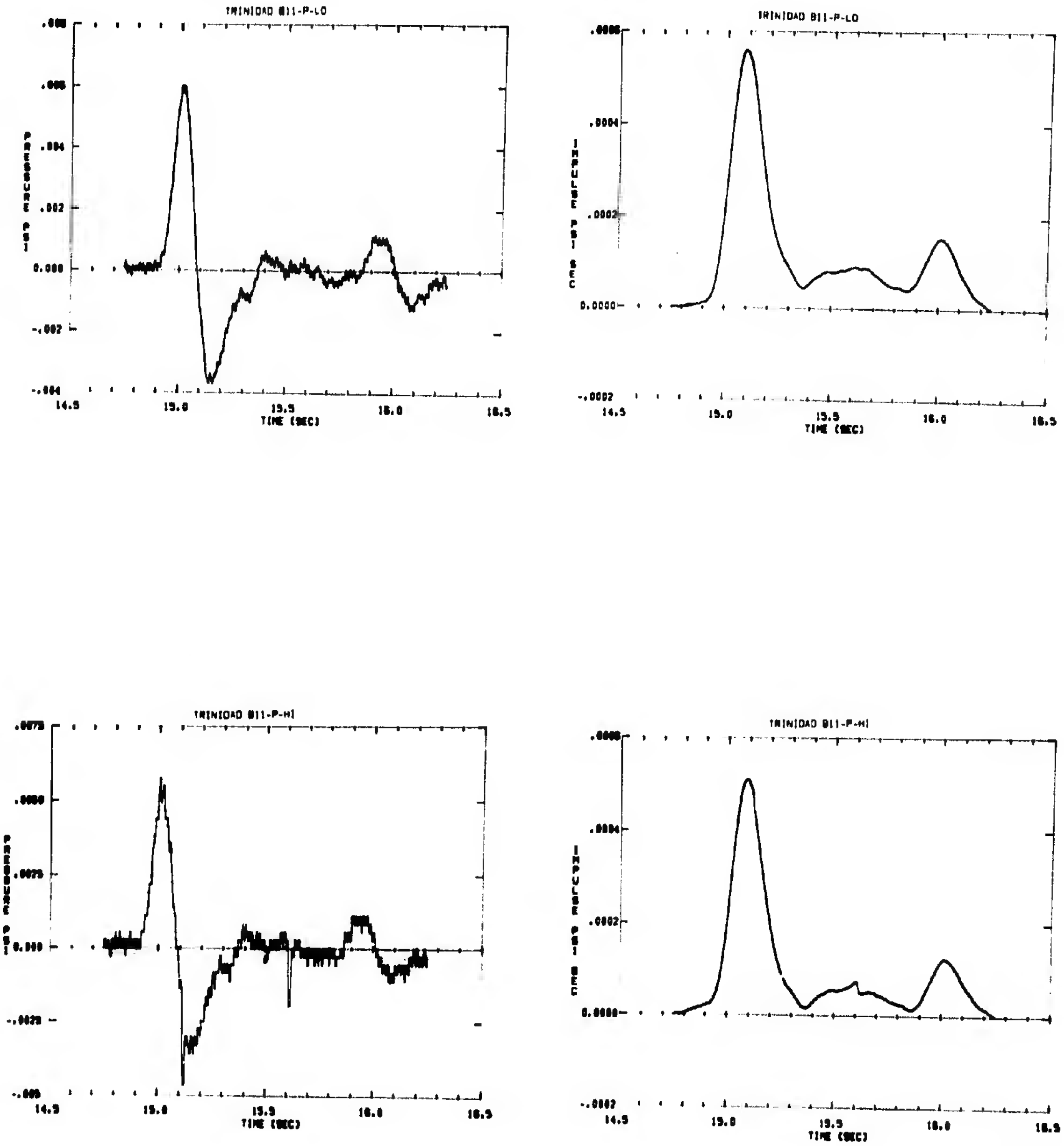

Figure B-34. Pressure-time and impulse-time for low-range gage (upper) and high-range gage (lower) for TRINIDAD Shot B-11, Station Piedmont

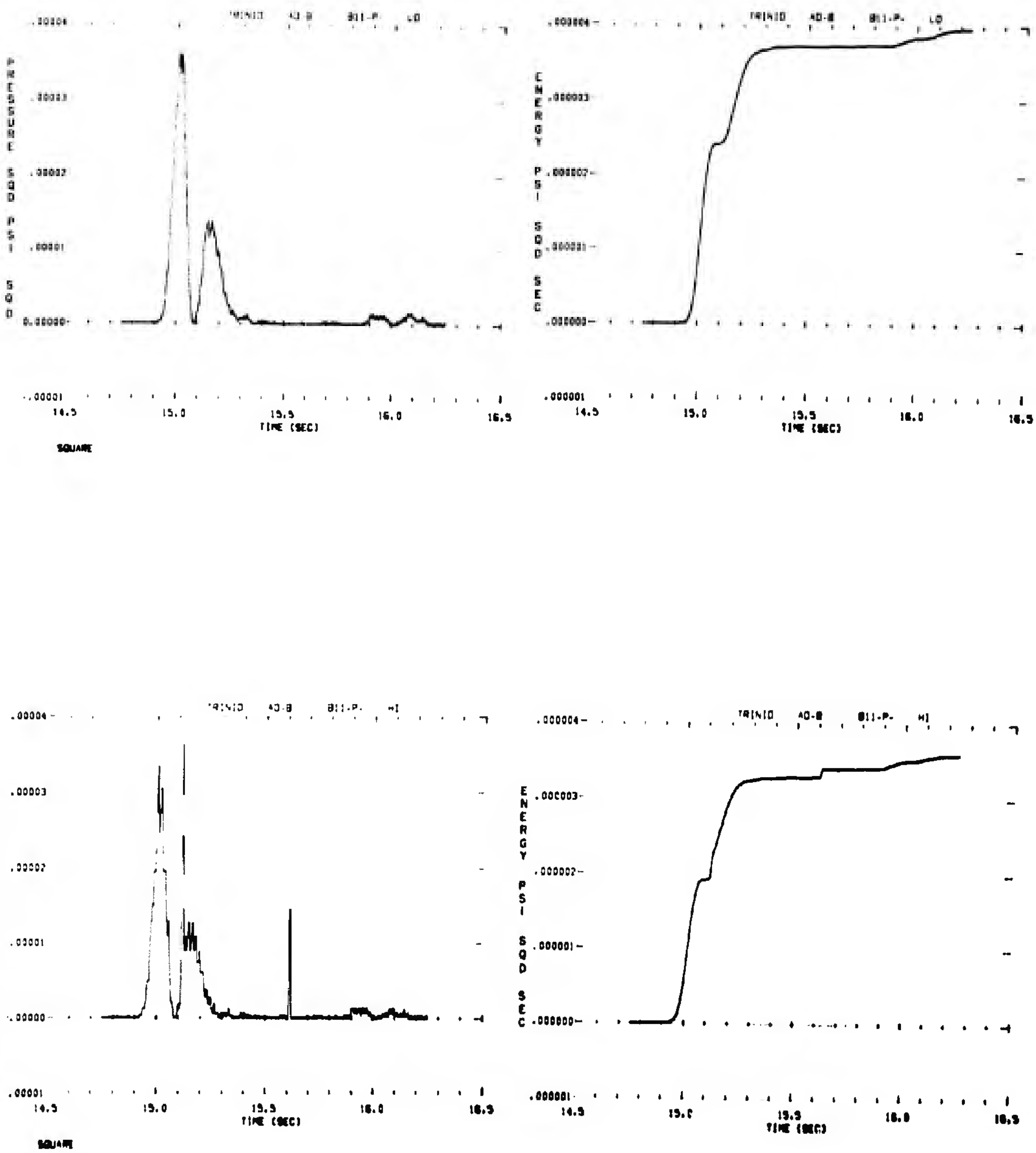

Figure B-35. Pressure-squared-time and Σp^2 - t for low-range gage (upper) and high-range gage (lower) for TRINIDAD Shot B-11, Station Piedmont

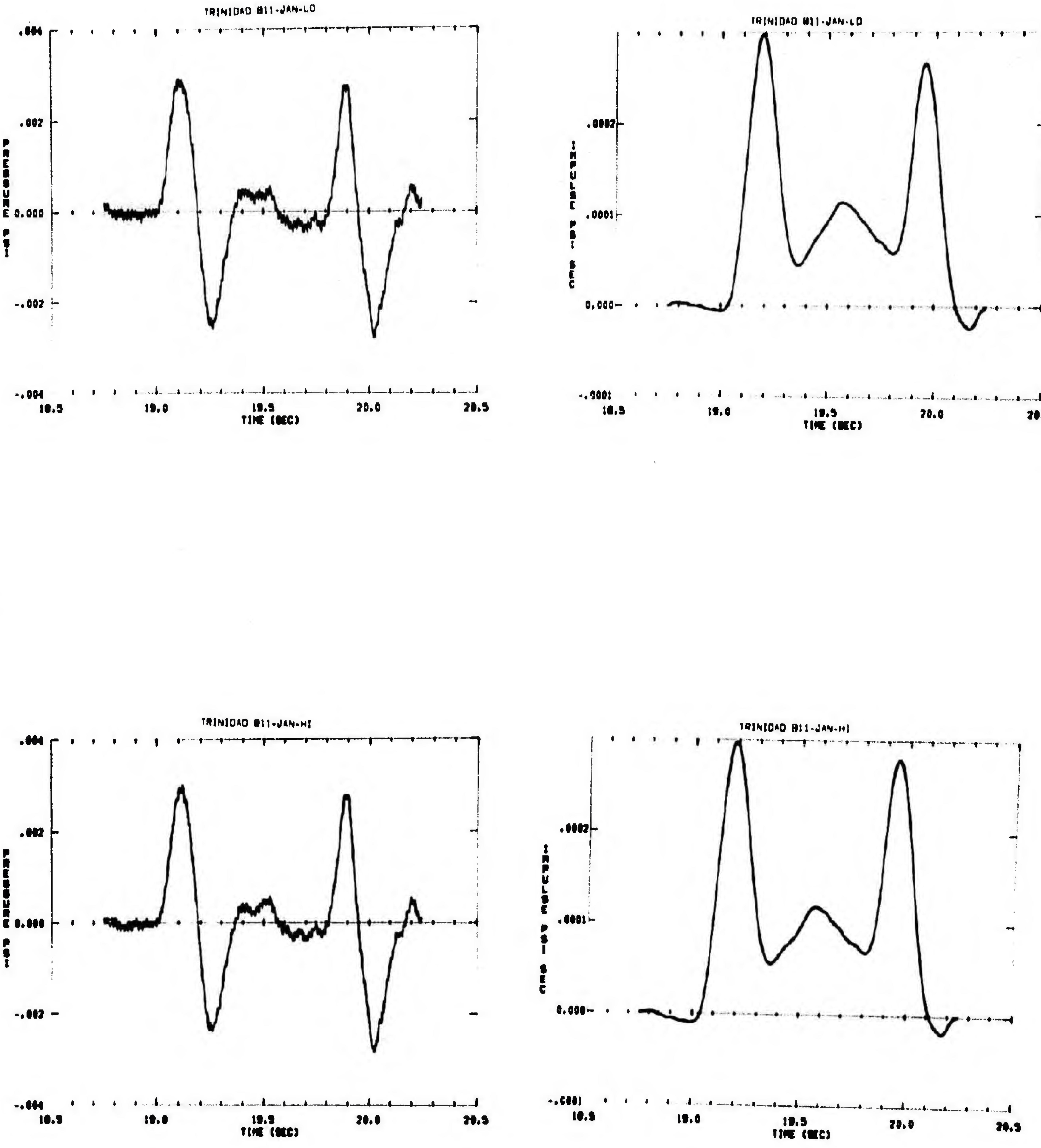

Figure B-36. Pressure-time and impulse-time for low-range gage (upper) and high-range gage (lower) for TRINIDAD Shot B-11, Station Jansen

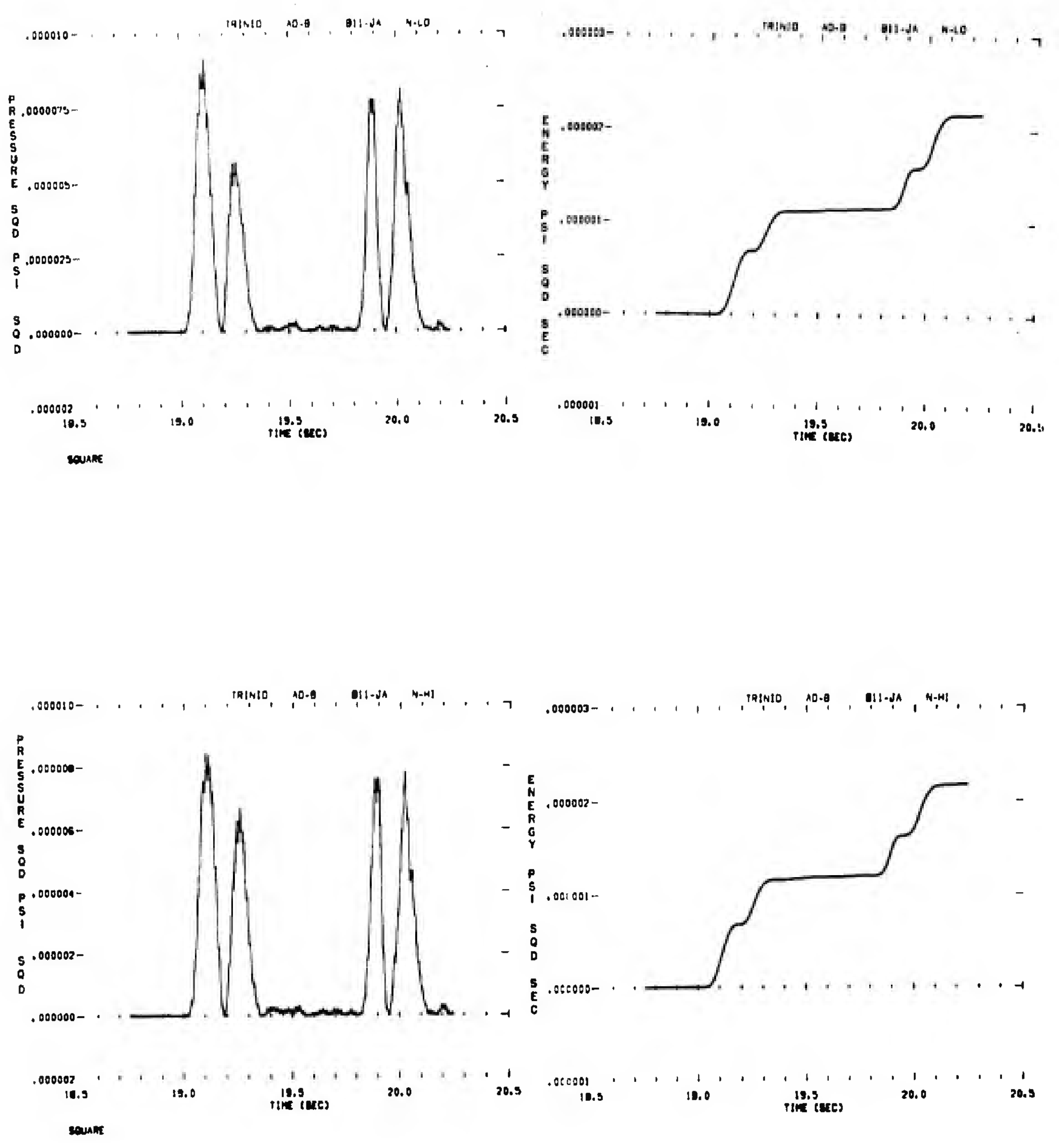

Figure B-37. Pressure-squared-time and Σp^2 - t for low-range gage (upper) and high-range gage (lower) for TRINIDAD Shot B-11, Station Jansen

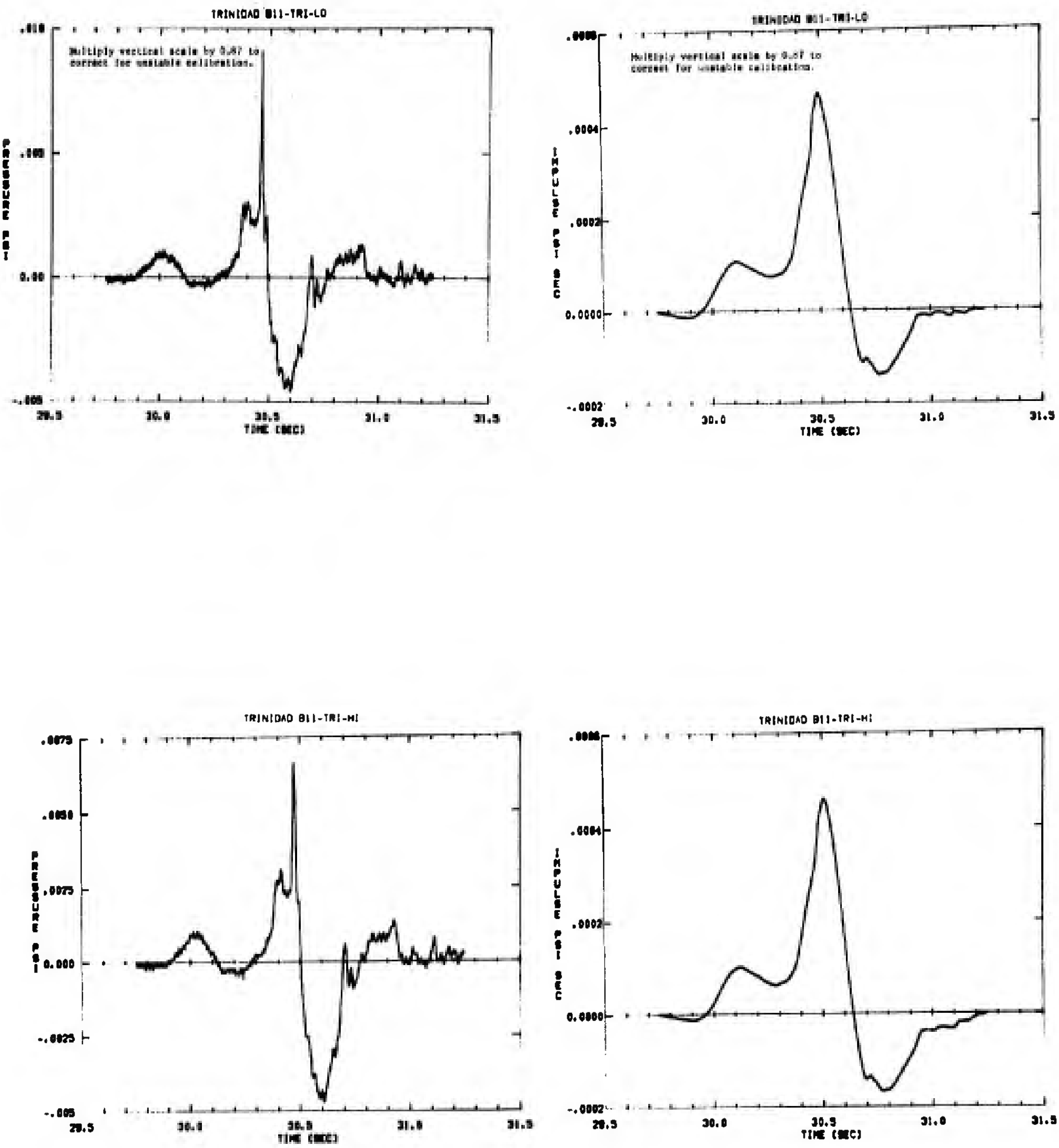

Figure B-38. Pressure-time and impulse-time for low-range gage (upper) and high-range gage (lower) for TRINIDAD Shot B-11, Station Trinidad

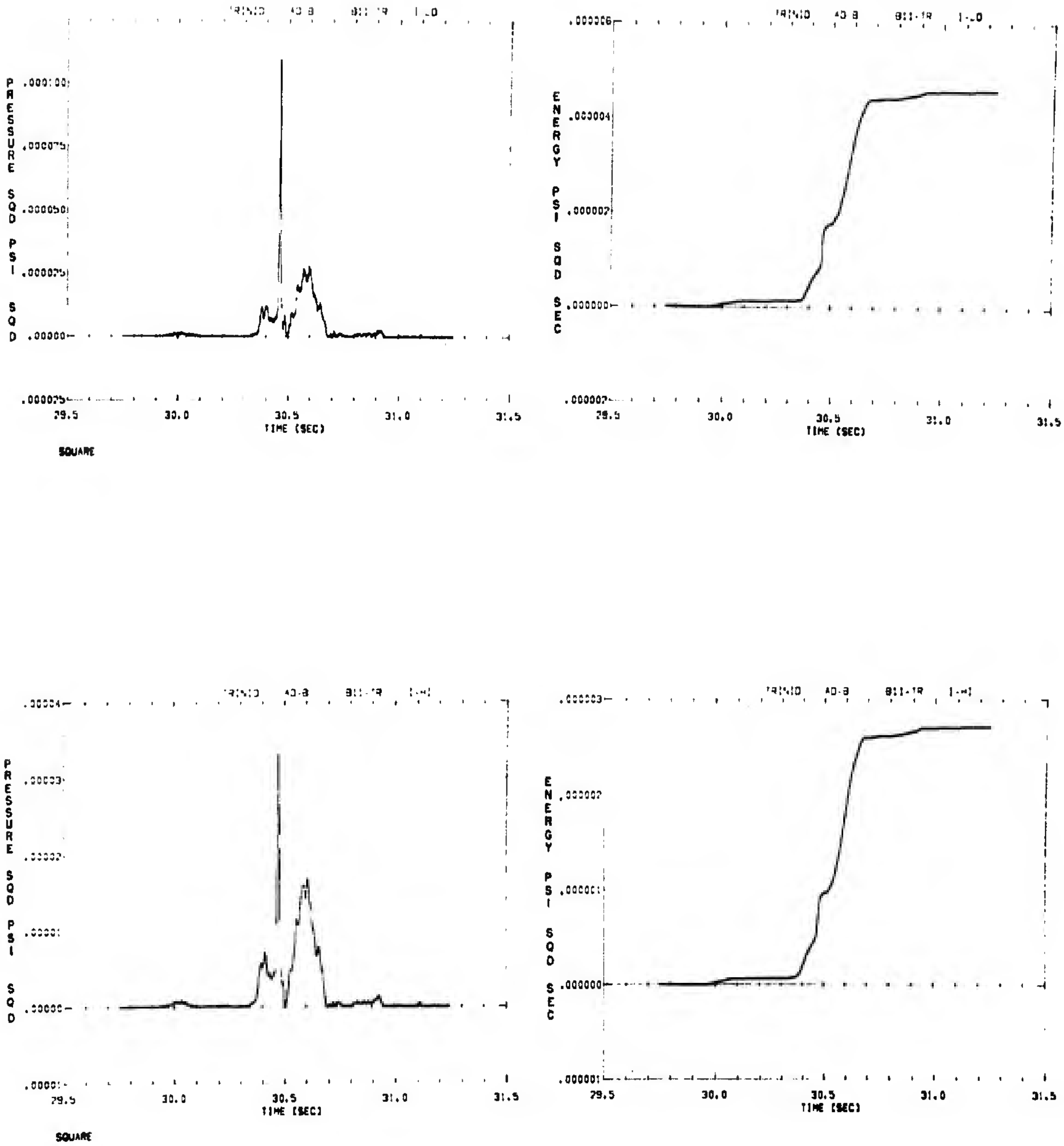

Figure B-39. Pressure-squared-time and Σp^2 - t for low-range gage (upper) and high-range gage (lower) for TRINIDAD Shot B-11, Station Trinidad

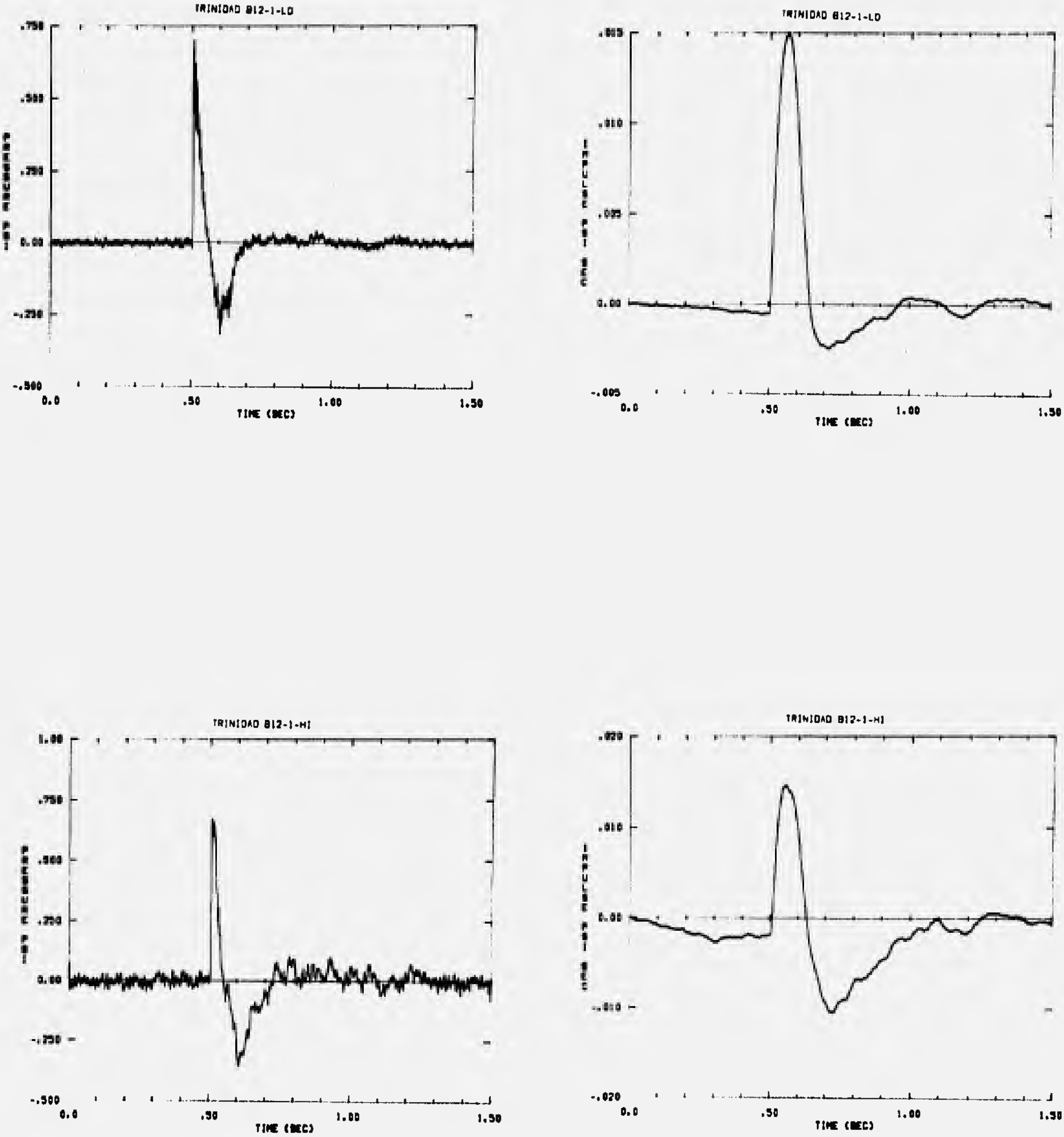

Figure B-40. Pressure-time and impulse-time for low-range gage (upper) and high-range gage (lower) for TRINIDAD Shot B-12, Station 1

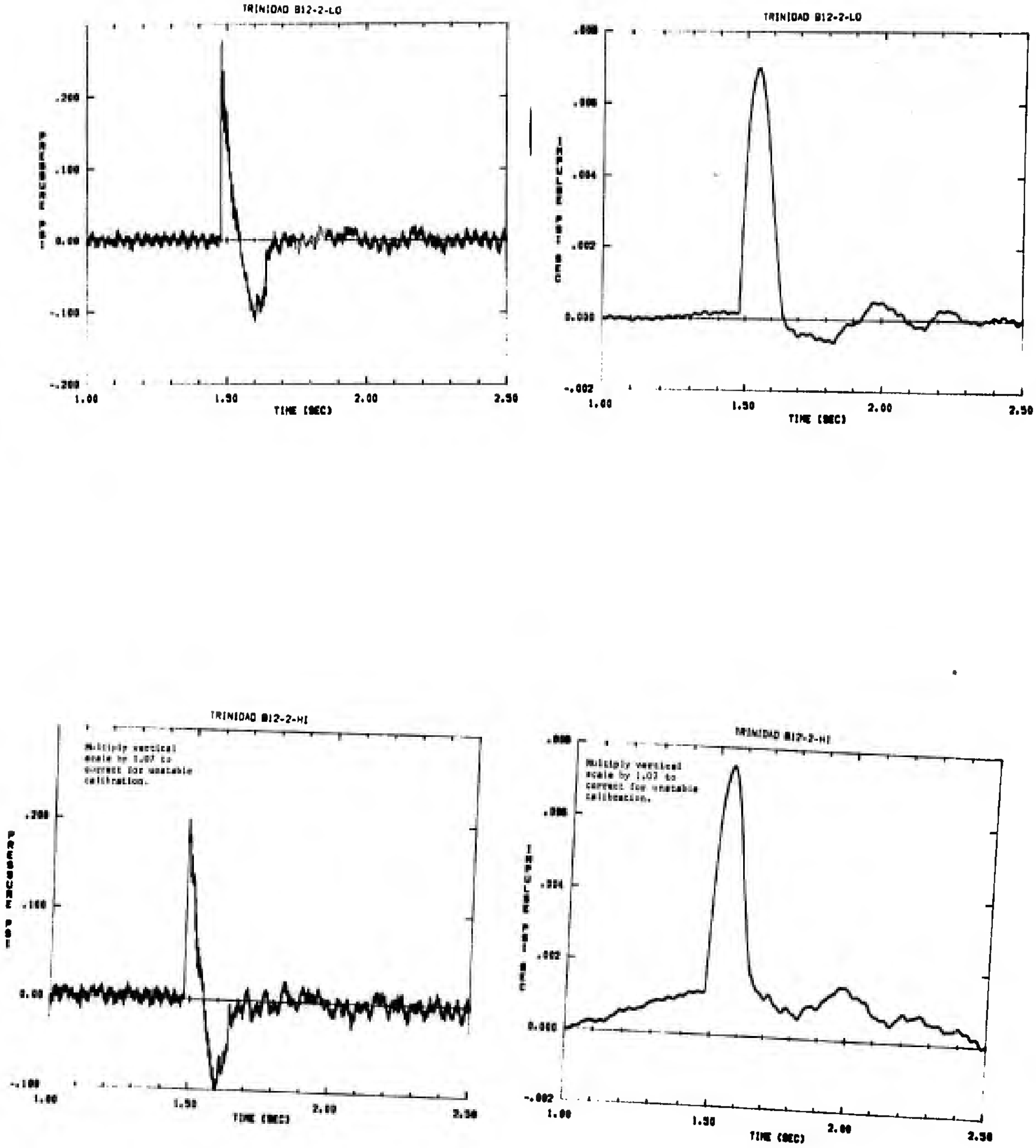

Figure B-41. Pressure-time and impulse-time for low-range gage (upper) and high-range gage (lower) for TRINIDAD Shot B-12, Station 2

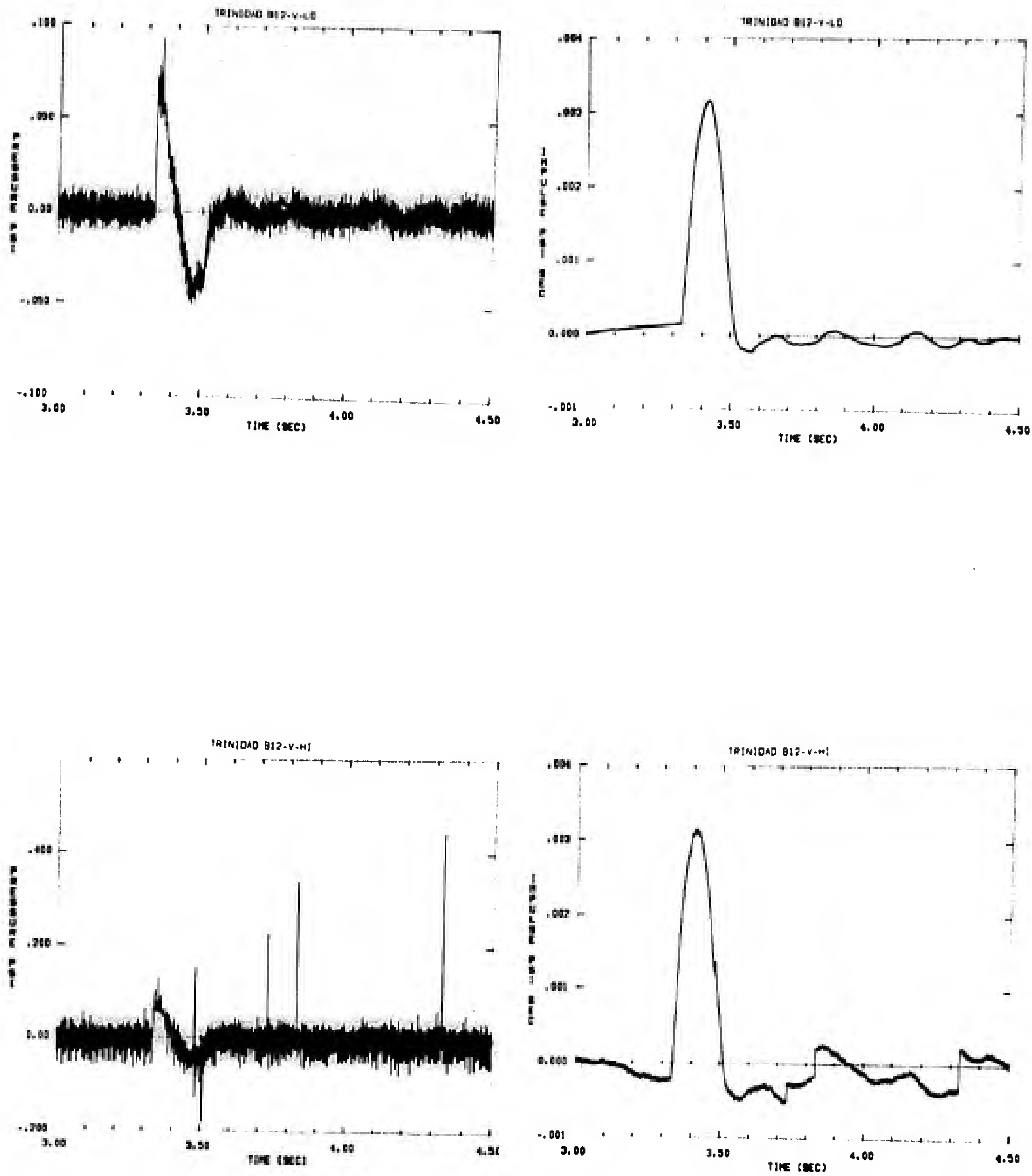

Figure B-42. Pressure-time and impulse-time for low-range gage (upper) and high-range gage (lower) for TRINIDAD Shot B-12, Station Viola

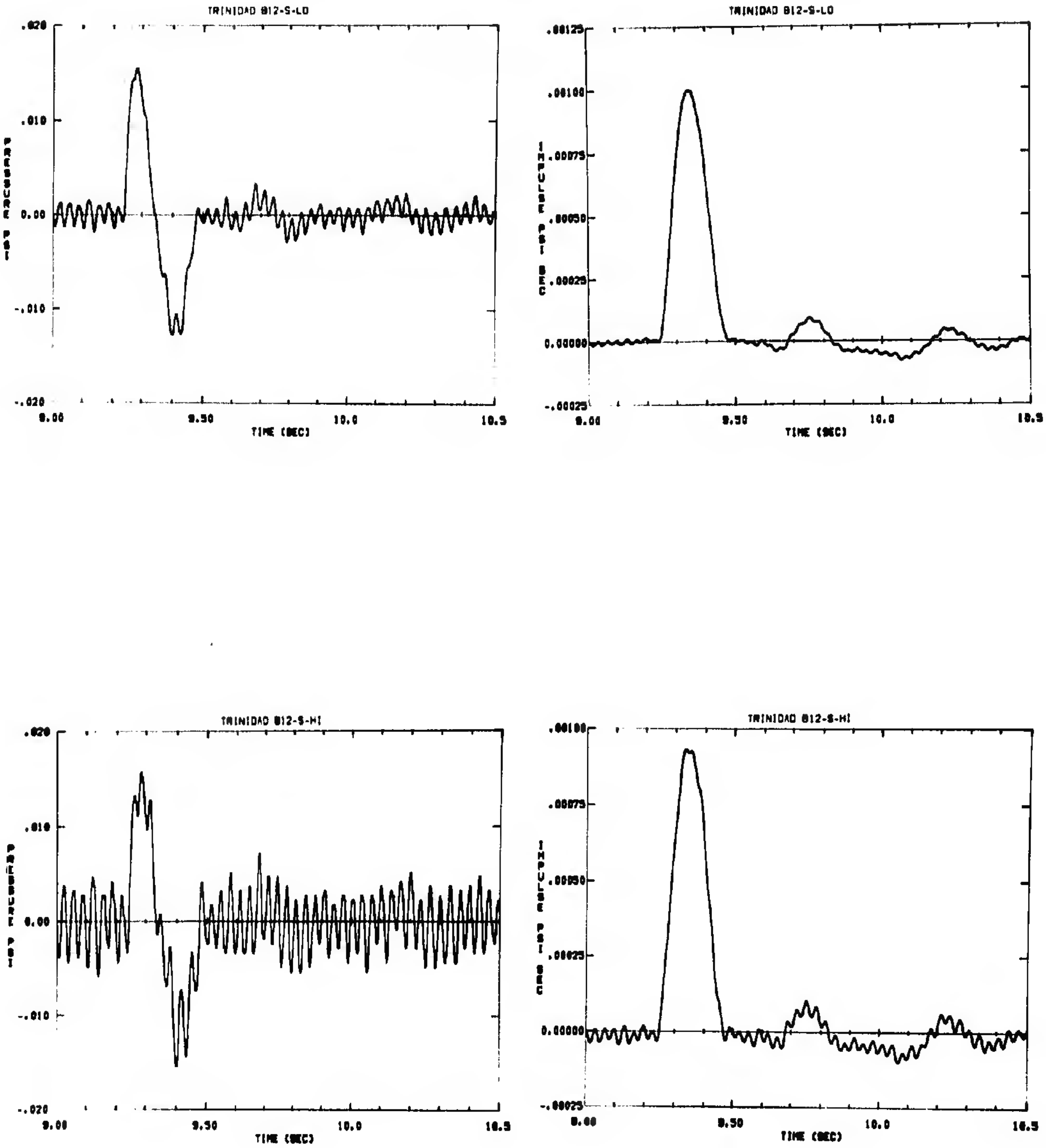

Figure B-43. Pressure-time and impulse-time for low-range gage (upper) and high-range gage (lower) for TRINIDAD Shot B12, Station Sopris

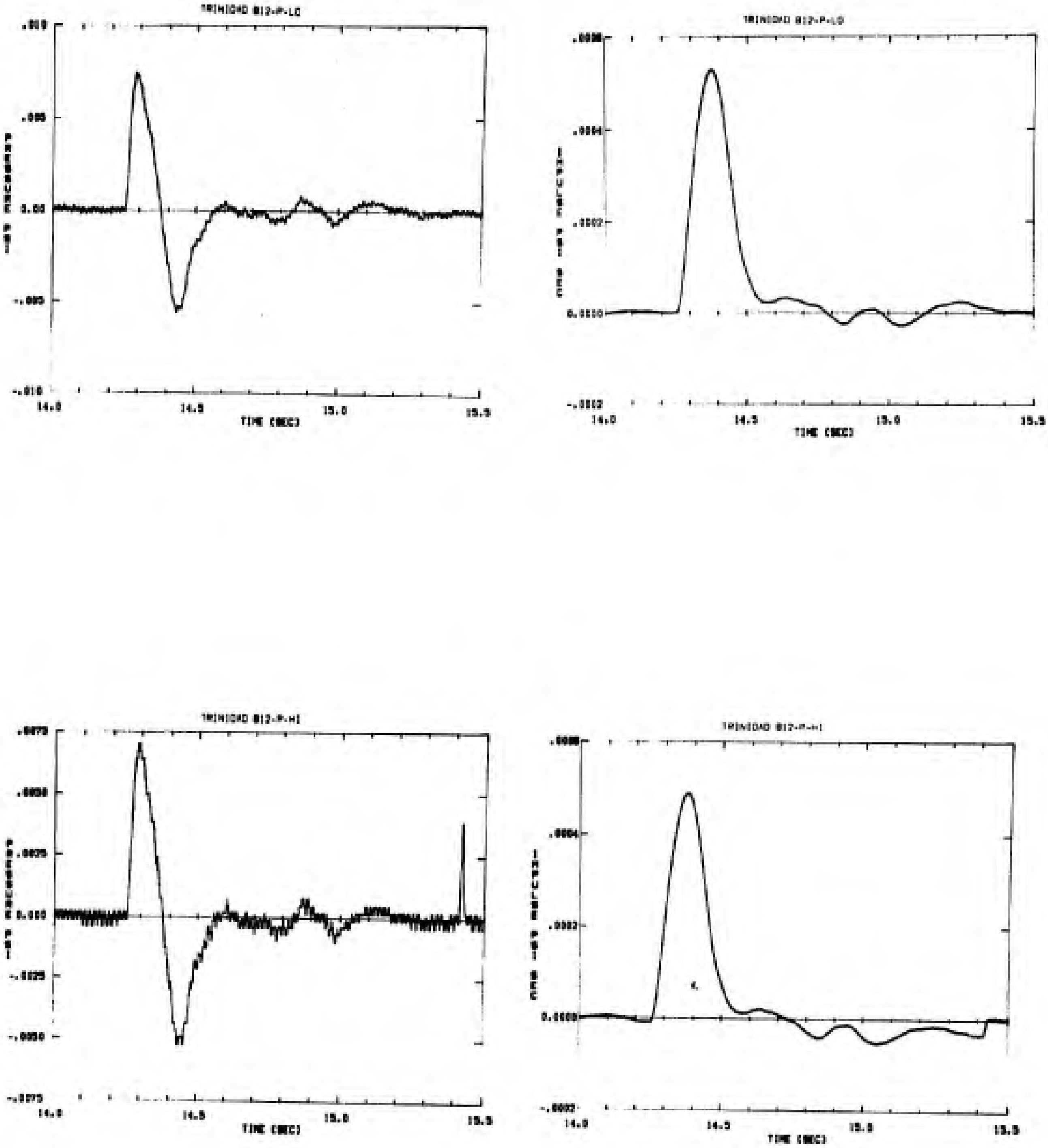

Figure B-44. Pressure-time and impulse-time for low-range gage (upper) and high-range gage (lower) for TRINIDAD Shot B-12, Station Piedmont

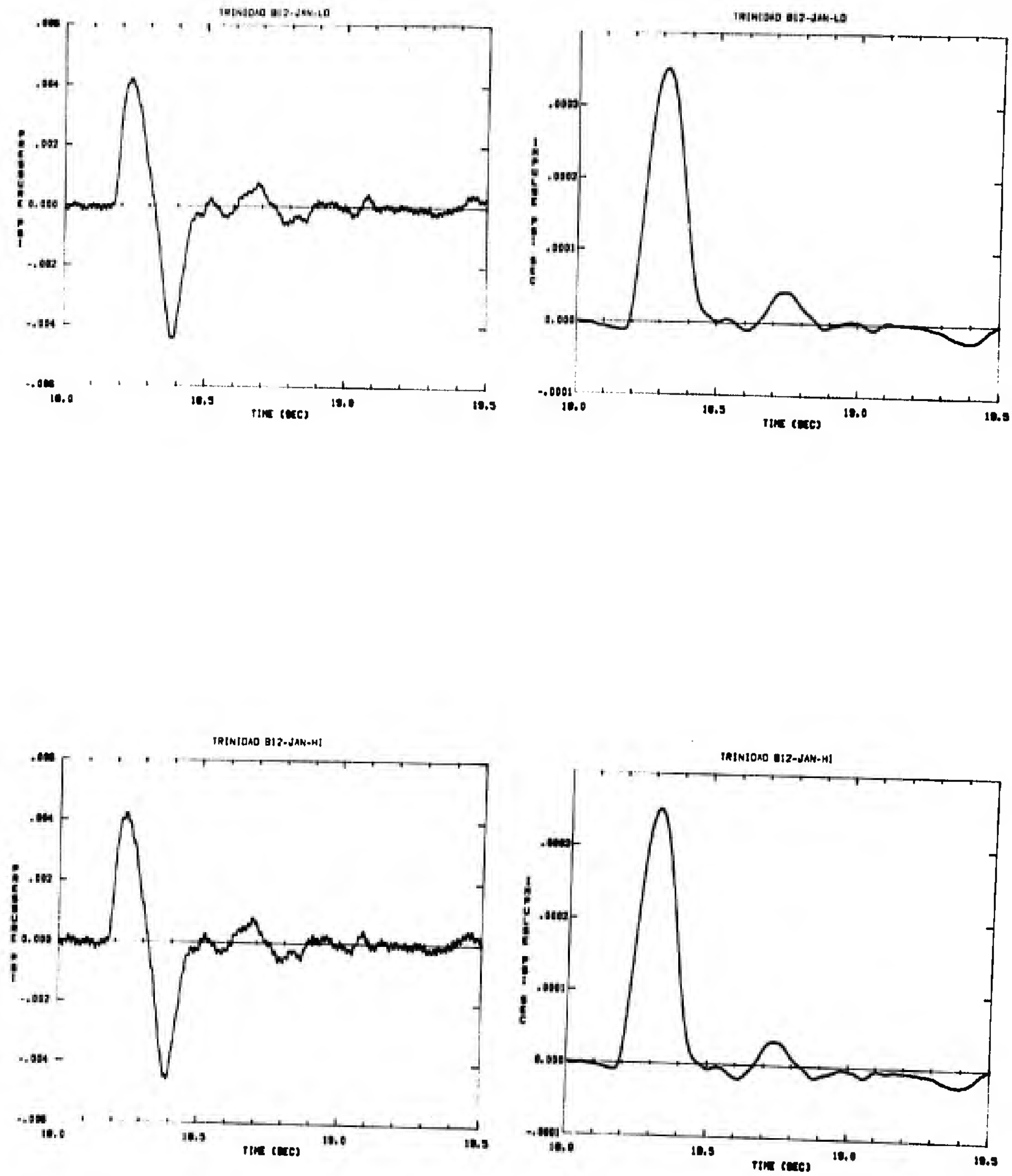

Figure B-45. Pressure-time and impulse-time for low-range gage (upper) and high-range gage (lower) for TRINIDAD Shot B-12, Station Jansen

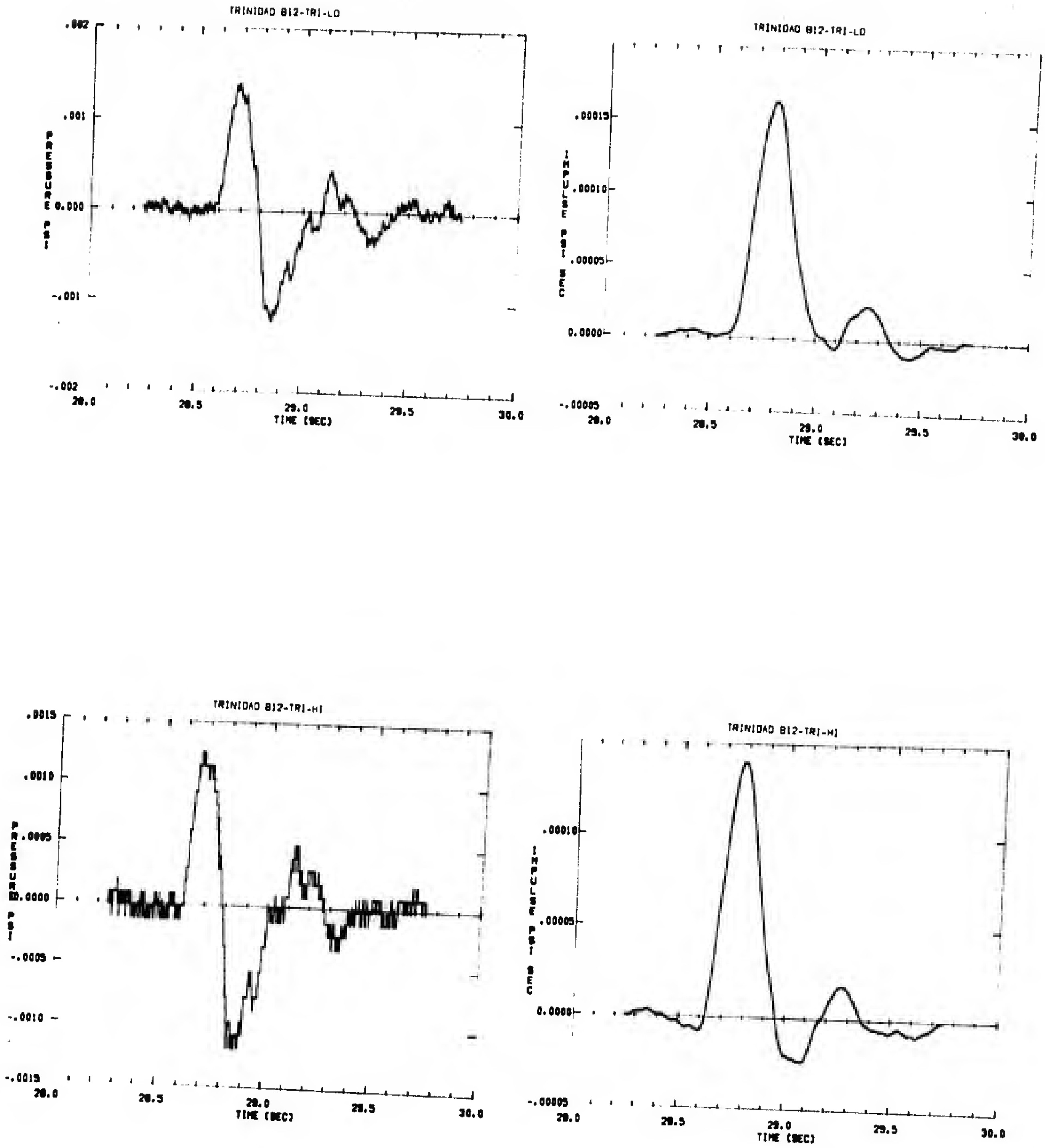

Figure B-46. Pressure-time and impulse-time for low-range gage (upper) and high-range gage (lower) for TRINIDAD Shot B-12, Station Trinidad

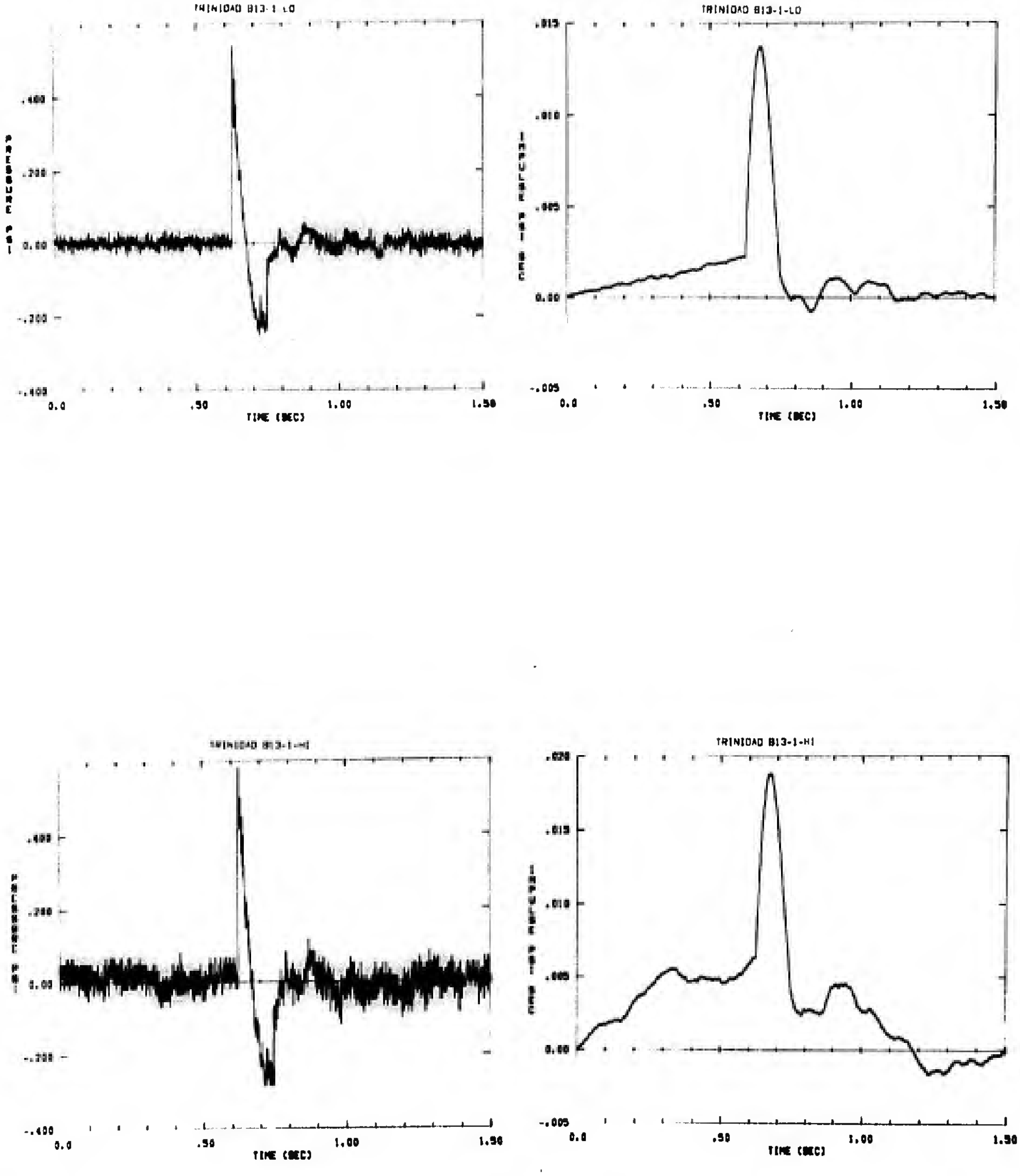

Figure B-47. Pressure-time and impulse-time for low-range gage (upper) and high-range gage (lower) for TRINIDAD Shot B-13, Station 1

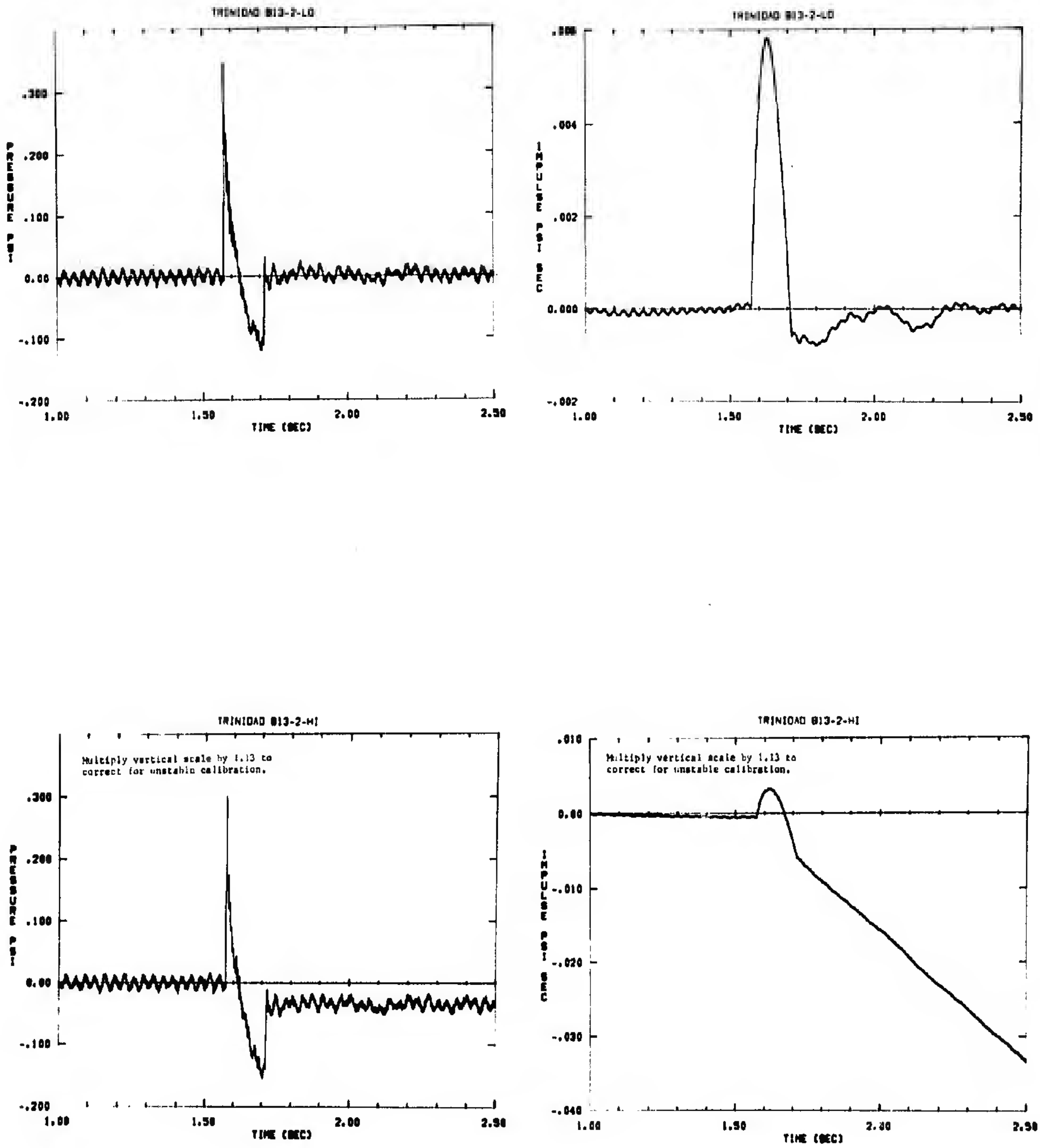

Figure B-48. Pressure-time and impulse-time for low-range gage (upper) and high-range gage (lower) for TRINIDAD Shot B-13, Station 2

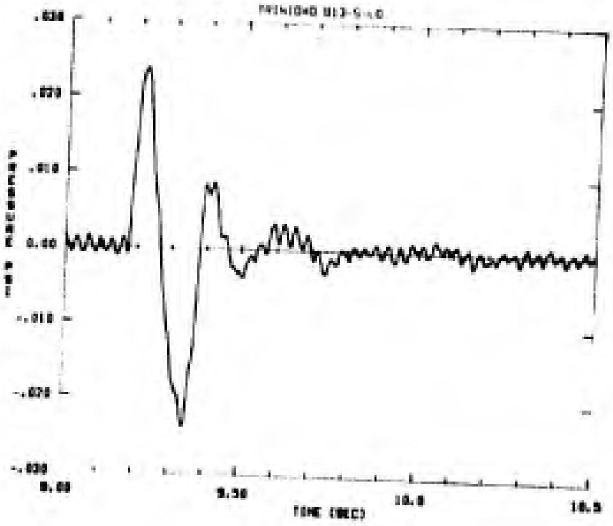

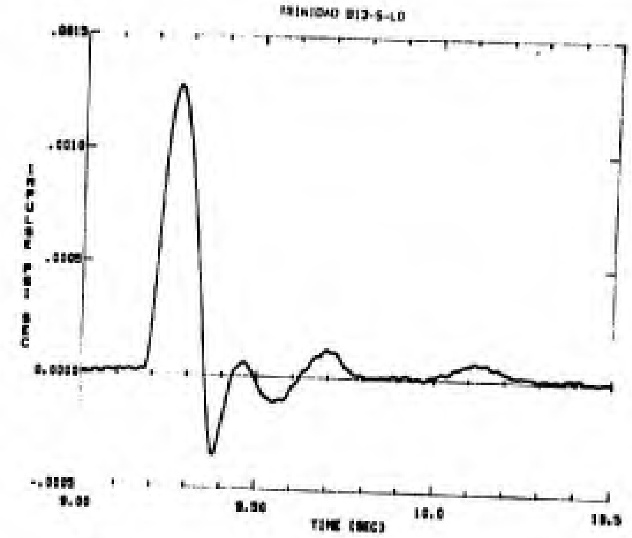

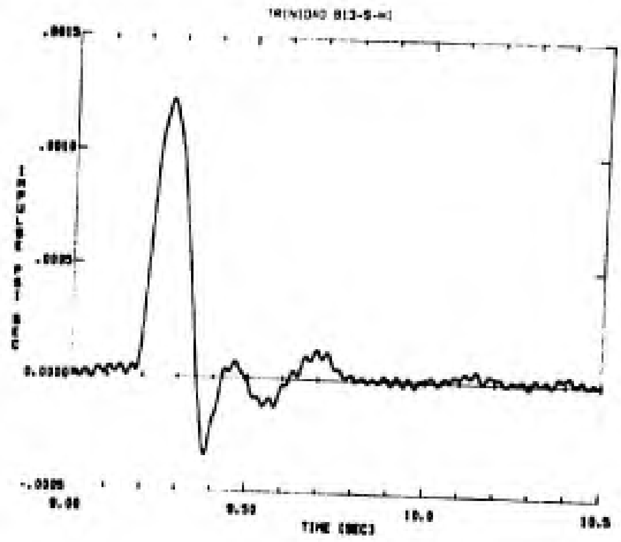

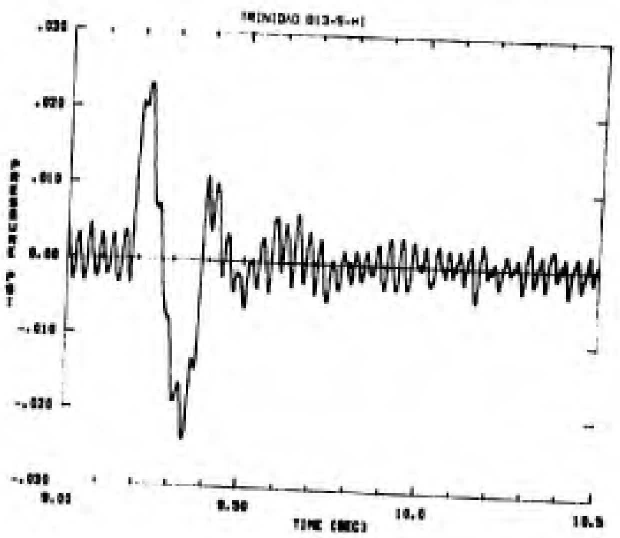

Figure B-49. Pressure-time and impulse-time for low-range gage (upper) and high-range gage (lower) for TRINIDAD Shot B-13, Station Sopris

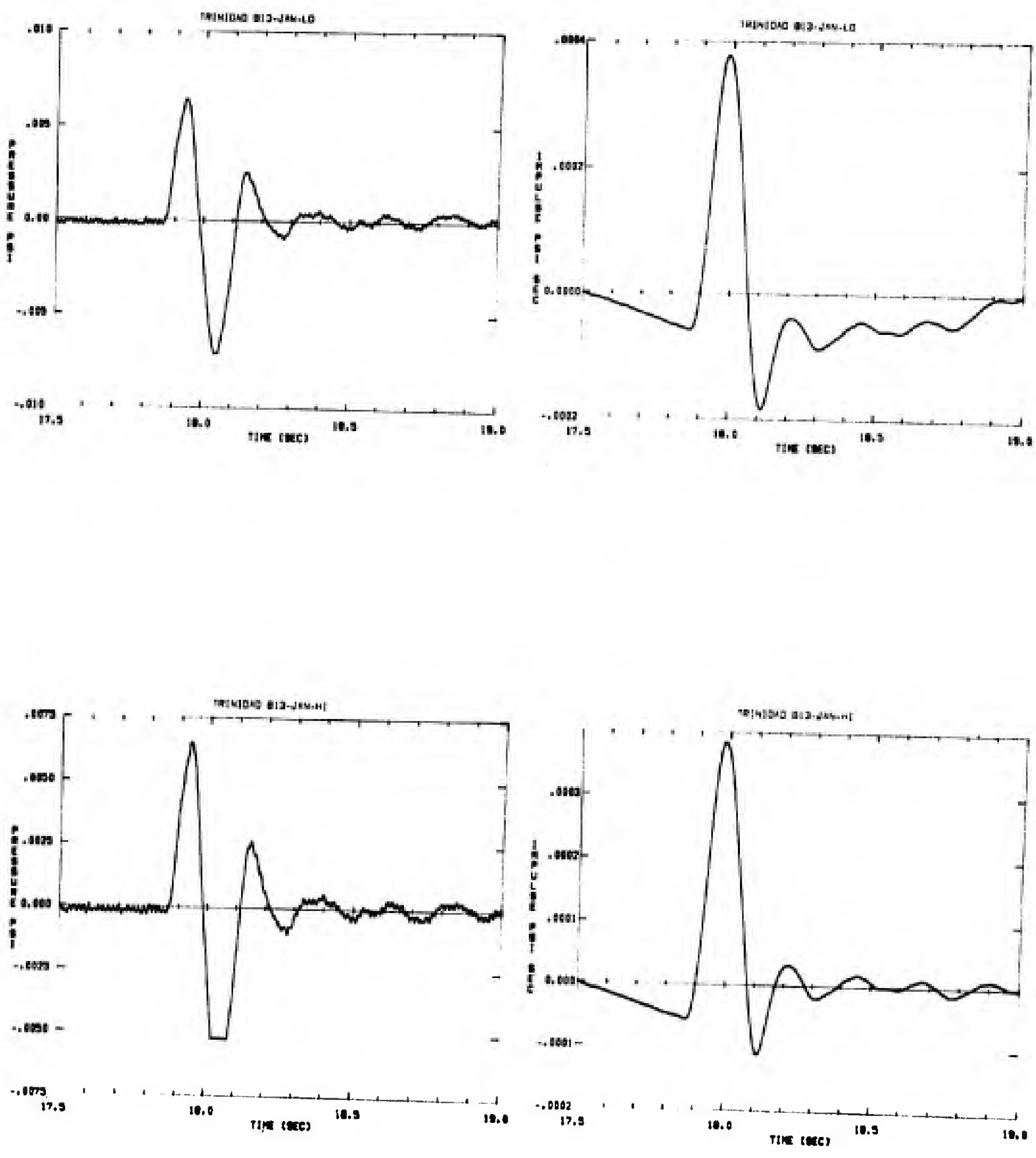

Figure B-50. Pressure-time and impulse-time for low-range gage (upper) and high-range gage (lower) for TRINIDAD Shot B-13, Station Jansen

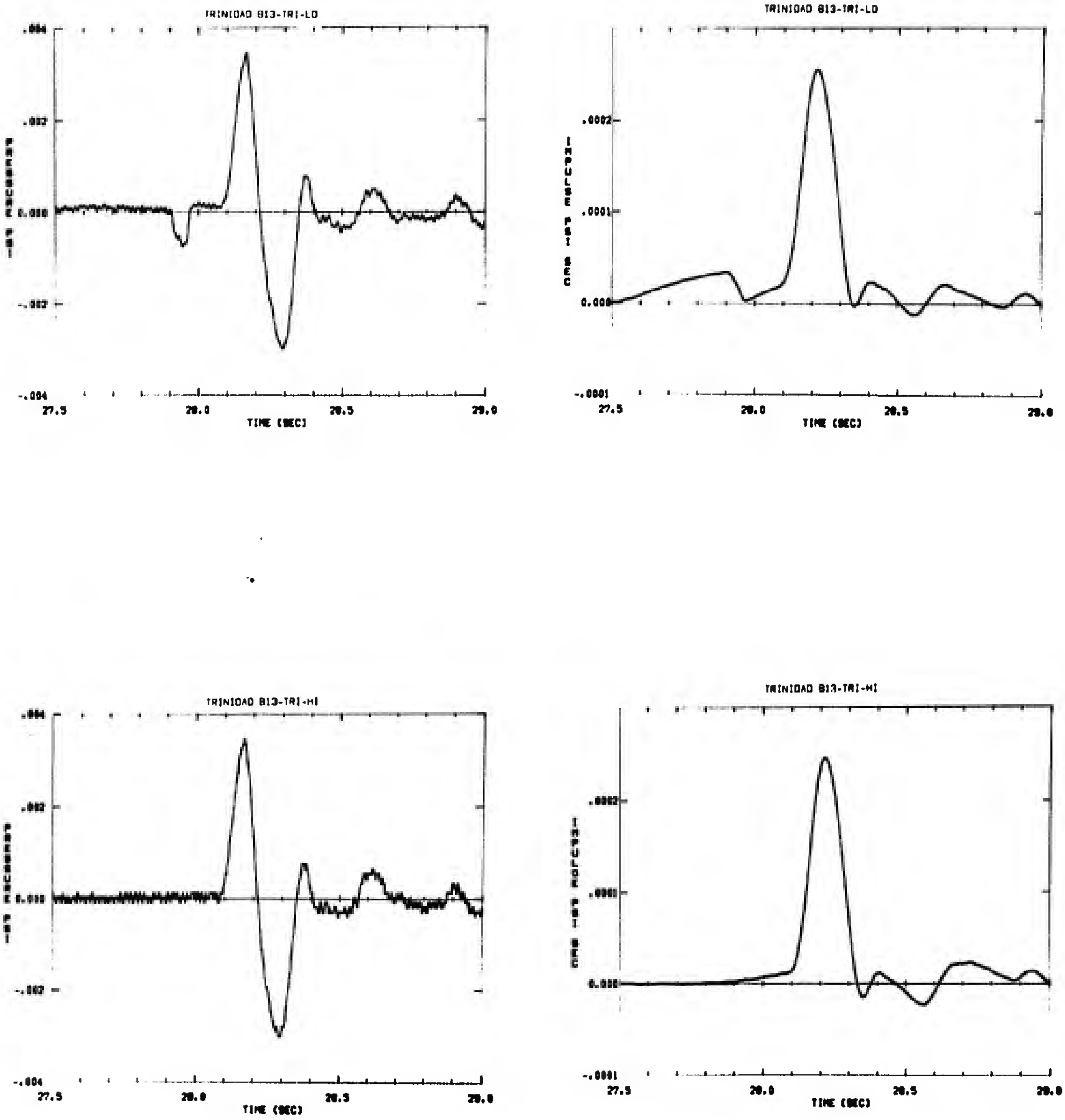

Figure B-51. Pressure-time and impulse-time for low-range gage (upper) and high-range gage (lower) for TRINIDAD Shot B-13, Station Trinidad

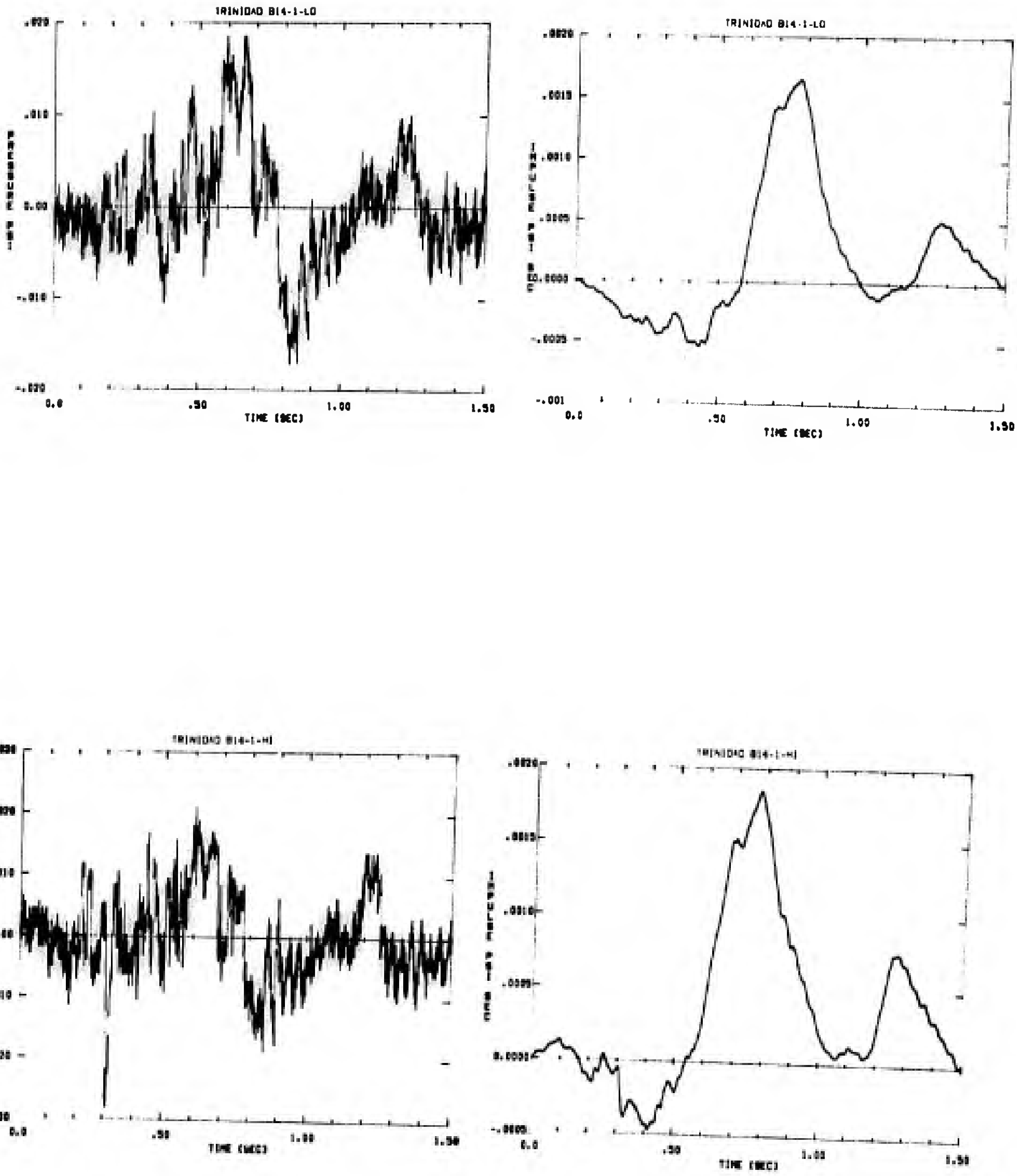

Figure B-52. Pressure-time and impulse-time for low-range gage (upper) and high-range gage (lower) for TRINIDAD Shot B-14, Station 1

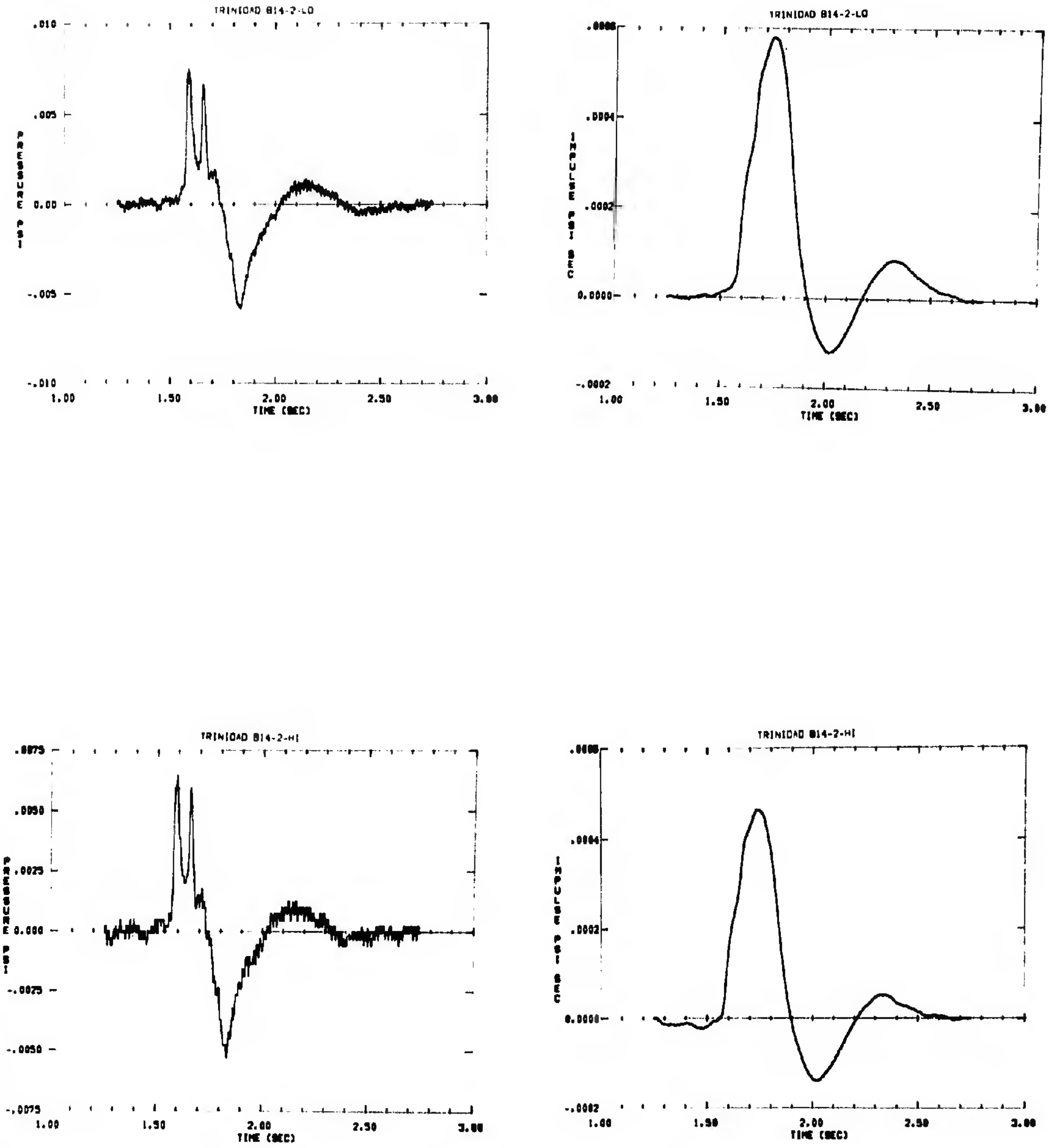

Figure B-53. Pressure-time and impulse-time for low-range gage (upper) and high-range gage (lower) for TRINIDAD Shot B-14, Station 2

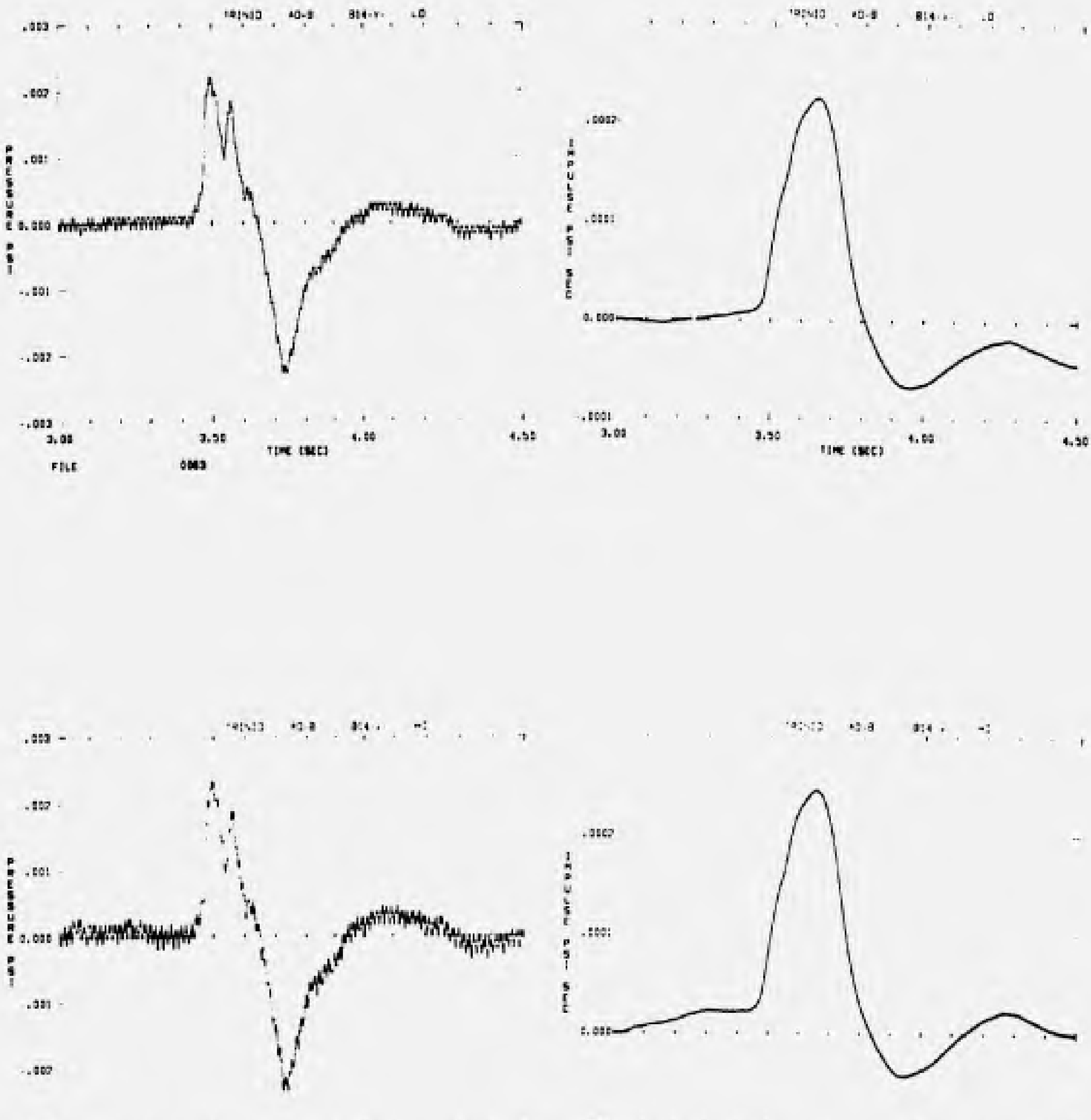

Figure B-54. Pressure-time and impulse-time for low-range gage (upper) and high-range gage (lower) for TRINIDAD Shot B-14, Station Viola

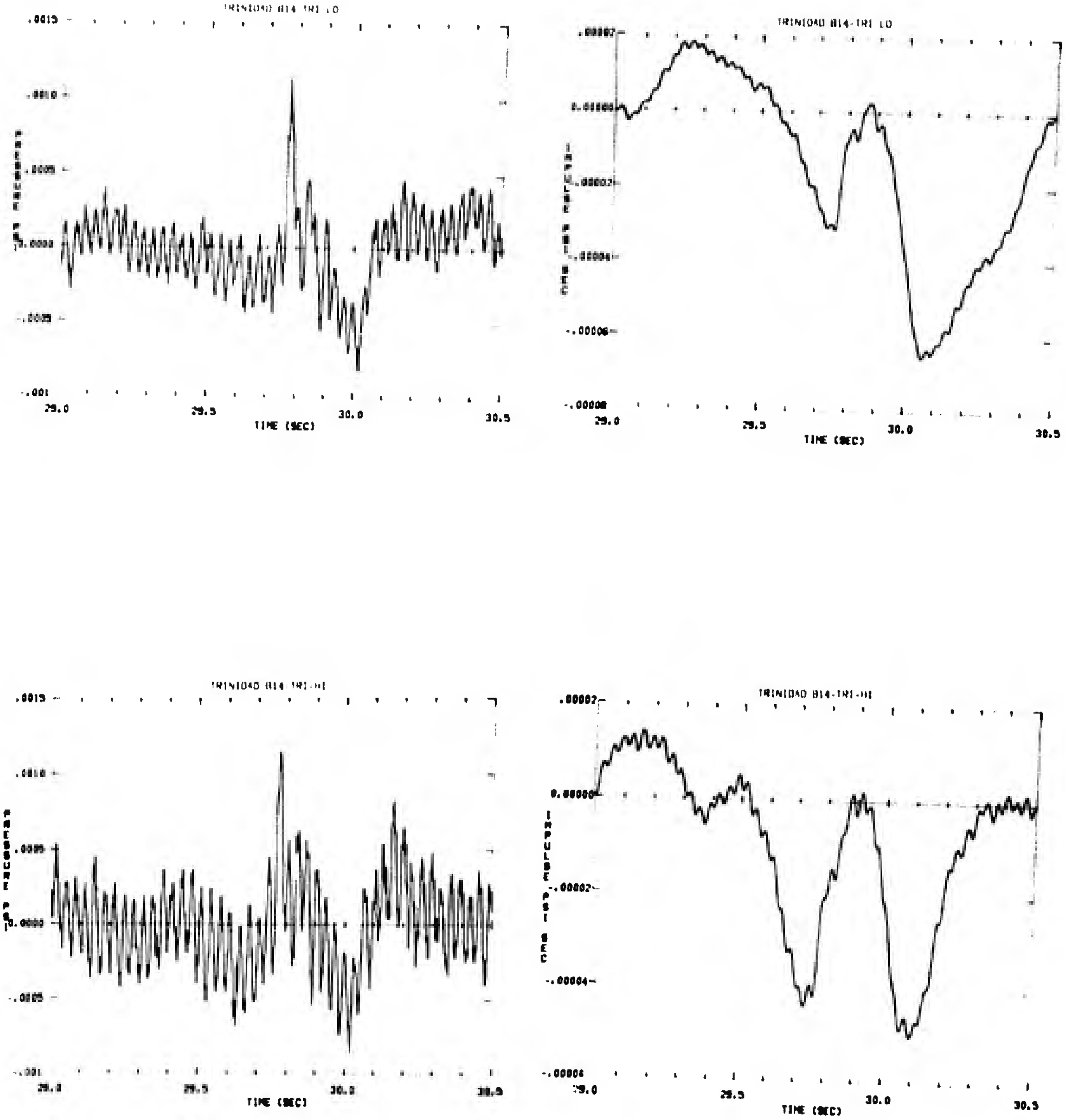

Figure B-55. Pressure-time and impulse-time for low-range gage (upper) and high-range gage (lower) for TRINIDAD Shot B-14, Station Trinidad

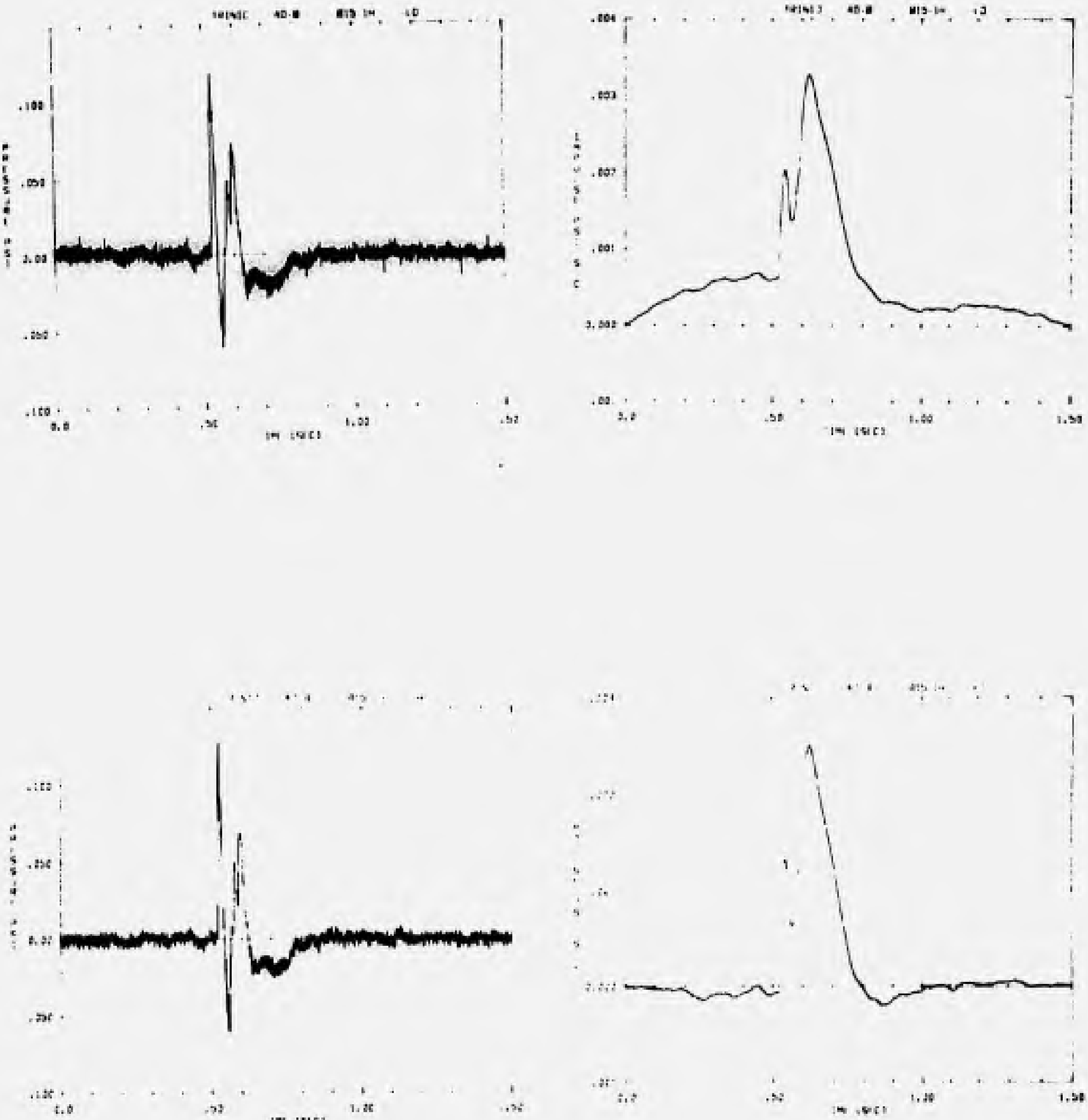

Figure B-56. Pressure-time and impulse-time for low-range gage (upper) and high-range gage (lower) for TRINIDAD Shot B-15, Station 1 High

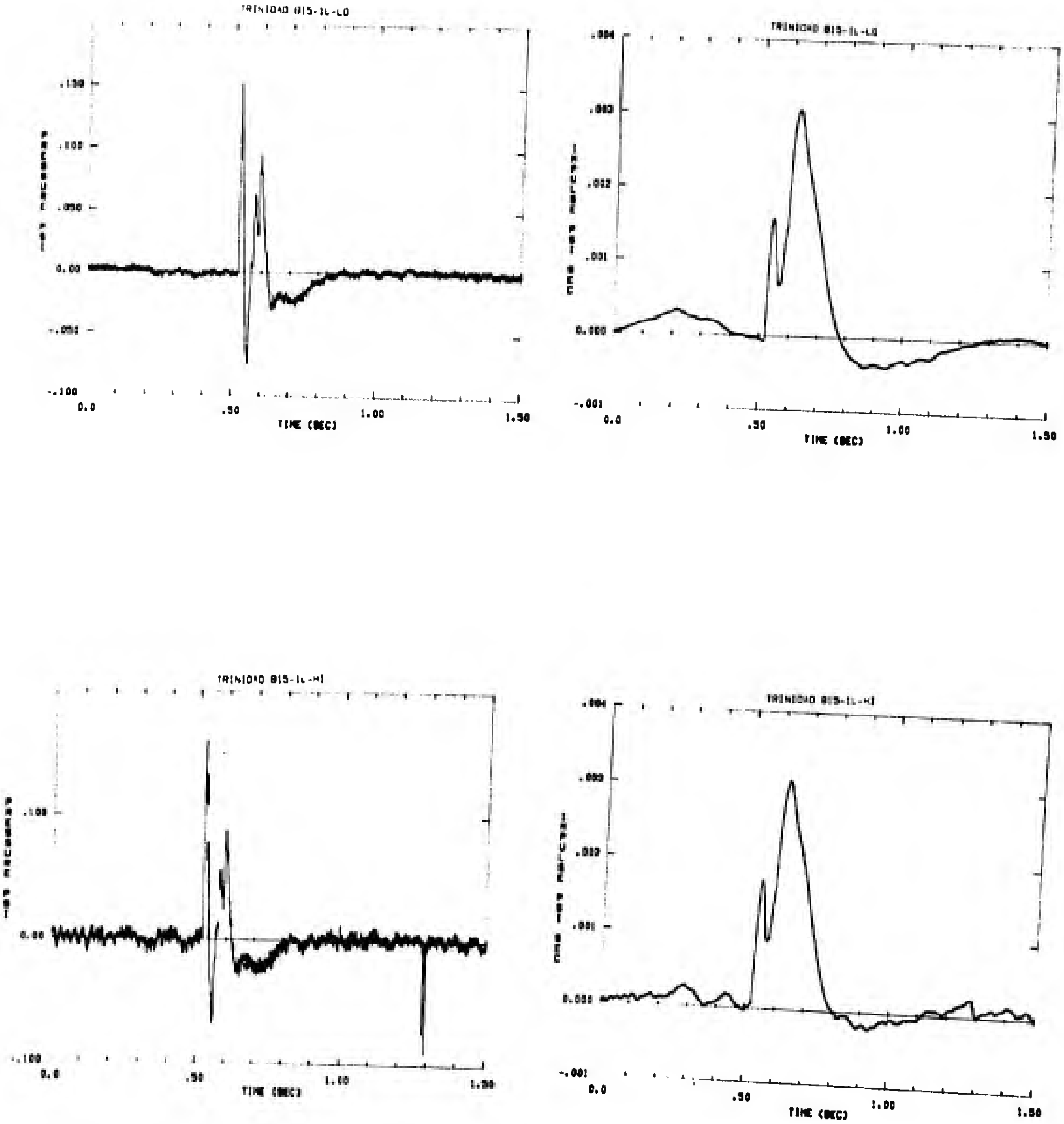

Figure B-57. Pressure-time and impulse-time for low-range gage (upper) and high-range gage (lower) for TRINIDAD Shot B-15, Station 1 Low

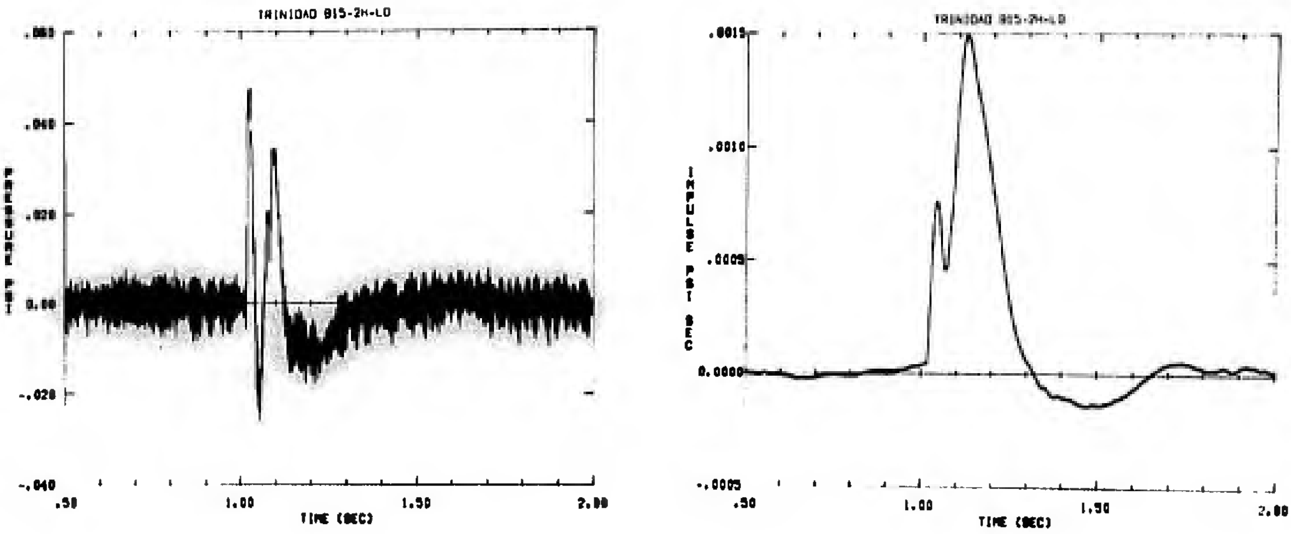

Figure B-58. Pressure-time and impulse-time for low-range gage for TRINIDAD Shot B-15, Station 2

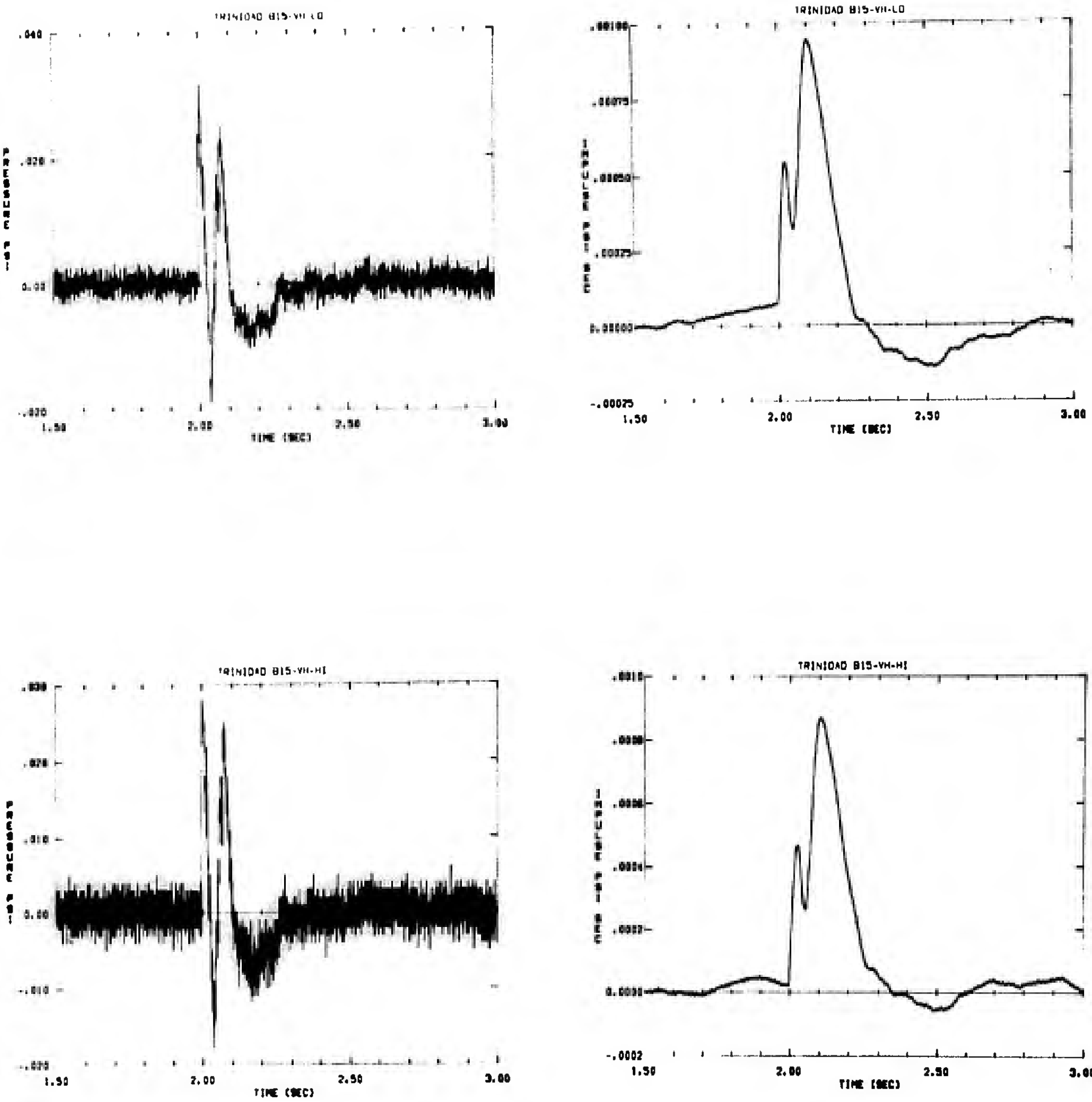

Figure B-59. Pressure-time and impulse-time for low-range gage (upper) and high-range gage (lower) for TRINIDAD Shot B-15, Station Viola High

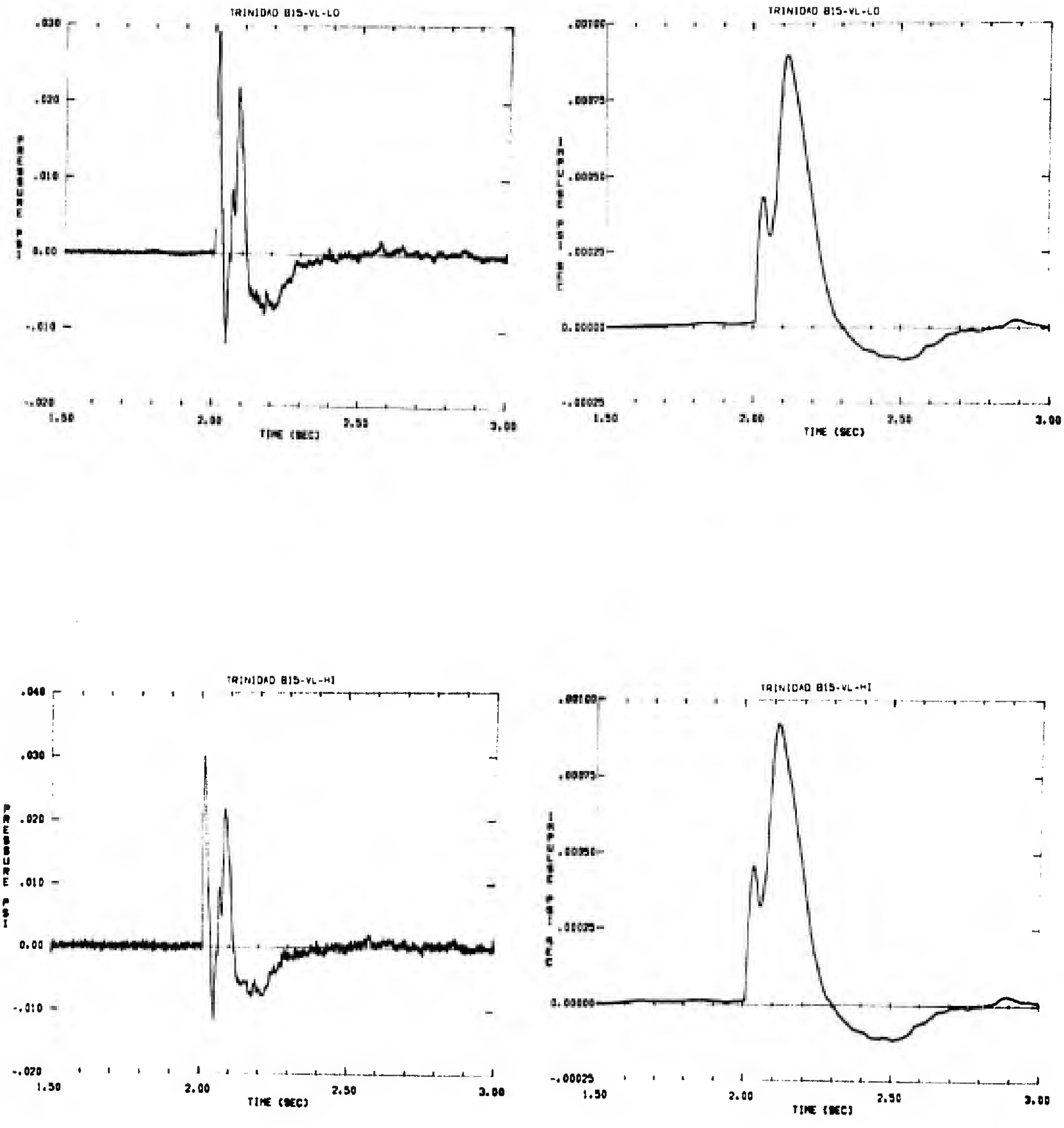

Figure B-60. Pressure-time and impulse-time for low-range gage (upper) and high-range gage (lower) for TRINIDAD Shot B-15, Station Viola Low

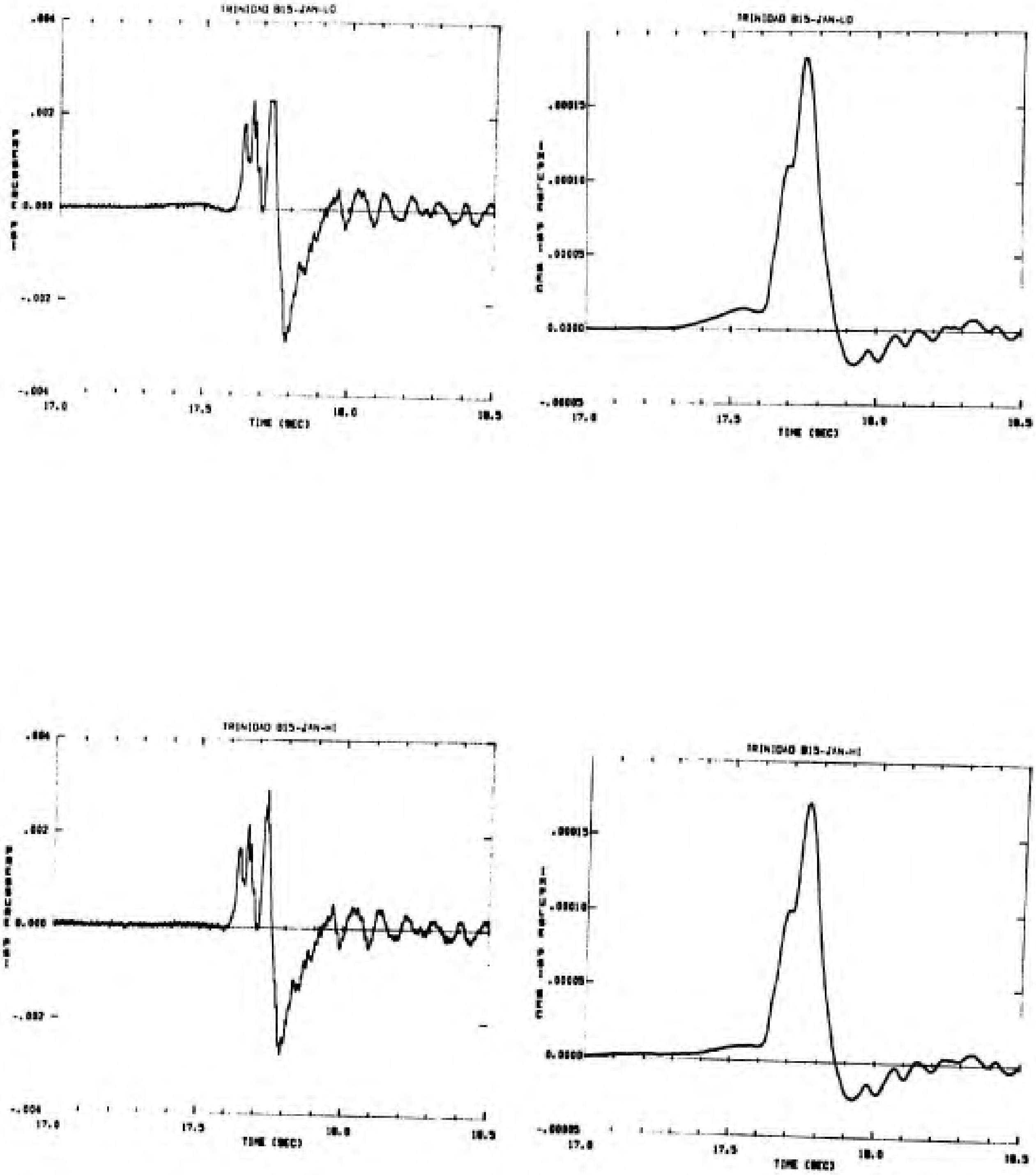

Figure B-61. Pressure-time and impulse-time for low-range gage (upper) and high-range gage (lower) for TRINIDAD Shot B-15, Station Jansen

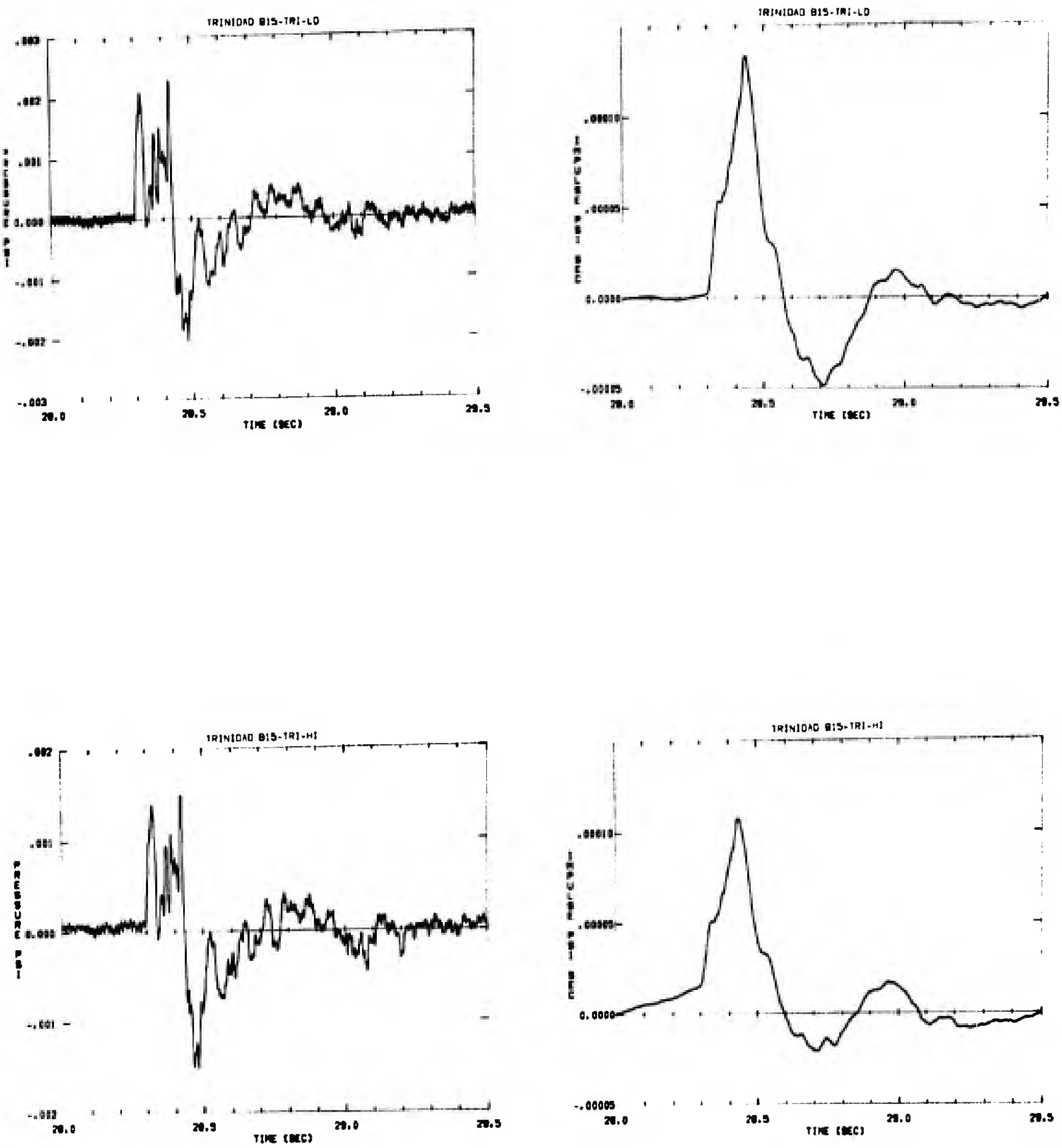

Figure B-62. Pressure-time and impulse-time for low-range gage (upper) and high-range gage (lower) for TRINIDAD Shot B-15, Station Trinidad

BLANK PAGE

APPENDIX C

Pressure-Time Records for the C Series

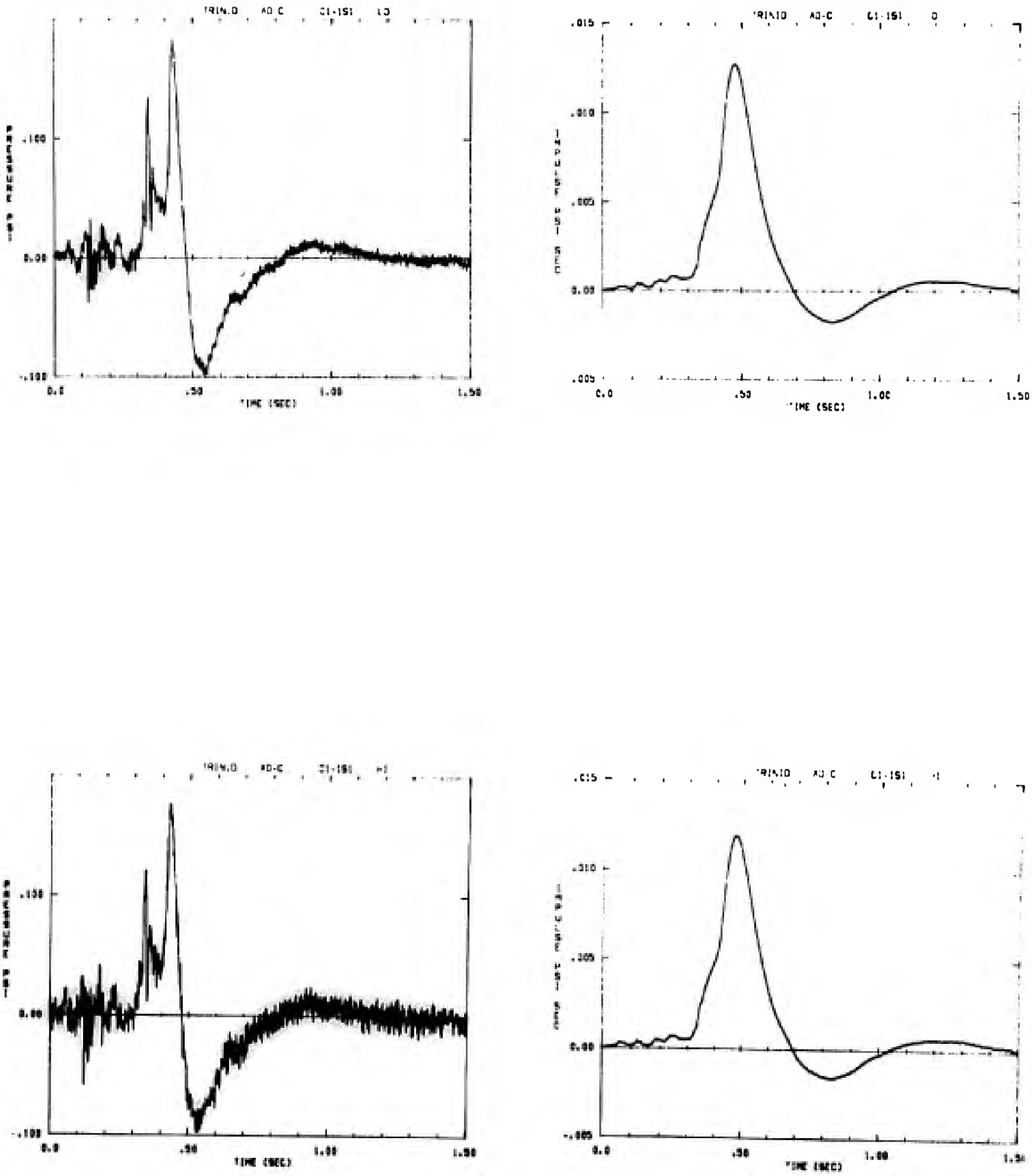

Figure C-1. Pressure-time and impulse-time for low-range gage (upper) and high-range gage (lower) for TRINIDAD Shot C-1, Station Side 1

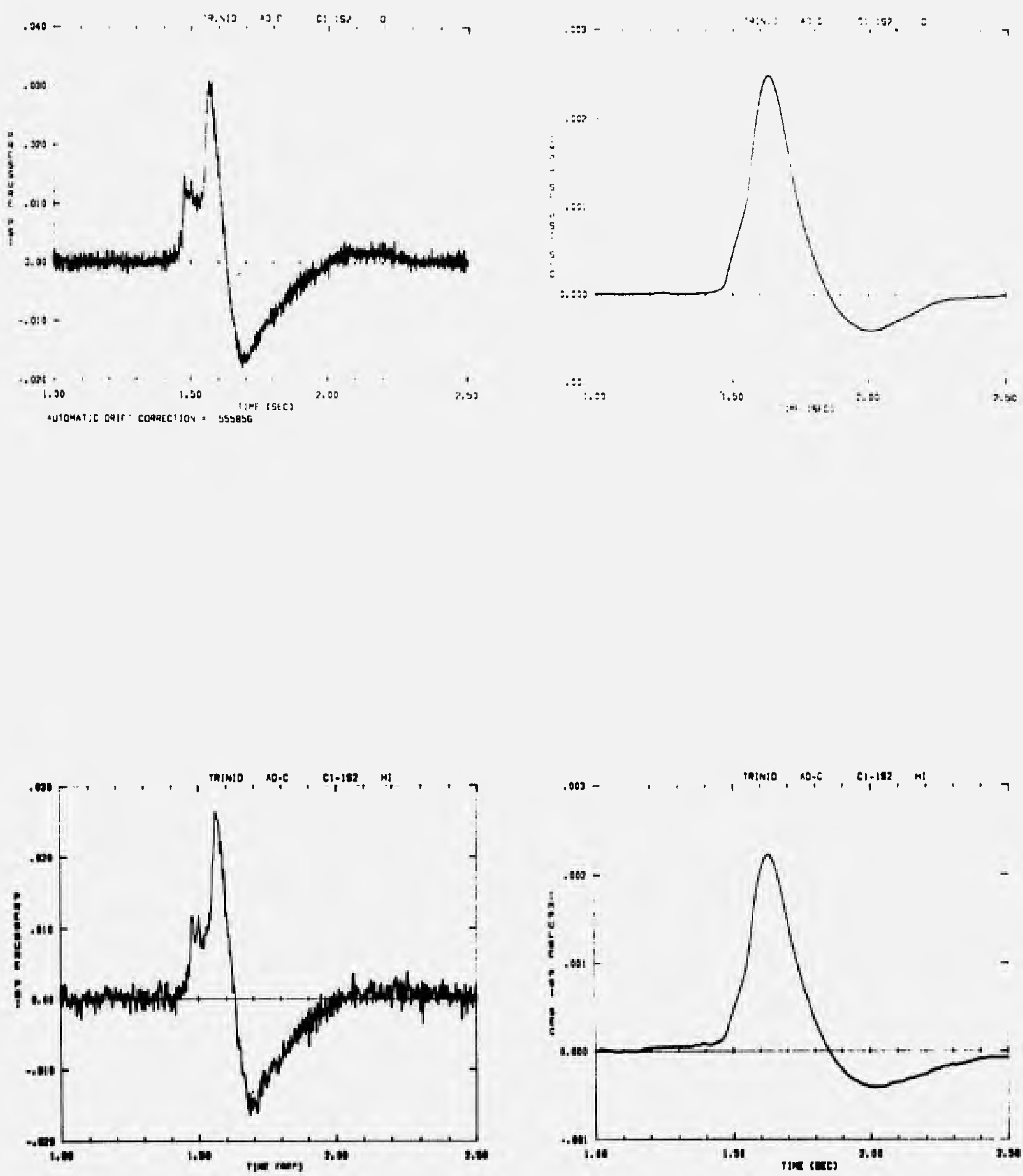

Figure C-2. Pressure-time and impulse-time for low-range gage (upper) and high-range gage (lower) for TRINIDAD Shot C-1, Station Side 2

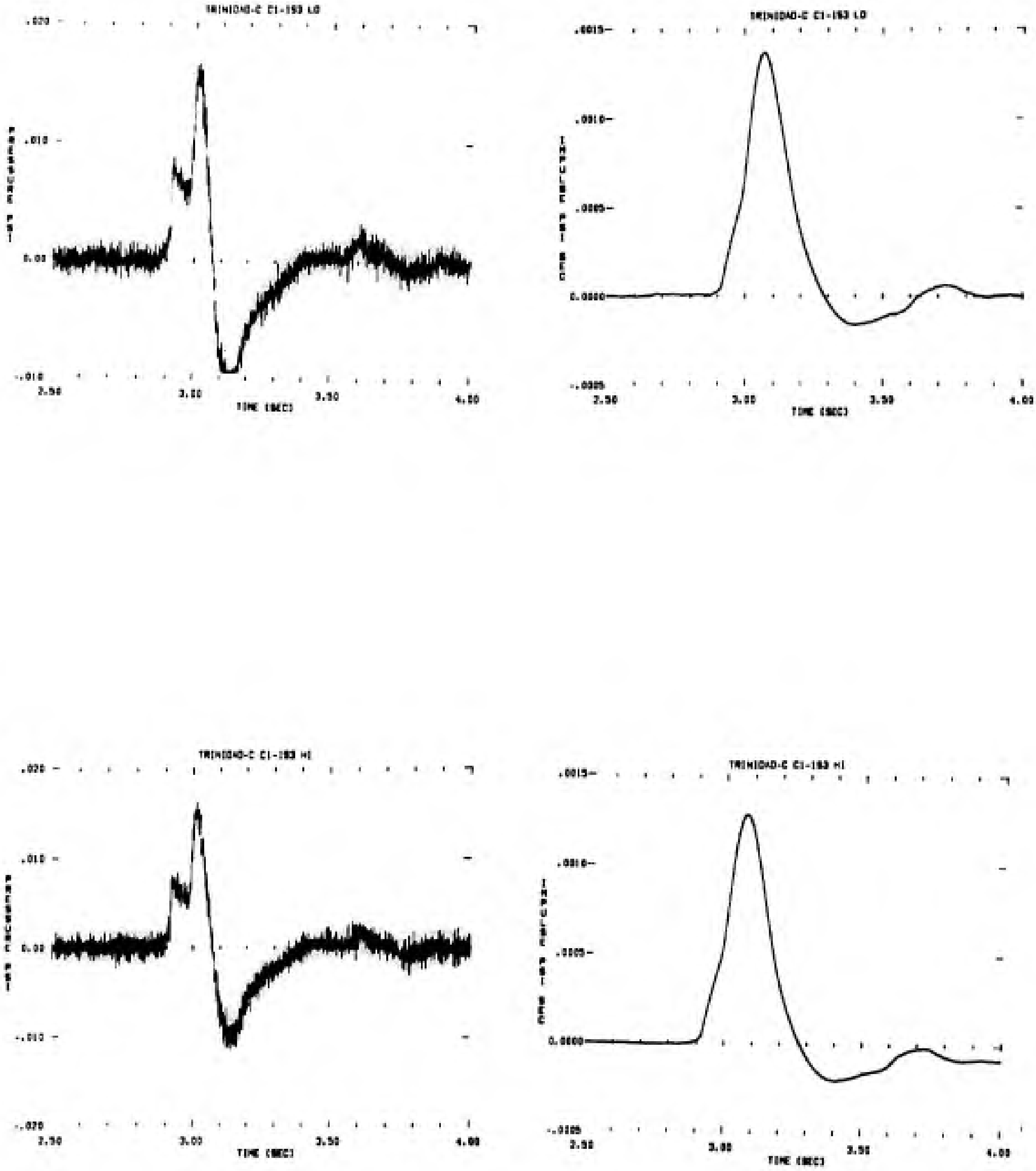

Figure C-3. Pressure-time and impulse-time for low-range gage (upper) and high-range gage (lower) for TRINIDAD Shot C-1, Station Side 3

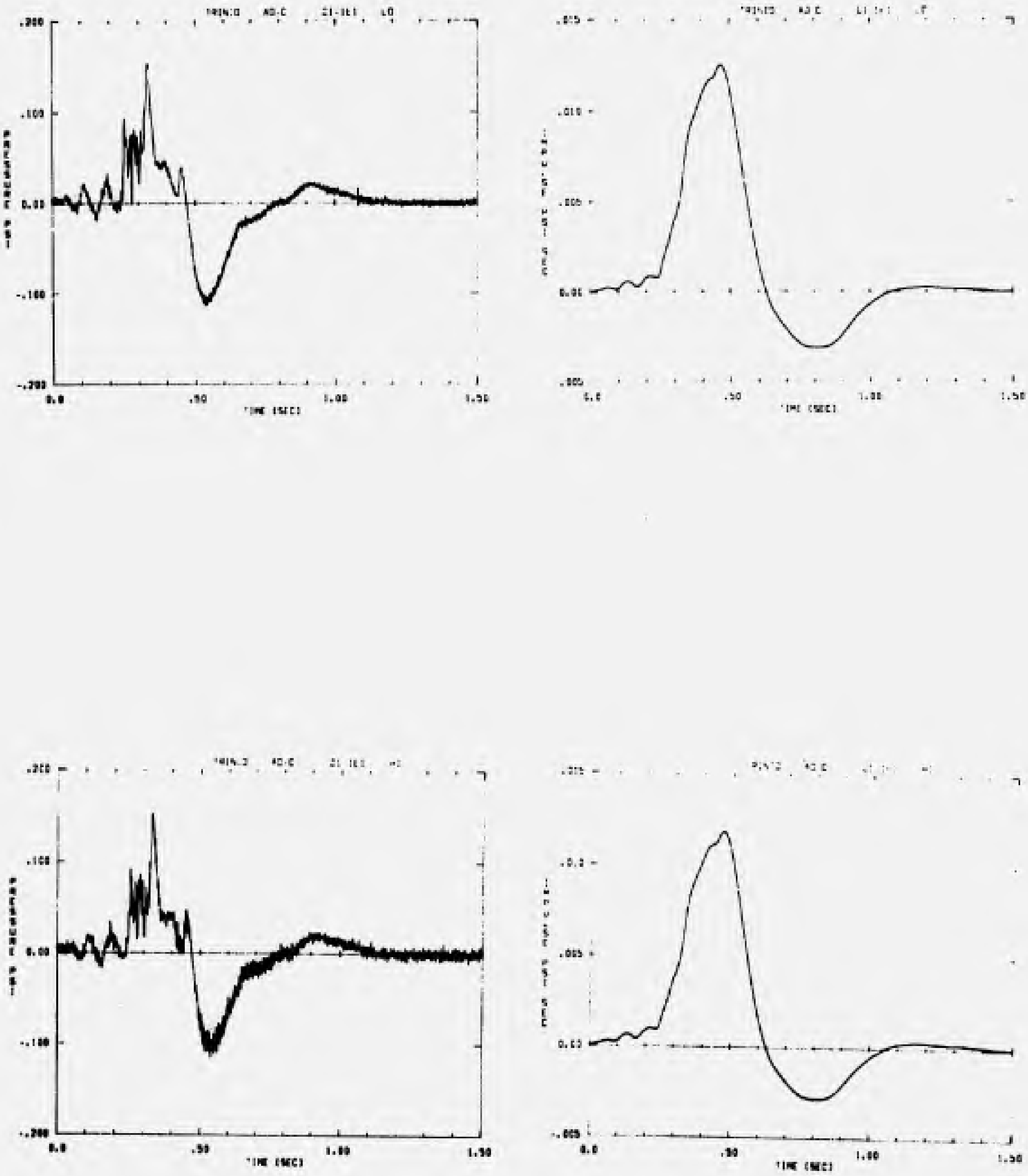

Figure C-4. Pressure-time and impulse-time for low-range gage (upper) and high-range gage (lower) for TRINIDAD Shot C-1, Station End 1

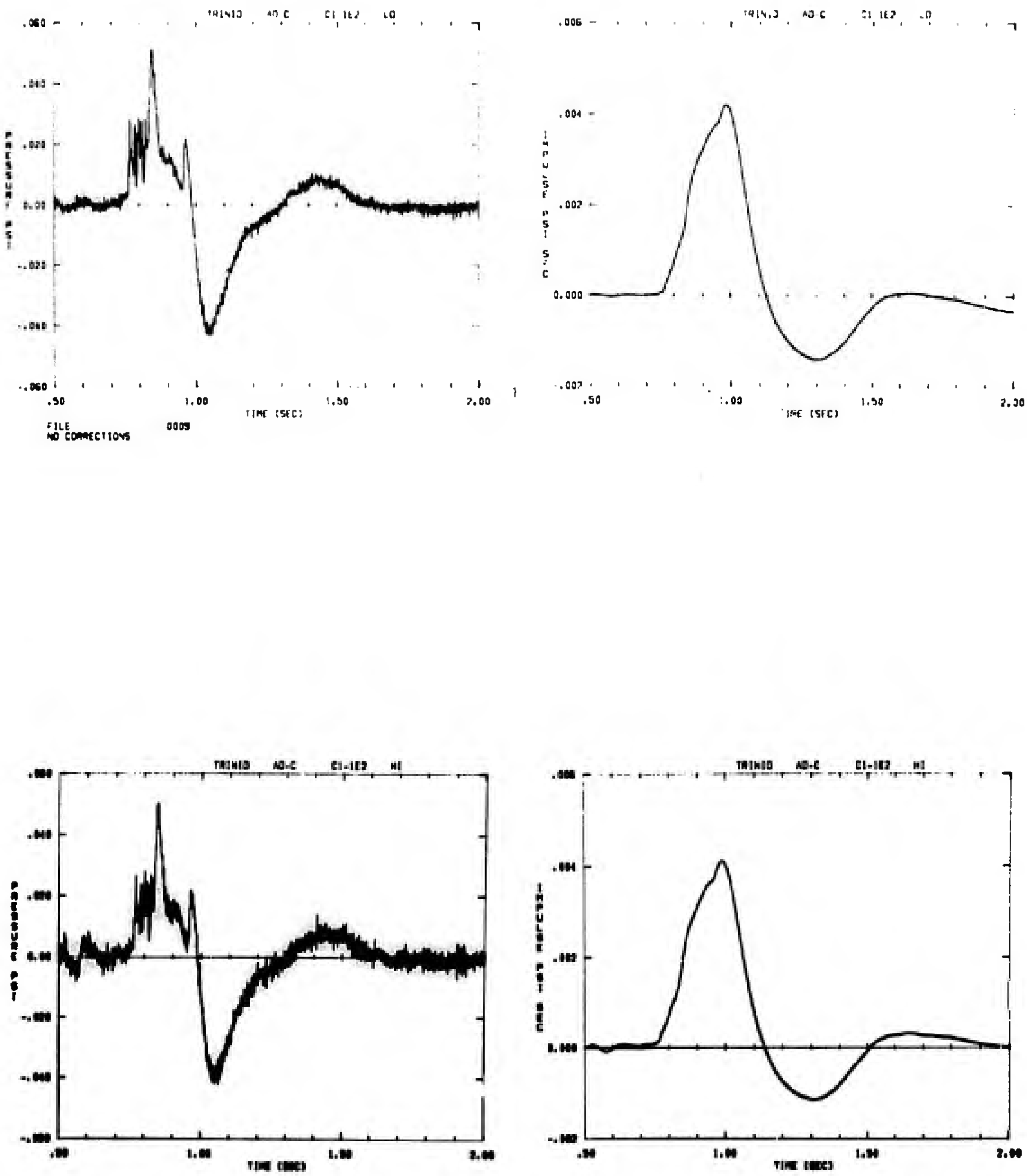

Figure C-5. Pressure-time and impulse-time for low-range gage (upper) and high-range gage (lower) for TRINIDAD Shot C-1, Station End 2

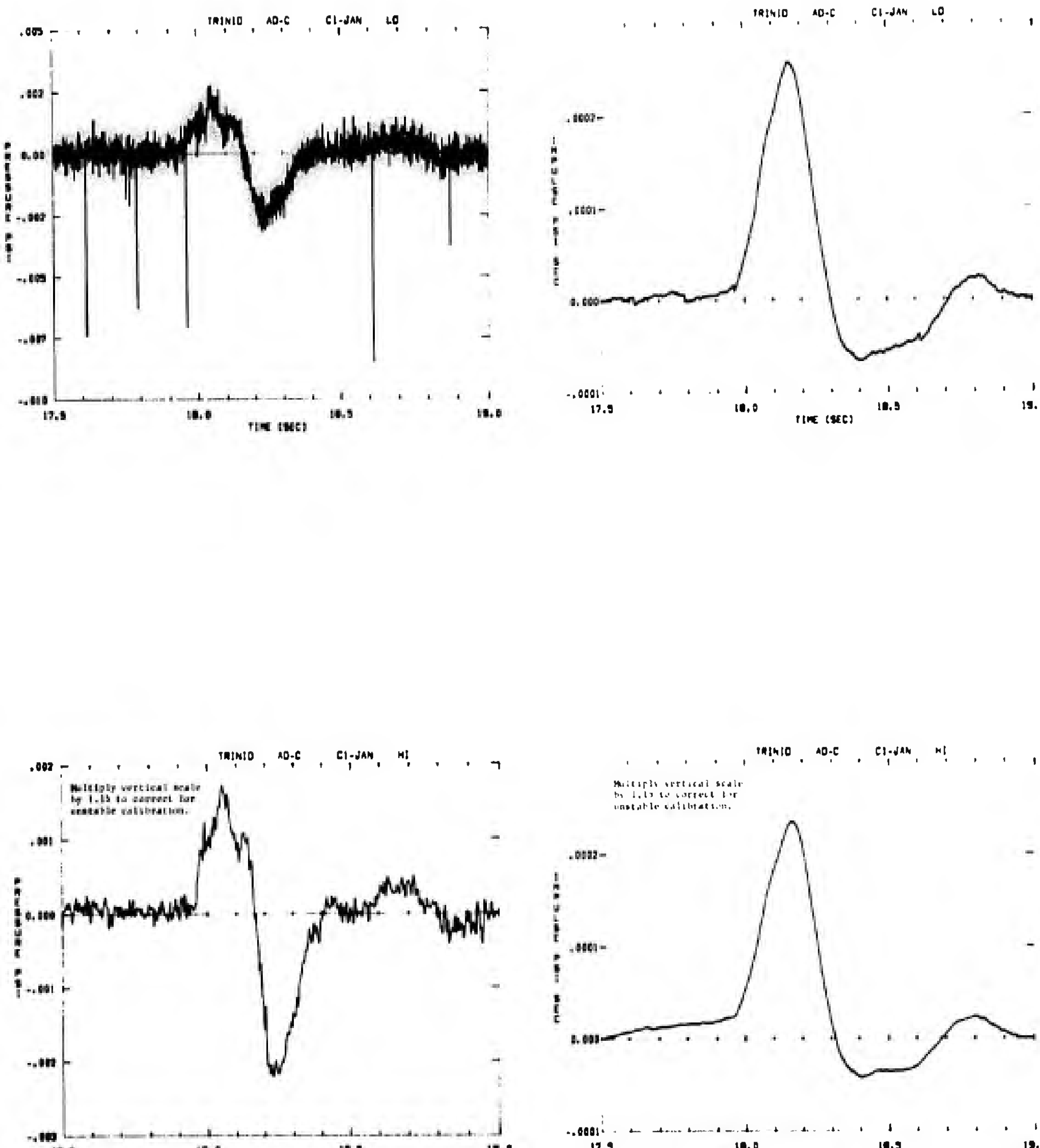

Figure C-6. Pressure-time and impulse-time for low-range gage (upper) and high-range gage (lower) for TRINIDAD Shot C-1, Station Jansen

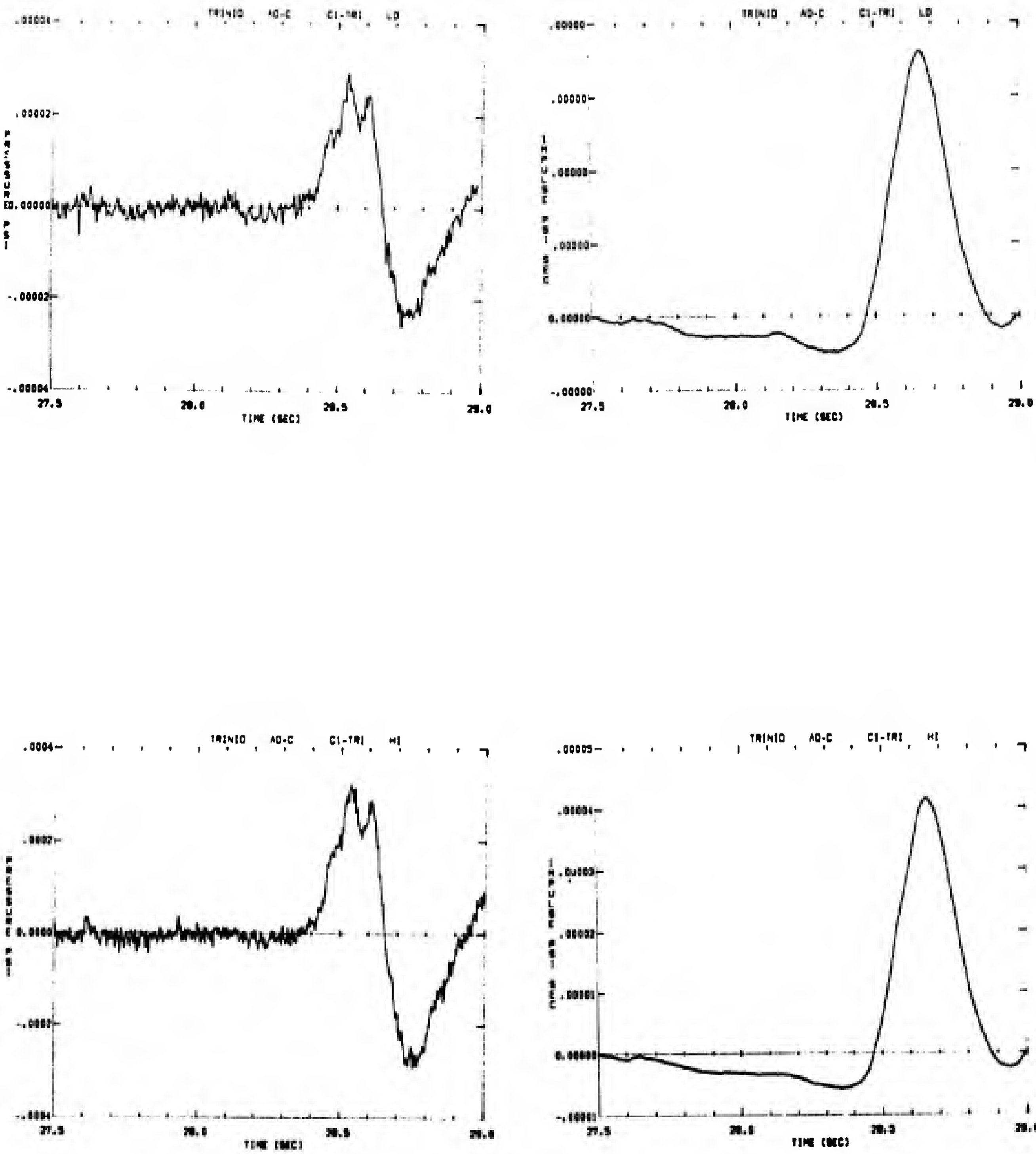

Figure C-7. Pressure-time and impulse-time for low-range gage (upper) and high-range gage (lower) for TRINIDAD Shot C-1, Station Trinidad

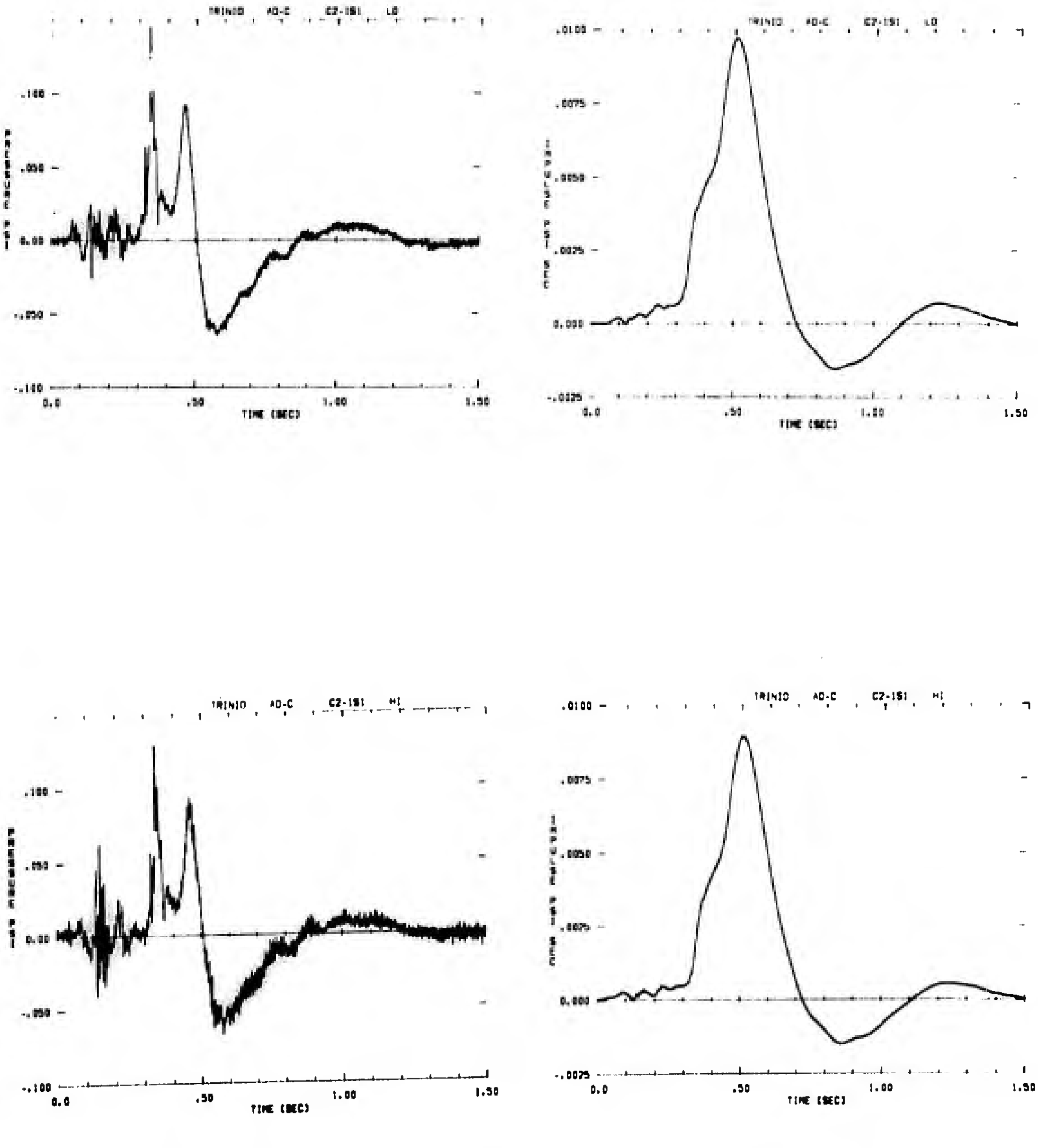

Figure C-8. Pressure-time and impulse-time for low-range gage (upper) and high-range gage (lower) for TRINIDAD Shot C-2, Station Side 1

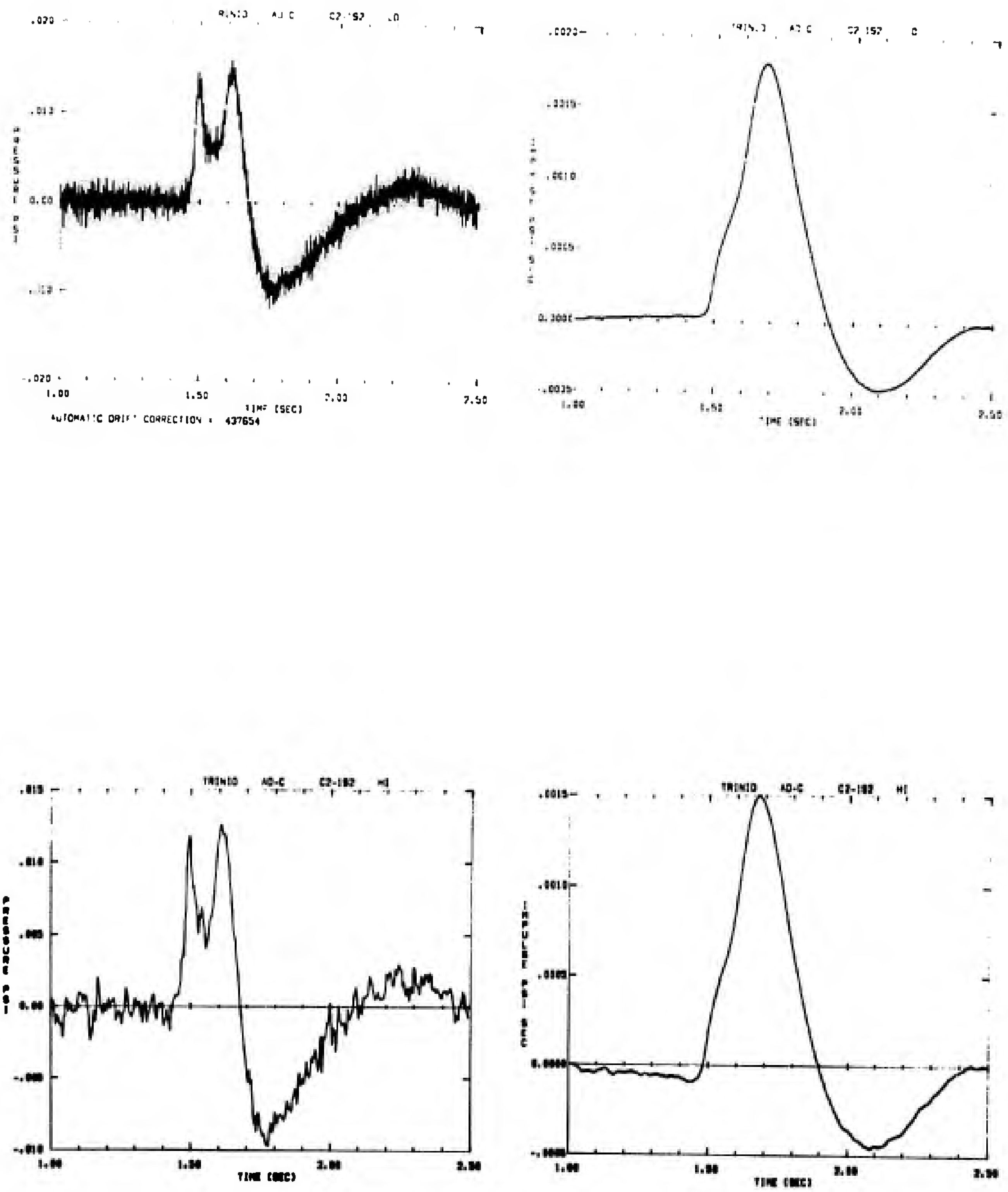

Figure C-9. Pressure-time and impulse-time for low-range gage (upper) and high-range gage (lower) for TRINIDAD Shot C-2, Station Side 2

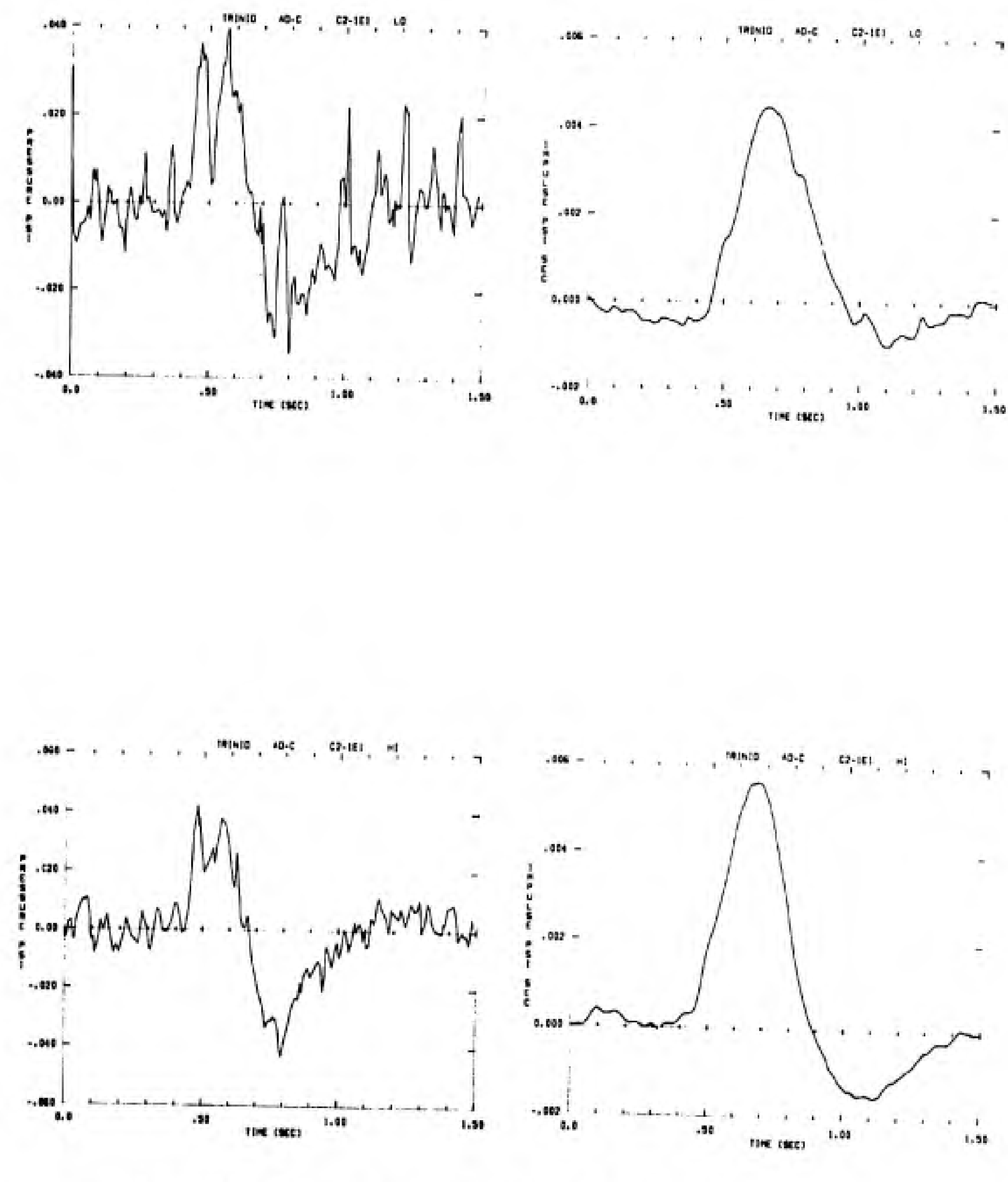

Figure C-10. Pressure-time and impulse-time for low-range gage (upper) and high-range gage (lower) for TRINIDAD Shot C-2, Station End 1

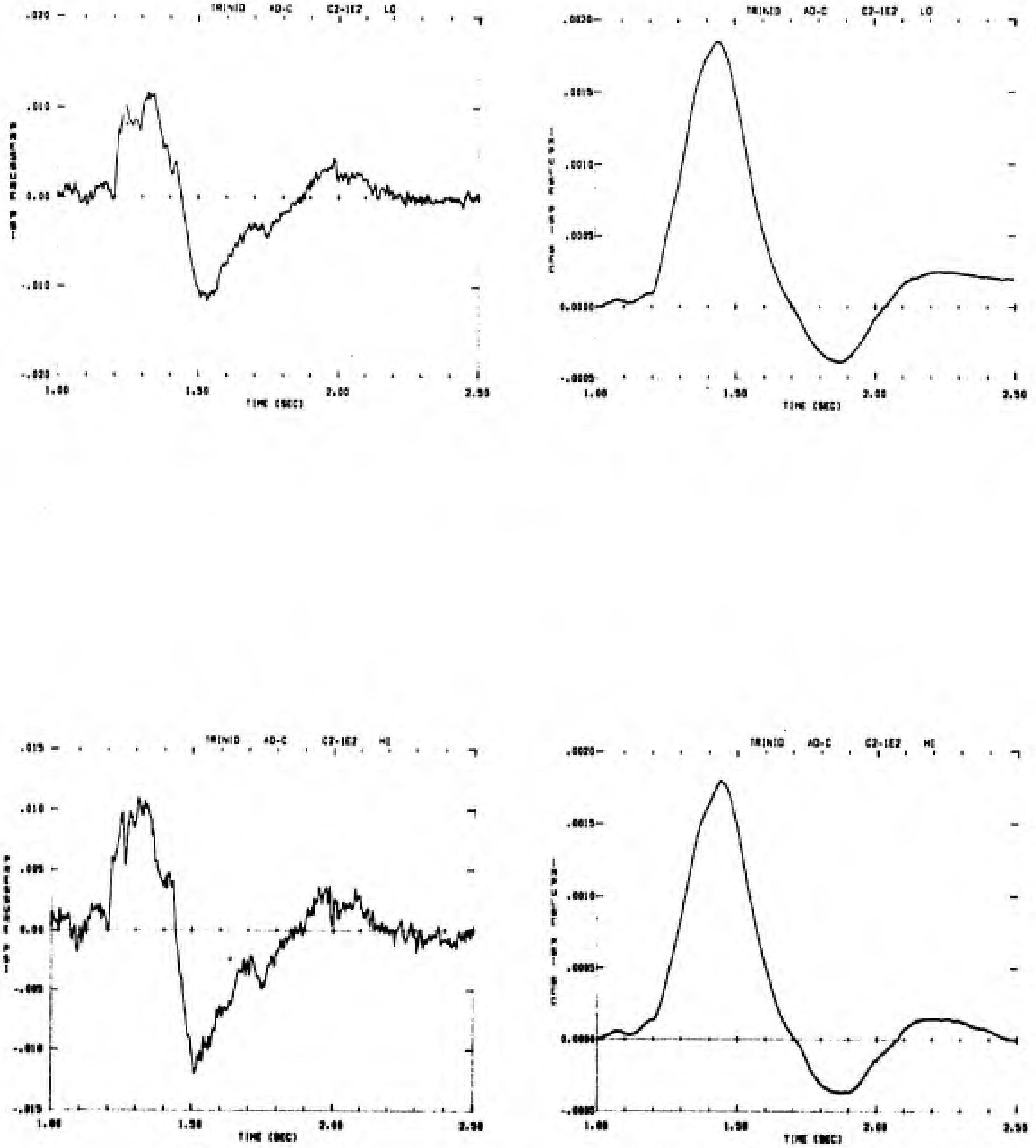

Figure C-11. Pressure-time and impulse-time for low-range gage (upper) and high-range gage (lower) for TRINIDAD Shot C-2, Station End 2

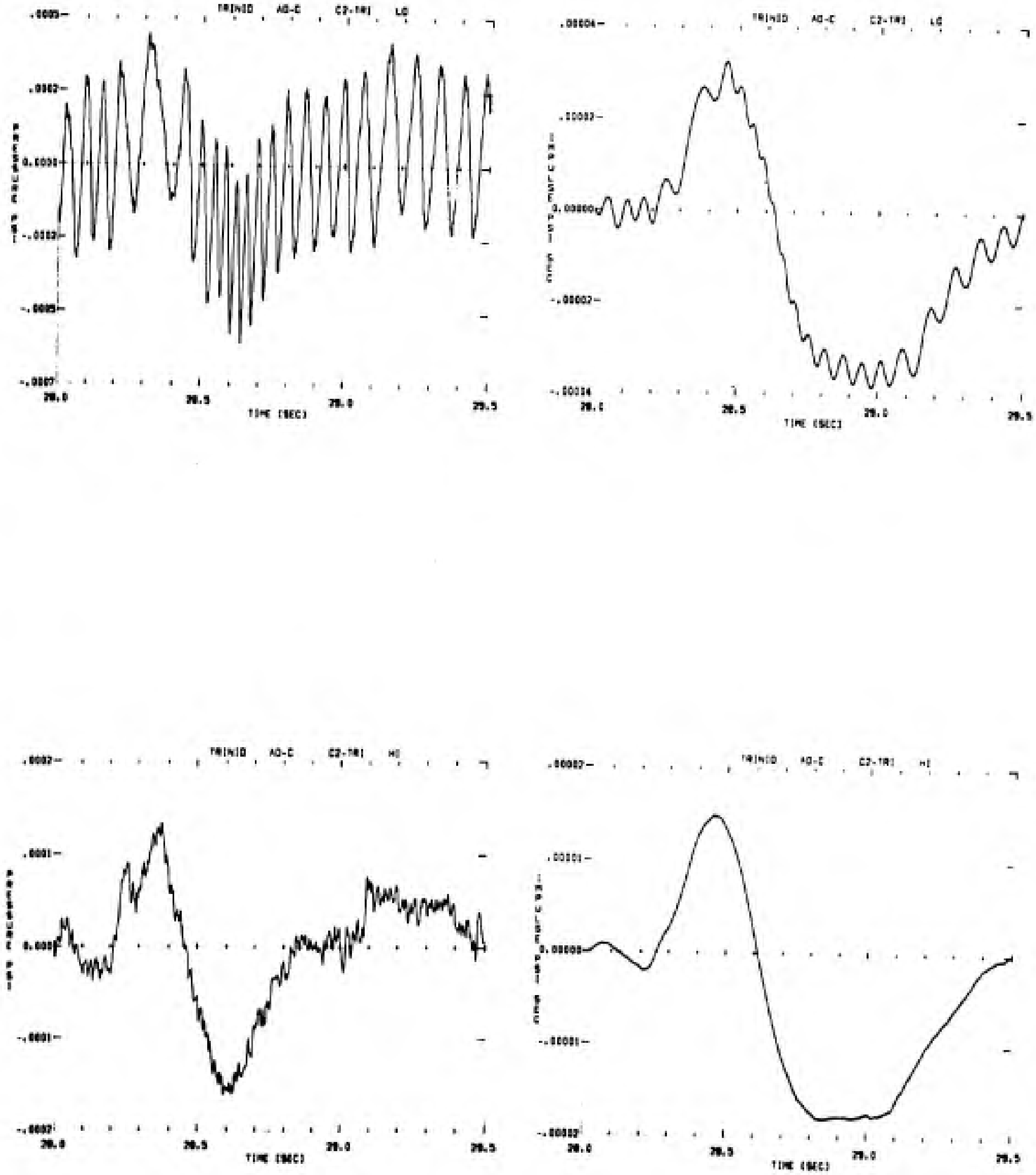

Figure C-12. Pressure-time and impulse-time for low-range gage (upper) and high-range gage (lower) for TRINIDAD Shot C-2, Station Trinidad

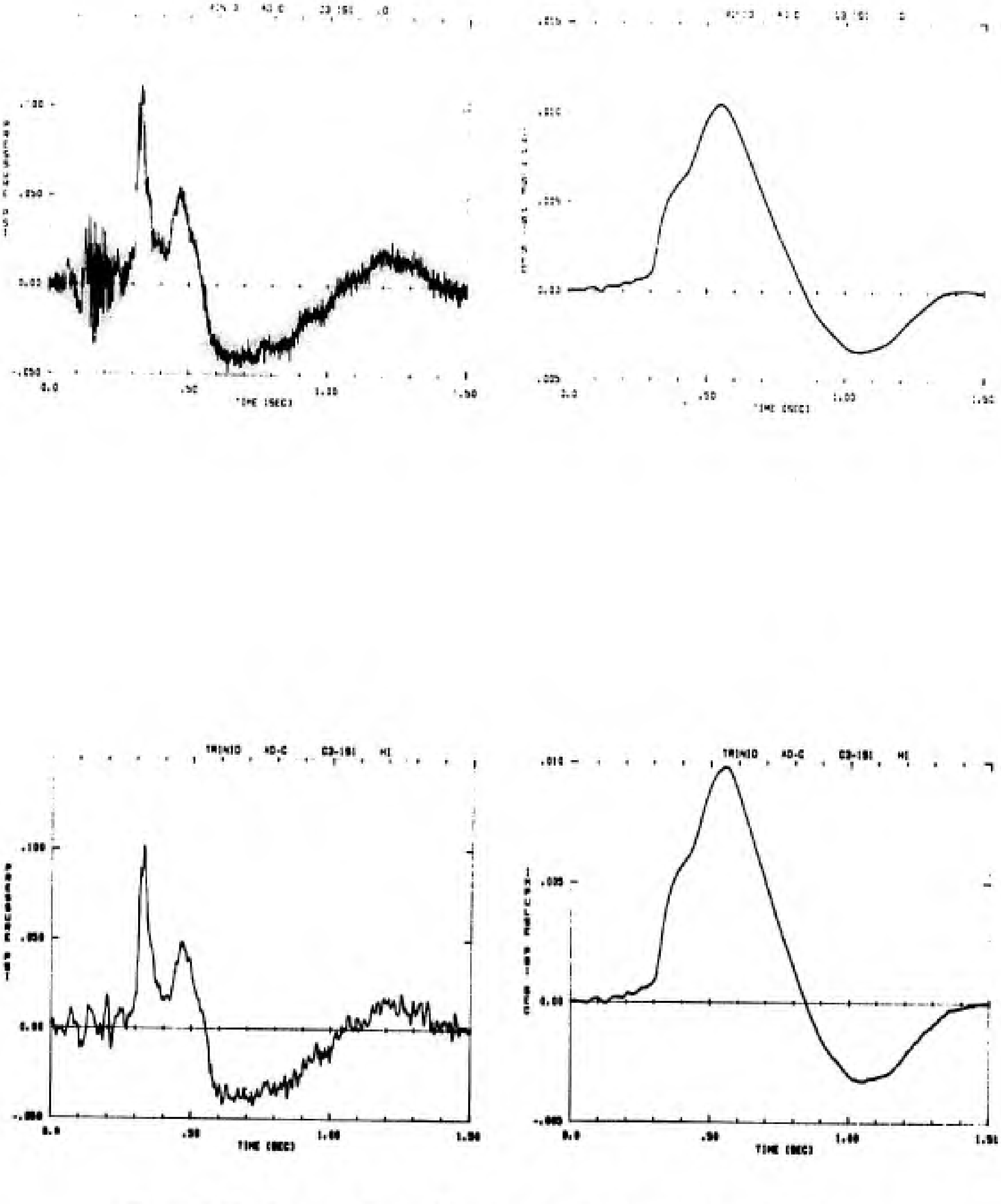

Figure C-13. Pressure-time and impulse-time for low-range gage (upper) and high-range gage (lower) for TRINIDAD Shot C-3, Station Side 1

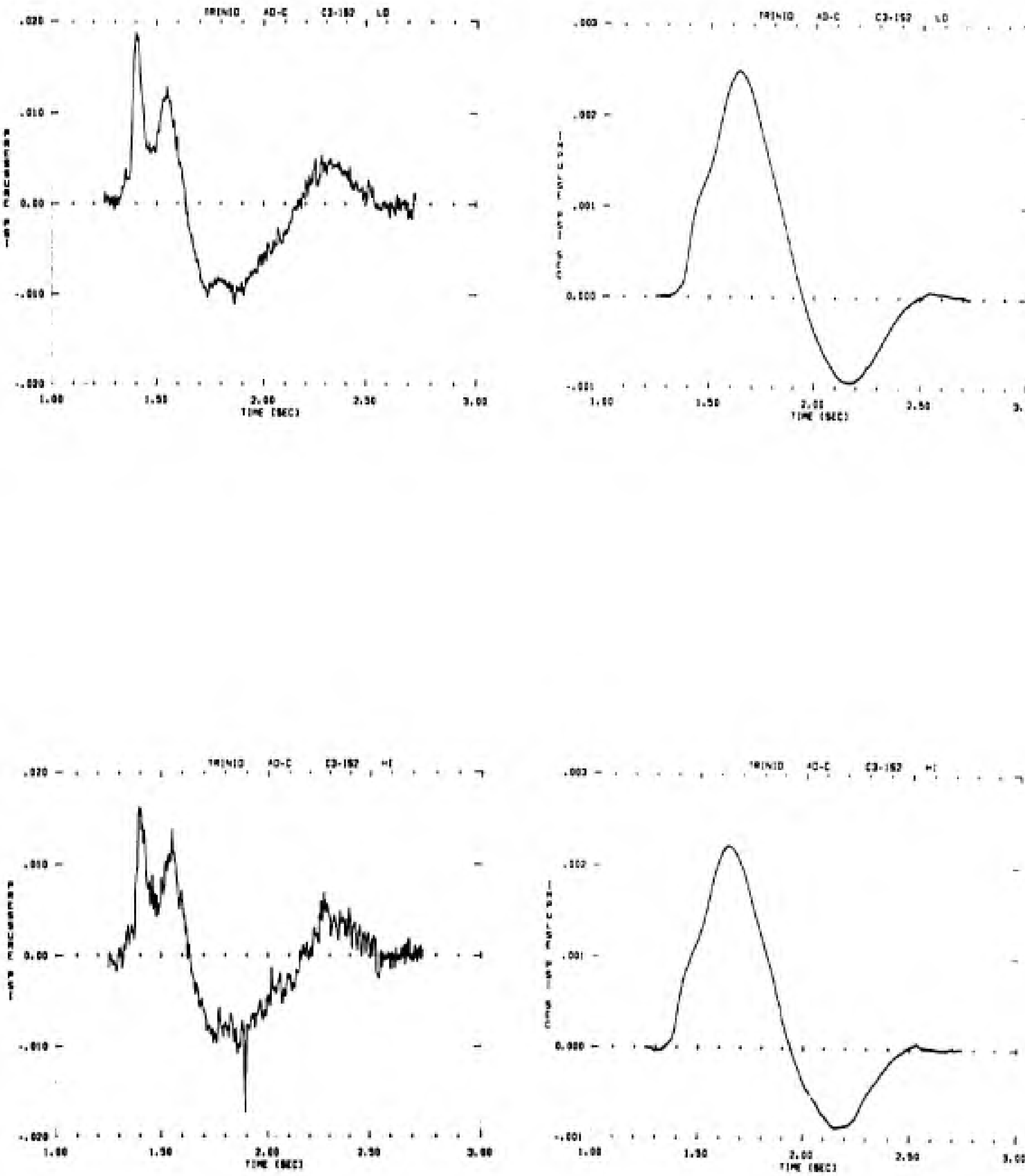

Figure C-14. Pressure-time and impulse-time for low-range gage (upper) and high-range gage (lower) for TRINIDAD Shot C-3, Station Side 2

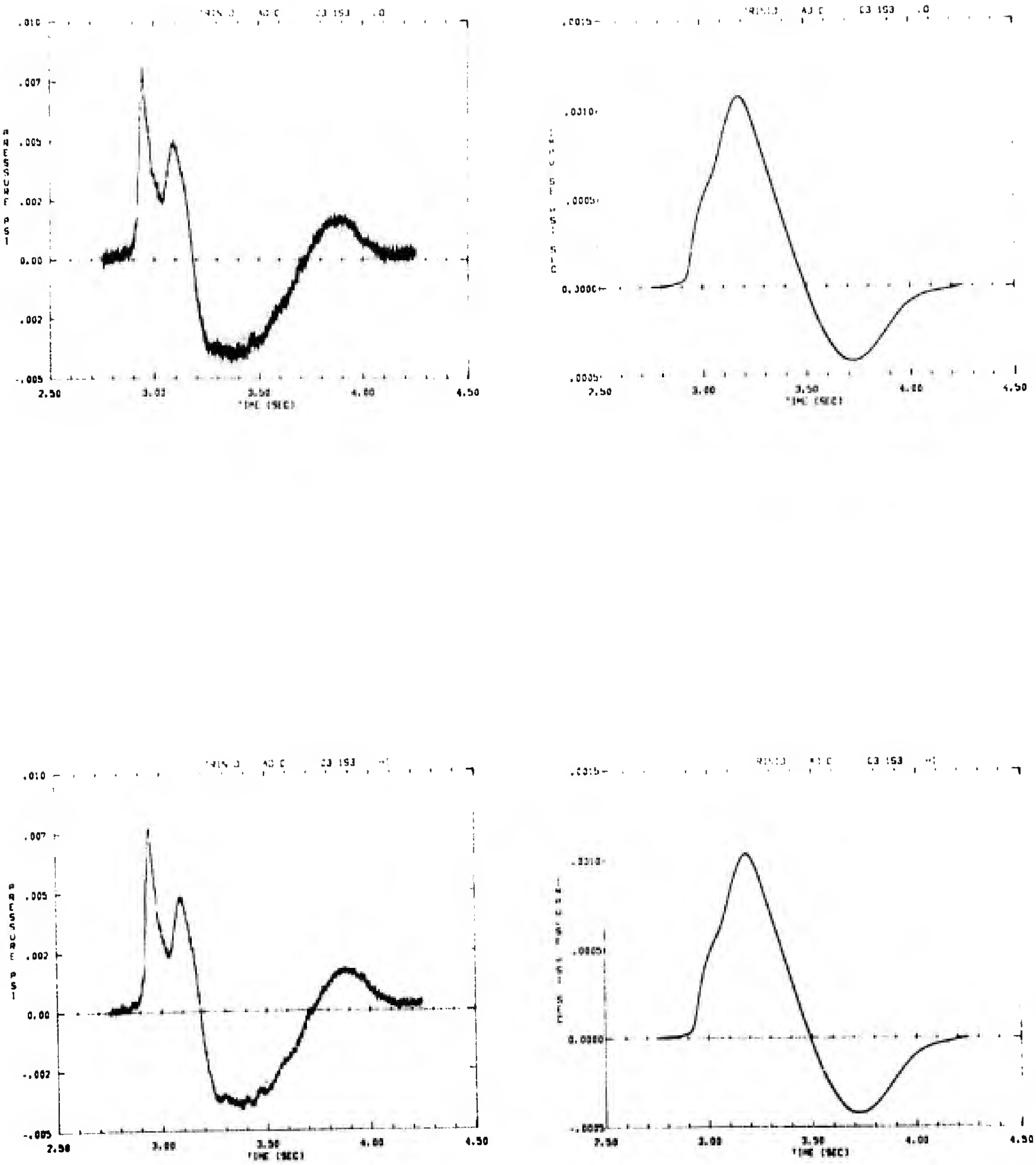

Figure C-15. Pressure-time and impulse-time for low-range gage (upper) and high-range gage (lower) for TRINIDAD Shot C-3, Station Side 3

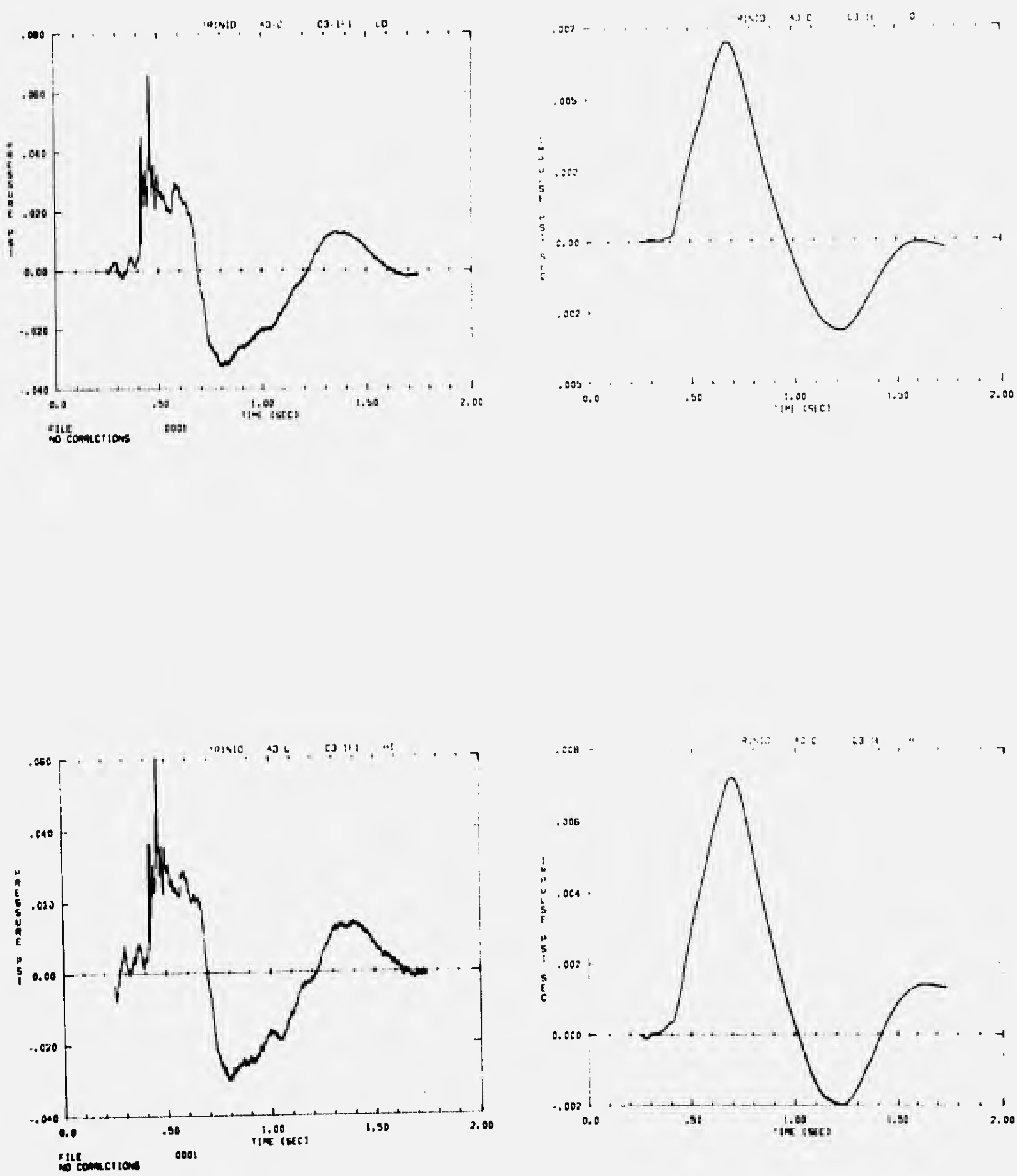

Figure C-16. Pressure-time and impulse-time for low-range gage (upper) and high-range gage (lower) for TRINIDAD Shot C-3, Station End 1

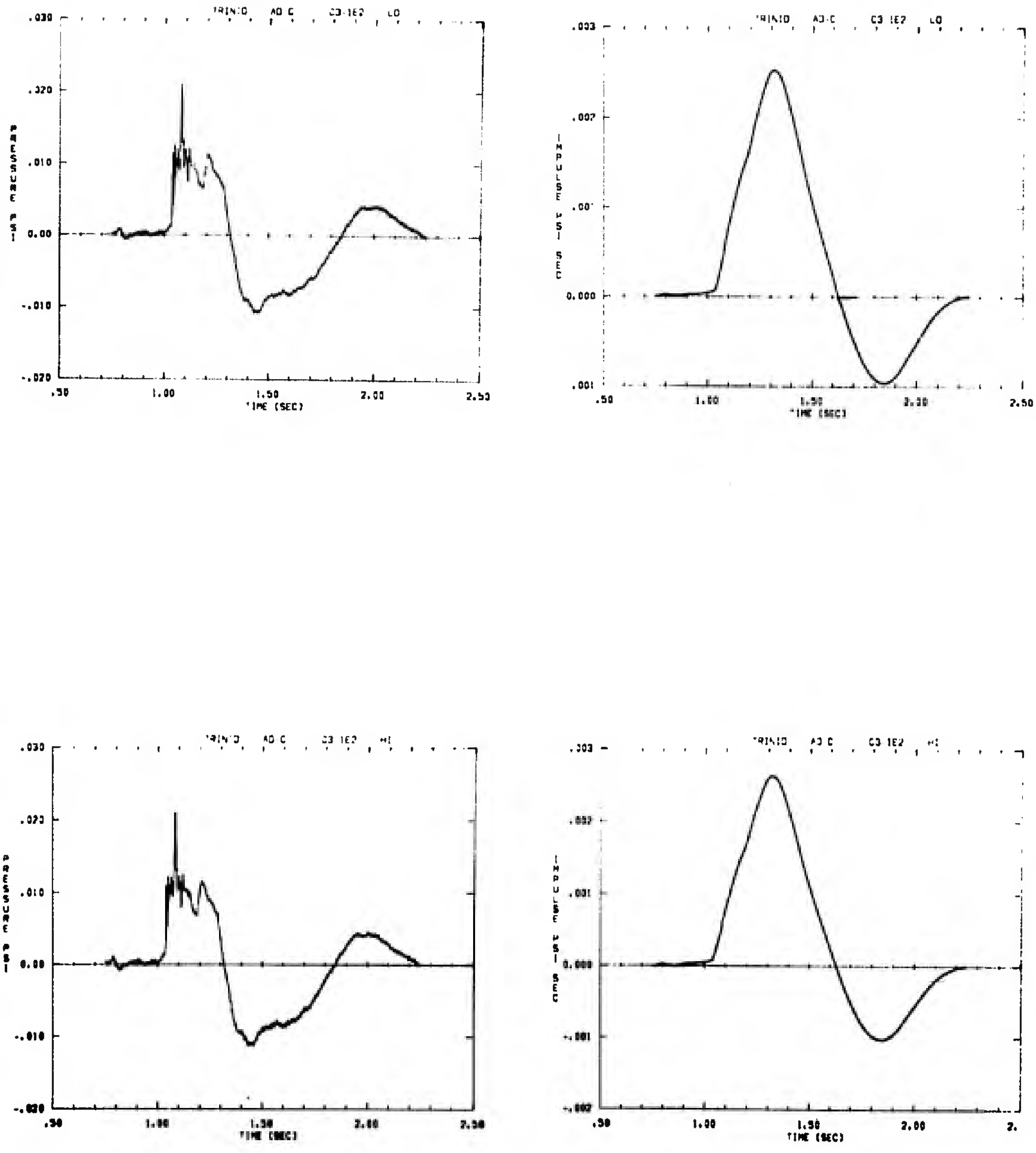

Figure C-17. Pressure-time and impulse-time for low-range gage (upper) and high-range gage (lower) for TRINIDAD Shot C-3, Station End 2

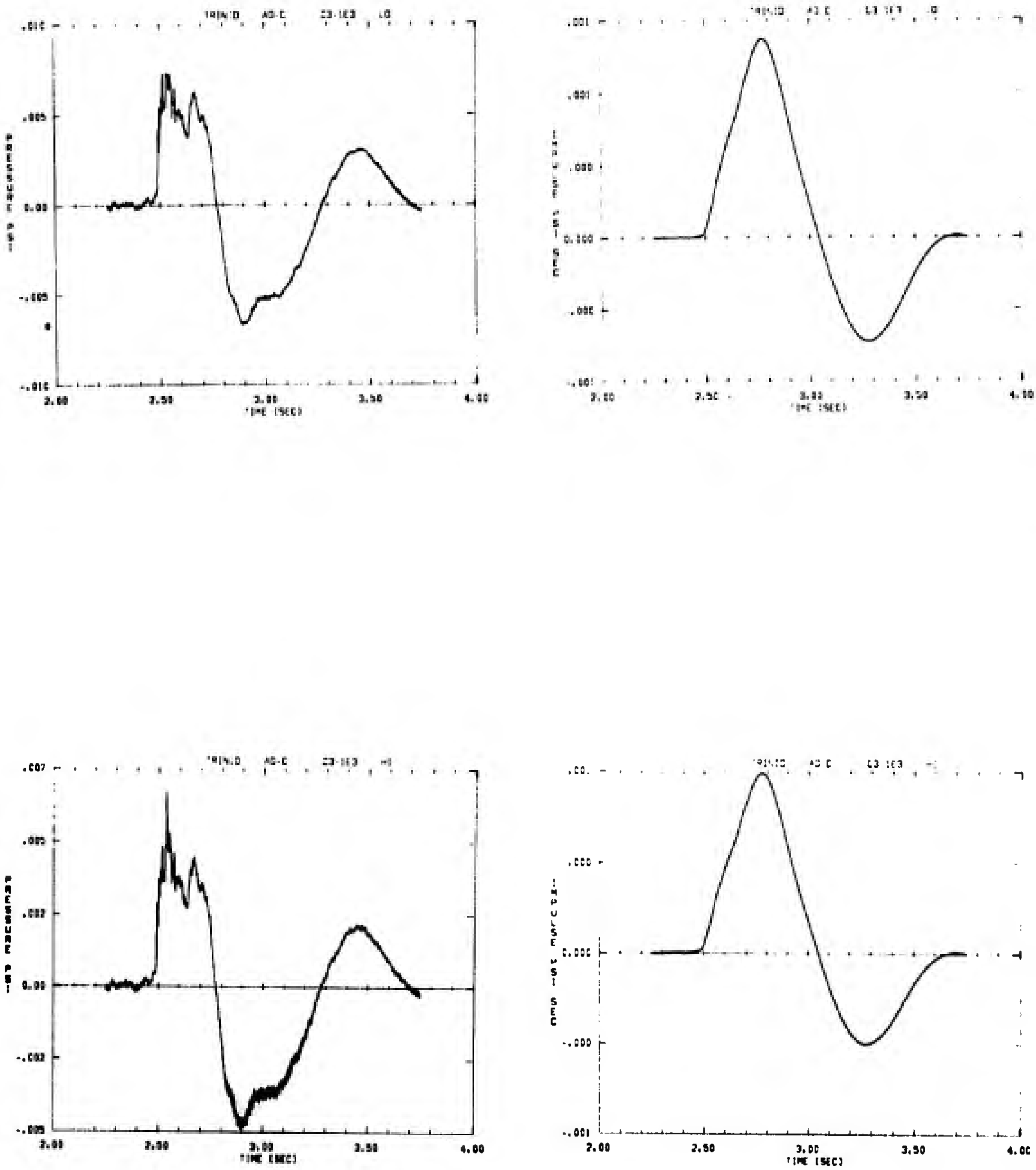

Figure C-18. Pressure-time and impulse-time for low-range gage (upper) and high-range gage (lower) for TRINIDAD Shot C-3, Station End 3

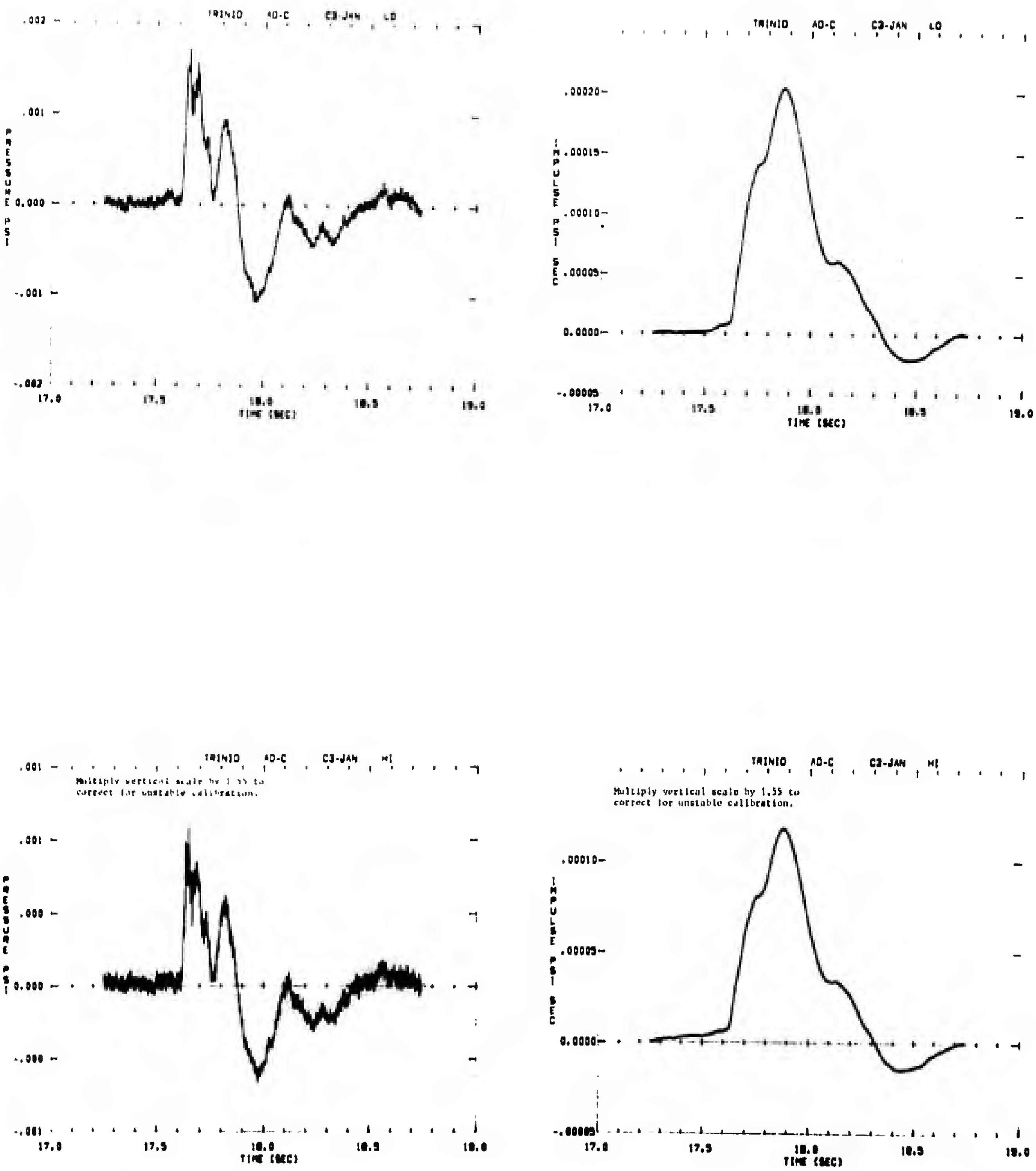

Figure C-19. Pressure-time and impulse-time for low-range gage (upper) and high-range gage (lower) for TRINIDAD Shot C-3, Station Jansen

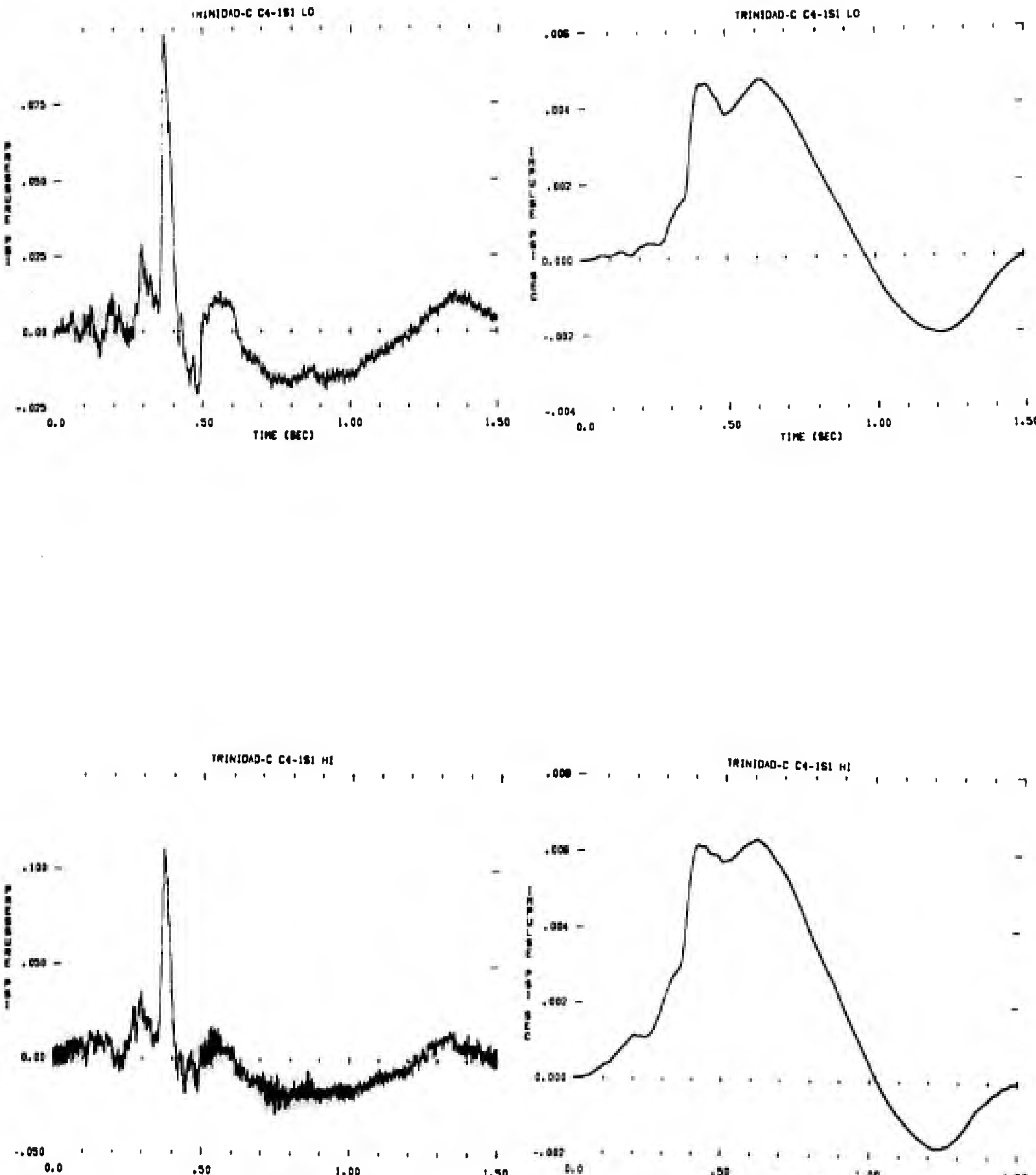

Figure C-20. Pressure-time and impulse-time for low-range gage (upper) and high-range gage (lower) for TRINIDAD Shot C-4, Station Side 1

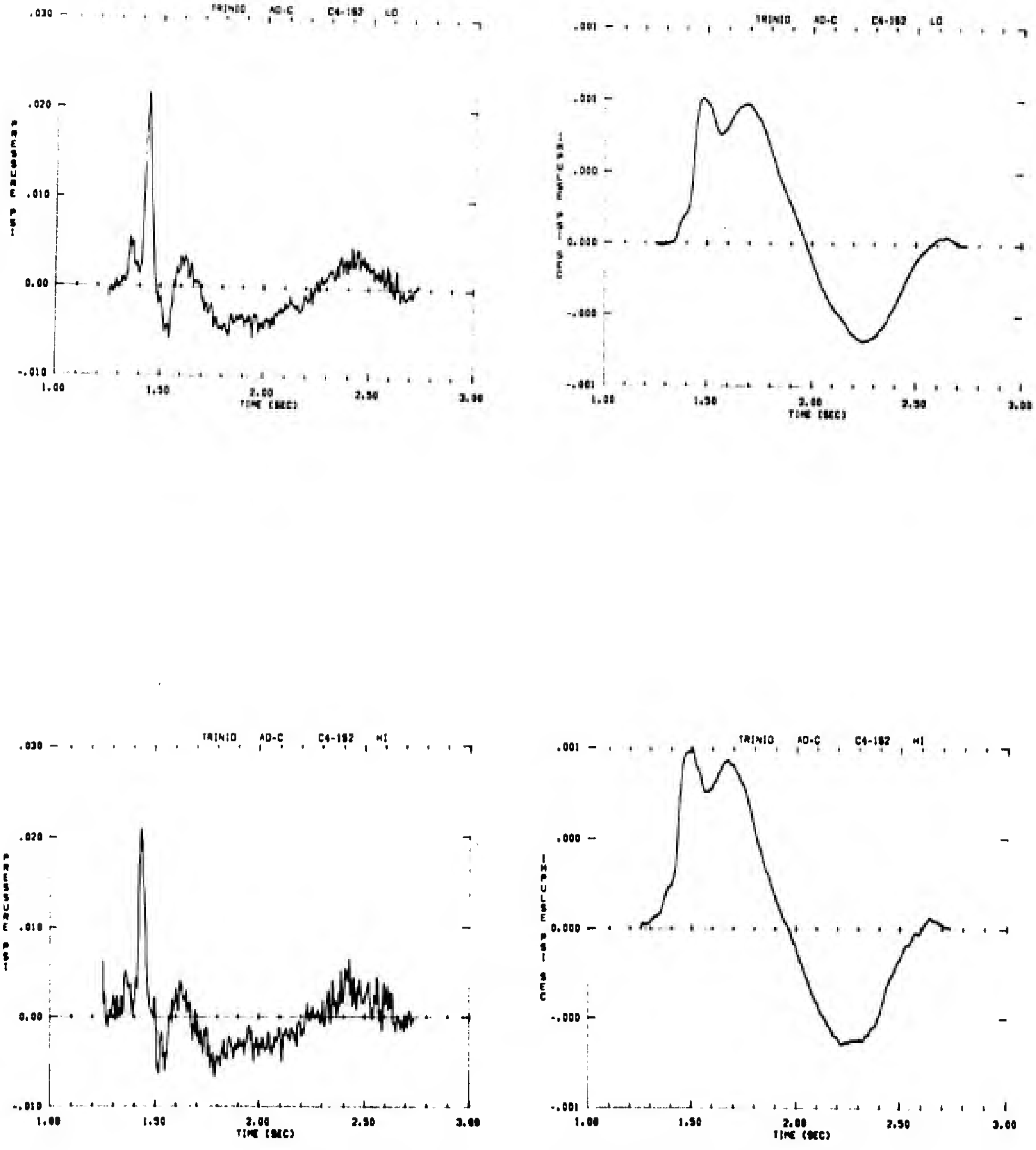

Figure C-21. Pressure-time and impulse-time for low-range gage (upper) and high-range gage (lower) for TRINIDAD Shot C-4, Station Side 2

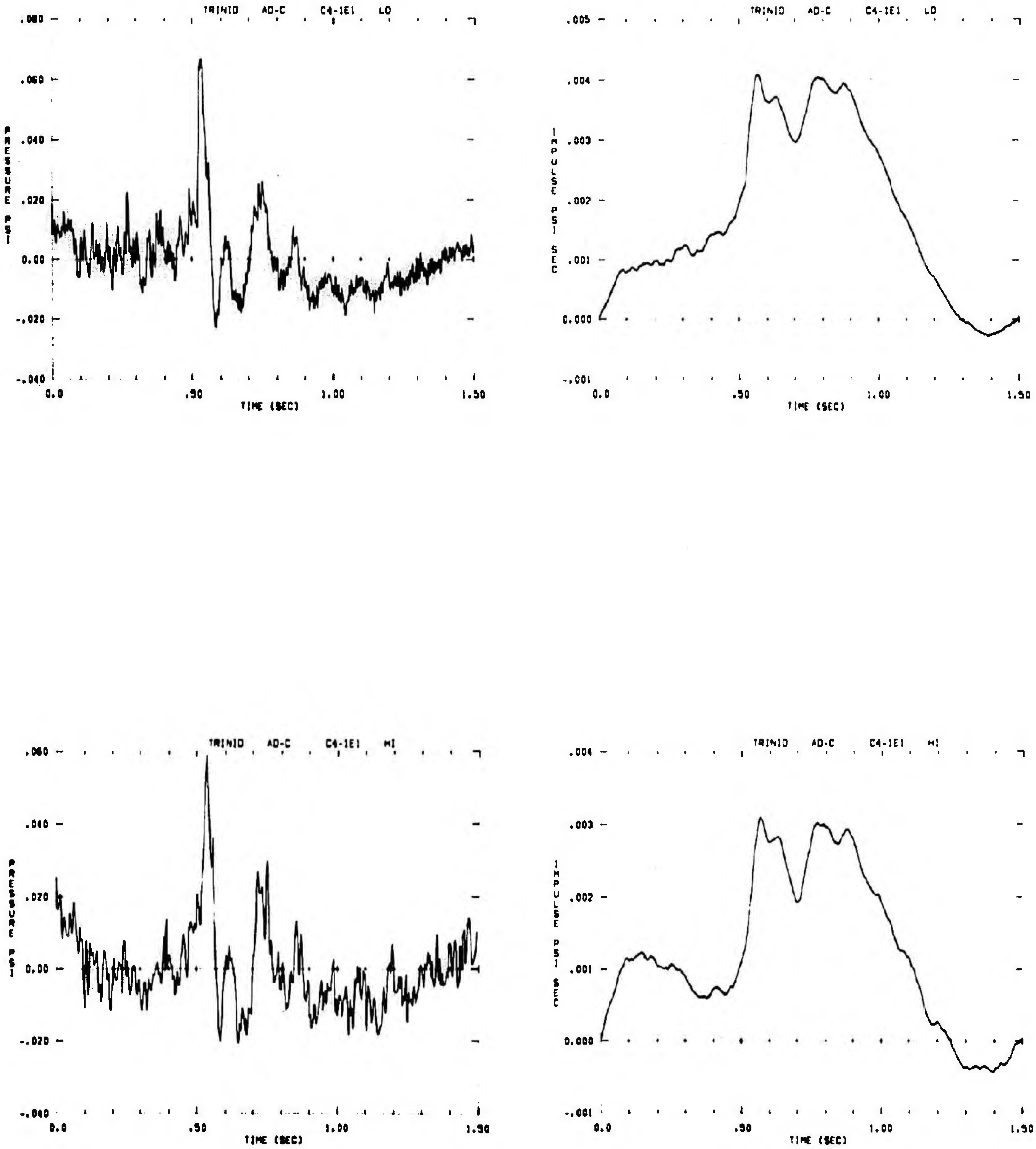

Figure C-22. Pressure-time and impulse-time for low-range gage (upper) and high-range gage (lower) for TRINIDAD Shot C-4, Station Initiated End 1

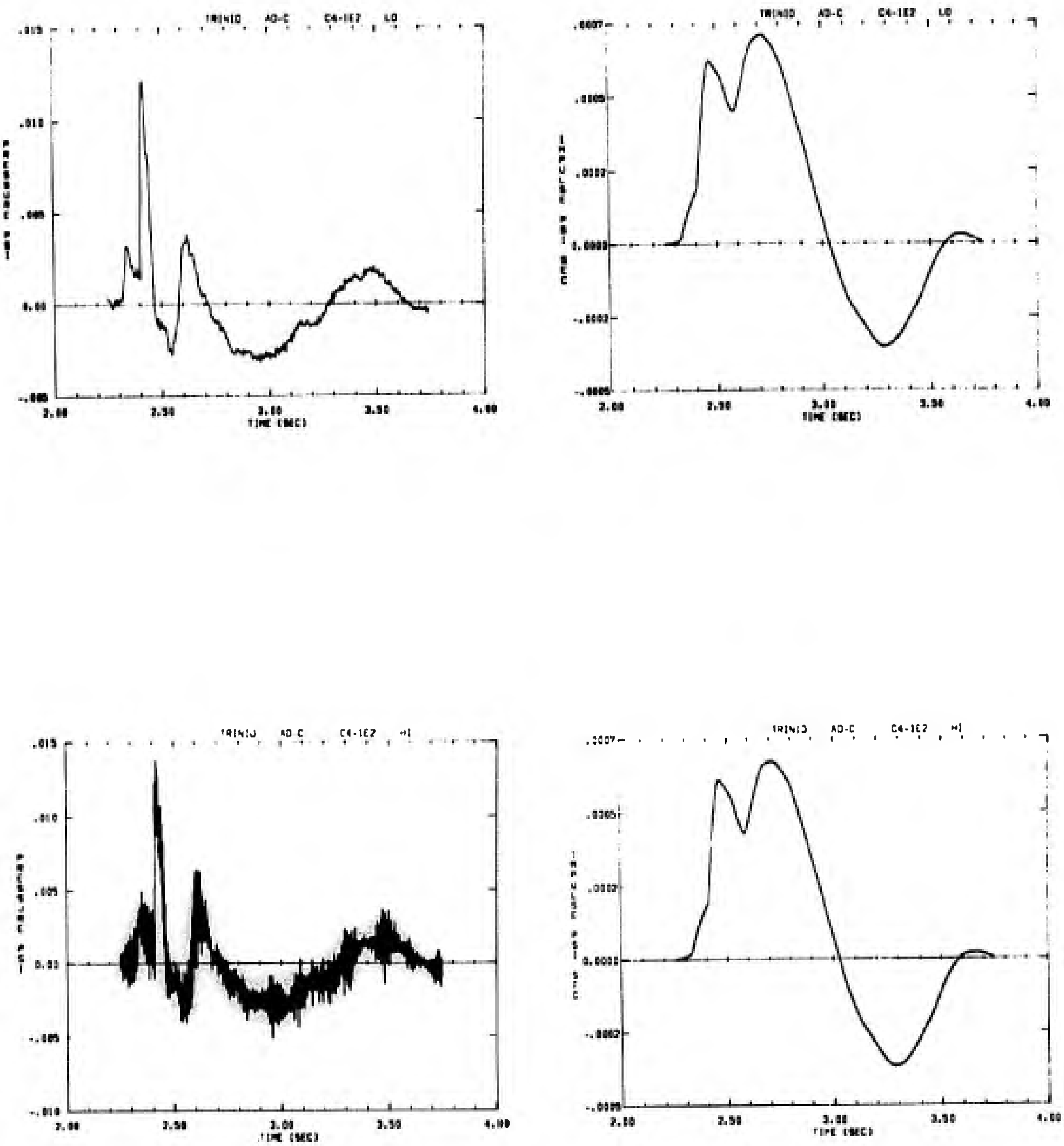

Figure C-23. Pressure-time and impulse-time for low-range gage (upper) and high-range gage (lower) for TRINIDAD Shot C-4, Station Initiated End 2

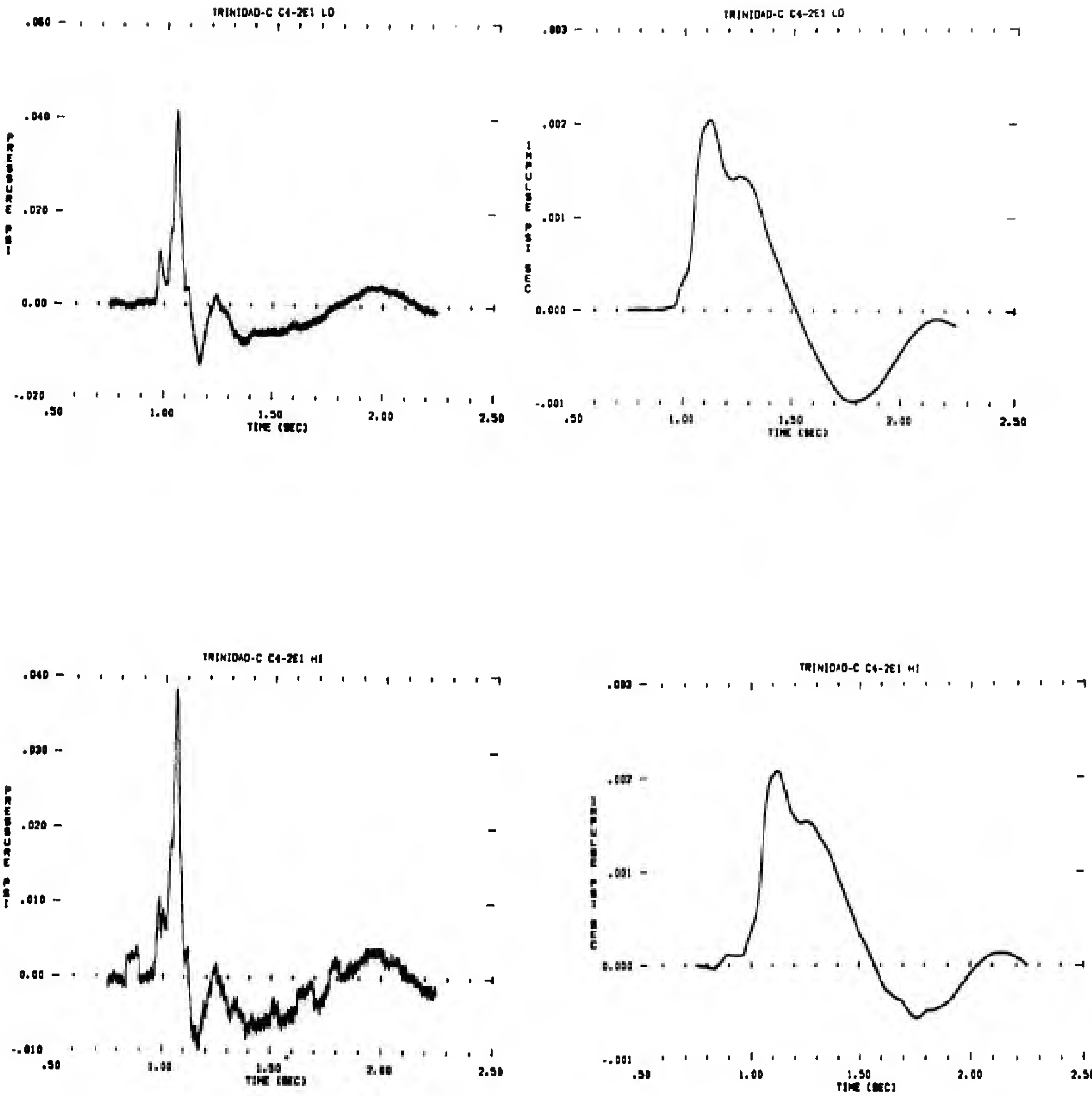

Figure C-24. Pressure-time and impulse-time for low-range gage (upper) and high-range gage (lower) for TRINIDAD Shot C-4, Station Opposite End 1

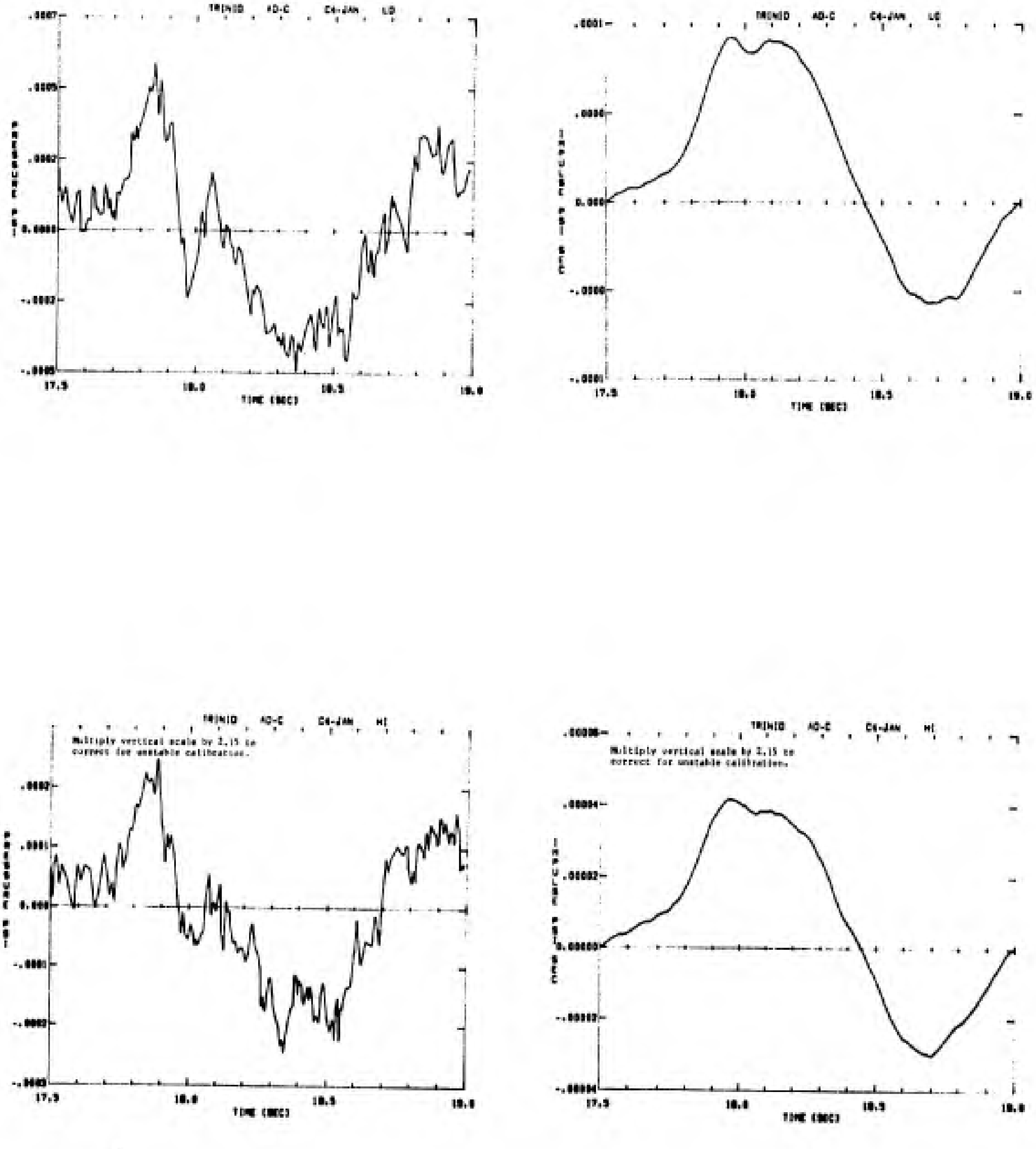

Figure C-25. Pressure-time and impulse-time for low-range gage (upper) and high-range gage (lower) for TRINIDAD Shot C-4, Station Jansen

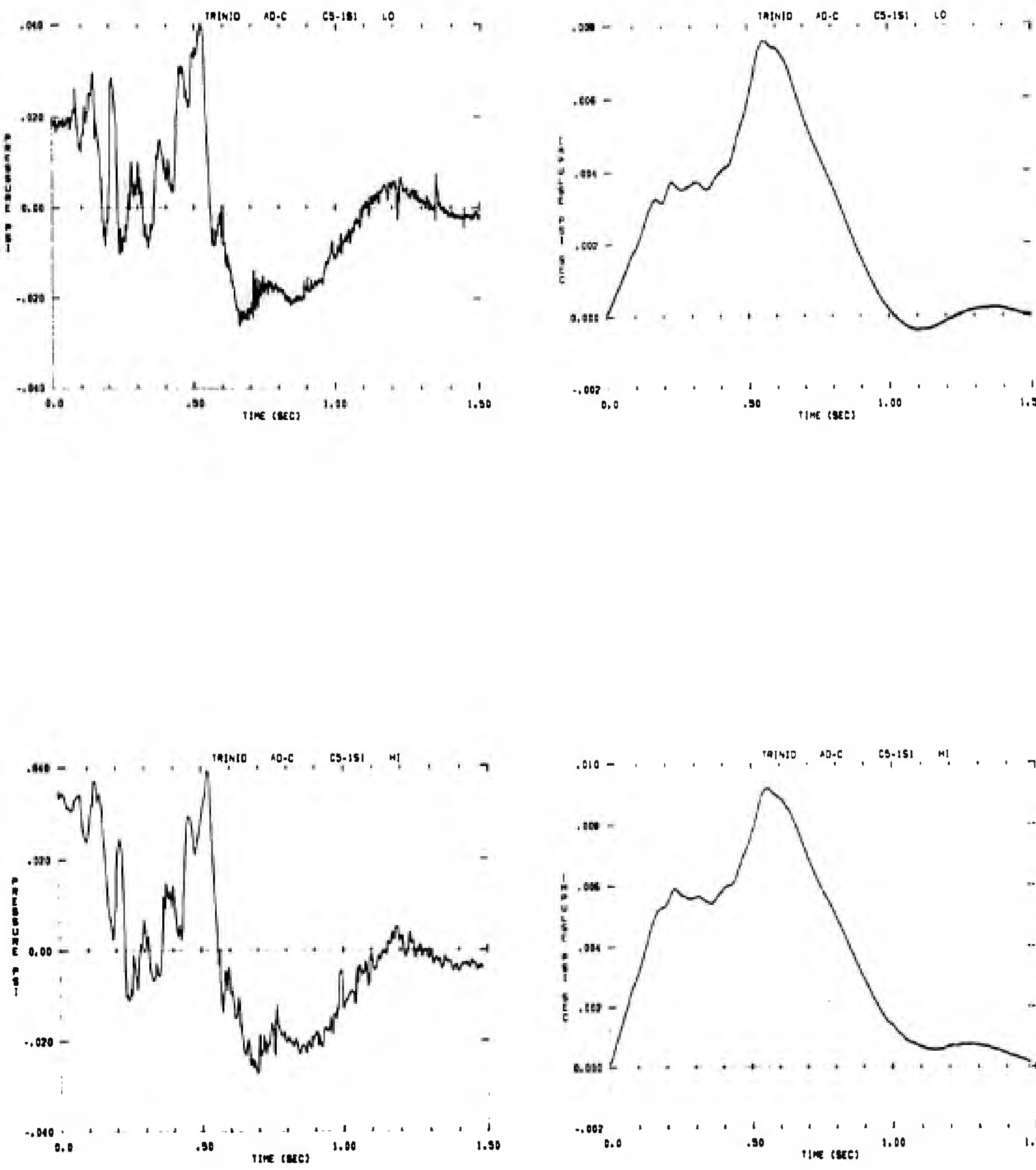

Figure C-26. Pressure-time and impulse-time for low-range gage (upper) and high-range gage (lower) for TRINIDAD Shot C-5, Station Side 1

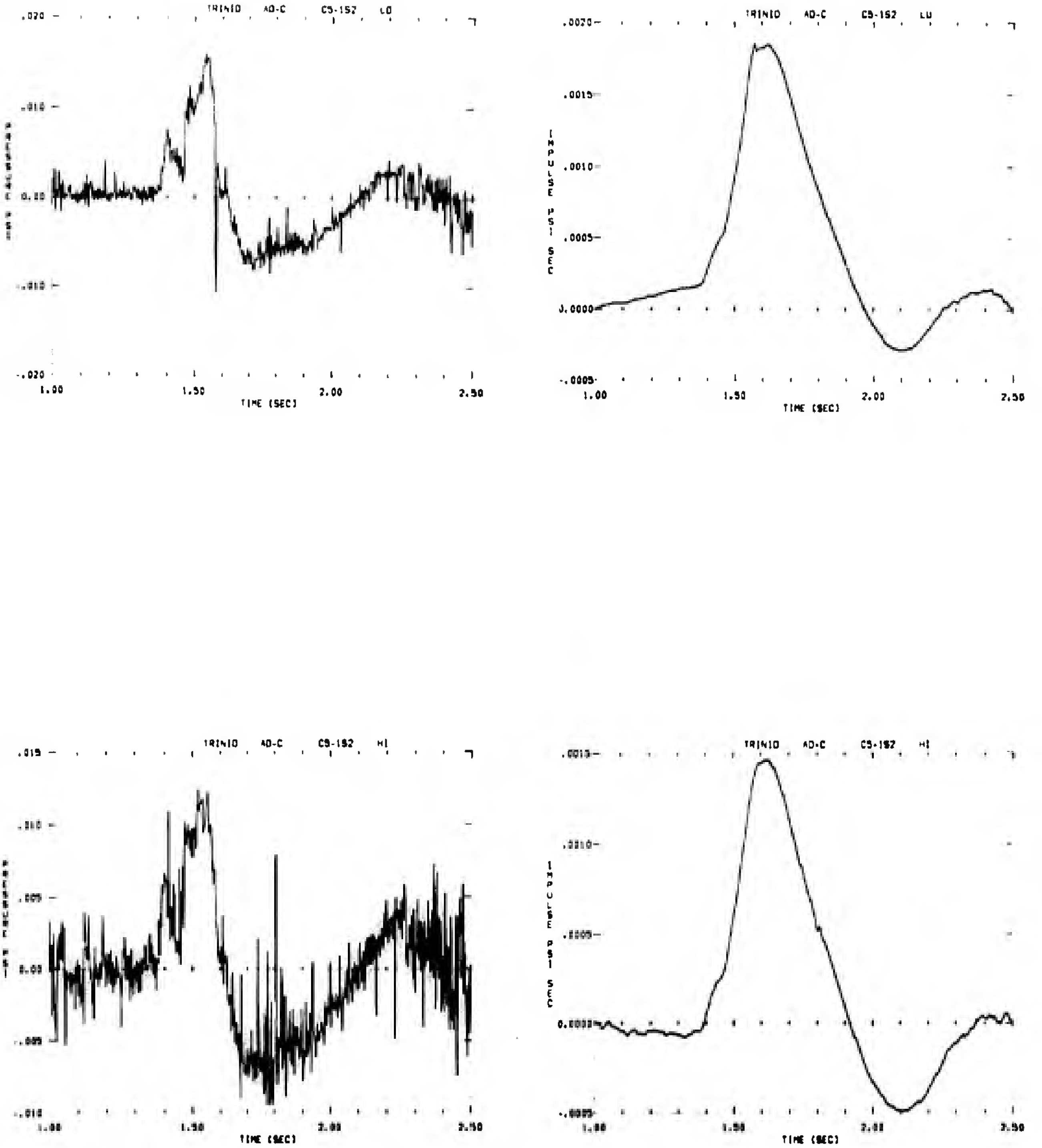

Figure C-27. Pressure-time and impulse-time for low-range gage (upper) and high-range gage (lower) for TRINIDAD Shot C-5, Station Side 2

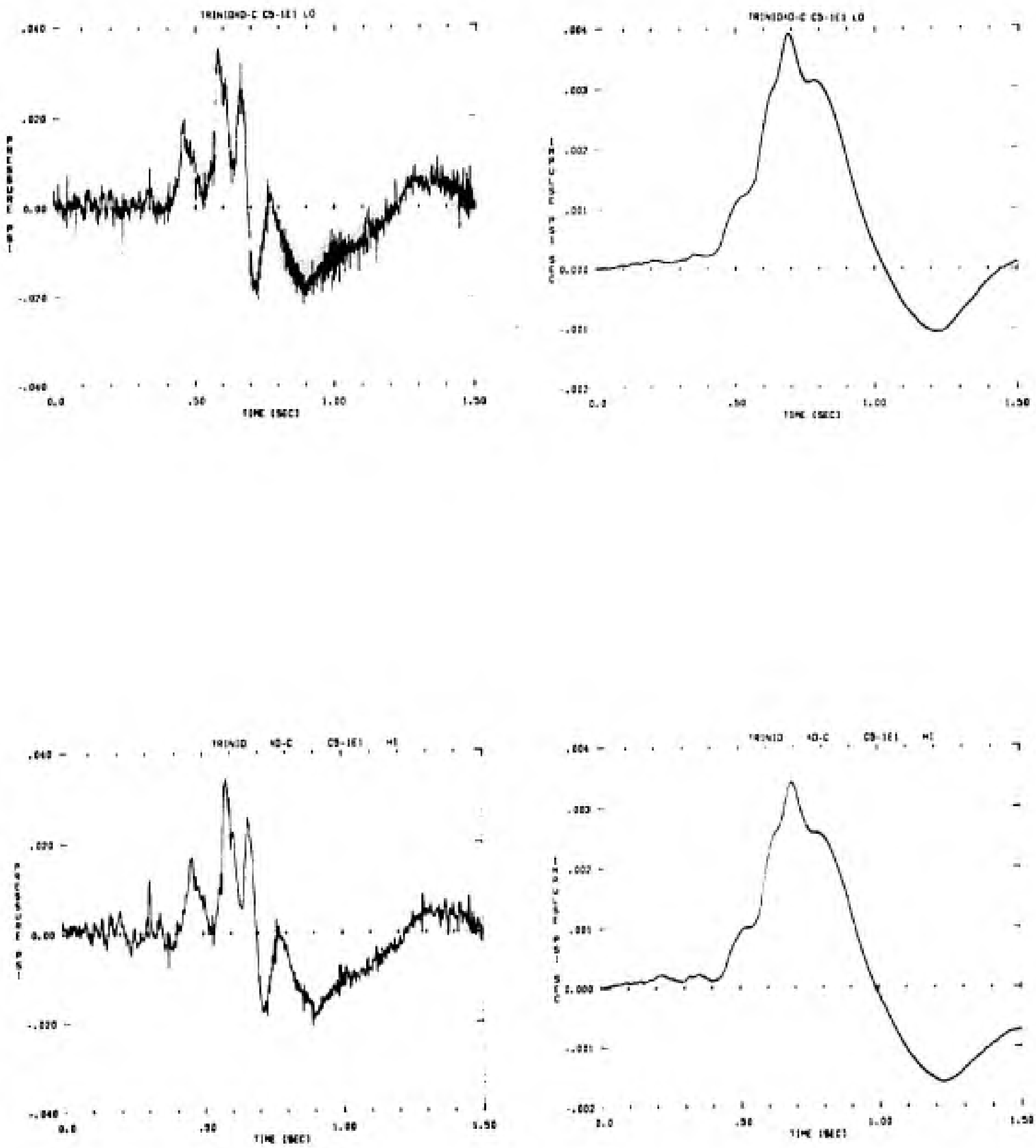

Figure C-28. Pressure-time and impulse-time for low-range gage (upper) and high-range gage (lower) for TRINIDAD Shot C-5, Station Initiated End 1

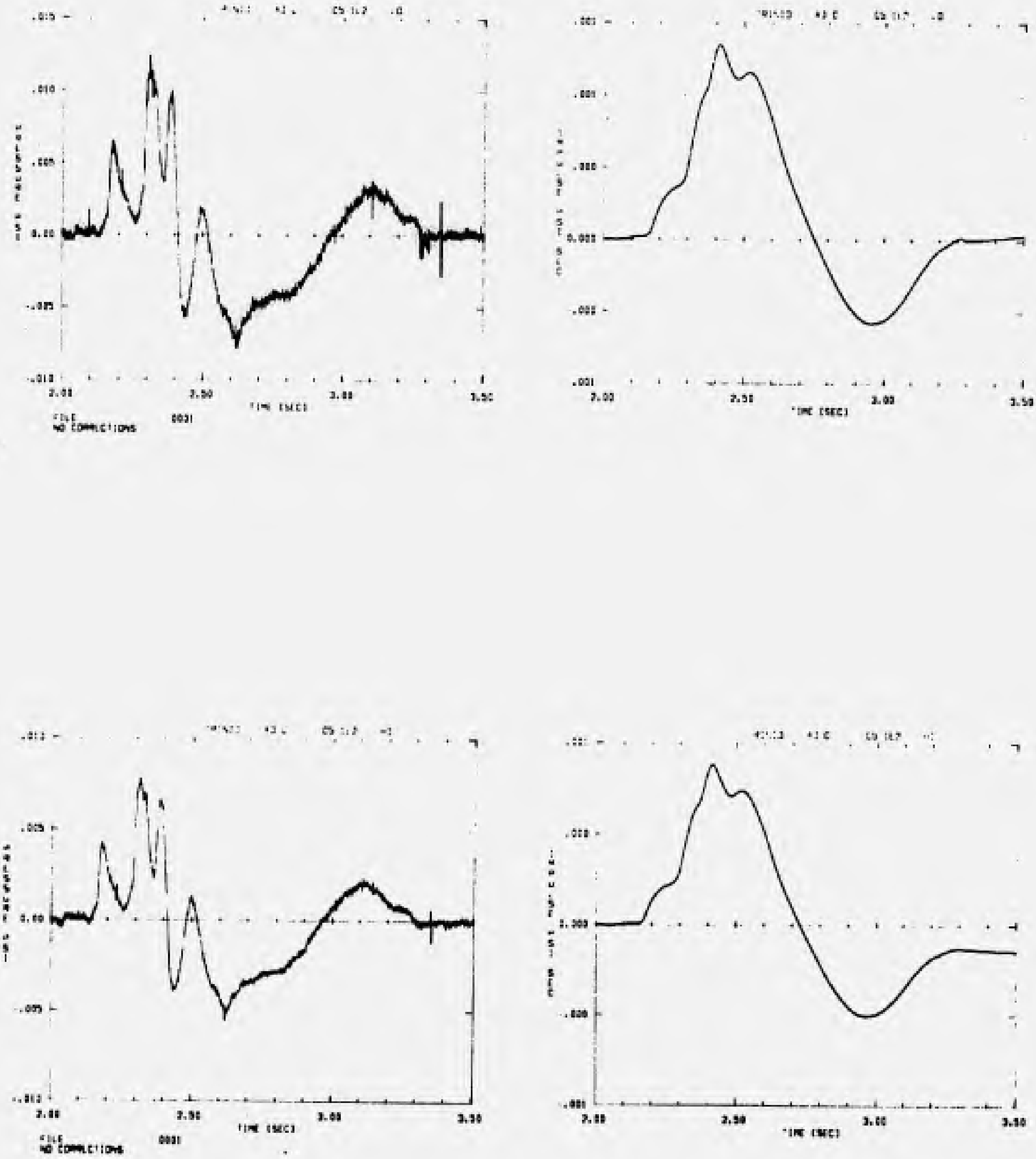

Figure C-29. Pressure-time and impulse-time for low-range gage (upper) and high-range gage (lower) for TRINIDAD Shot C-5, Station Initiated End 2

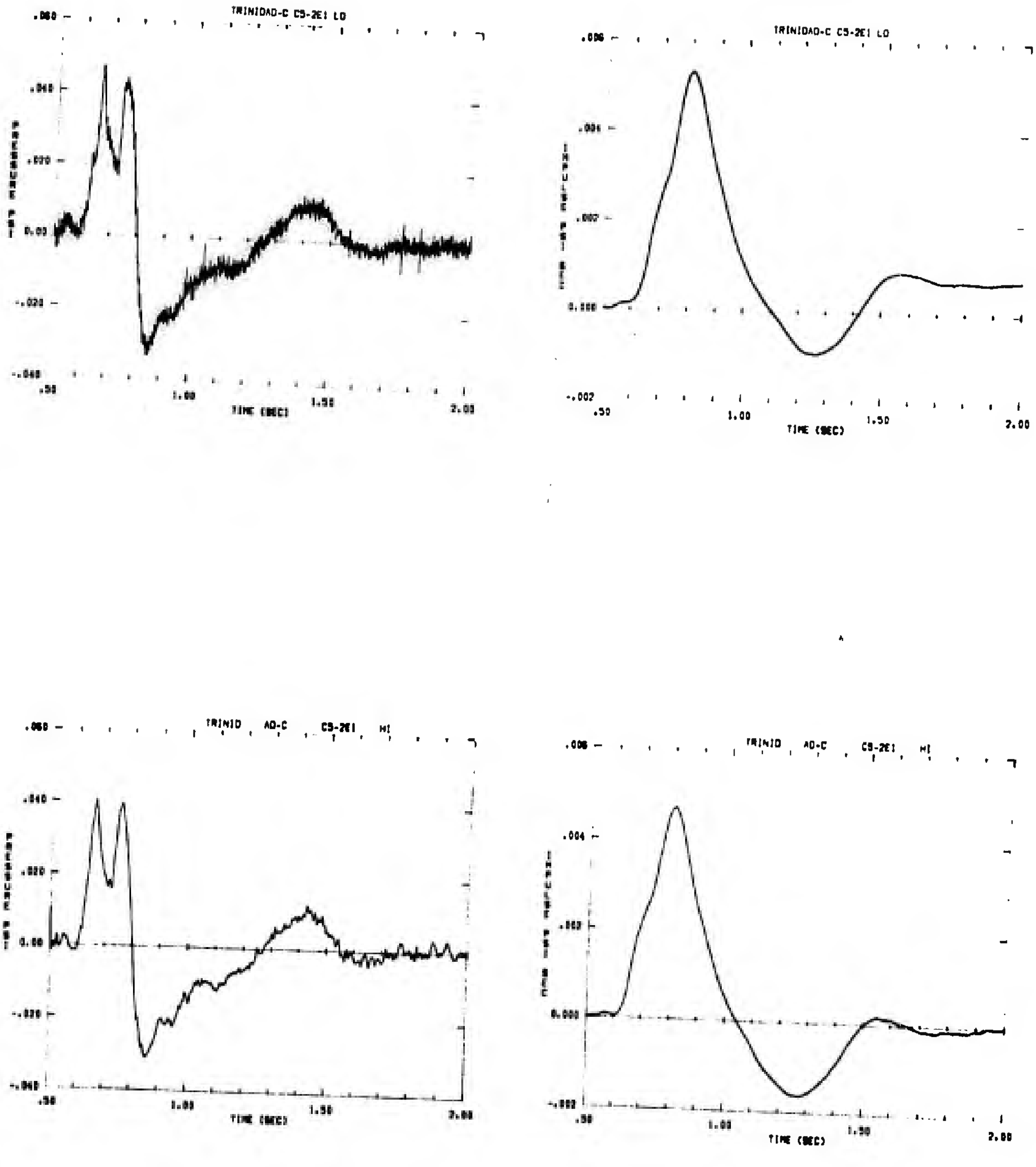

Figure C-30. Pressure-time and impulse-time for low-range gage (upper) and high-range gage (lower) for TRINIDAD Shot C-5, Station Opposite End 1

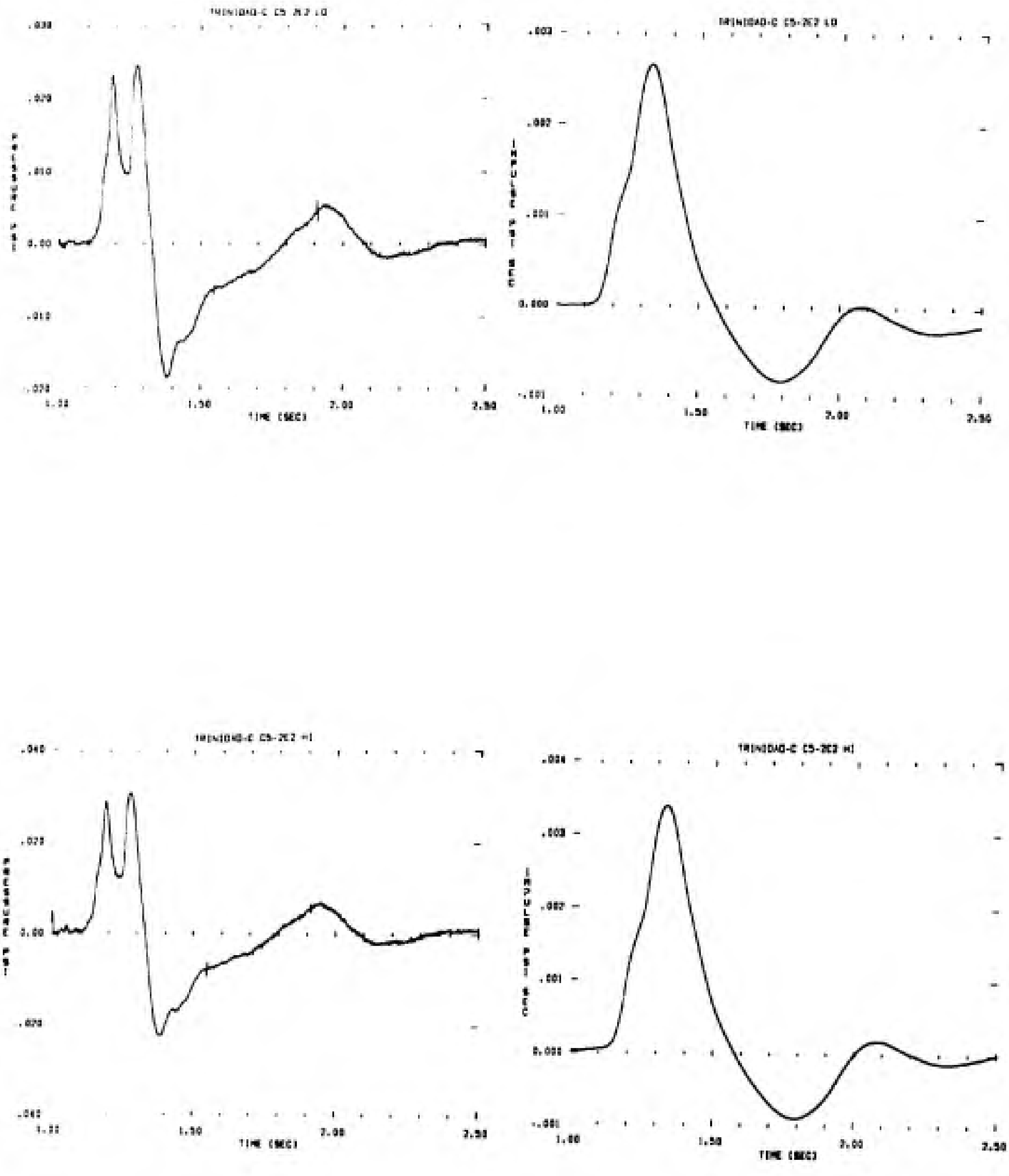

Figure C-31. Pressure-time and impulse-time for low-range gage (upper) and high-range gage (lower) for TRINIDAD Shot C-5, Station Opposite End 2

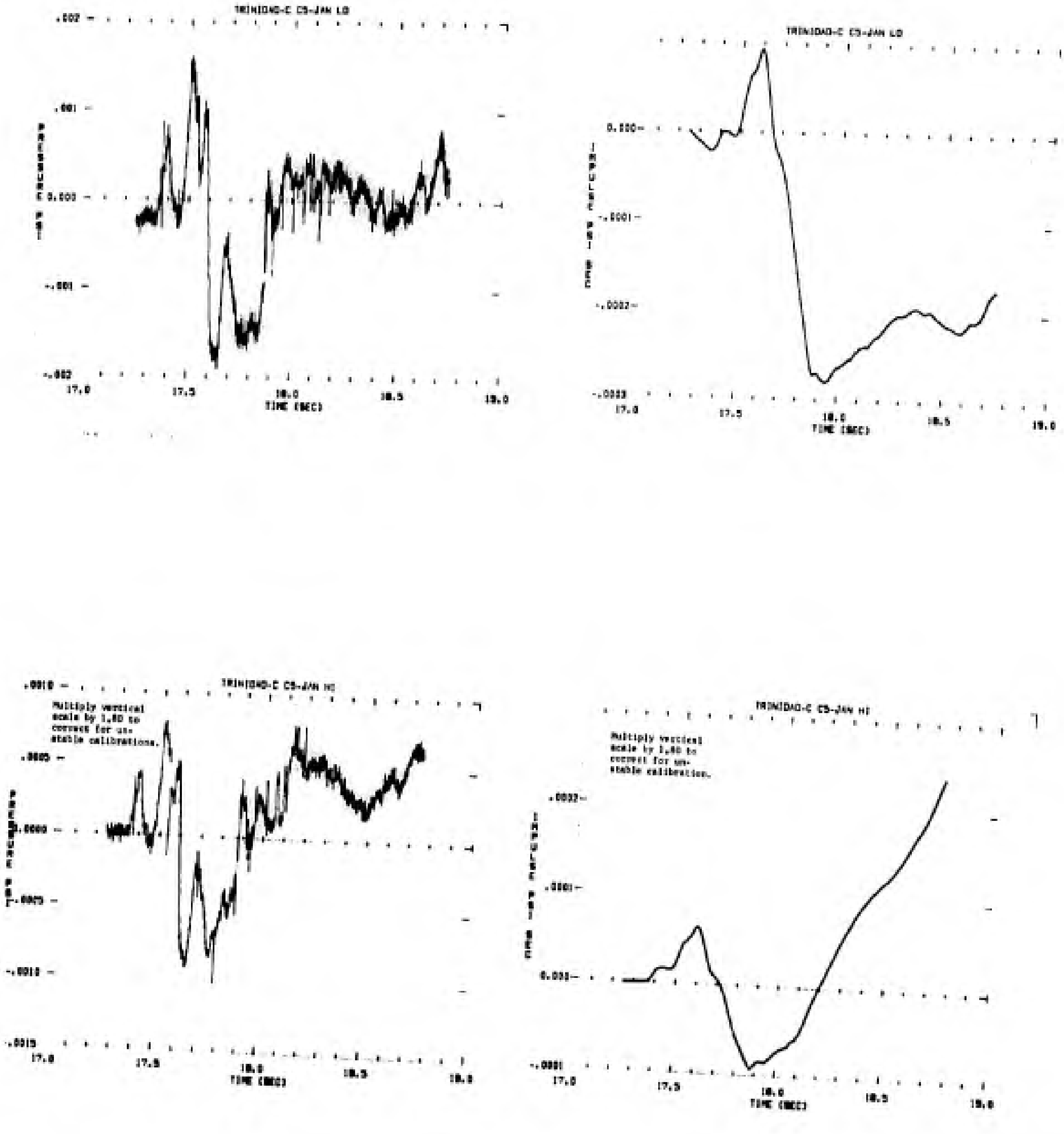

Figure C-32. Pressure-time and impulse-time for low-range gage (upper) and high-range gage (lower) for TRINIDAD Shot C-5, Station Jansen

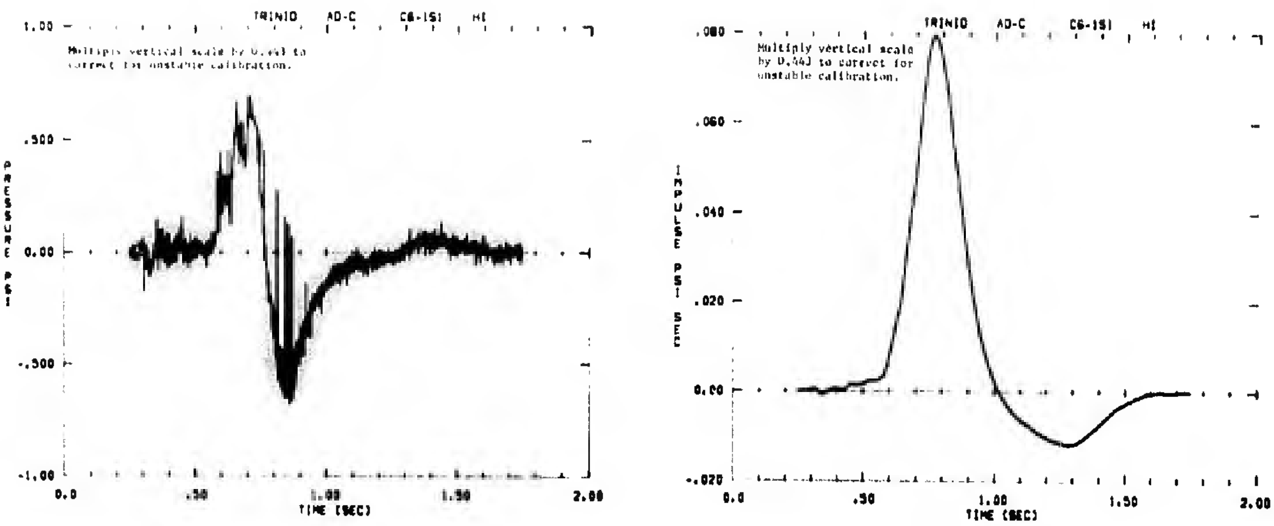

Figure C-33. Pressure-time and impulse-time for high-range gage for TRINIDAD Shot C-6, Station Side 1

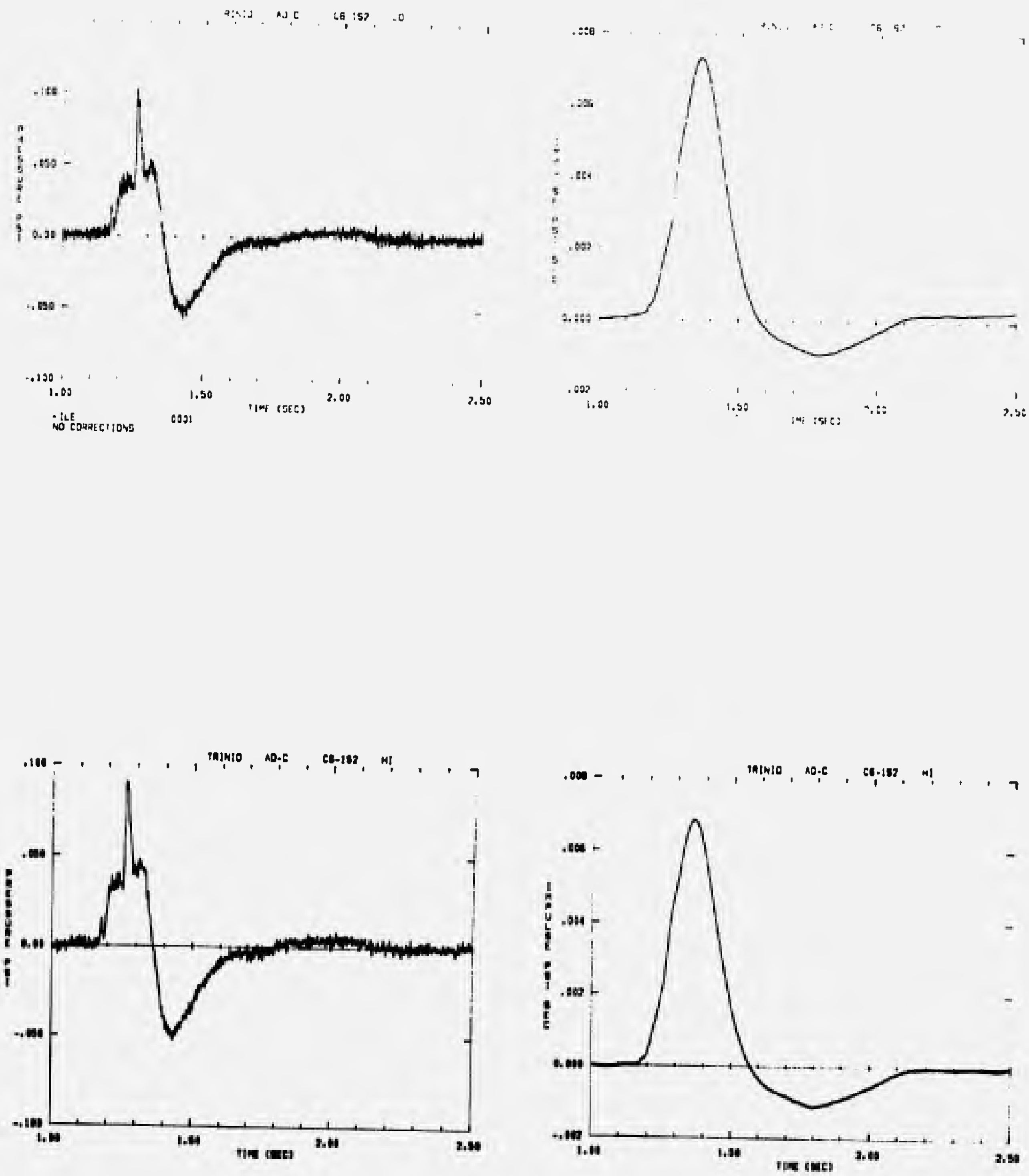

Figure C-34. Pressure-time and impulse-time for low-range gage (upper) and high-range gage (lower) for TRINIDAD Shot C-6, Station Side 2

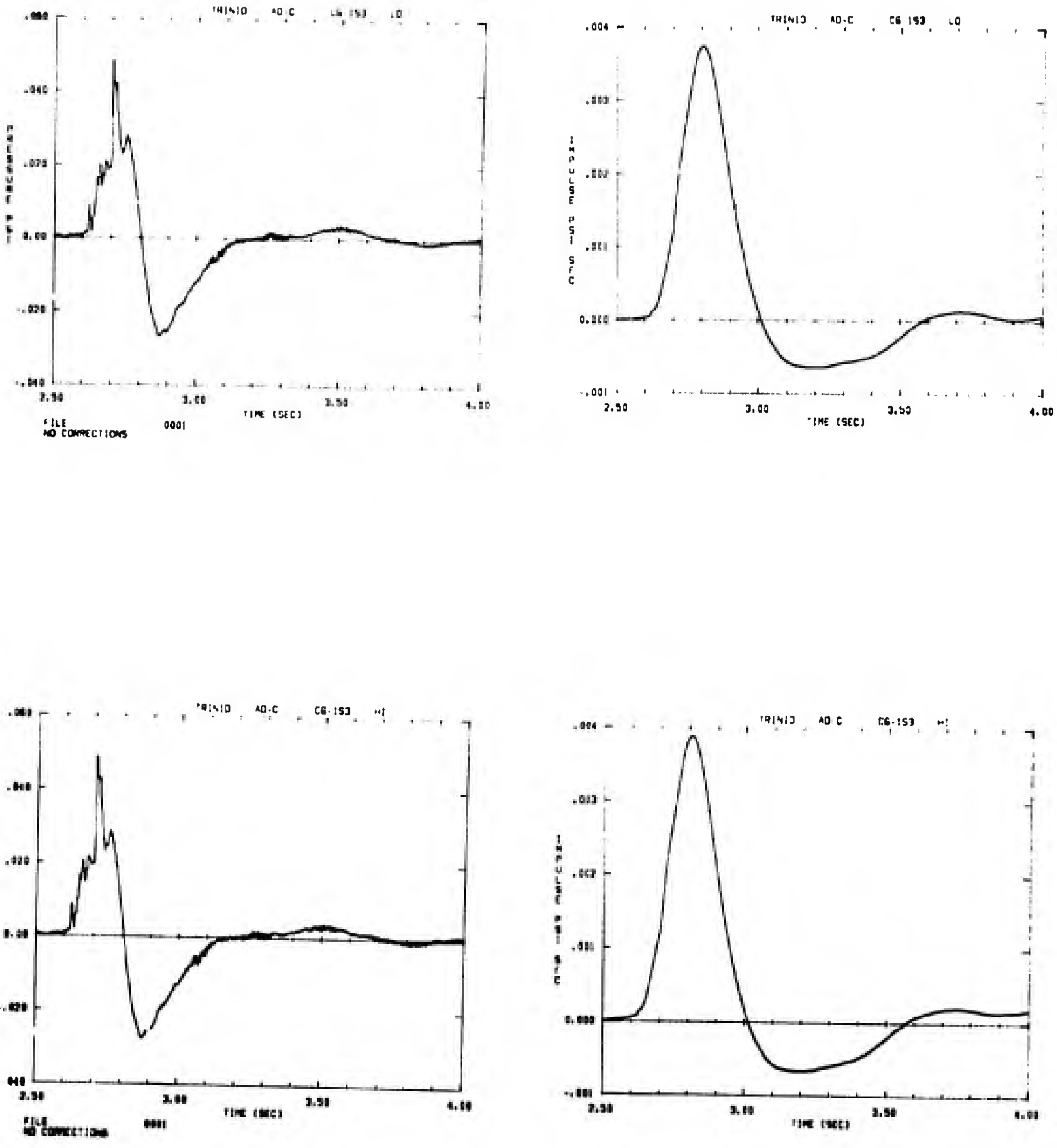

Figure C-35. Pressure-time and impulse-time for low-range gage (upper) and high-range gage (lower) for TRINIDAD Shot C-6, Station Side 3

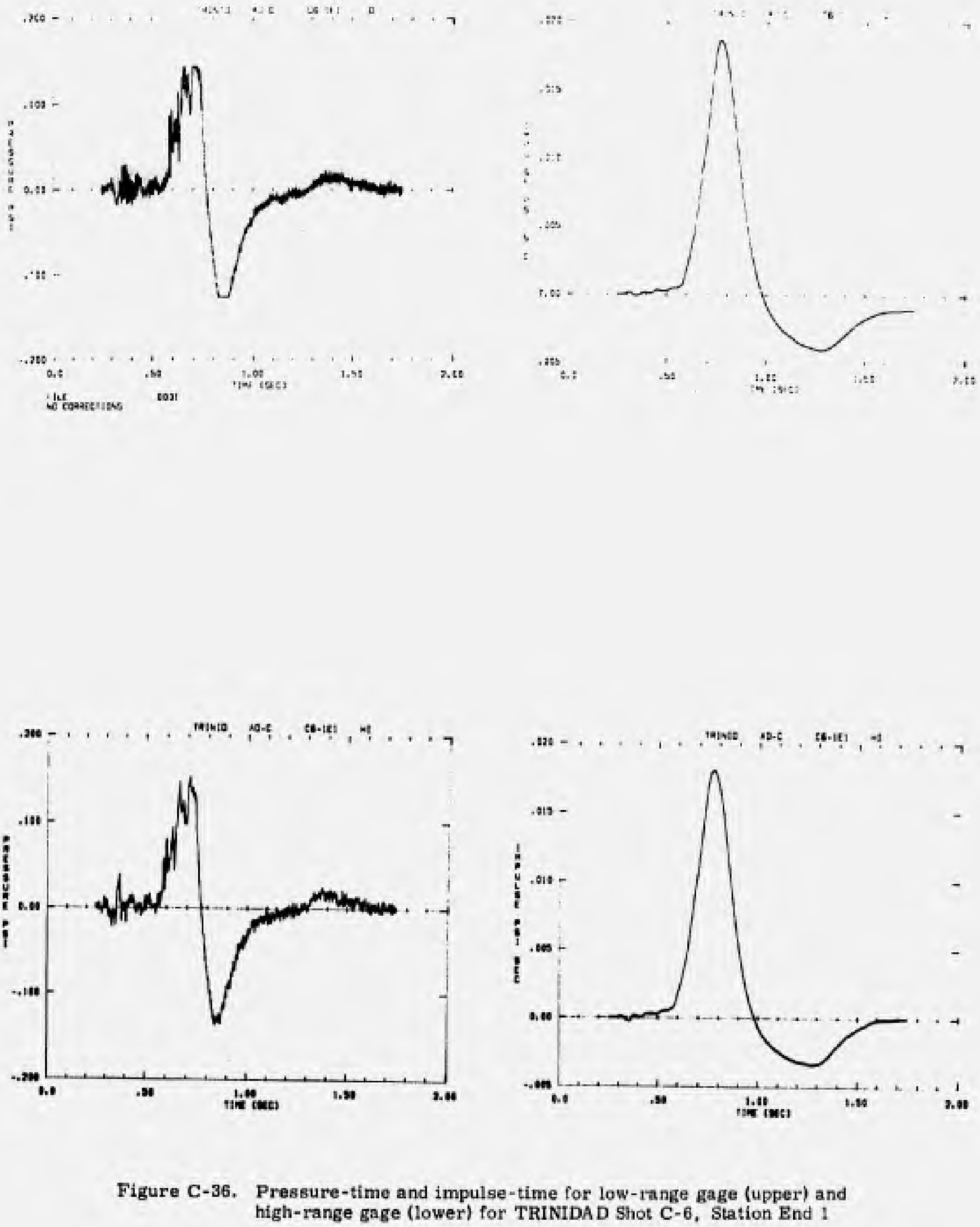

Figure C-36. Pressure-time and impulse-time for low-range gage (upper) and high-range gage (lower) for TRINIDAD Shot C-6, Station End 1

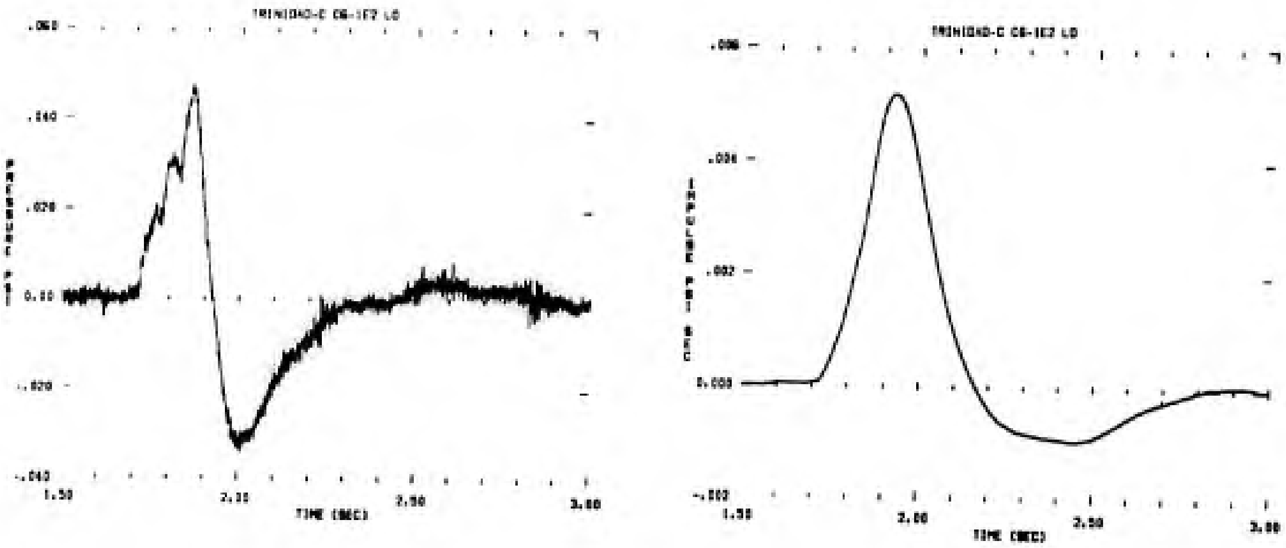

Figure C-37. Pressure-time and impulse-time for high-range gage for TRINIDAD Shot C-6, Station End 2

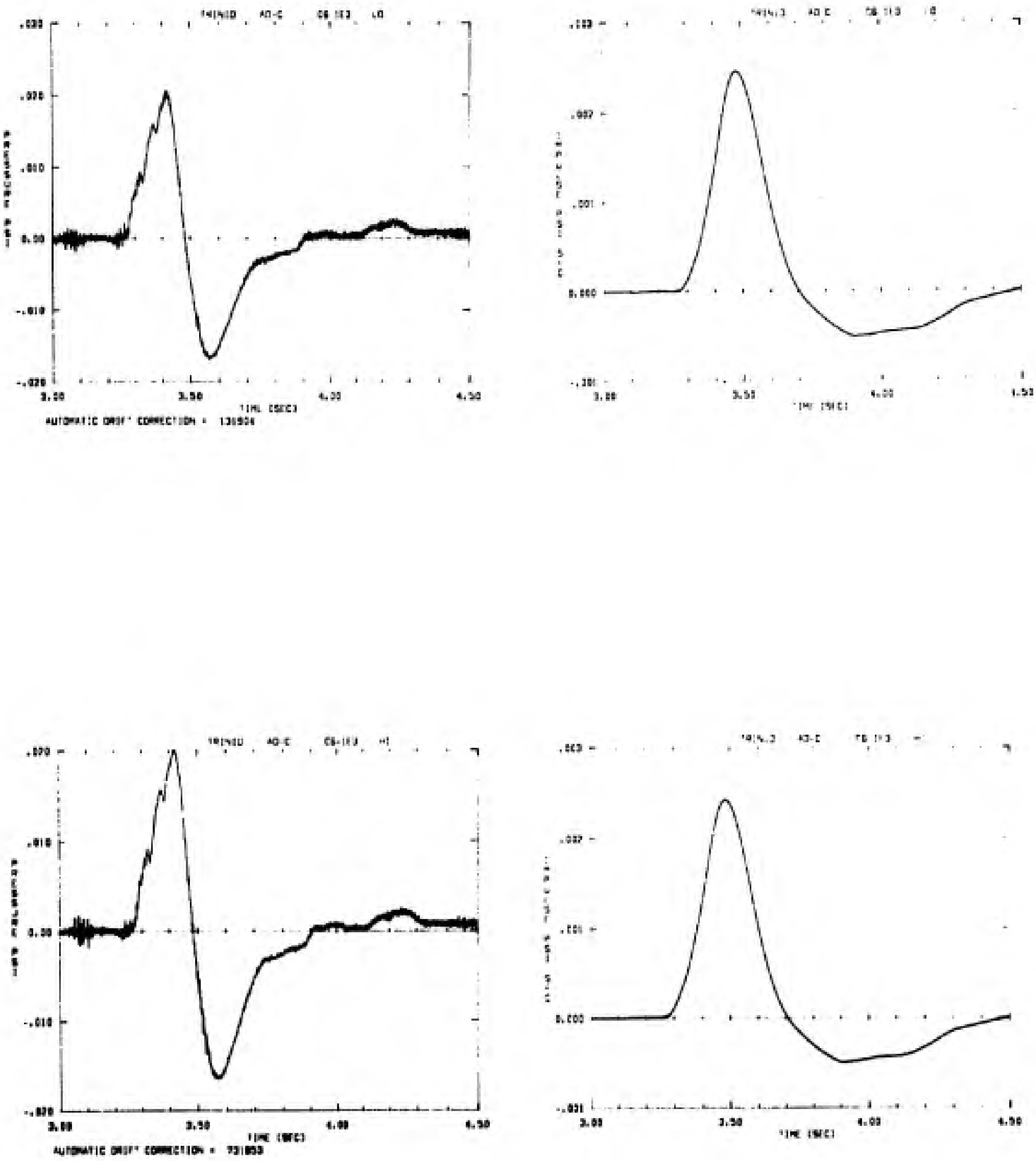

Figure C-38. Pressure-time and impulse-time for low-range gage (upper) and high-range gage (lower) for TRINIDAD Shot C-6, Station End 3

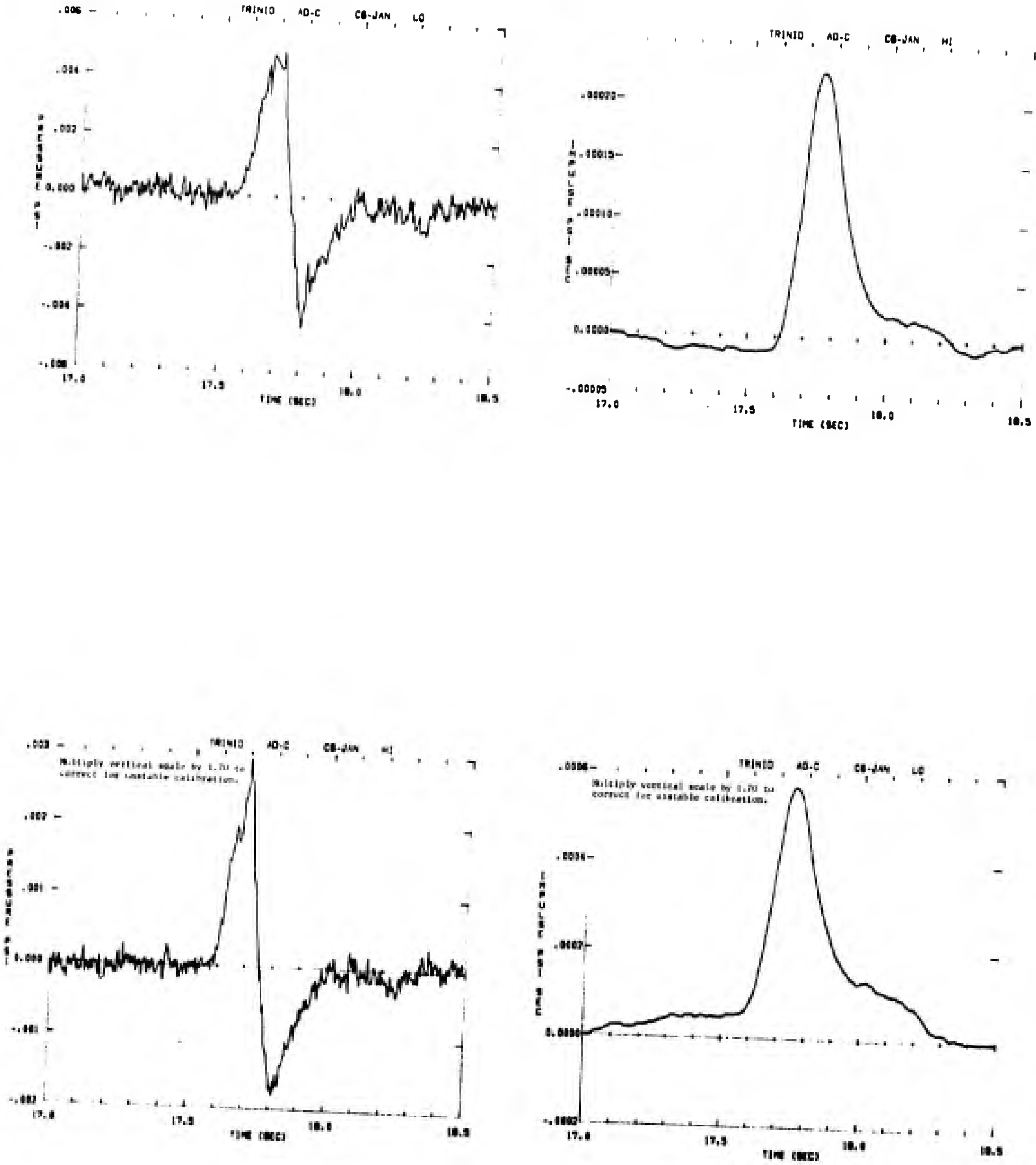

Figure C-39. Pressure-time and impulse-time for low-range gage (upper) and high-range gage (lower) for TRINIDAD Shot C-6, Station Jansen

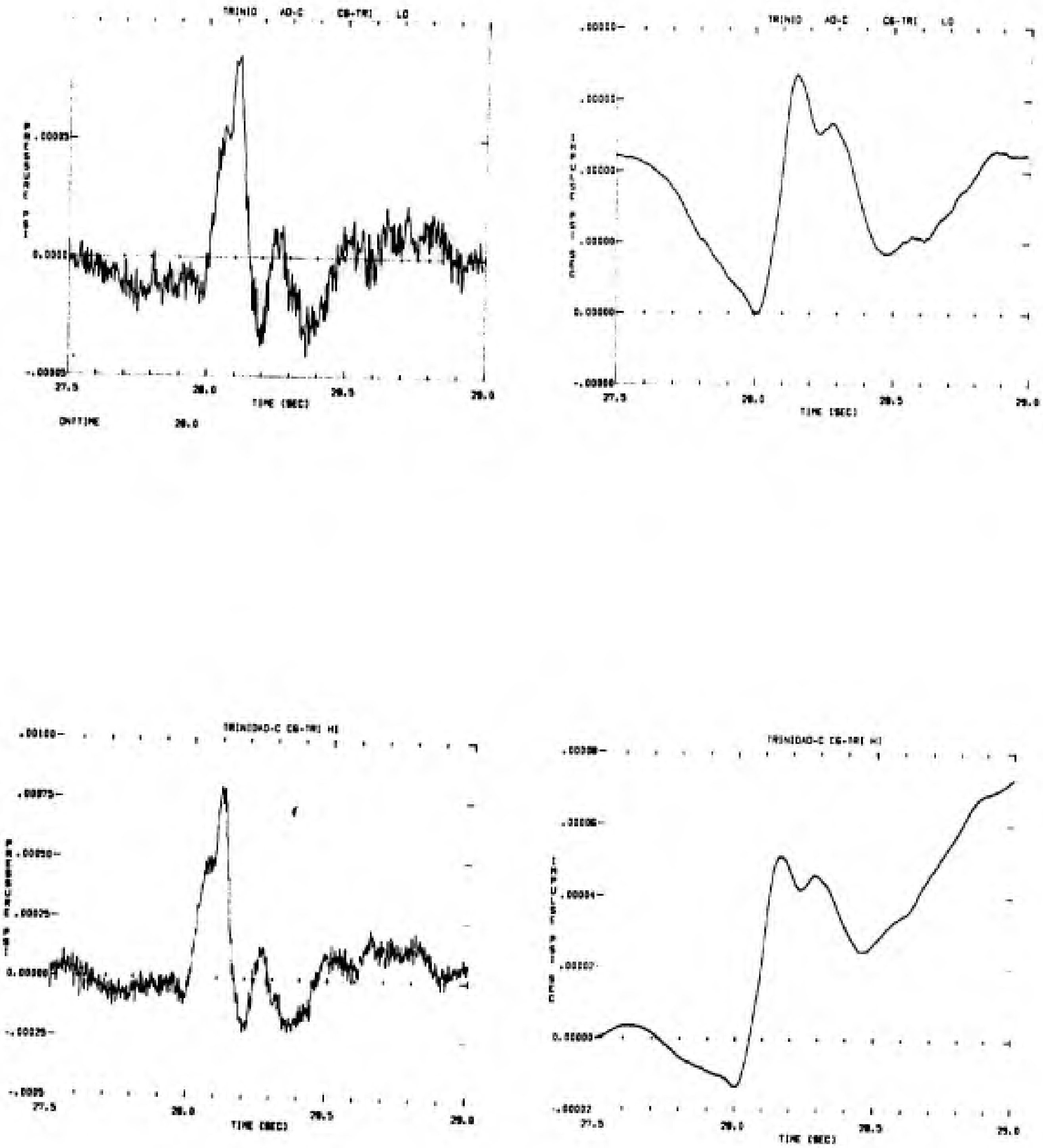

Figure C-40. Pressure-time and impulse-time for low-range gage (upper) and high-range gage (lower) for TRINIDAD Shot C-6, Station Trinidad

BLANK PAGE

APPENDIX D

Pressure-Time Records for the D Series

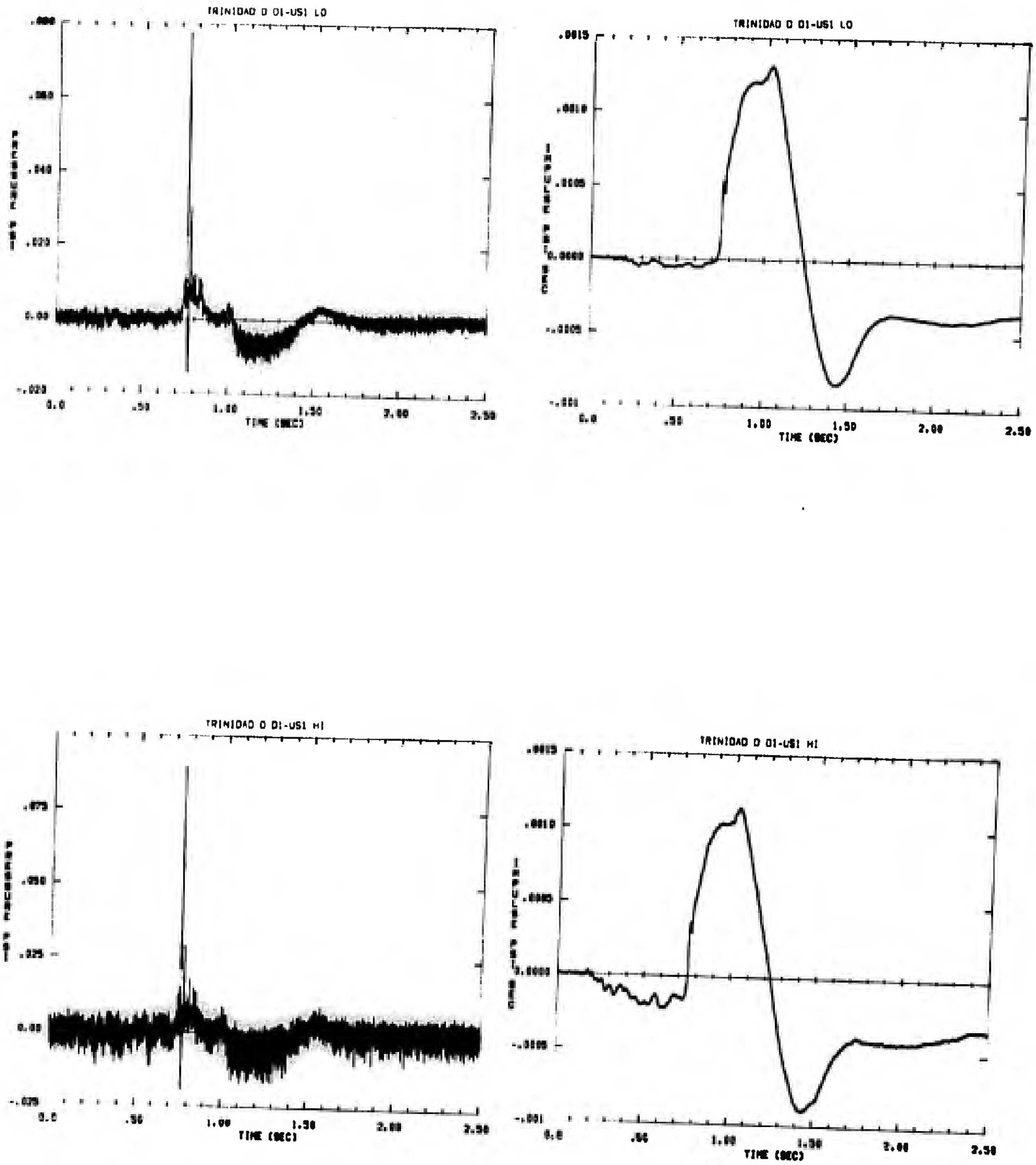

Figure D-1. Pressure-time and impulse-time for low-range gage (upper) and high-range gage (lower) for TRINIDAD Shot D-1, Station Uphill, Side 1

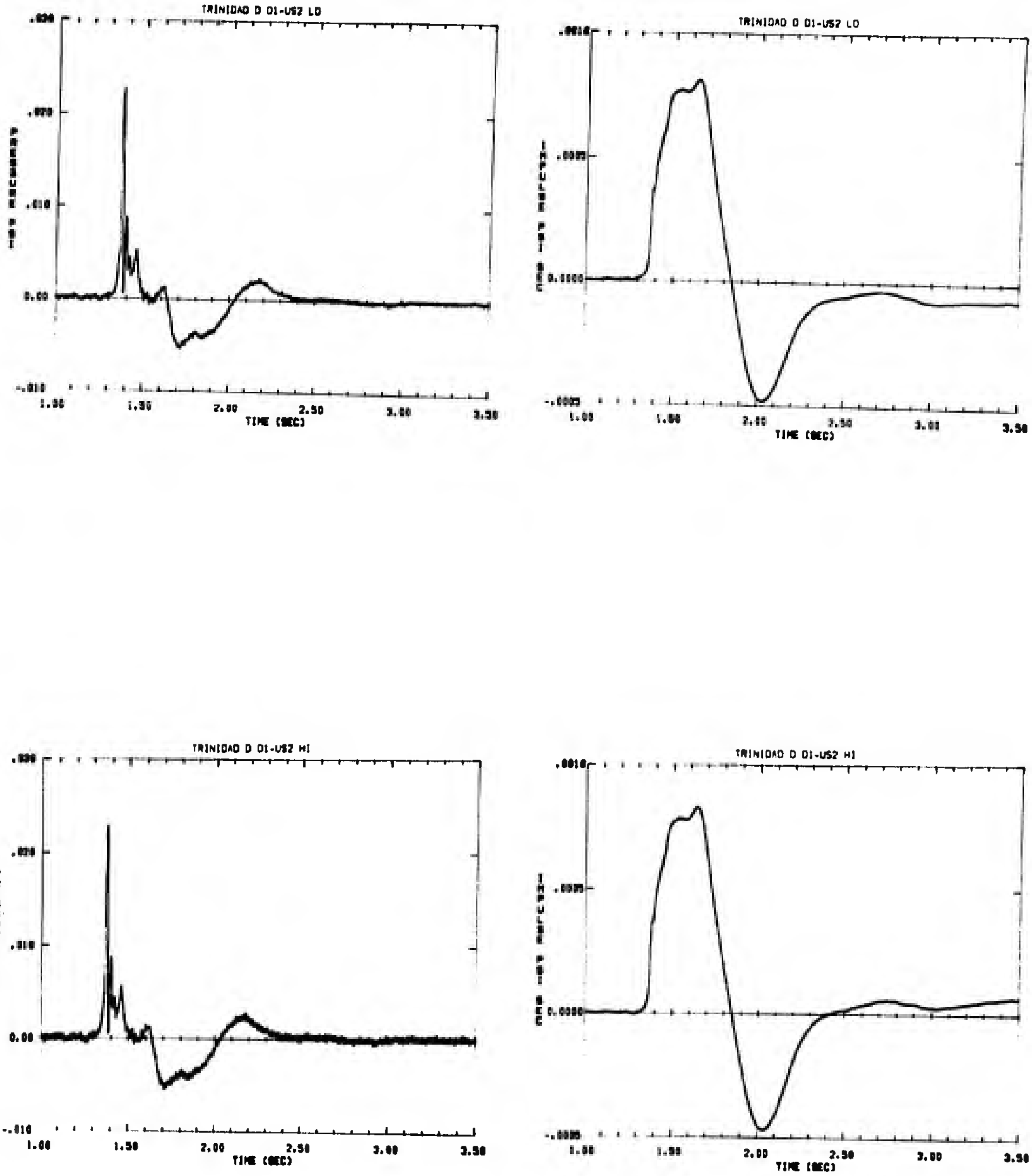

Figure D-2. Pressure-time and impulse-time for low-range gage (upper) and high-range gage (lower) for TRINIDAD Shot D-1, Station Uphill Side 2

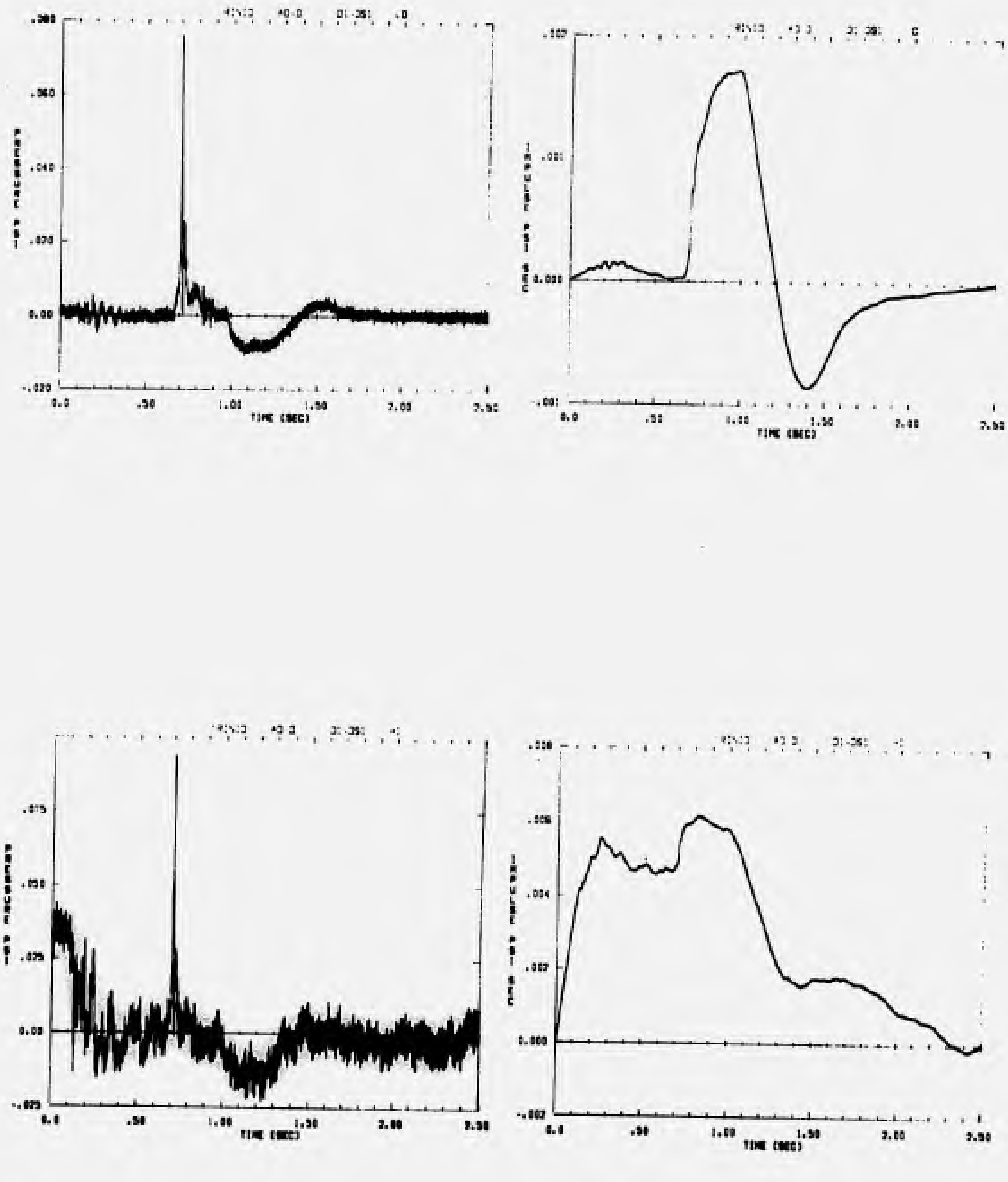

Figure D-3. Pressure-time and impulse-time for low-range gage (upper) and high-range gage (lower) for TRINIDAD Shot D-1, Station Downhill Side 1

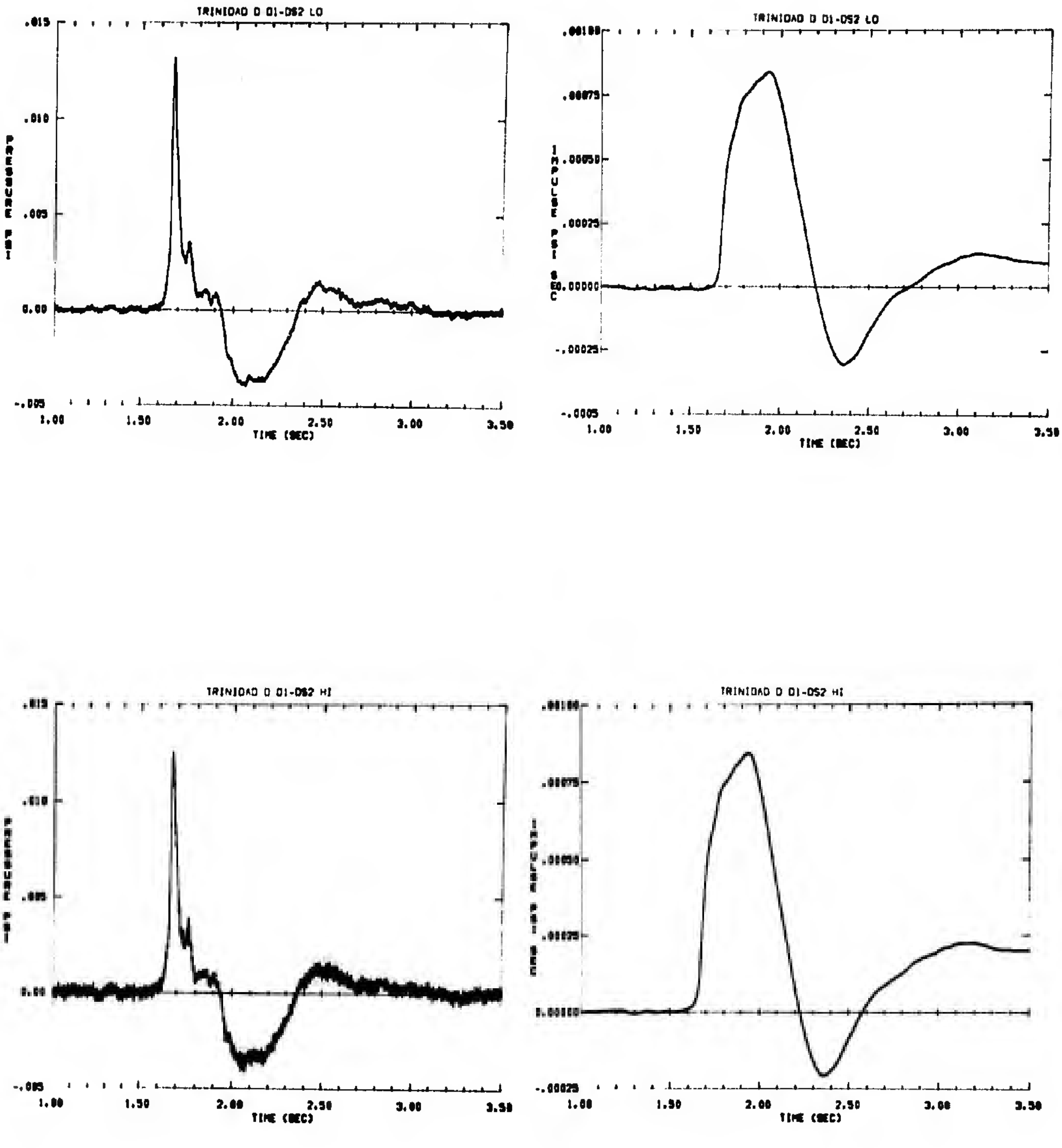

Figure D-4. Pressure-time and impulse-time for low-range gage (upper) and high-range gage (lower) for TRINIDAD Shot D-1, Station Downhill Side 2

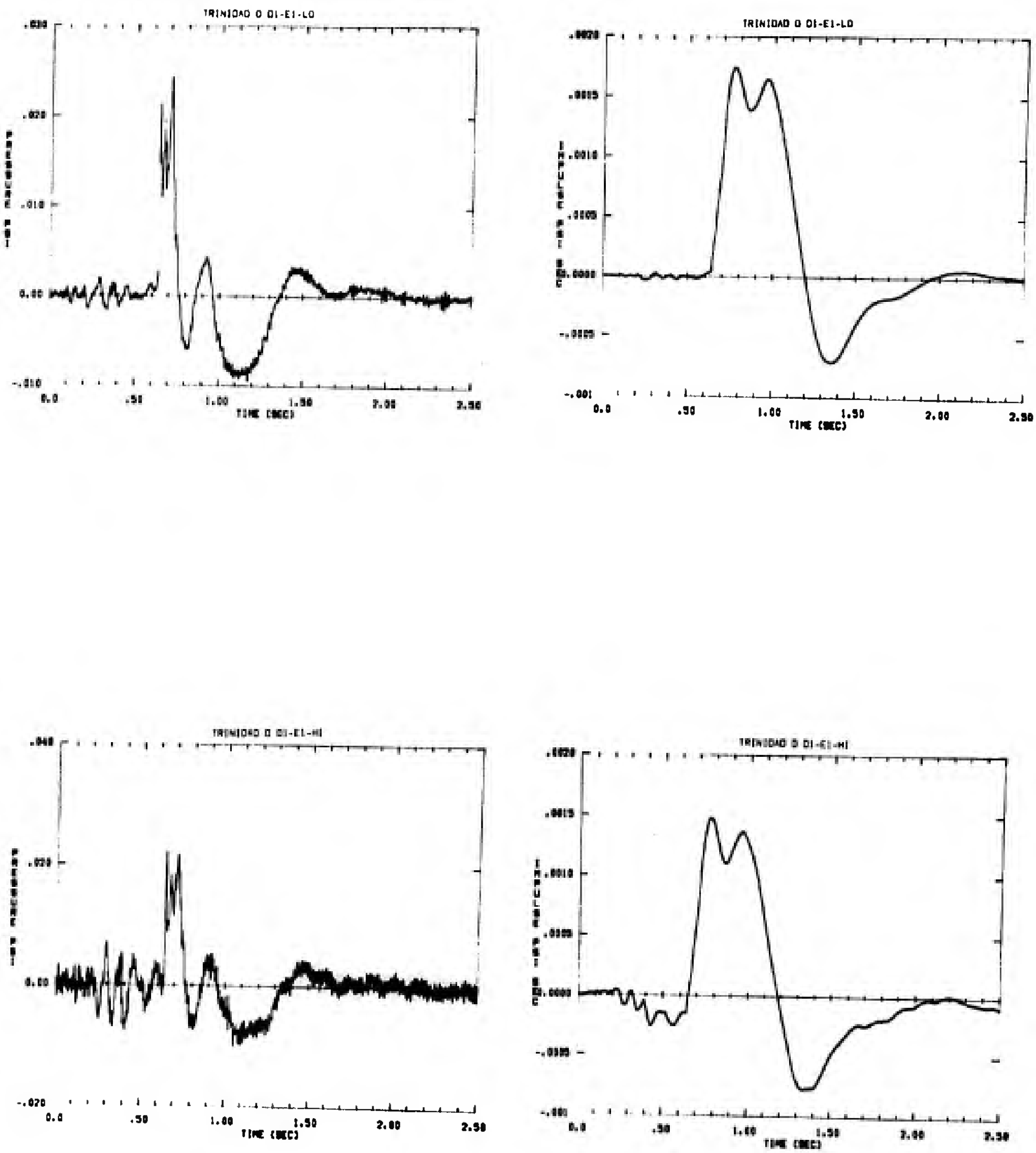

Figure D-5. Pressure-time and impulse-time for low-range gage (upper) and high-range gage (lower) for TRINIDAD Shot D-1, Station End 1

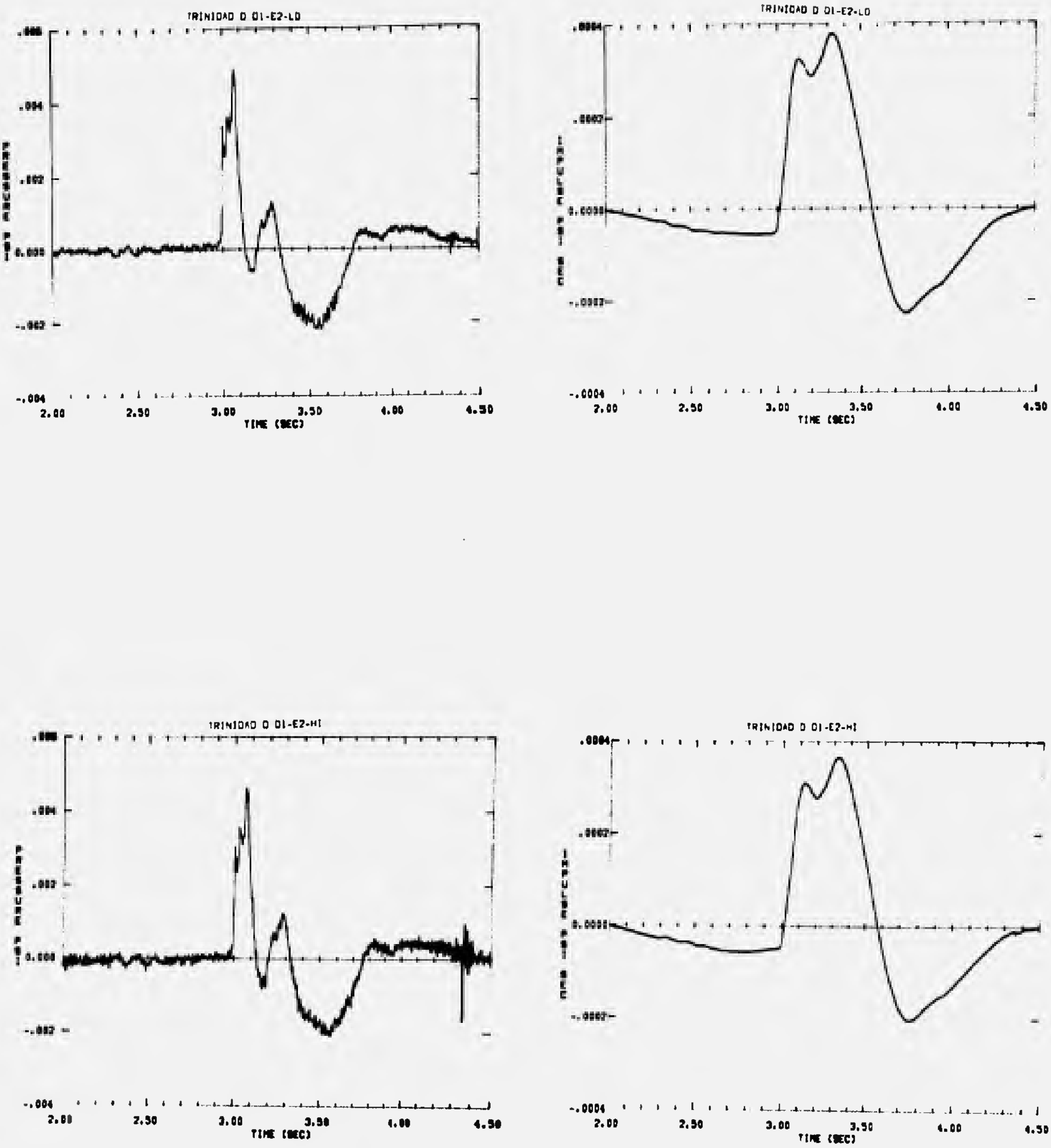

Figure D-6. Pressure-time and impulse-time for low-range gage (upper) and high-range gage (lower) for TRINIDAD Shot D-1, Station End 2

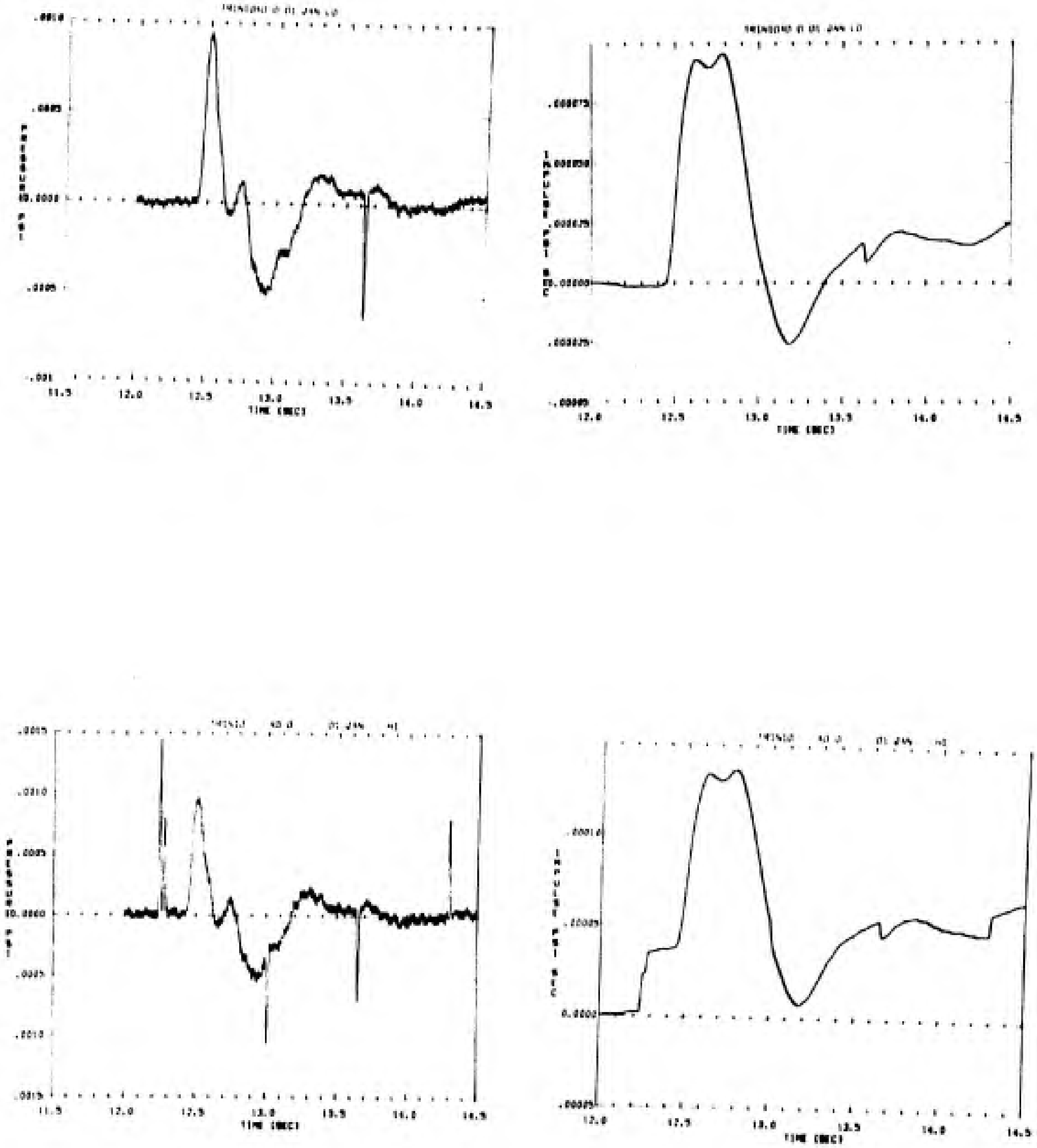

Figure D-7. Pressure-time and impulse-time for low-range gage (upper) and high-range gage (lower) for TRINIDAD Shot D-1, Station Jansen

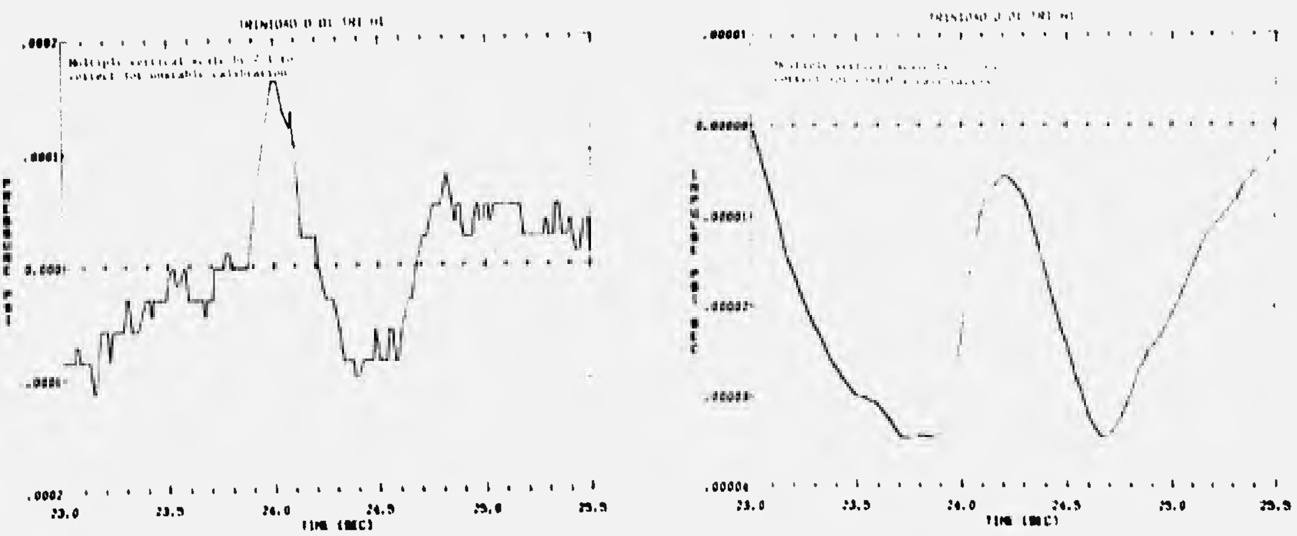

Figure D-8. Pressure-time and impulse-time for high-range gage for TRINIDAD Shot D-1, Station Trinidad

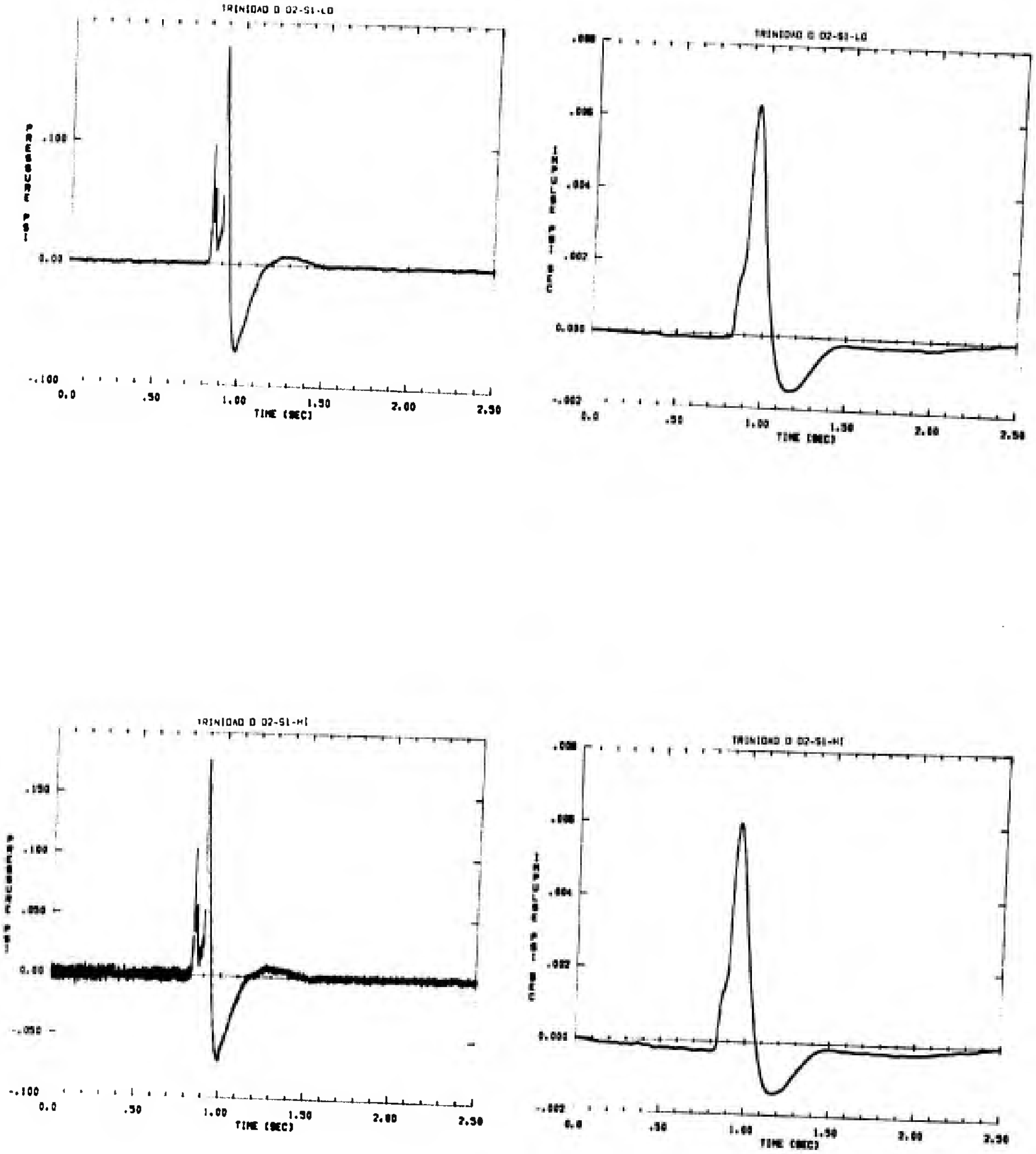

Figure D-9. Pressure-time and impulse-time for low-range gage (upper) and high-range gage (lower) for TRINIDAD Shot D-2, Station Side 1

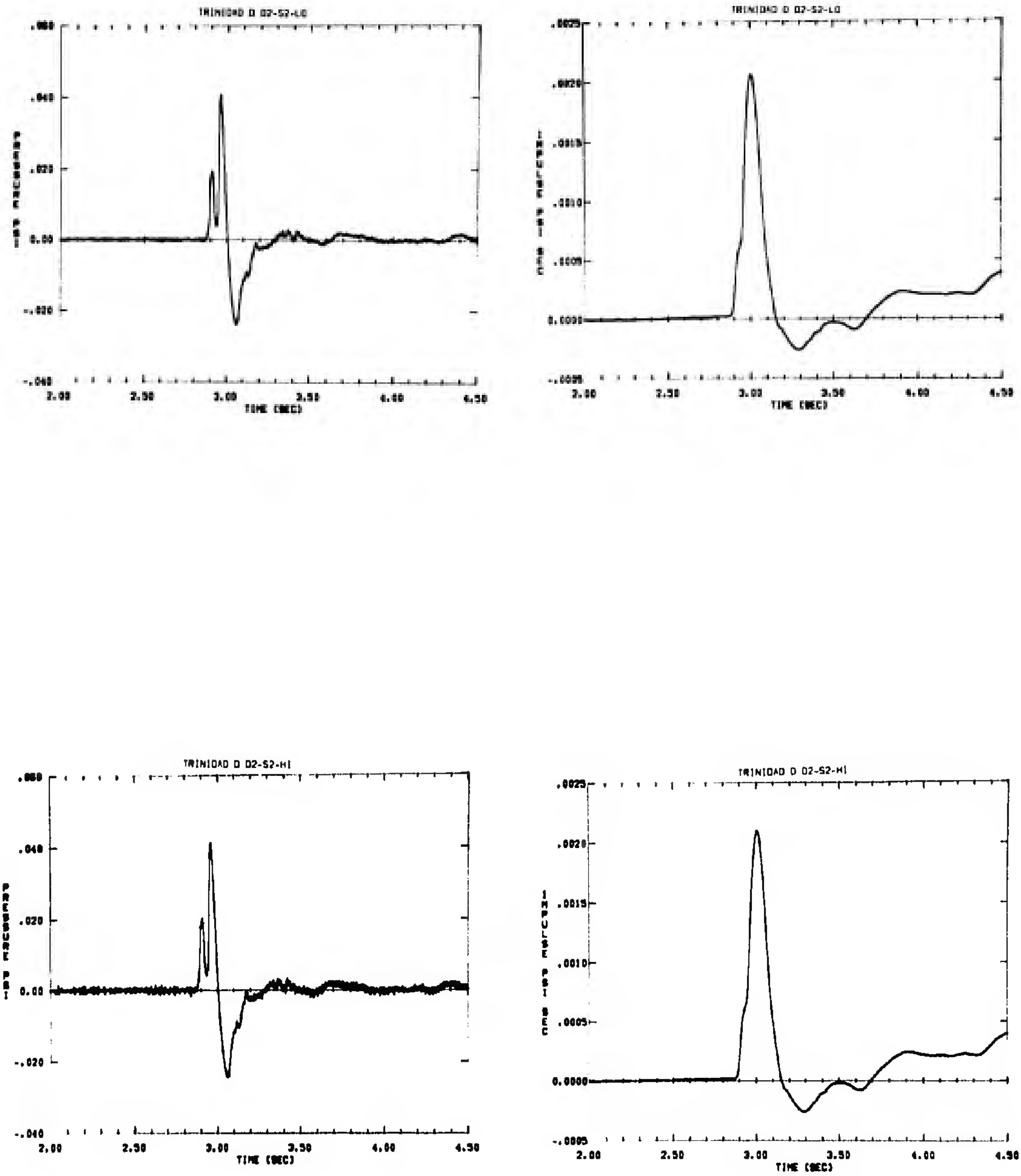

Figure D-10. Pressure-time and impulse-time for low-range gage (upper) and high-range gage (lower) for TRINIDAD Shot D-2, Station Side 2

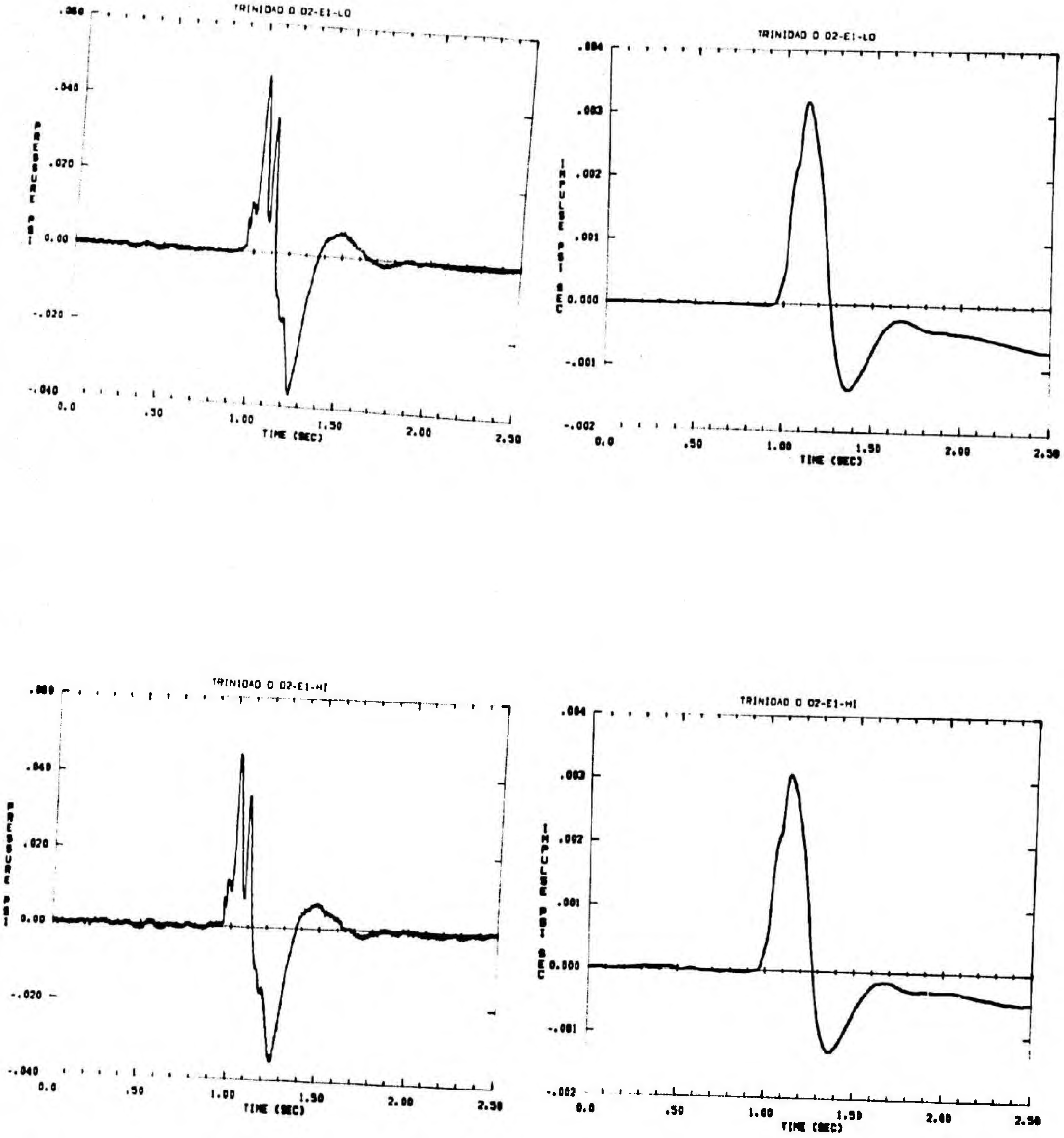

Figure D-11. Pressure-time and impulse-time for low-range gage (upper) and high-range gage (lower) for TRINIDAD Shot D-2, Station End 1

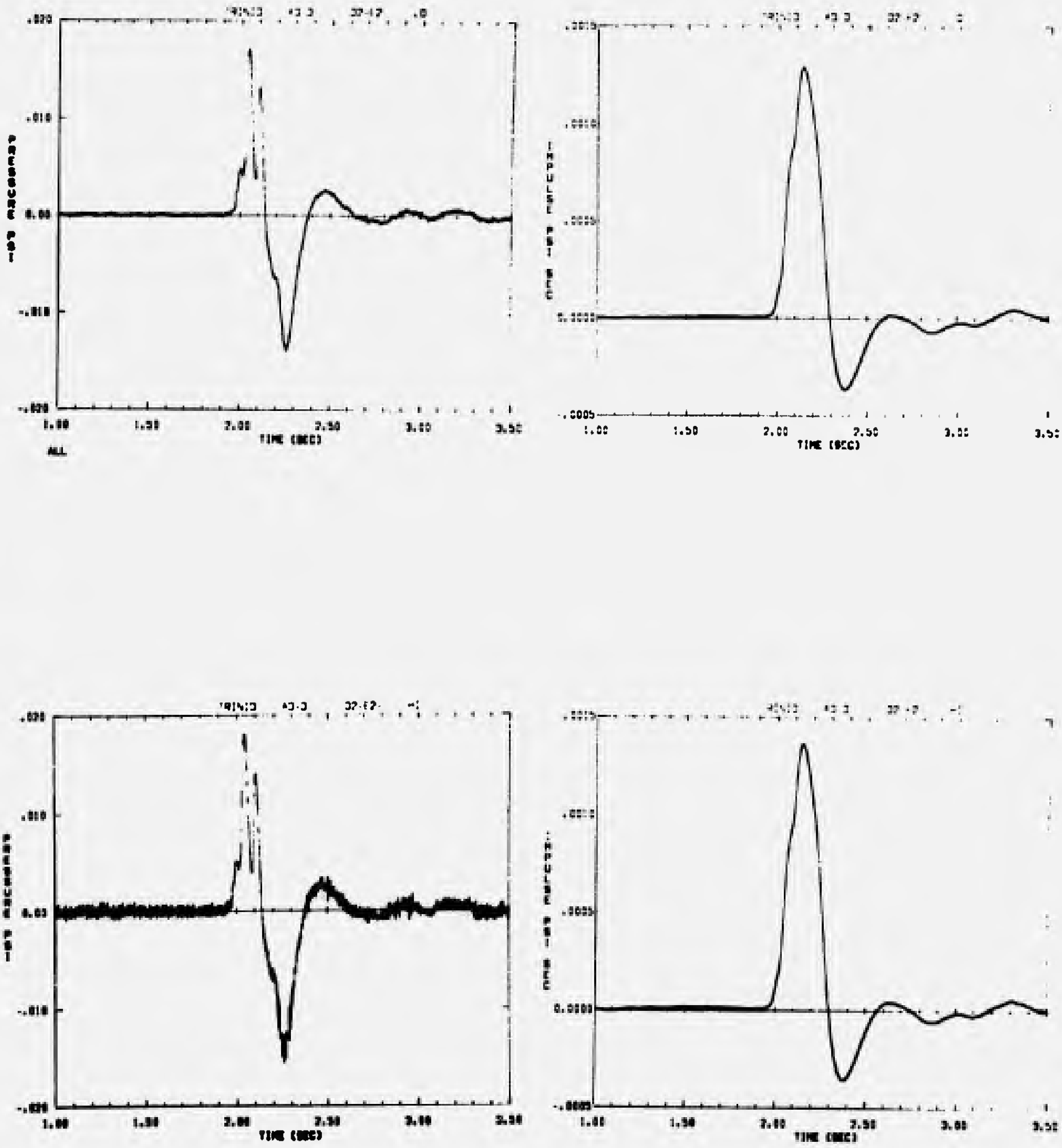

Figure D-12. Pressure-time and impulse-time for low-range gage (upper) and high-range gage (lower) for TRINIDAD Shot D-2, End 2

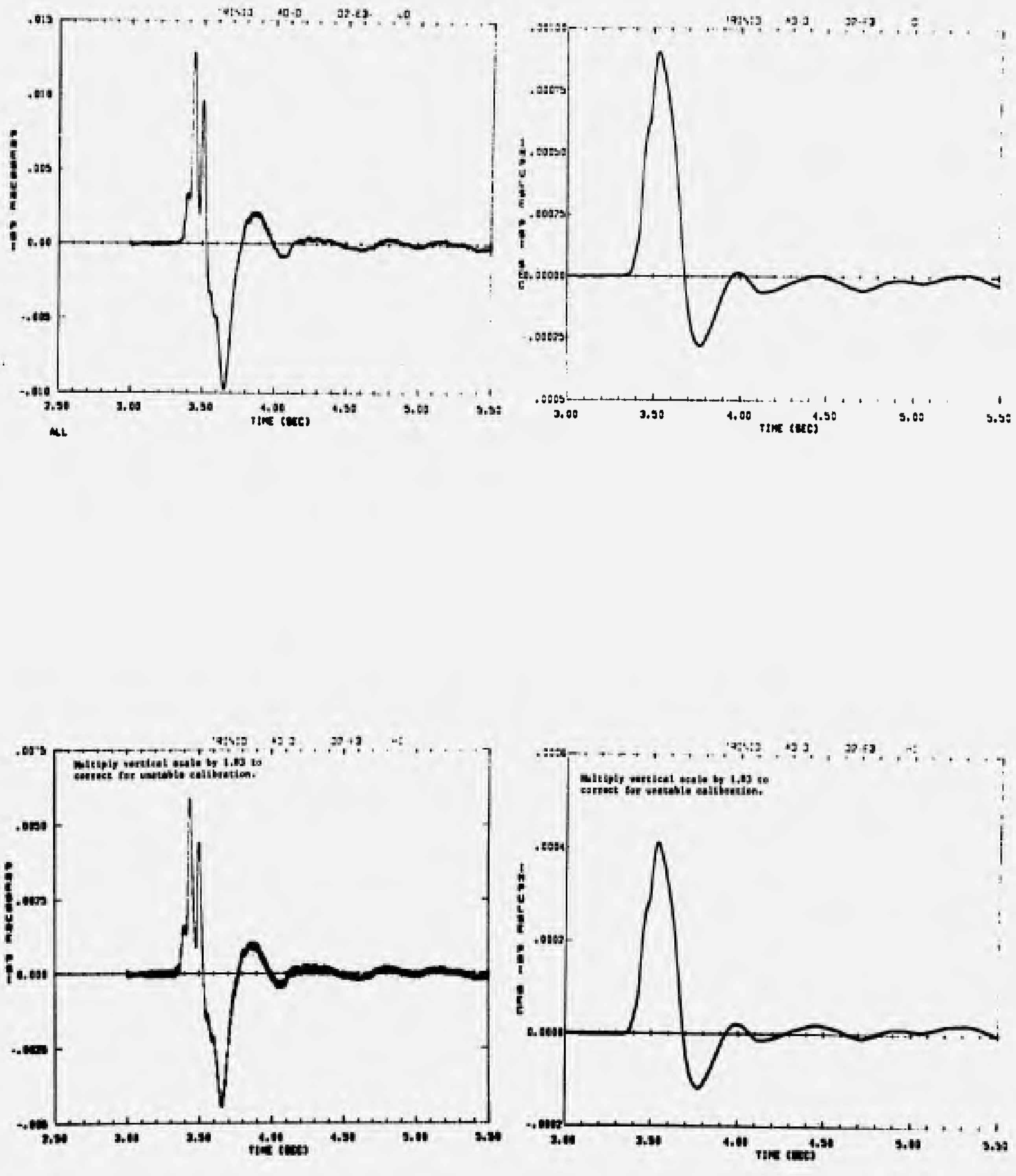

Figure D-13. Pressure-time and impulse-time for low-range gage (upper) and high-range gage (lower) for TRINIDAD Shot D-2, Station End 3

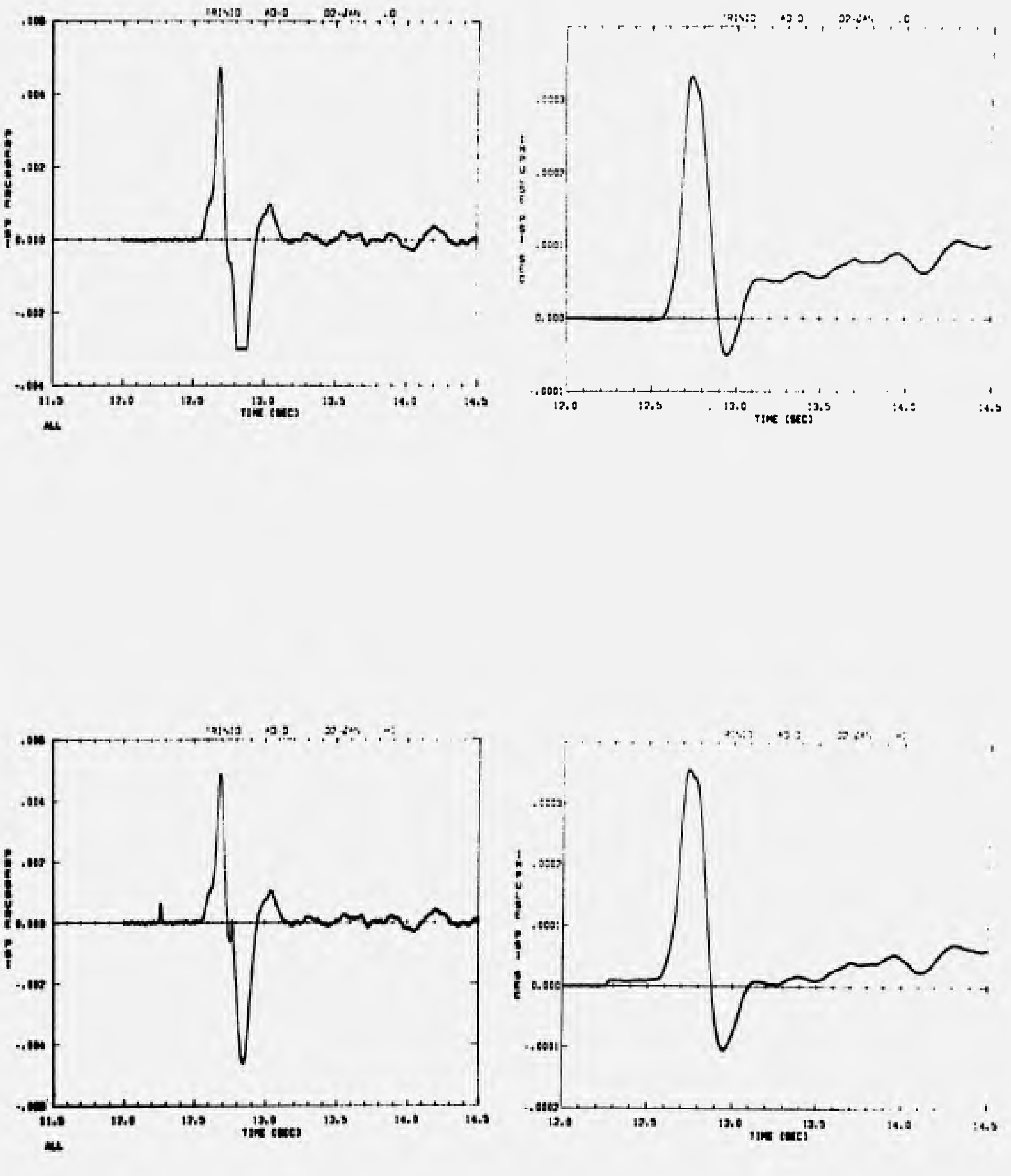

Figure D-14. Pressure-time and impulse-time for low-range gage (upper) and high-range gage (lower) for TRINIDAD Shot D-2, Station Jansen

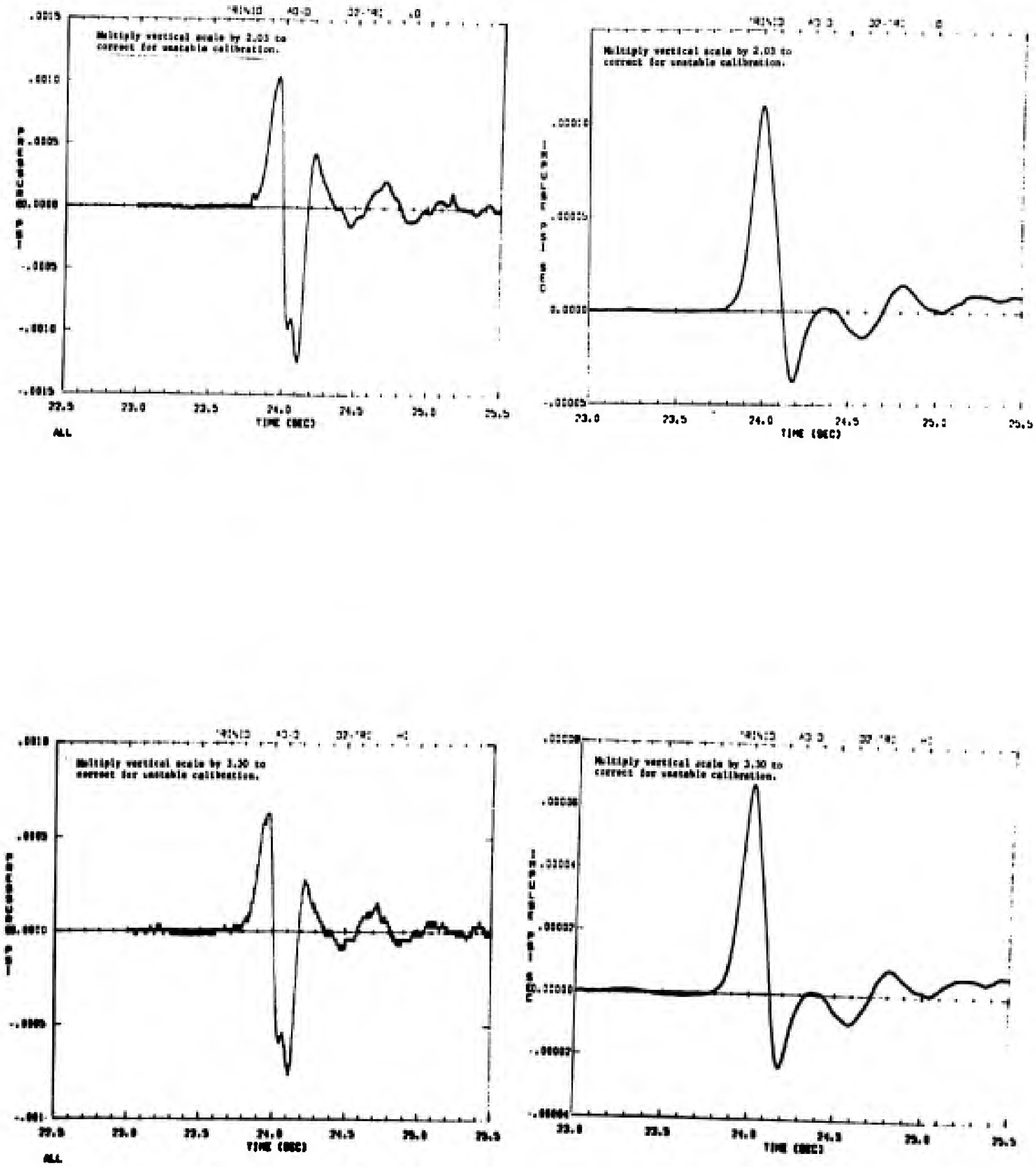

Figure D-15. Pressure-time and impulse-time for low-range gage (upper) and high-range gage (lower) for TRINIDAD Shot D-2, Station Trinidad

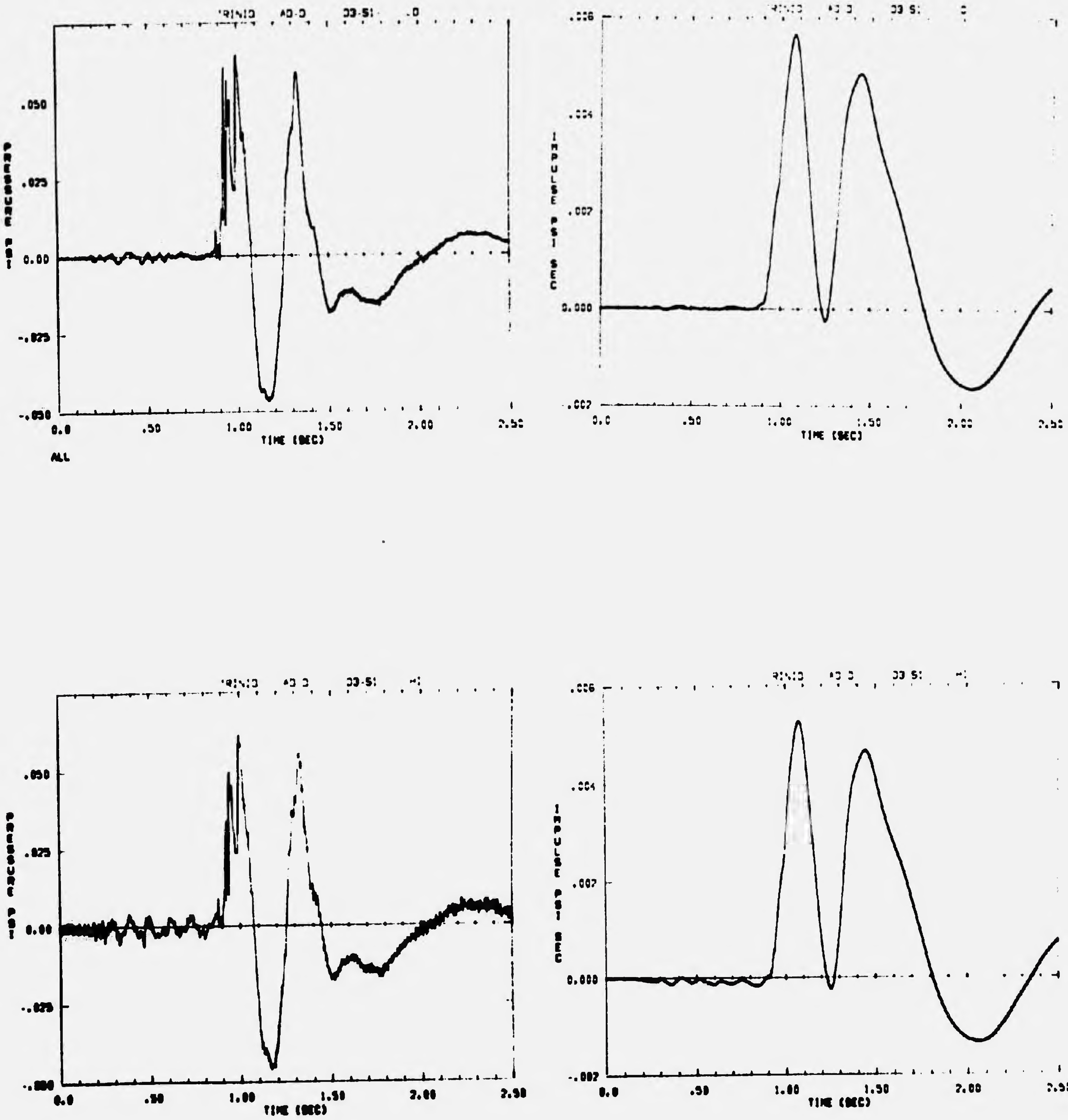

Figure D-16. Pressure-time and impulse-time for low-range gage (upper) and high-range gage (lower) for TRINIDAD Shot D-3, Station Side 1

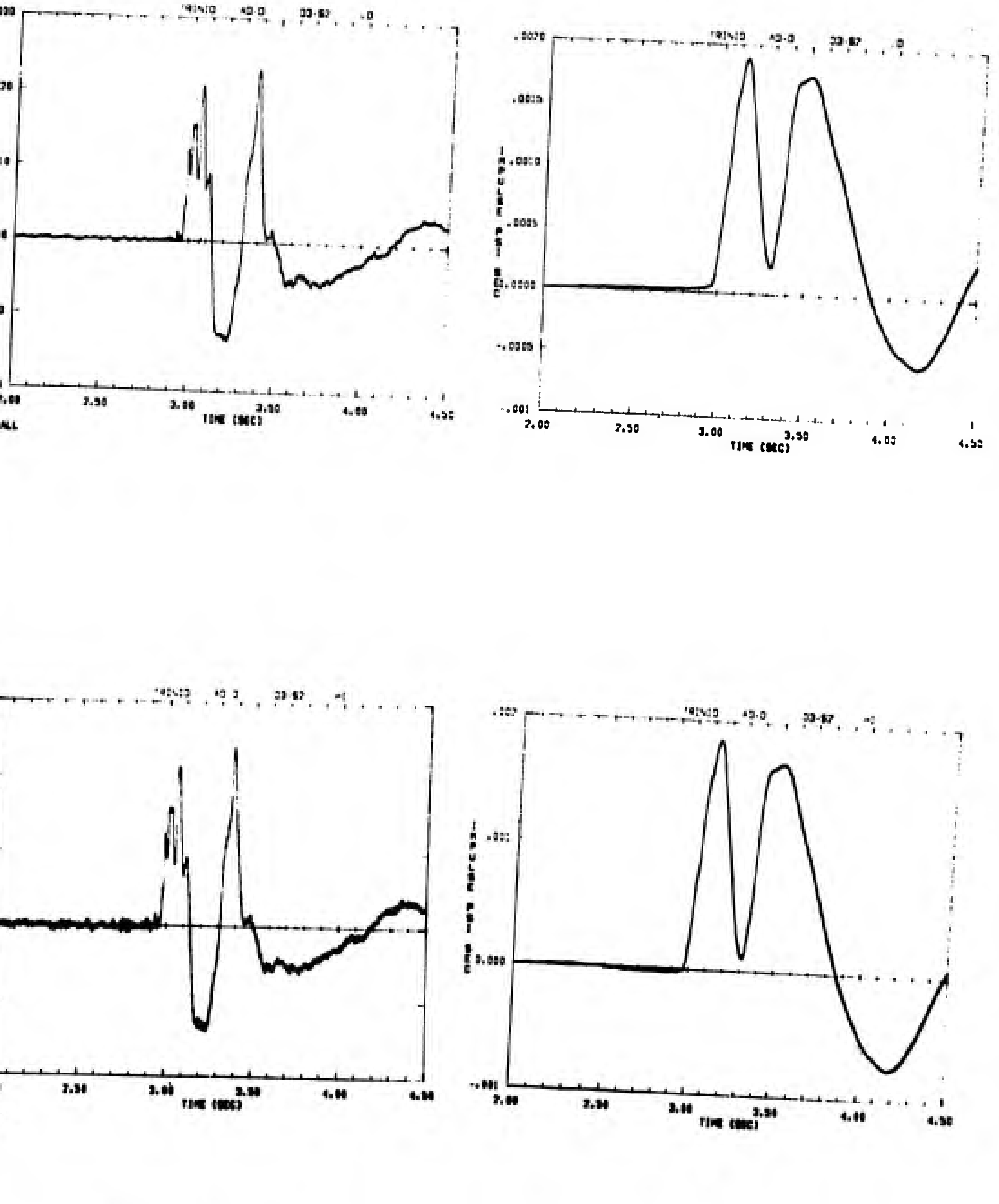

Figure D-17. Pressure-time and impulse-time for low-range gage (upper) and high-range gage (lower) for TRINIDAD Shot D-3, Station Side 2

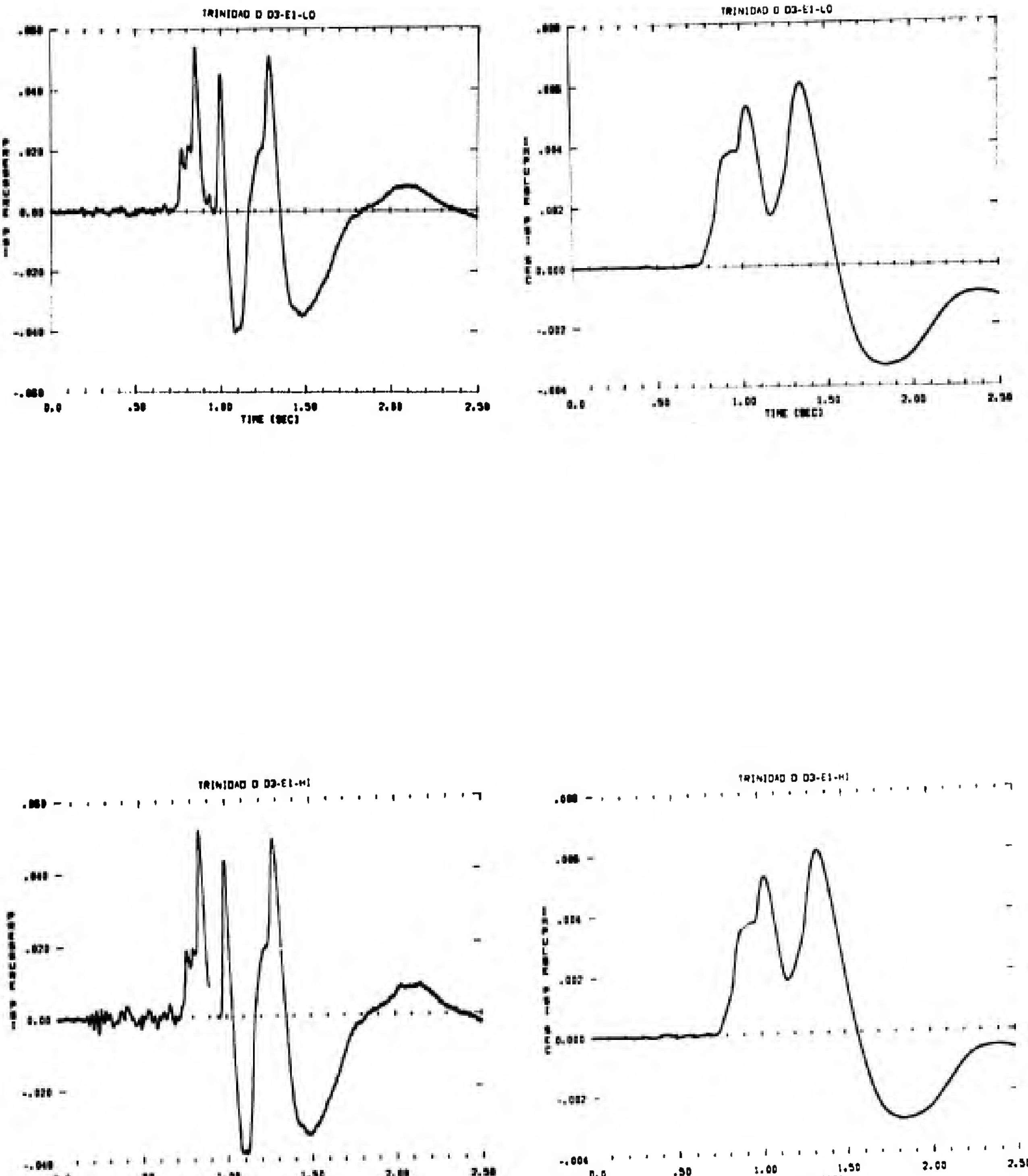

Figure D-18. Pressure-time and impulse-time for low-range gage (upper) and high-range gage (lower) for TRINIDAD Shot D-3, Station End 1

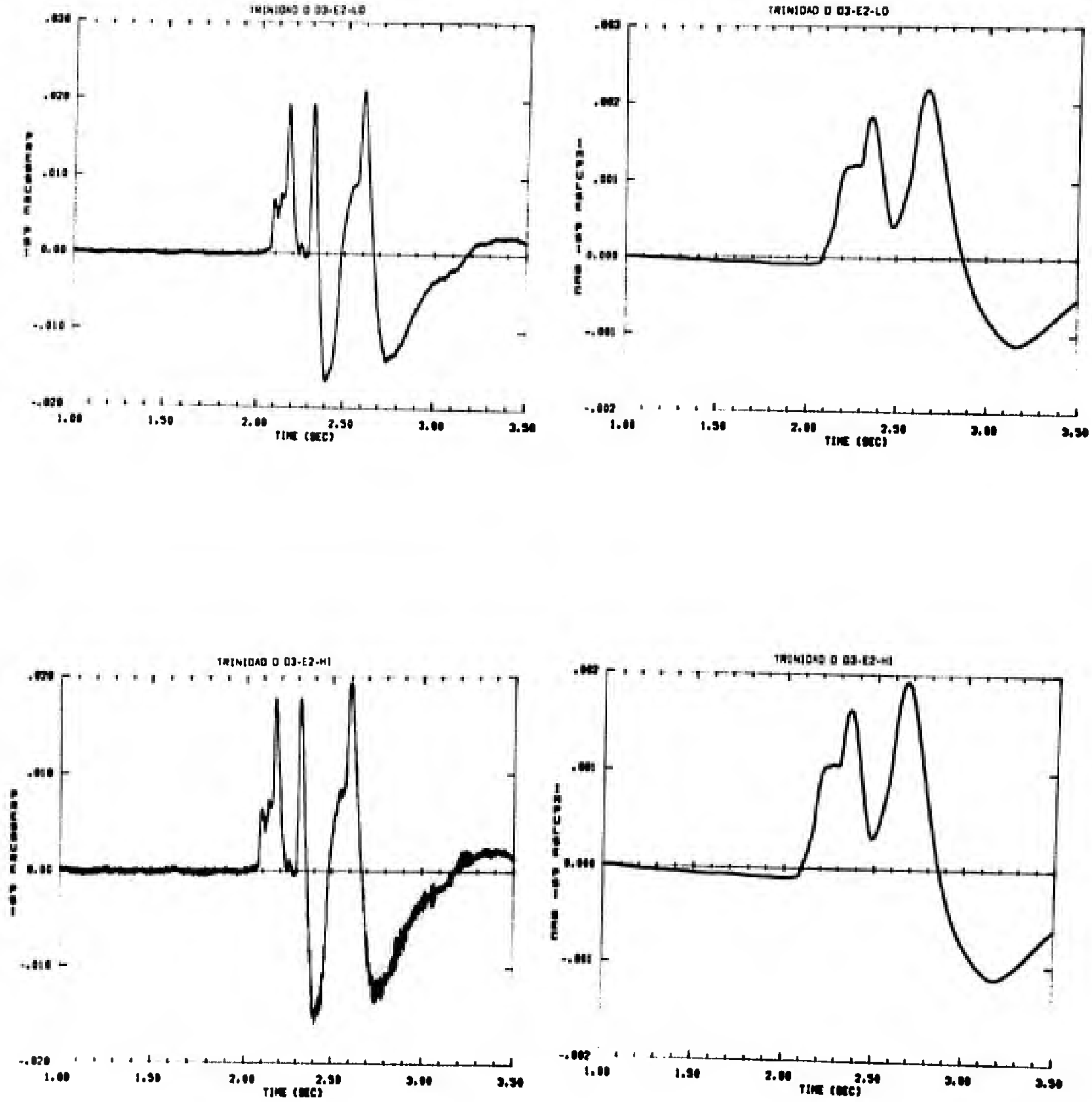

Figure D-19. Pressure-time and impulse-time for low-range gage (upper) and high-range gage (lower) for TRINIDAD Shot D-3, Station End 2

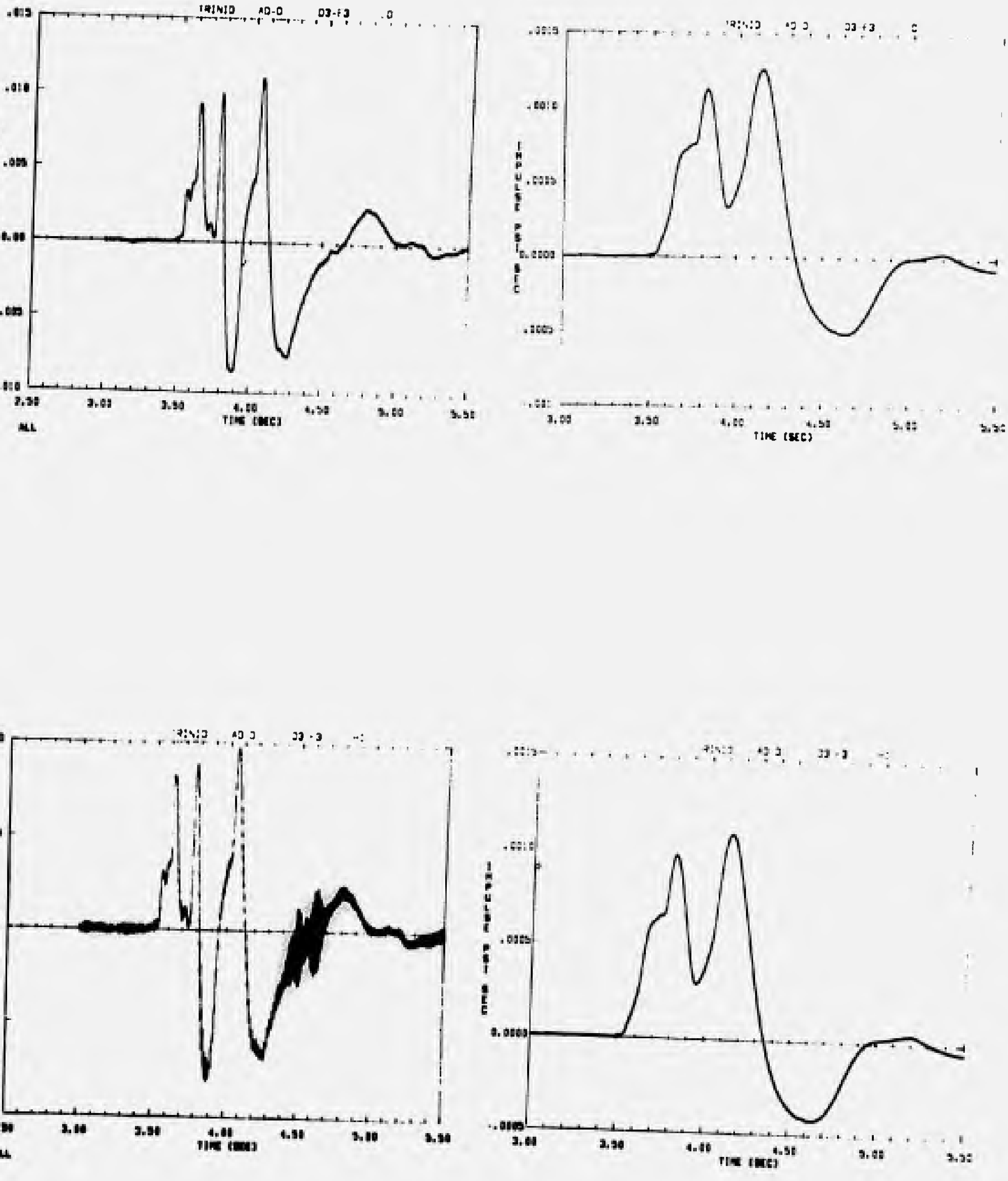

Figure D-20. Pressure-time and impulse-time for low-range gage (upper) and high-range gage (lower) for TRINIDAD Shot D-3, End 3

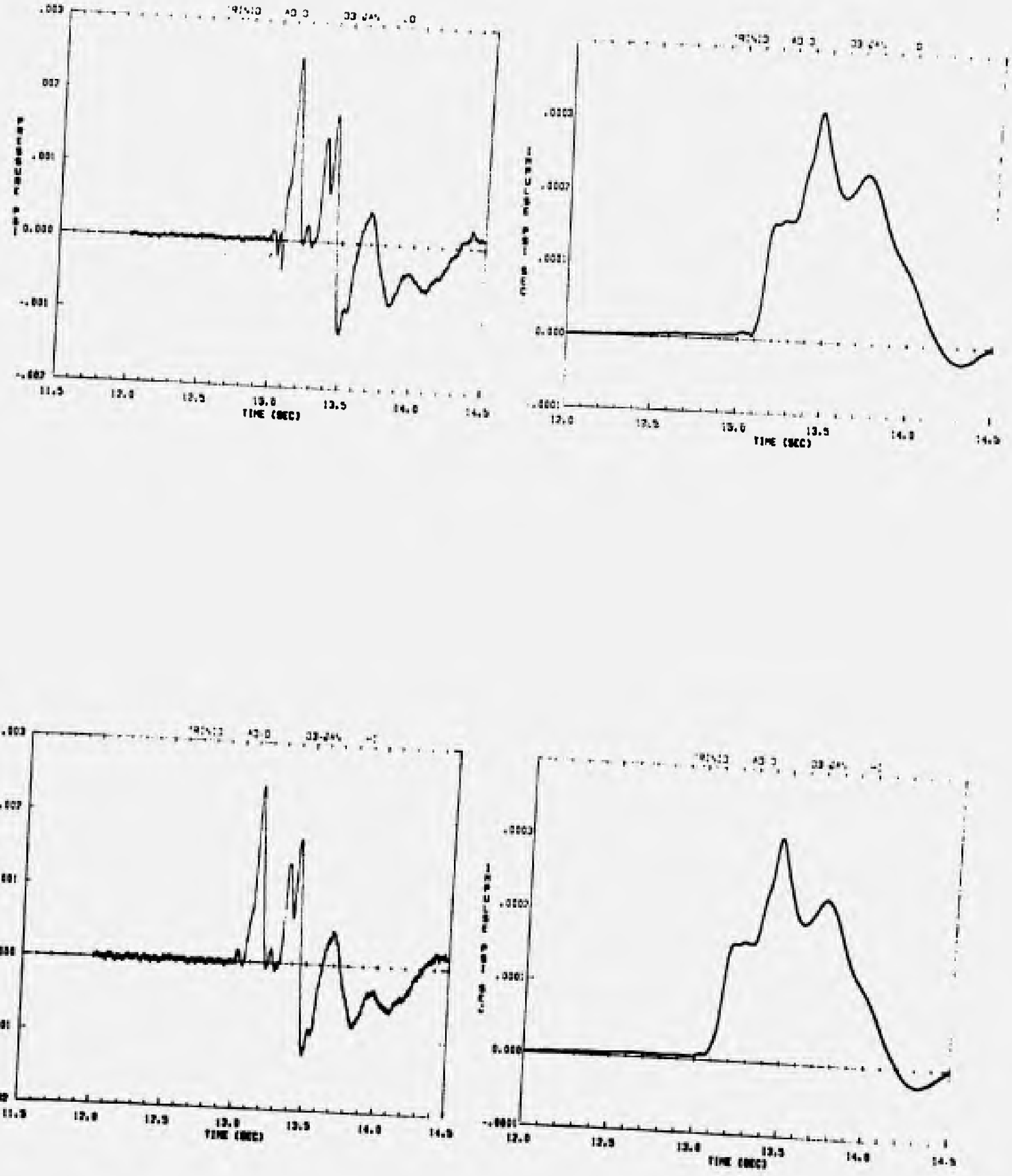

Figure D-21. Pressure-time and impulse-time for low-range gage (upper) and high-range gage (lower) for TRINIDAD Shot D-3, Station Jansen

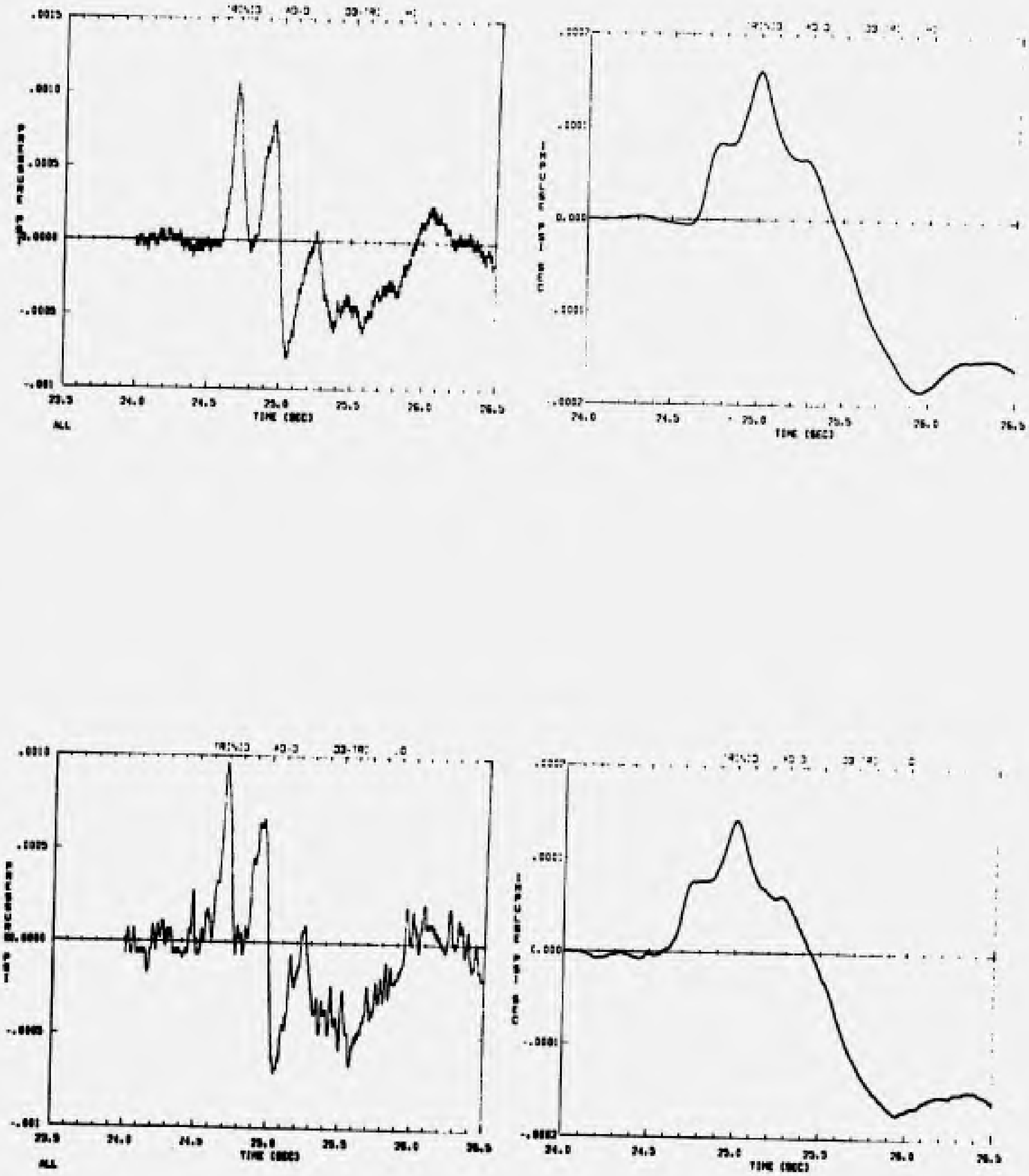

Figure D-22. Pressure-time and impulse-time for low-range gage (upper) and high-range gage (lower) for TRINIDAD Shot D-3, Station Trinidad

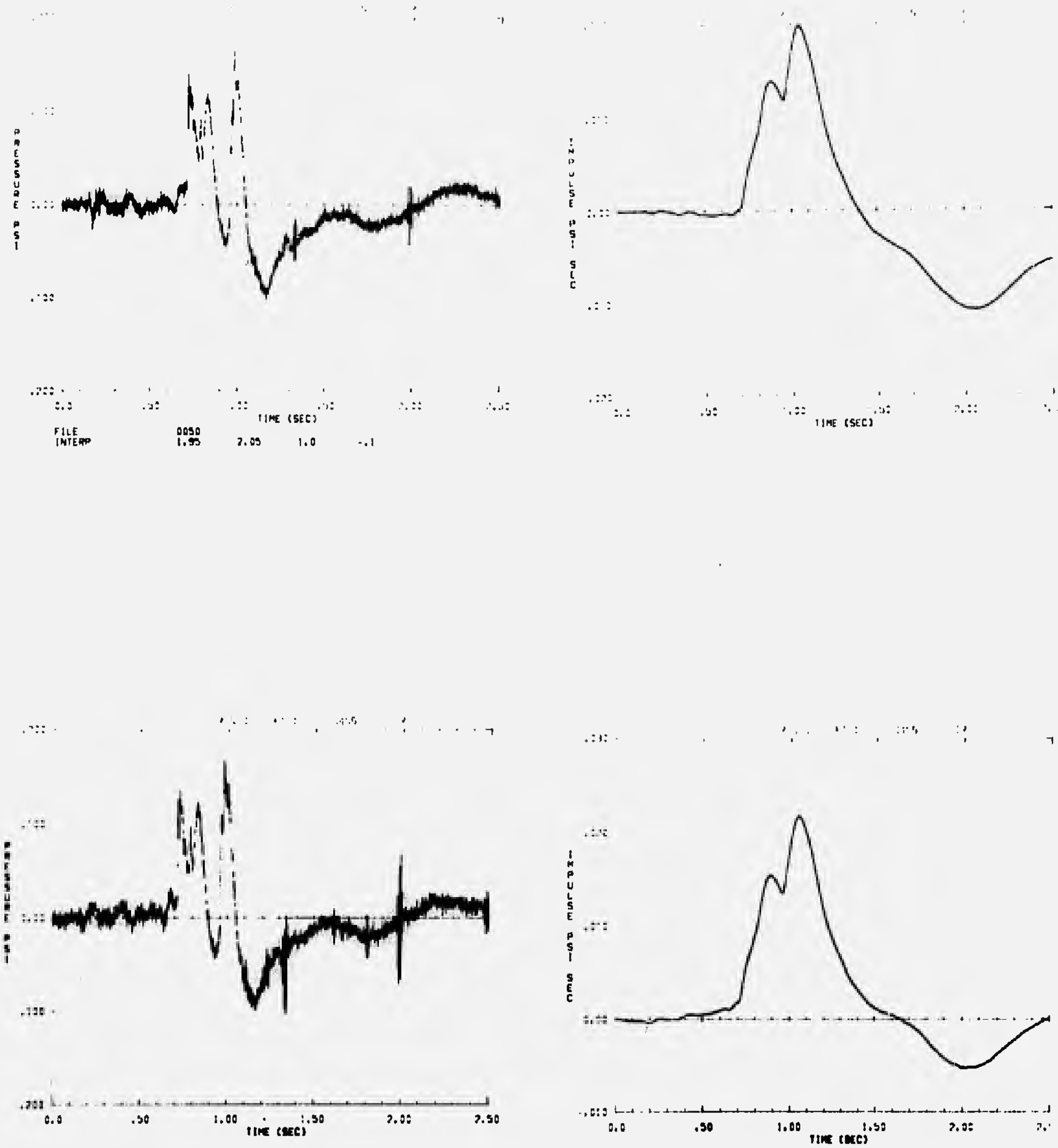

Figure D-23. Pressure-time and impulse-time for low-range gage (upper) and high-range gage (lower) for TRINIDAD Shot D-4, Station North Side 1

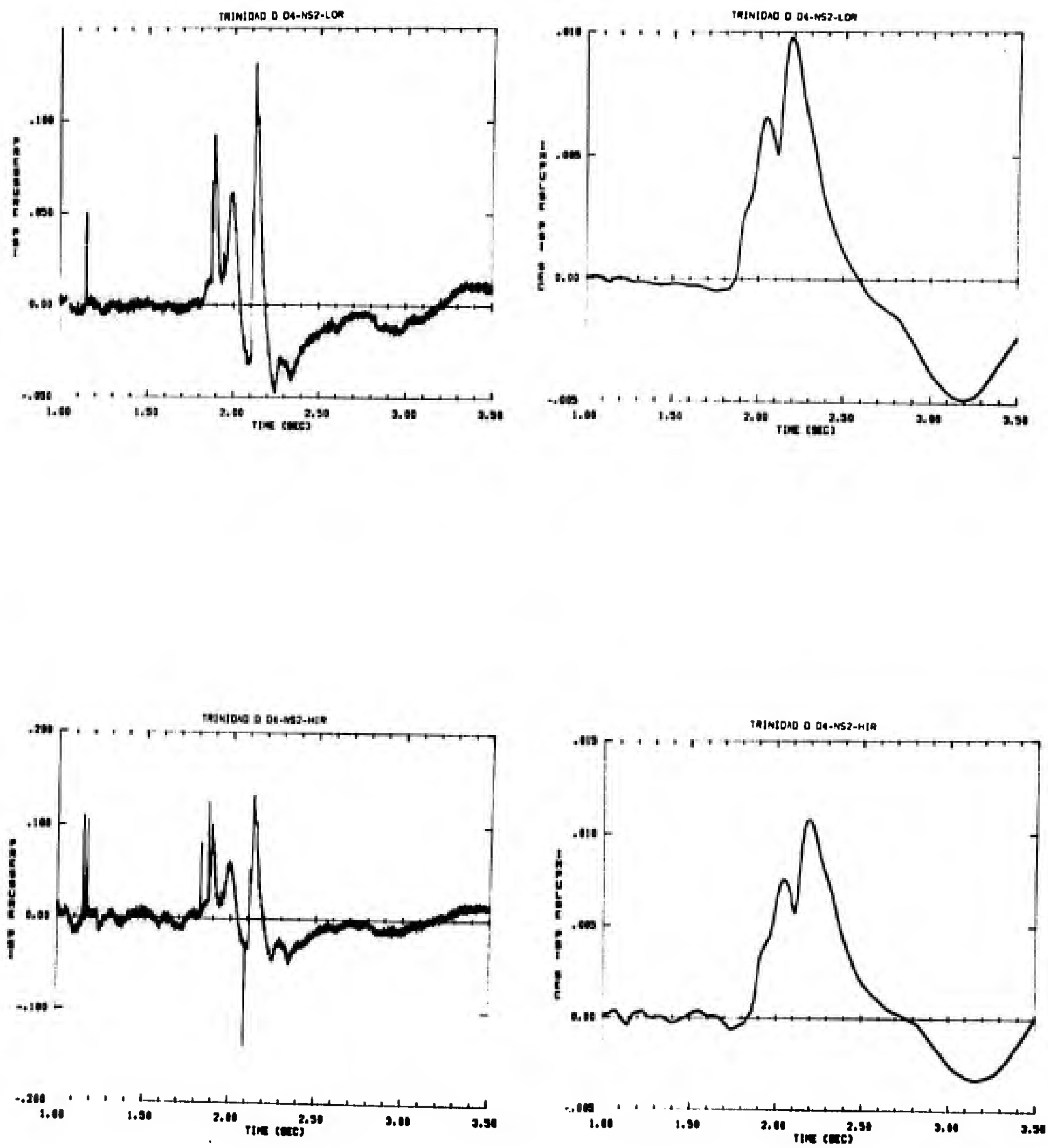

Figure D-24. Pressure-time and impulse-time for low-range gage (upper) and high-range gage (lower) for TRINIDAD Shot D-4, Station North Side 2

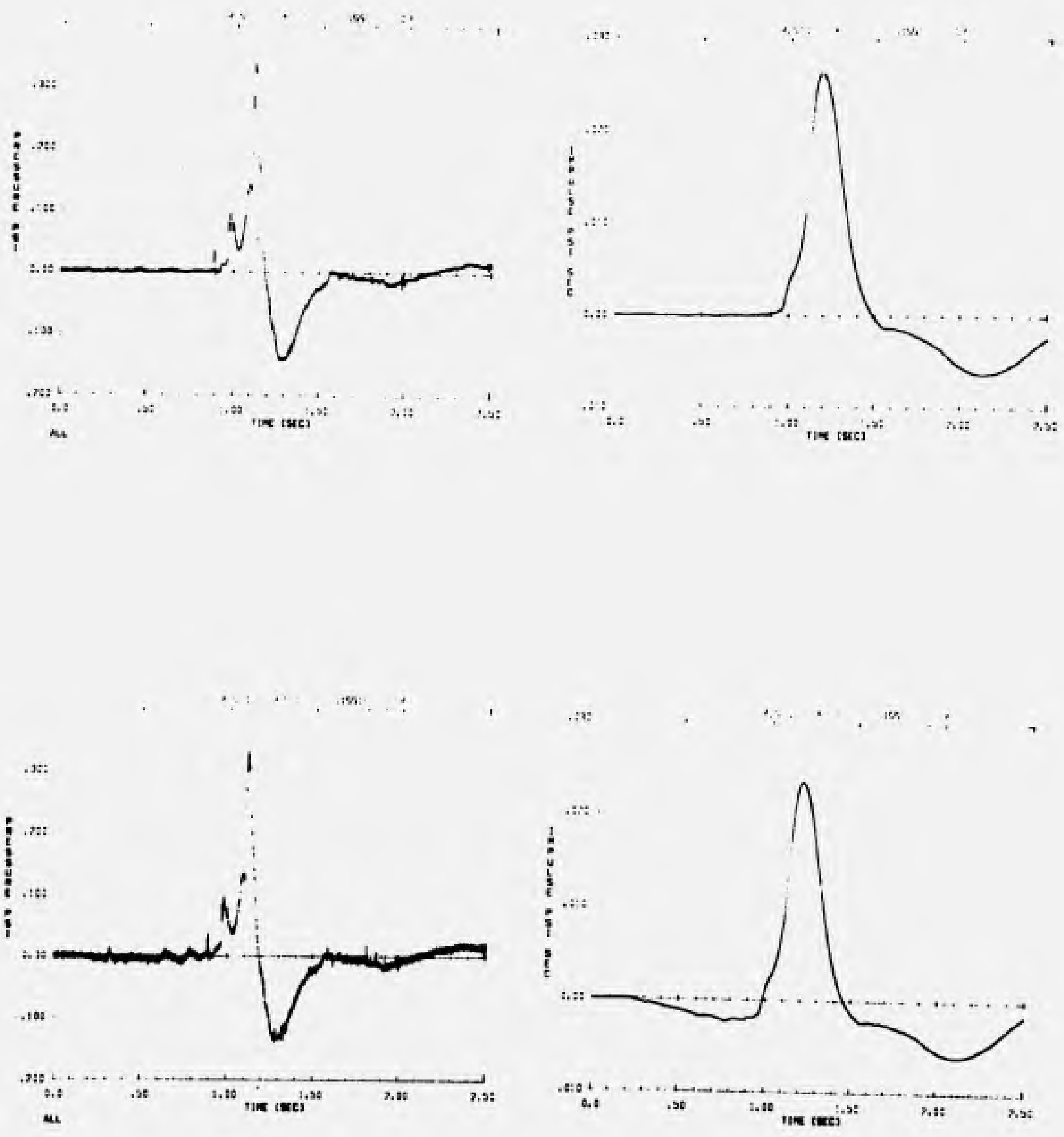

Figure D-25. Pressure-time and impulse-time for low-range gage (upper) and high-range gage (lower) for TRINIDAD Shot D-4, Station South Side

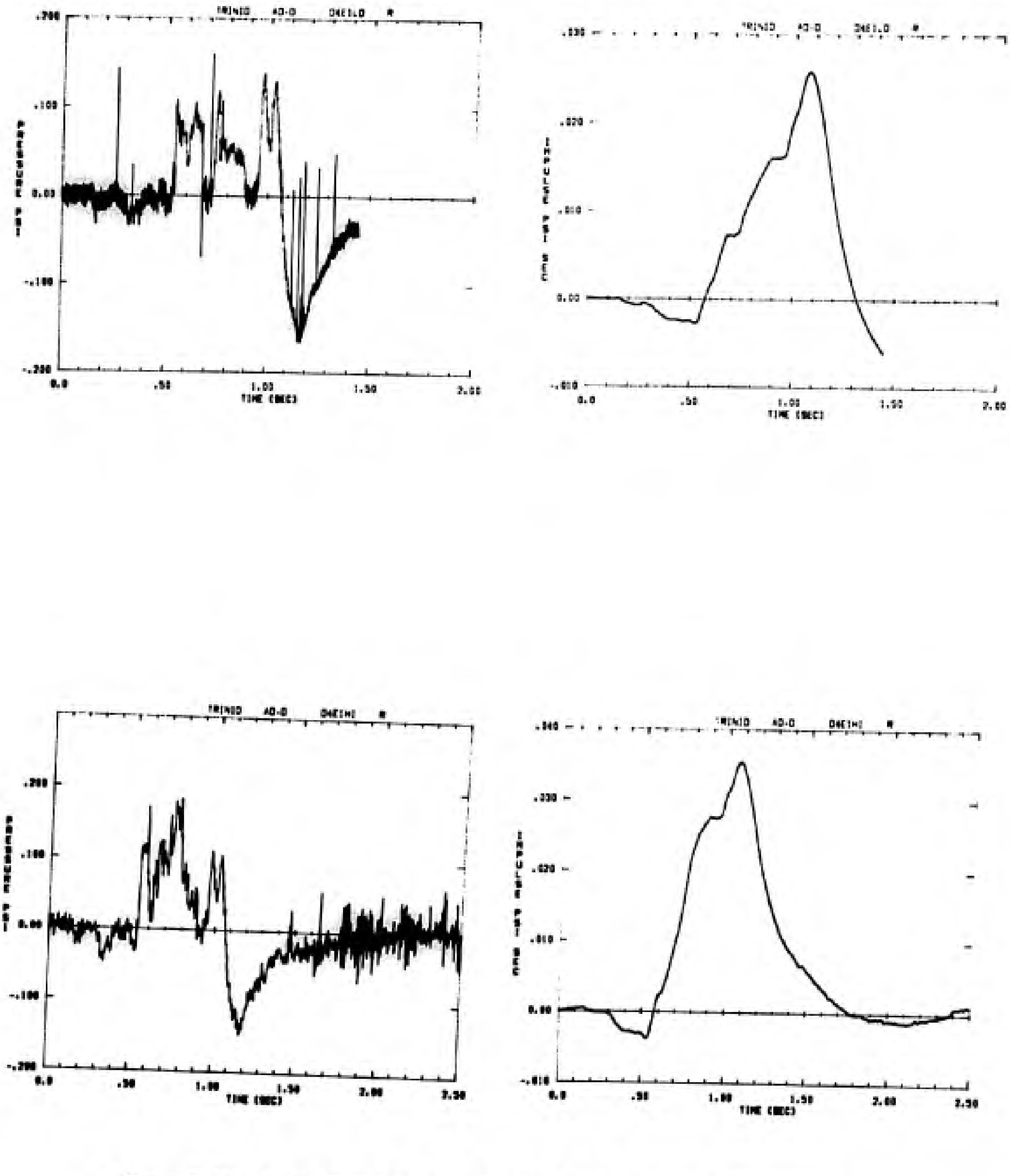

Figure D-26. Pressure-time and impulse-time for low-range gage (upper) and high-range gage (lower) for TRINIDAD Shot D-4, Station End 1

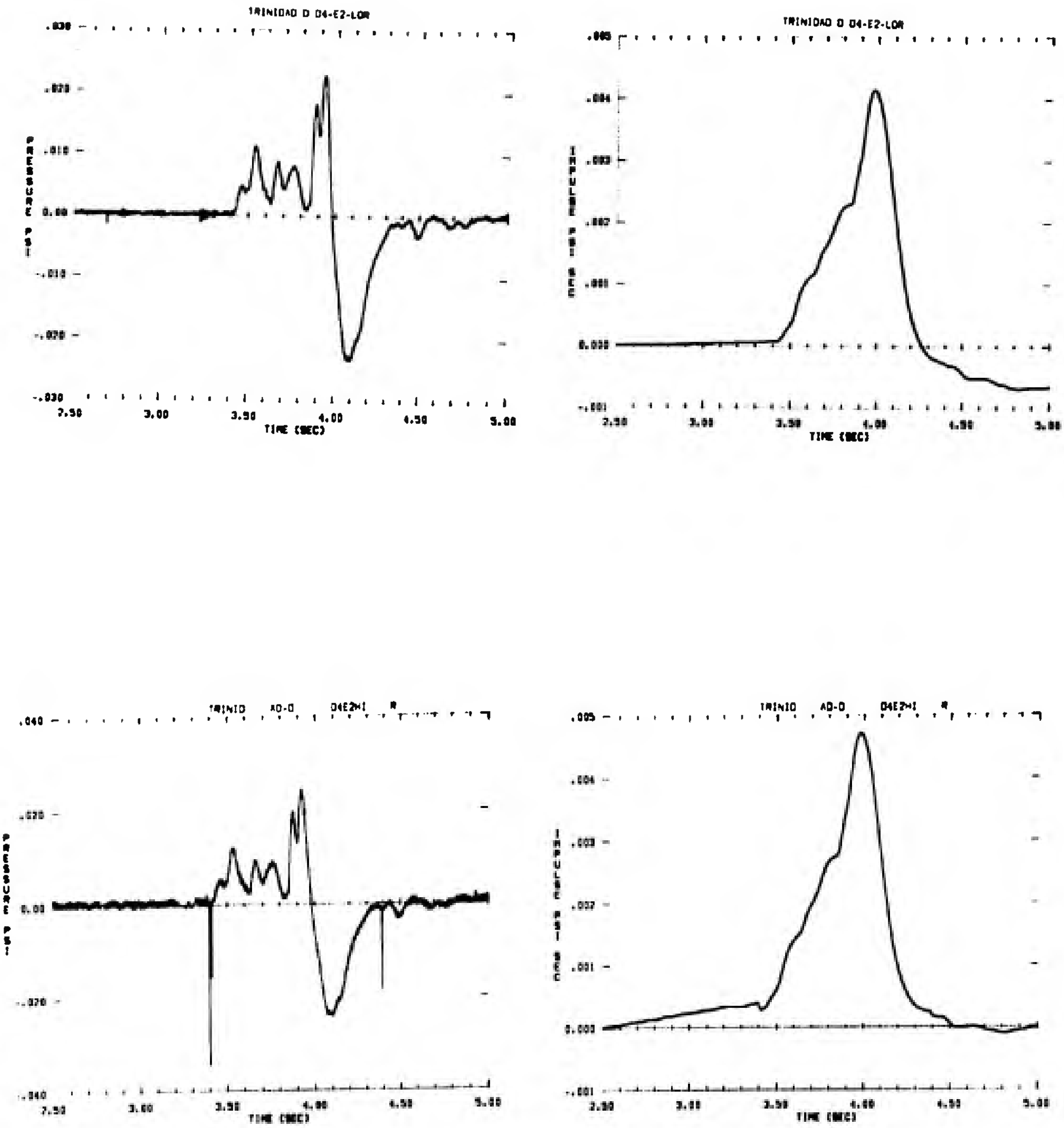

Figure D-27. Pressure-time and impulse-time for low-range gage (upper) and high-range gage (lower) for TRINIDAD Shot D-4, Station End 2

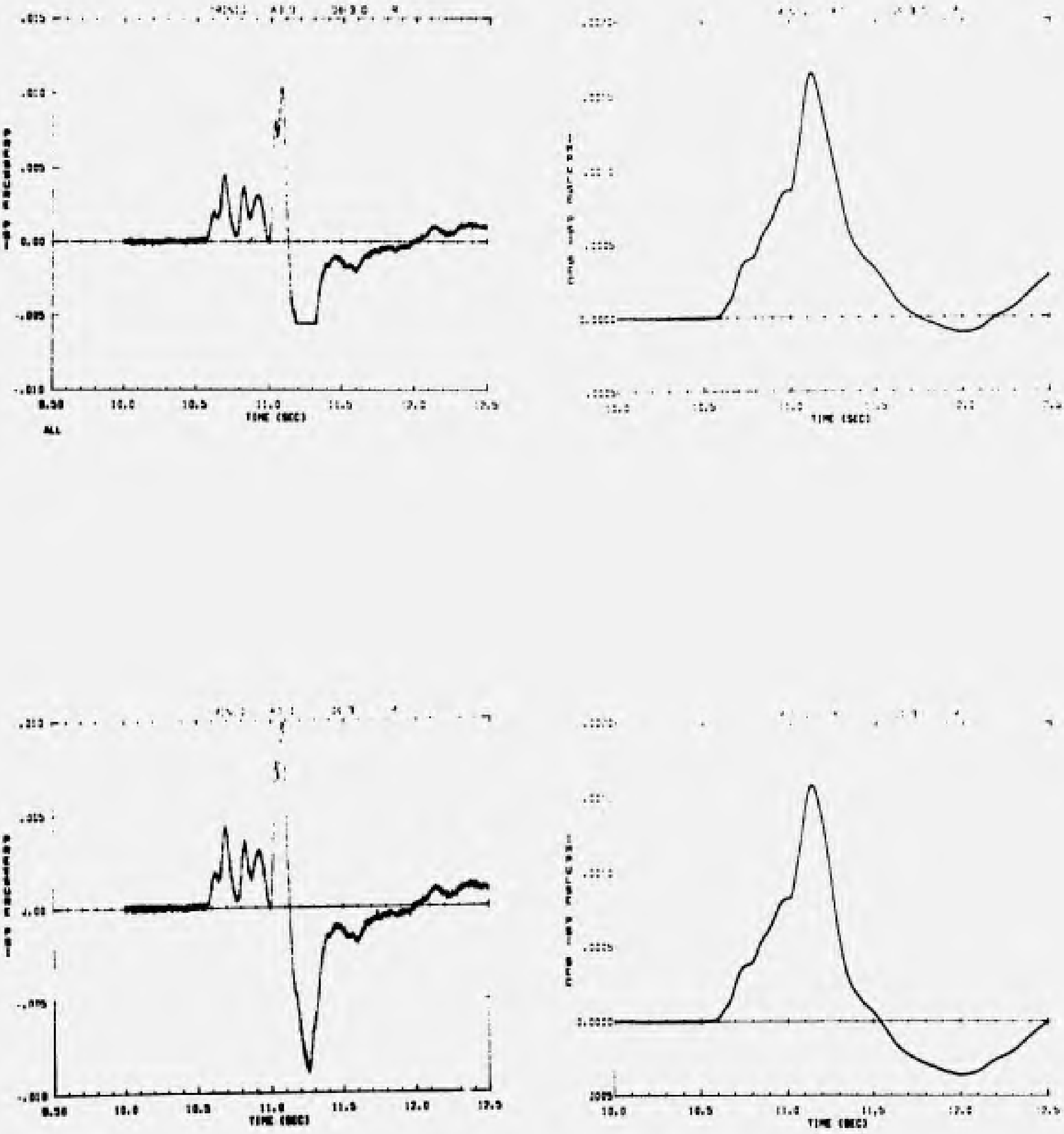

Figure D-28. Pressure-time and impulse-time for low-range gage (upper) and high-range gage (lower) for TRINIDAD Shot D-4, Station End 3

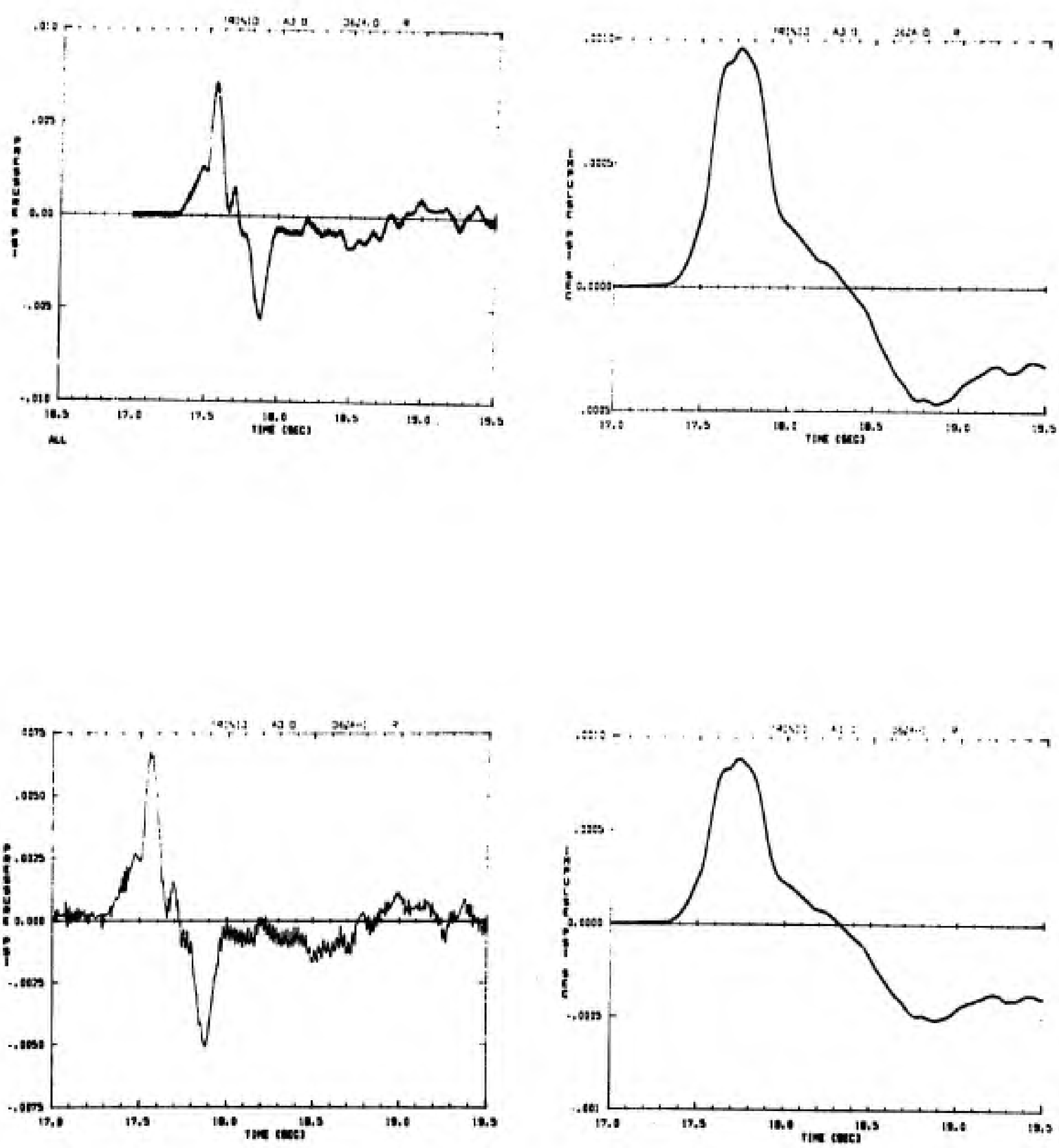

Figure D-29. Pressure-time and impulse-time for low-range gage (upper) and high-range gage (lower) for TRINIDAD Shot D-4, Station Jansen